Évaluation des effets des incendies sur la capacité de protection des forêts contre les chutes de blocs dans les Alpes françaises

S. Dupire

Communauté
UNIVERSITÉ Grenoble Alpes

THÈSE

POUR OBTENIR LE GRADE DE

**DOCTEUR DE LA
COMMUNAUTÉ UNIVERSITÉ GRENOBLE ALPES**

SPÉCIALITÉ : **SCIENCE DE LA TERRE, DE L'UNIVERS ET DE L'ENVIRONNEMENT (CESTUE)**

ARRÊTÉ MINISTÉRIEL : 25 MAI 2006

PRÉSENTÉE PAR
SYLVAIN DUPIRE

THÈSE DIRIGÉE PAR **THOMAS CURT**, CHERCHEUR, IRSTEA
ET CODIRIGÉE PAR **SYLVAIN BIGOT**, ENSEIGNANT-CHERCHEUR, UGA

PRÉPARÉE AU SEIN DU CENTRE **IRSTEA DE GRENOBLE**
DANS L'**ÉCOLE DOCTORALE TERRE, UNIVERS, ENVIRONNEMENT**

Évaluation des effets des incendies sur la capacité de protection des forêts contre les chutes de blocs dans les Alpes françaises

Assessing wildfires effects on the protection capability of forests against rockfalls in the French Alps

THÈSE SOUTENUE PUBLIQUEMENT LE **13 AVRIL 2018**,
DEVANT LE JURY COMPOSÉ DE :

MONSIEUR MARKUS STOFFEL
Professeur, Université de Genève, Suisse, Président du jury
MADAME ALEXIA STOKES
Directrice de Recherche, INRA Centre Occitanie-Montpellier, Rapporteur
MONSIEUR MARCO CONEDERA
Directeur de Recherche, Institut Fédéral WSL, Suisse, Rapporteur
MONSIEUR EMANUELE LINGUA
Maître de conférences, Université de Padoue, Italie, Examinateur
MONSIEUR THOMAS CURT
Directeur de recherche, IRSTEA Aix-en-Provence, Directeur de thèse
MONSIEUR SYLVAIN BIGOT
Professeur, Université Grenoble Alpes, Co-Directeur de thèse
MONSIEUR LAURENT BORGNIET
Ingénieur de recherche, IRSTEA Grenoble, Examinateur

Remerciements

Ce mémoire de thèse rend compte de trois années de travail menées au centre Irstea de Grenoble. Je tiens ici à remercier tous ceux qui ont rendu cette aventure possible. Précisons que tout a commencé six ans plus tôt suite à mon recrutement en tant que chargé d'études par Frédéric BERGER. Les personnes rencontrées au centre et les missions qui m'ont été confiées m'ont peu à peu donné le goût pour la recherche jusqu'à présenter cette thèse de doctorat.

Je tiens tout d'abord à remercier mon directeur de thèse, Thomas CURT, directeur de recherche à Irstea Aix-en-Provence, pour son accompagnement (à longue distance) tout au long de la thèse. Nos échanges et ses conseils ont ainsi permis de cibler les points d'investigations essentiels et d'améliorer les interprétations des résultats.
Je remercie également Sylvain BIGOT, Professeur à l'Université Grenoble Alpes et co-directeur de la thèse, pour son accompagnement sur des sujets scientifiques parfois éloignés de ses activités. Je lui suis très reconnaissant des conseils et directives qu'il a su m'apporter ainsi que de son soutien administratif qui a grandement facilité mon service d'enseignement à l'Institut de Géographie Alpine de Grenoble.
Merci également à Laurent BORGNIET, ingénieur de recherche à Irstea, pour avoir participé à l'encadrement de ma thèse.

Je remercie chaleureusement Franck BOURRIER et Jean-Matthieu MONNET, respectivement chargé de recherche et ingénieur de recherche à Irstea, pour nos échanges réguliers sur ce travail de thèse et pour m'avoir conseillé à de nombreuses reprises. Leur implication a largement contribué à la réussite de ce travail de thèse.

Je remercie aussi Luuk DORREN, professeur à l'Université de Bern, Max BRUCCIAMACHIE, enseignant-chercheur à AgroParisTech, et Hélène DE POMMERY, ingénieure à la DDT de l'Isère, pour leur soutien scientifique et technique et leur disponibilité à l'occasion des comités de pilotage.

J'adresse aussi mes remerciements à l'ensemble des membres de feu l'équipe PIER et particulièrement à Frédéric BERGER, ingénieur de recherche à Irstea, qui a réussi à insuffler, parmi nous, un état d'esprit amical pour endurer ce travail de thèse. Merci à David, mon colocataire de bureau, pour m'avoir offert de nombreuses franches rigolades. Merci à Jean-Baba, pour ses incomptables éclairages plus qu'utiles dans bien des sujets qu'ils soient scientifiques ou non ! Merci à Eric et Pascal pour leurs coups de main sur le terrain.

Je remercie enfin ma famille. Mes parents qui m'ont toujours soutenu que ce soit pour les études ou les autres projets de la vie. Bertille et Anouk (arrivée en cours de thèse) qui m'ont supporté dans cette aventure et ont apporté l'équilibre extraprofessionnel essentiel pour affronter pareil travail.

Résumé

Les chutes de blocs constituent un aléa naturel majeur dans les Alpes françaises en raison de leur probabilité d'occurrence spatiale et temporelle très élevée. Les forêts peuvent constituer une solution naturelle et efficace pour atténuer ce phénomène tout en protégeant les populations et leurs infrastructures. Cependant, ce service écosystémique peut être perturbé par d'autres aléas naturels comme les feux de forêts, susceptibles d'être plus fréquents et intenses dans le contexte actuel et futur de changements climatiques.

Cette thèse propose ainsi d'**évaluer les effets des incendies sur la capacité de protection des forêts contre les chutes de blocs dans les Alpes françaises**.

Une méthodologie pour évaluer la capacité de protection d'une forêt contre les chutes de blocs est d'abord développée et consiste à utiliser des simulations de propagation de chutes de blocs réalisées sur 3886 placettes forestières des Alpes françaises pour calculer trois indicateurs quantitatifs évaluant la réduction de la fréquence (*BARI*), de l'intensité (*MIRI*) et la réduction globale (*ORPI*) de l'aléa chutes de blocs dues à la présence d'une forêt. Ces indicateurs sont utilisés pour identifier les variables forestières prépondérantes pour évaluer la capacité de protection : la longueur boisée sur le versant, la surface terrière et le diamètre moyen. Les peuplements présentant une distribution hétérogène des diamètres et composés de plusieurs essences offrent généralement une meilleure protection que les peuplements monospécifiques et réguliers, soulignant ainsi l'influence de la diversité forestière. Cette thèse montre ainsi que les taillis présentent les capacités de protection les plus élevées, suivis par les futaies feuillues et les futaies mixtes ; les peuplements résineux venant en dernier.

Les évolutions spatiales et temporelles des conditions climatiques favorables aux incendies, étudiées sur la période 1959-2015, révèlent un contraste majeur entre les Alpes du Sud qui ont connu une forte augmentation (en intensité, fréquence, durée et saisonnalité) surtout à haute altitude, et les Alpes du Nord, où une légère hausse est observée à basse altitude, mais aucune tendance significative n'est observée à haute altitude. Ces résultats sont ensuite utilisés pour définir trois types de feux (d'hiver, d'été moyen et d'été très sec) pour lesquels la mortalité post-incendie est étudiée à l'échelle de l'arbre et du peuplement forestier. Ces analyses montrent que seuls les feux d'été sont susceptibles d'affecter significativement les peuplements, en particulier à basse altitude où les peuplements feuillus (notamment les taillis) dominent.

L'effet des incendies sur la capacité de protection des forêts est évalué en comparant les simulations de propagation de chutes de blocs sans feu aux simulations après chaque type de feu pour lesquelles les arbres avec une forte probabilité de mortalité post-feu ne sont pas pris en compte. Les valeurs de *ORPI* pour chaque placette forestière et chaque type de feu sont ainsi calculées et comparées au scénario de référence sans feu, permettant ainsi d'évaluer quantitativement la réduction de la capacité de protection. Les peuplements de basse altitude, soumis à des conditions climatiques plus chaudes et sèches, présentent des réductions de la capacité de protection après des feux d'été de l'ordre de 60 à 100 %. Il s'agit principalement de taillis et de futaies feuillues. À plus haute altitude, la réduction est de l'ordre de 30 à 65 %.

En conclusion, ce travail de thèse propose une méthode originale pour quantifier la capacité de protection d'une forêt contre les chutes de blocs avant et après un incendie et alimente les connaissances sur ces deux aléas naturels et les risques associés. L'analyse multi-aléas conduite en fin de thèse permet d'appréhender les effets cascades potentiels à l'échelle du peuplement forestier et de quatre territoires bioclimatiquement homogènes des Alpes françaises.

Mots-clés : Forêts de montagne · Aléas naturels · Alpes françaises · Chutes de blocs · Feux de forêt · Analyse multi-aléas · Effets cascades · Forêts de protection · Changements climatiques · Services écosystémiques · Simulations numériques

Abstract

Rockfalls are a major natural hazard in the French Alps due to their high probability of spatial and temporal occurrence. Forests constitute an efficient nature-based solution to mitigate this hazard while protecting human lives and assets. However, this ecosystem service may be disrupted by others natural hazards such as wildfires likely to be more frequent and intense in the current and future context of climate changes.

This PhD thesis proposes to **assess the effects of fires on the protection capability of forests against rockfalls in the French Alps**.

A methodology to evaluate the protection capability of a forest against rockfalls is first developed. It consists in modelling rockfalls propagations on 3886 forest plots taken in the French Alps to calculate three quantitative indicators that assess the reduction of the frequency ($BARI$), the intensity ($MIRI$) and the overall reduction ($ORPI$) of rockfalls due to the presence of a forest. These indicators are used to identify the predominant forest variables for assessing the protective effect : the length of forest along the slope, the basal area and the mean diameter. Forest stands with a heterogeneous distribution of diameters and made up of several tree species generally offer a better protection than mono-specific and regular stands, thus underlining the influence of forest diversity. This work shows that coppices have the highest protection capabilities, followed by hight stands dominated by deciduous species and mixed stands ; coniferous stands coming last.

Spatio-temporal trends in fire weather in the French Alps are investigated over the period 1959-2015 and reveal a major contrast between Southern Alps which experienced a strong increase (in intensity, frequency, duration and seasonality) especially at high elevation, and Northern Alps, where a slight increase at low elevation and no significant trends at high elevation are observed. These results are then used to define three types of fires (winter, summer, and dry summer) for which post-fire tree mortality is studied at the tree and forest stands levels. These analyses show that only summer fires are likely to significantly affect the forest ecosystems, particularly at low elevations where deciduous stands (especially coppice) dominate.

The effect of fires on the protection capabilities of forests is assessed by comparing rockfalls propagation simulations without fire to simulations after each type of fire in which the trees with a high post-fire mortality are not taken into account. $ORPI$ values for each forest plot and fire type are thus calculated and compared to the reference scenario without fire thus making it possible to quantitatively assess the reduction of the protection capabilities. Low elevation stands, subject to warmer and drier climatic conditions, show reductions of the protective effect in the range 60-100%. It mainly concerns coppices and deciduous stands. At high elevation, the reduction is in the range 30- 65%.

In conclusion, this PhD thesis proposes an original method to quantify the protection capabilities of a forest against rockfalls before and after a fire and improve the knowledge of these two natural hazards and their associated risks. The multi-hazard analysis conducted at the end of the thesis makes it possible to understand the potential cascading effects in the main forest types and four bio-climatically homogeneous territories of the French Alps.

Keywords : Mountain forests · Natural hazards · French Alps · Rockfalls · Forest fire · Multi-hazard analysis · Cascading effect · Protection forest · Climate changes · Ecosystem services · Numerical modelling

Table des matières

Première partie

Introduction

CHAPITRE 1

Contexte

1.1 Contexte général

Les zones de montagne sont particulièrement concernées par une concentration élevée d'aléas naturels notamment du fait de caractéristiques topographiques et climatiques favorables aux aléas (Hewitt, 2014). Dans les Alpes françaises, ils peuvent être de plusieurs natures : géophysique (avalanches, glissements de terrain, éboulements rocheux, tremblements de terre), hydrologique (crues torrentielles, coulées de boue, inondations, sécheresse), atmosphérique (tempêtes, orages violents) ou encore biophysique (feux de forêts) (Gill et al., 2014). Ces phénomènes naturels potentiellement dangereux constituent des risques lorsqu'ils menacent des personnes, des infrastructures ou encore des atouts économiques, environnementaux, sociaux ou culturels ; regroupés sous le terme "d'enjeux" (Naaim-Bouvet et al., 2015). Un risque naturel est ainsi défini par la combinaison d'un aléa et d'un ou plusieurs enjeux, chacun caractérisé par une vulnérabilité (perte physique, sociale, économique ou environnementale liée à l'aléa) (IPCC, 2012).

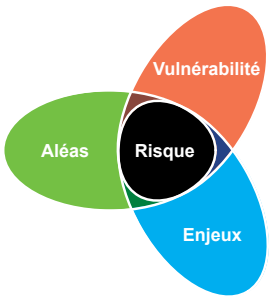

Figure 1.1 – Les trois composantes de la "rose des risques" (d'après IPCC (2012)).

En pratique, la gestion des risques naturels vise à réduire le danger en agissant sur une ou plusieurs composantes du risque (Fig. 1.1). Ainsi, il est parfois possible de réduire le nombre d'enjeux menacés en réglementant leur implantation ou leur transit dans les zones touchées par différents aléas. C'est notamment la vocation des plans de prévention des risques naturels (PPRN) en France. Ce document réglementaire détaille par exemple les zones inondables où toute construction sera prohibée. Les enjeux peuvent aussi être spécifiquement conçus pour résister à un aléa particulier. C'est notamment le cas des maisons construites selon des normes antisismiques dans les régions régulièrement touchées par les tremblements de terre. Enfin, la dernière stratégie consiste à agir directement sur l'aléa en réduisant sa fréquence et/ou son intensité au niveau des enjeux. C'est ainsi que de nombreux ouvrages de protection ont été mis en place en France depuis

le milieu du XIX^{e} siècle afin de limiter les effets des avalanches (Eckert et al., 2009), des crues torrentielles (Piton et al., 2016) ou encore de l'érosion (Giordano, 1994).

Le rôle des écosystèmes de montagne dans l'atténuation de certains aléas naturels est aussi très important (Rey, 2017; Brang et al., 2001). C'est notamment le cas des forêts en ce qui concerne les chutes de blocs rocheux (Fig. 1.2.a et 1.2.b) qui, malgré une intensité relativement modérée, constituent un aléa majeur dans les Alpes en raison de leur probabilité d'occurrence très élevée à la fois spatialement et temporellement. Il serait ainsi très coûteux et illusoire de vouloir mettre en place des ouvrages de protection de génie civil partout où ce phénomène est susceptible d'avoir lieu. Le maintien et la bonne gestion des forêts de montagne constituent ainsi une mesure de protection contre les chutes de blocs à large échelle, naturelle, efficace et économique (Notaro et al., 2012; Wehrli et al., 2006).

(a) Crédit : E. Mermin. Irstea (2007)

(b) Crédit : F. Berger. Irstea (2007)

(c) Crédit : S. Dupire. Irstea (2007)

Figure 1.2 – Exemples de blocs arrêtés en forêt communale de Sainte-Foy-Tarentaise, Savoie, France (a) et en forêt communale de Boutat, Isère, France (b). Panneau de signalisation sur une route en Corse, France (c).

Ce service écosystémique particulier pourrait cependant être lourdement altéré par d'autres aléas naturels tels que les tempêtes, les feux de forêts ou encore les sécheresses, tous susceptibles d'être de plus en plus fréquents et intenses dans le contexte actuel de changements climatiques, notamment en montagne (Pachauri et al., 2014; Gobiet et al., 2014). Le cas des feux de forêts est particulièrement préoccupant car, ces dernières années, des incendies intenses ont été observés dans tout le massif alpin notamment lors de la vague de chaleur et la canicule prolongée de l'été 2003 (Fig. 1.3) (Poumadère et al., 2005; Luterbacher et al., 2004).

(a) Champagny-en-Vanoise Savoie, France Crédit : D. Mouchené (2003)

(b) Montagne du Néron, Grenoble-Alpes-Métropole, Isère, France. Crédit : A. Herrault (2003)

Figure 1.3 – Incendies déclarés lors de l'été 2003 dans les Alpes françaises.

Dans les régions méridionales, l'augmentation des chutes de bloc suite à des feux de forêts est régulièrement observée, notamment par les gestionnaires des routes (Fig. 1.2.c), en raison de la fréquence plus importante des incendies. Dans les Alpes, cette altération de l'effet protecteur des forêts pourrait prendre une dimension plus grande du fait d'une forte densité d'enjeux situés à l'aval d'écosystèmes *a priori* moins adaptés au feu. Les questions et les craintes des acteurs locaux sont ainsi nombreuses.

Ce travail de thèse vise à contribuer aux réflexions mises en œuvre pour améliorer la gestion des risques naturels et leur prise en compte par les gestionnaires forestiers (Programme 181 "Prévention de risques" du Ministère en charge des risques naturels et projets de recherche ANR SAMCO et H2020 NAIAD). Il s'intéresse plus particulièrement à la capacité de protection contre les chutes de blocs des forêts des Alpes françaises (Fig. 1.4) et à la dégradation potentielle de cette protection naturelle en cas d'incendie. Plusieurs échelles d'analyses sont prises en compte afin d'alimenter les réflexions et la prise de décision aux niveaux local et régional.

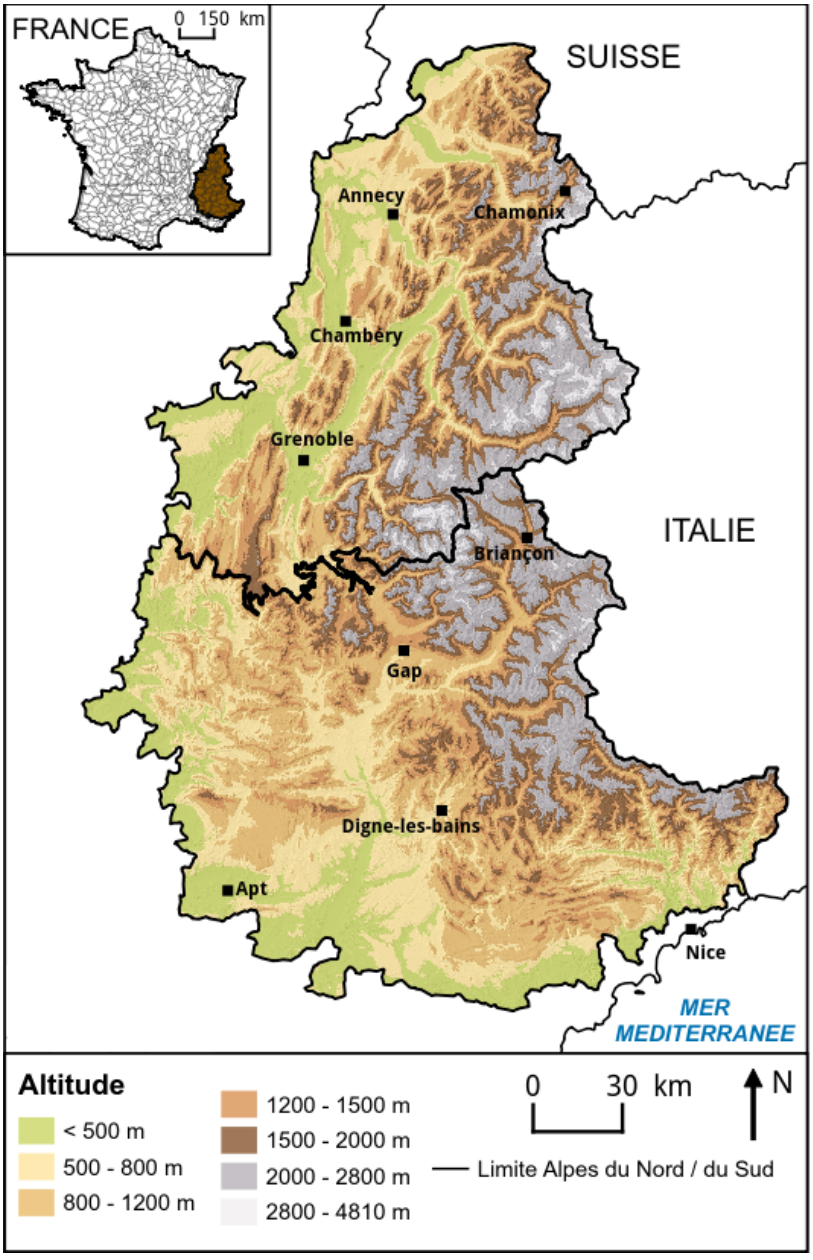

Figure 1.4 – Carte des Alpes françaises.

1.2 État de l'art

1.2.1 Forêts et aléa chutes de blocs

1.2.1.1 L'aléa chutes de blocs

Une chute de blocs est définie par la mise en mouvement soudaine d'une ou plusieurs masses rocheuses généralement suivie d'une phase de propagation rapide le long d'un versant (Selby, 1993). On distingue les chutes de blocs des éboulements en masse en fonction du volume mobilisé et du processus physique impliqué : propagation d'objets solides de seulement quelques mètres cubes pour les premières contre propagation d'un fluide de centaines jusqu'à millions de mètres cubes pour les seconds (Bourrier et al., 2013; Whalley, 1984). Plusieurs facteurs influencent le déclenchement de ce phénomène. La nature des roches et l'existence de fissures, failles ou discontinuités au sein des parois rocheuses sont ainsi les principaux facteurs géologiques (Vidrih et al., 2001; Coutard et al., 1989). Les conditions climatiques et notamment les périodes de gel/dégel ou de très fortes précipitations favorisent aussi les détachements de blocs (Matsuoka et al., 1999). Enfin, les activités humaines sont parfois à l'origine de chutes de blocs par exemple en cas de changements de pratiques et d'occupations du sol (Dorren, 2003). Selon les services du Ministère en charge des risques naturels, entre 25% et 55% des communes alpines sont concernés par l'aléa chute de blocs selon les départements (Géorisques, 2017). De plus, les observations de terrain des services de Restauration des Terrains de Montagnes (RTM-ONF) témoignent d'une activité importante comparée à d'autres aléas, avec des événements d'une période de retour pouvant aller d'un seul jour à quelques années selon les volumes et les zones considérés. Ce phénomène présente donc une forte probabilité spatiale et temporelle. Les chutes de blocs peuvent avoir de lourdes conséquences allant de dégâts matériels importants (Fig. 1.5) à des atteintes physiques voire mortelles aux personnes.

(a) Crédit : S. Gominet - IRMa (2007)

(b) Crédit : S. Gominet - IRMa (2002)

(c) Crédit : S. Gominet - IRMa (2015)

(d) Crédit : S. Gominet - IRMa (2015)

Figure 1.5 – Dégâts occasionnés par des chutes de blocs sur (a) une route départementale en Isère, (b) une habitation à Lumbin en Isère, (c) une voie ferrée et (d) un bâtiment industriel à Moûtiers en Savoie.

Une chute de blocs peut être décomposée en trois phases successives : (1) le détachement du bloc d'une zone de départ, (2) sa propagation le long d'un versant en interaction avec le milieu et (3) son arrêt en bas de versant ou dans une structure de protection (Ritchie, 1963). Les principaux travaux sur la première phase de l'aléa se sont attachés à proposer des méthodes pour identifier les zones de départ (Frayssines, 2005; Falaise, 2001) et estimer la probabilité de détachement (Hantz et al., 2003; Dussauge-Peisser et al., 2002). Si l'estimation des volumes et l'identification et la localisation des zones de départ sont désormais relativement fiables, quantifier la probabilité de départ des blocs demeure encore très complexe en raison des nombreux processus impliqués. La phase d'arrêt des blocs a surtout été étudiée en vue d'améliorer le dimensionnement des ouvrages de protection de génie civil tels que les filets (Nicot et al., 2001; Peila et al., 1998) ou les merlons (Lambert et al., 2013).

La communauté scientifique est surtout très active en termes de recherches sur la phase de propagation des blocs rocheux le long d'un versant (Toe et al., 2017a; Leine et al., 2014; Volkwein et al., 2011; Bourrier et al., 2009; Dorren et al., 2006a; Lied, 1977; Heim, 1932). Cette phase est décrite comme une succession de vols libres, d'interactions avec le sol et d'impacts sur des obstacles (arbres, ouvrages de protection, enjeux...). Tous ces travaux ont abouti au développement de plusieurs logiciels et modèles d'analyse trajectographique tels que Conefall 1.0 (Evans et al., 1993), RAMMS-ROCKFALL (Christen, 2012) ou encore Rockyfor3D (Dorren, 2015). Les plus élaborés d'entre eux permettent de prendre en compte la végétation en augmentant artificiellement la rugosité du terrain, voire même en modélisant explicitement les impacts des blocs sur les arbres (Toe et al., 2017b; Dorren, 2015).

1.2.1.2 Les forêts de protection contre les chutes de bloc

De nombreuses études ont démontré que les forêts constituent une structure de protection efficace et peu coûteuse contre les chutes de blocs (Notaro et al., 2012; Wehrli et al., 2006; Wehrli et al., 2005), en particulier lorsque le volume des blocs reste modéré (< 5 m^3) (Berger et al., 2002). Les forêts sont essentiellement efficaces dans les zones de propagation et d'arrêt (Fig. 1.6) où les impacts contre les arbres vont modifier la vitesse et la trajectoire des blocs (Dorren et al., 2006a). En multipliant les impacts contre des arbres, l'énergie cinétique totale d'un bloc est progressivement réduite (Toe et al., 2017b; Bertrand et al., 2013; Dorren et al., 2006b) et, si le nombre d'impacts est suffisant, le bloc finira par s'arrêter dans le versant. Les forêts contribuent donc à réduire à la fois l'énergie (intensité de l'aléa) et le nombre (fréquence de l'aléa) de blocs pouvant atteindre les enjeux situés à l'aval d'un versant.

De manière intuitive, les premières recherches sur l'effet protecteur des forêts (Wasser et al., 1996; Gsteiger, 1993) ont cherché à appréhender la probabilité d'impacts contre les arbres à partir de variables dendrométriques simples (densité de tiges et surface terrière). C'est sur ces bases que des valeurs cibles de variables forestières ont été proposées empiriquement afin d'optimiser l'effet protecteur des forêts comme par exemple dans le modèle Rockfor^{NET} (Berger et al., 2007). Ces démarches ont été largement utilisées pour la rédaction des guides de sylvicultures de montagne en France (Ancelin et al., 2006), Italie (Berretti et al., 2006) et Suisse (Dorren et al., 2015). Bien qu'elles présentent l'avantage d'être faciles à mettre en œuvre par les gestionnaires forestiers, ces approches sont principalement fondées sur des observations d'experts et un nombre réduit de résultats issus d'expérimentations. Elles demeurent, de fait, insuffisantes en vue de quantifier l'efficacité de la protection et comprendre en détail les processus fonctionnels impliqués dans l'interaction entre la forêt et les chutes de blocs.

Certains modèles plus récents, comme Rockyfor3D (Dorren, 2015), permettent une meilleure prise en compte des processus physiques impliqués y compris les impacts contre les arbres. De plus, ils ajoutent une dimension spatiale aux analyses qui se limitaient jusqu'alors à des profils en long. Il est ainsi possible d'accéder à une description relativement précise de la trajectoire des blocs sur un versant (boisé ou non) ainsi qu'à des données sur l'énergie et le nombre de blocs

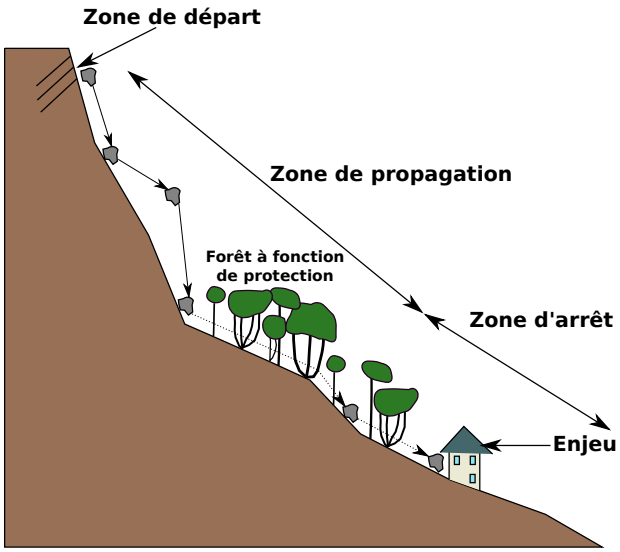

Figure 1.6 – Localisation schématique des forêts de protection contre les chutes de blocs sur un versant.

passant par n'importe quel point de la zone d'étude. Ces modèles trajectographiques ont surtout été utilisés pour des analyses d'aléa sur des sites pilotes bien définis (Dorren et al., 2006a; Stoffel et al., 2006). Plusieurs exemples d'utilisation à des fins forestières peuvent aussi être cités. Toe (2016) et Radtke et al. (2014) ont ainsi mis en avant la forte capacité de protection des taillis. Fuhr et al. (2015) ont démontré que le bois mort laissé en forêt avait une capacité de protection non négligeable à court terme. Enfin, Monnet et al. (2017) ont montré qu'à nombre de tiges constant, l'organisation spatiale des tiges avait une influence faible sur la fonction de protection des forêts comparée à d'autres paramètres comme le type de sol. Si ces études tendent à souligner des variables forestières prépondérantes (surface terrière, diamètre moyen, nombre de tiges), la diversité des types de forêt étudiés reste limitée et peu d'études proposent d'utiliser ces modèles afin de quantifier l'effet protecteur des forêts (Toe, 2016; Radtke et al., 2014).

Malgré la nette amélioration par rapport à l'approche empirique initiale, les outils comme Rockyfor3D utilisent des relations mathématiques très simplifiées pour décrire à la fois les rebonds des blocs sur le sol et les impacts contre les arbres (Toe et al., 2017c). Avec l'augmentation constante des capacités de calcul, une nouvelle génération de modèles de propagation devrait voir le jour (Toe et al., 2017a). Basés sur des modélisations par éléments discrets (DEM), ces modèles permettent une description très précise des rebonds au sol (Bourrier et al., 2009) et des impacts sur les arbres (Toe et al., 2017b). La prise en compte de ces derniers a notamment été fortement améliorée par de nombreux essais mécaniques sur des tiges de bois verts de plusieurs espèces (Barré, 2017; Toe, 2016; Olmedo et al., 2015) qui ont, entre autres, mis en évidence une plus forte disparité des capacités mécaniques au sein d'une même espèce qu'entre deux espèces différentes. Les freins à l'utilisation de tels modèles sont aujourd'hui le temps de calcul nécessaire ainsi que la disponibilité de données expérimentales permettant leur calibration. Cependant, ils représentent certainement une grande avancée dans la caractérisation de l'effet protecteur des forêts.

1.2.2 Feux de forêts dans les Alpes

1.2.2.1 L'aléa incendie (ou feu) de végétation

Les incendies, ou feux de végétation sont des perturbations affectant les écosystèmes terrestres depuis des millions d'années (Scott et al., 2006) y compris dans les Alpes (Power et al., 2008). Pour qu'un feux de végétation se déclare et se propage, quatre facteurs indispensables doivent être réunis (Bradstock, 2010; Archibald et al., 2009) (Fig. 1.7).

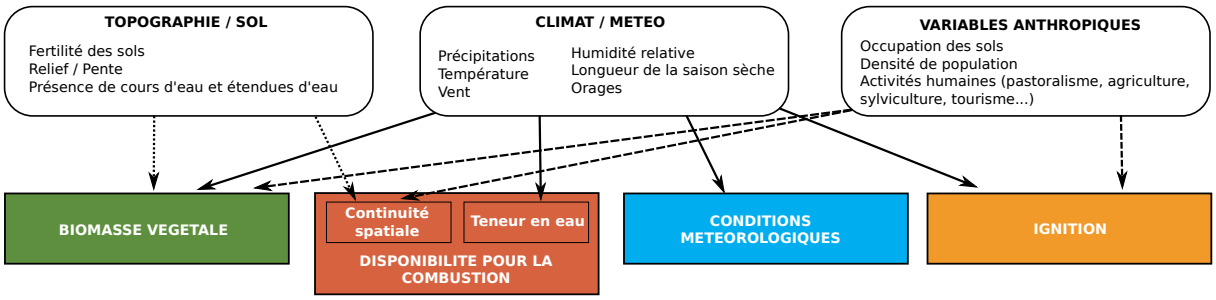

Figure 1.7 – Schéma conceptuel des quatre facteurs indispensables au départ et la propagation d'un feu de végétation (rectangles de couleur) ainsi que des principales variables climatiques, topographiques et anthropiques les influençant (rectangle en blanc). D'après Bradstock (2010); Archibald et al. (2009).

Le premier facteur est la biomasse végétale dont la présence et le type vont dépendre des caractéristiques climatiques (température, précipitation...), édaphiques (fertilité des sols) et des activités humaines. La biomasse contenue dans les strates basses (litière, herbacées et ligneux bas) participe tout particulièrement au départ et à la propagation des feux (Curt et al., 2013; Bessie et al., 1995).

Le deuxième facteur englobe l'état hydrique et la continuité spatiale du combustible qui vont déterminer la part du combustible disponible pour la combustion (Hantson et al., 2015). Les faibles taux de teneur en eau de la végétation, généralement observés pendant les périodes chaudes et sèches, favorisent ainsi l'éclosion et la propagation des feux (Loehman et al., 2014). La continuité spatiale de la végétation influence essentiellement la propagation du feu, c'est ainsi un élément clé dans la lutte contre les incendies. En effet, le feu ne pourra pas se propager plus loin s'il y a une rupture horizontale du combustible (changement d'occupation des sols, infrastructures routières, cours d'eau...) ; c'est le principe des coupes-feux (Rigolot, 2002). De même, si une strate verticale est absente dans un peuplement forestier, le feu pourra difficilement monter en cime.

Le troisième facteur est la présence de conditions météorologiques favorables telles que les températures élevées, l'absence de précipitations, le vent ou encore une humidité de l'air très faible qui vont faciliter l'ignition et la propagation des feux (Ruffault et al., 2017a). C'est à partir de ces variables que Météo-France calcule quotidiennement l'indice Forêt-Météo (IFM), directement inspiré du Fire Weather Index (FWI) initialement mis en place au Canada (Van Wagner, 1987). L'IFM est ainsi utilisé à des fins d'aide à la décision pour la lutte contre les incendies afin de réglementer l'accès aux zones les plus à risque et de prépositionner les moyens de lutte.

Enfin, le dernier facteur indispensable est l'ignition à partir d'une source de chaleur. En France, cette source de chaleur est principalement d'origine anthropique (Curt et al., 2016) et le plus souvent involontaire. En montagne, les impacts de foudre peuvent cependant représenter jusqu'à 15% des départs de feu (Müller et al., 2015; Reineking et al., 2010), ils sont d'ailleurs à l'origine des deux feux de l'été 2003 illustrés précédemment (Fig. 1.3).

Parce qu'il influence chacun de ces facteurs (Fig. 1.7), le climat est un moteur prépondérant de

l'activité des incendies dans le monde (Hantson et al., 2015; Moritz et al., 2012). L'augmentation globale de la température et l'extension des sécheresses devraient contribuer à un renforcement de la fréquence mais aussi de l'intensité des feux (Schumacher et al., 2006), tandis que des sécheresses exceptionnelles comme lors de l'été 2003 favorisent des incendies importants et intenses (Ruffault et al., 2016).

1.2.2.2 Description physique des feux

Le front actif d'un feu de forêt (Fig. 1.8) comporte trois caractéristiques : (1) il se propage, (2) il consomme du combustible et (3) il produit de l'énergie sous forme de chaleur (Van Wagner, 1970).

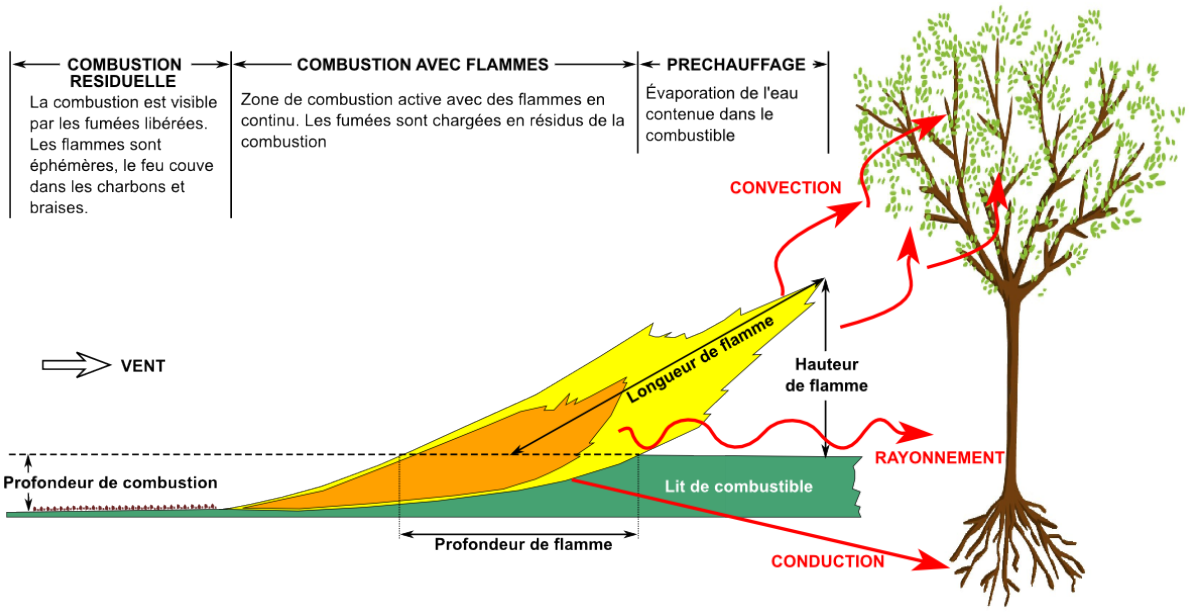

Figure 1.8 – Coupe transversale du front de flammes d'un feu sur terrain plat avec des conditions ventées. Les trois étapes de la pyrolyse sont présentées (préchauffage du combustible, combustion active avec flamme et combustion résiduelle des charbons et braises). Les processus de transfert de chaleur depuis le front de flammes vers les différents tissus d'un arbre sont schématisés en rouge. D'après Michaletz et al. (2007); Alexander (1982).

Dans le language courant, l'intensité d'un feu désigne la chaleur produite par le front de flamme (Byram, 1959):

$$I = PCI \times MC \times V \tag{1.1}$$

où I est l'intensité du front de flammes ($kW \cdot m^{-1}$), PCI est le pouvoir calorifique du combustible ($kW \cdot kg^{-1}$), MC est la masse de combustible consumée par unité de surface (dans la zone de combustion active) ($kg \cdot m^{-2}$) et V est la vitesse du front de flammes ($m \cdot s^{-1}$). Le PCI est très variable en fonction de l'état hydrique et de la nature de la végétation et MC est difficile à estimer en conditions réelles. Ainsi ces grandeurs ont surtout été estimées empiriquement à partir de feux expérimentaux et d'essais en laboratoire (Peterson et al., 1986; Alexander, 1982). La vitesse du front de flamme V est en revanche mesurable sur le terrain tout comme la longueur et la profondeur du front de flammes (Fig. 1.8). Ainsi ces grandeurs sont couramment utilisées pour caractériser un feu et estimer la durée d'exposition de la végétation aux flammes.

C'est l'exposition à la chaleur produite par la combustion qui est responsable des dommages causés aux racines, au tronc et/ou au feuillage des arbres (Dickinson et al., 2001). Il est important de distinguer la température qui mesure l'énergie moléculaire, de la chaleur qui est l'énergie

associée au déplacement des molécules. Ainsi, la chaleur peut être transférée tandis que la température restera constante. Le transfert de chaleur se produit selon trois processus :

1. La conduction est la transmission de proche en proche de l'énergie, elle a surtout lieu au niveau des racines et de la base du tronc ;

2. Le rayonnement thermique est le principal mode de propagation de l'énergie dans les feux de forêt, il s'agit d'ondes infrarouges qui affectent particulièrement le tronc ;

3. La convection, caractérisée par des mouvements d'air chaud et de fumées, affecte surtout le feuillage des arbres (Michaletz et al., 2007). Ce dernier processus est d'autant plus important que la pente et le vent sont forts.

1.2.2.3 Les différents types de feux

Un feu peut prendre différentes formes en fonction du combustible (distribution spatiale, charge et état hydrique) et des conditions météorologiques et topographiques. Nous détaillerons ici les trois types de feu (Fig. 1.9) susceptibles de se produire dans les Alpes, parfois même simultanément lors d'un même évènement (Valese et al., 2011).

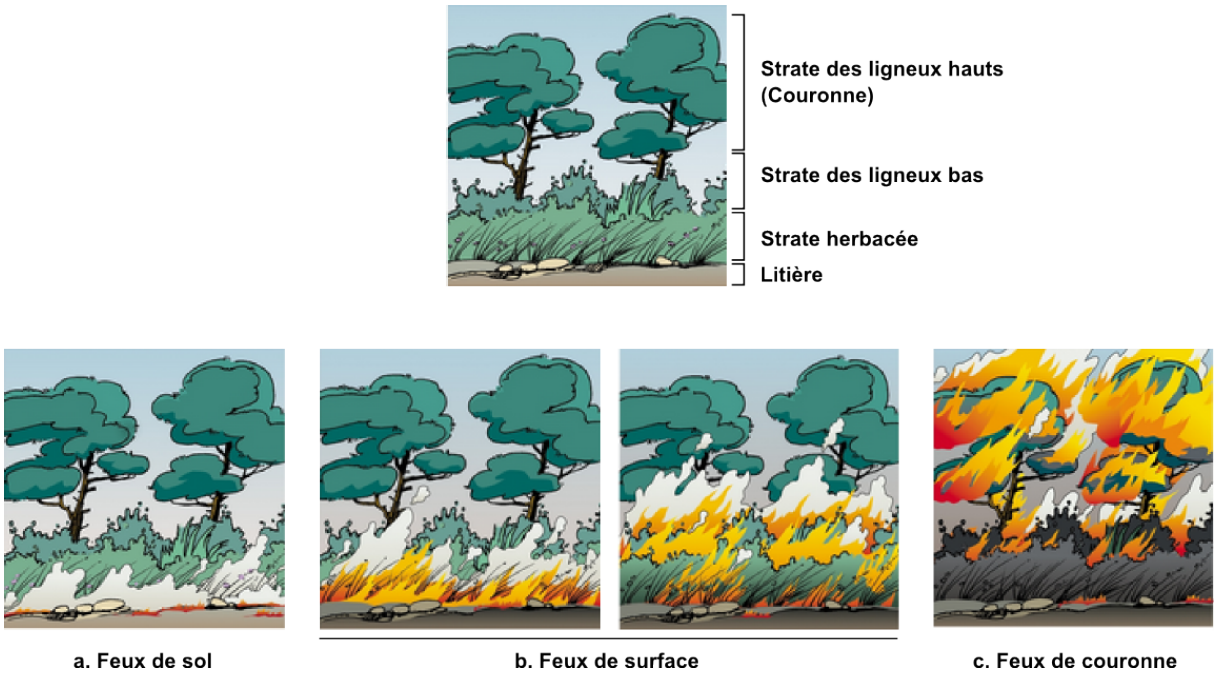

Figure 1.9 – Les différents types de feux de végétation. D'après Géorisques (2017).

Les feux de sol (a) se développent dans les couches organiques du sol (litière et l'humus). Ils se propagent habituellement sans flamme à travers les racines avec une vitesse de propagation faible. Ce type de feu peut être très destructeur en cas de longue durée car il s'attaque au système racinaire (Hartford et al., 1992). De plus, ces incendies peuvent entraîner une diminution du sol en raison de la perte des caractéristiques structurales due à la combustion de la matière organique. Le fait qu'il couve généralement en profondeur présente des difficultés pour le détecter et le contenir.

Les feux de surface (b) sont caractérisés par une vitesse de propagation moyenne à rapide (en cas de vent et/ou de pente) et une hauteur de flamme limitée qui affecte principalement les strates basses de la végétation : la partie supérieure de la litière, la strate herbacée et les ligneux bas. Généralement, les arbres ne sont affectés qu'au niveau de leur tronc tandis que la canopée

reste intacte. Cependant, si la chaleur développée est importante et/ou la zone régulièrement affectée par plusieurs incendies sur une période restreinte, la combustion basale du tronc peut endommager le cambium et s'avérer fatale pour les arbres (Bova et al., 2005).

Les feux de couronne (c) affectent toutes les strates de la végétation depuis la litière jusqu'à la couronne. Il arrive plus rarement que le feu se propage de couronne en couronne indépendamment des strates inférieures. Ce type de feux libère une grande énergie et leur vitesse de propagation est très rapide (Keeley, 2009). Comme pour les feux de surface, ils sont d'autant plus intenses que le vent est fort et le combustible sec. Ils affectent plus souvent les forêts de conifères en raison de la forte teneur en résine et composés volatiles qui favorisent le passage en cime du feu (Coudour, 2015). Comme les feux de couronne sont difficiles à contenir, ils produisent des dommages importants causant la mort de la plupart des plantes.

1.2.2.4 Les régimes d'incendie de forêts dans les Alpes françaises

Les incendies sont présents depuis des milliers d'années dans les Alpes. L'analyse des cicatrices de feux passés sur les troncs ou des charbons de bois dans les sols montre, par exemple, que le feu est passé environ tous les 100 ans dans certaines forêts de mélèzes ou toutes les quelques années dans des pelouses pâturées et brûlées par l'homme (Carcaillet, 1998). Les feux d'origine humaine destinés à la culture sur brûlis ou à l'écobuage - ou plus rarement les feux déclenchés par la foudre - ont ainsi profondément modifié la végétation alpine en diminuant la présence d'espèces sensibles au feu (sapin, frêne, tilleul) et en favorisant des espèces résistantes (Wick et al., 2006; Tinner et al., 2005; Tinner et al., 1999).

Dans la classification proposée par Meyn et al. (2007), les écosystèmes alpins se situent aujourd'hui, pour la plupart, dans la catégorie des «écosystèmes riches en biomasse et rarement secs» avec des conditions favorables à la croissance de la végétation. Par conséquent, parmi les quatre facteurs exposés précédemment (Fig. 1.7), ceux qui limitent le départ des feux sont principalement la part de combustible disponible pour la combustion (teneur en eau élevée de la végétation) et les sources d'ignition.
Ces deux facteurs limitants influencent les régimes d'incendies des Alpes qui se caractérisent par deux saisons de feux. La première saison a lieu en hiver, surtout aux plus faibles altitudes. Elle se caractérise par de petits feux de surface (généralement < 1 ha), de faible intensité, et principalement dus aux activités humaines et notamment aux pratiques d'écobuages. La seconde saison se tient en été avec des feux de surfaces plus grands (1-10 ha) et plus intenses. Plus rarement, de grands feux pouvant passer en couronne se déclarent. Ils sont surtout observés pendant des épisodes de sécheresse exceptionnelle comme lors de l'été 2003 (Poumadère et al., 2005; Luterbacher et al., 2004). La part de feux estivaux d'origine naturelle (impacts de foudre) se situe autour de 15% (Müller et al., 2013) avec une distribution plus élevée en altitude.

Au cours des dernières décennies, la fréquence moyenne annuelle d'incendies de forêt est de 130 dans les Alpes françaises du sud pour une surface brûlée moyenne annuelle d'environ 900 ha (dont 70% pendant l'été) (Prométhée, 2017). Dans les Alpes française du Nord, plus froides et plus humides, ces chiffres sont de 35 feux en moyenne pour 80 ha (dont 55% en été) (BDIFF, 2017).

Dans les prochaines années, ces chiffres pourraient augmenter significativement en raison de l'accumulation de combustible (abandon des terres et du pastoralisme) et des changements climatiques (augmentation des températures et de la fréquence d'événements extrêmes) qui devraient être plus marqués en montagne (Wastl et al., 2012; Beniston, 2005). Les feux de forêts pourraient ainsi davantage perturber la structure et le fonctionnement des écosystèmes et, par conséquent, les nombreux services qu'ils fournissent aux sociétés humaines.

1.2.3 Analyse multi-aléas

Dans les zones de montagne, la diversité des aléas naturels présents implique que différents aléas naturels peuvent sévir au même endroit et/ou au même moment (Fig. 1.10).

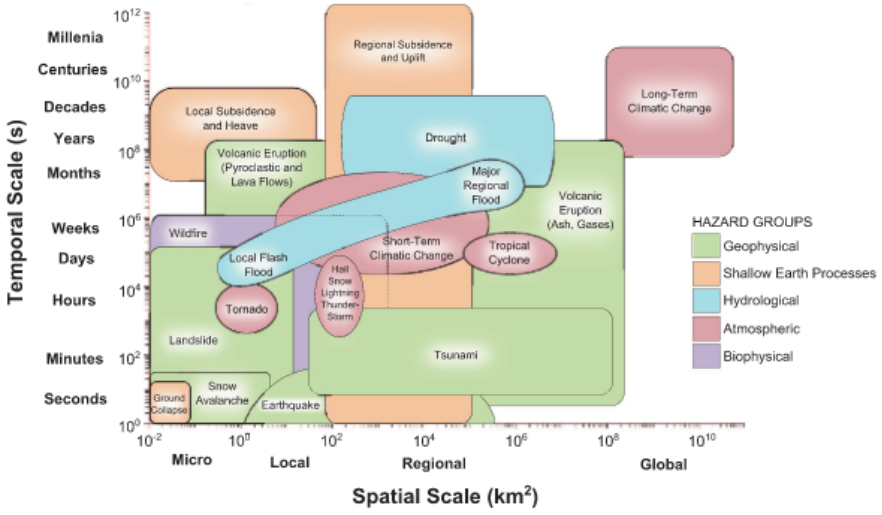

Group	Hazard	References
Geophysical	Earthquake	*Dixon* [1991]; *Ilk et al.* [2005]; *Minster* [2013]
	Tsunami	*Chelton* [2001]; *Ilk et al.* [2005]
	Volcanic Eruption	*Dixon* [1991]; *Ilk et al.* [2005]
	Landslide	*Waugh* [2000]; *Malamud et al.* [2004]; *Winter et al.* [2005]
	Snow Avalanche	*Waugh* [2000]; *Winter et al.* [2005]; *Lemke et al.* [2007]
Hydrological	Flood	*Hirschboeck* [1988]
	Drought	*Edwards* [1999]
Shallow Earth Processes	Regional Subsidence and Uplift	---
	Local Subsidence and Heave	---
	Ground Collapse	*Cooper* [1998]
Atmospheric	Tropical Cyclone	*Edwards* [1999]; *Grenci and Nese* [2006]; *Laing and Evans* [2011]; *Hirschboeck* [1988]
	Tornado	*Grenci and Nese* [2006]; *Laing and Evans* [2011]
	Hail, Snow, Lightning, Thunder Storm	*Edwards* [1999]; *Grenci and Nese* [2006]; *Laing and Evans* [2011]; *Hirschboeck* [1988]
	Long-Term Climatic Change	*Edwards* [1999]; *Chelton* [2001]; *Laing and Evans* [2011]
	Short-Term Climatic Change	*Chelton* [2001]; *Laing and Evans* [2011]; *Hirschboeck* [1988]
Biophysical	Wildfire	*Malamud et al.* [1998]; *Hincks et al.* [2013]

Figure 1.10 – Échelles spatiales et temporelles pour 16 aléas naturels en fonction de leur origine. D'après Gill et al. (2014).

La démarche classique d'évaluation d'un aléa ou d'un risque naturel consiste à considérer le phénomène comme isolé ou indépendant des autres aléas potentiels (Kappes et al., 2012). Dans un travail récent, Newman et al. (2017) ont étudié une centaine d'articles scientifiques dans le domaine des risques naturels et ont montré que la plupart des efforts ont été déployés pour identifier les zones de risque et évaluer les conséquences économiques résultant des pertes directes d'un aléa. Cependant, très peu d'articles ont envisagé des changements de ces risques liés à d'autres aléas ou à des processus globaux comme les changements climatiques. Ainsi, l'essentiel des analyses multi-aléas s'attachent à étudier chaque phénomène individuellement et identifier les zones où plusieurs aléas peuvent coexister spatialement et/ou temporellement (Montz et al., 2017; Vacchiano et al., 2016). Cependant, cette approche peut conduire à des plans d'action erronés qui sous-estiment le risque global et l'importance d'autres aléas pourtant considérés comme mineurs lorsqu'ils sont pris individuellement (Budimir et al., 2014; Mignan et al., 2014). Les dommages globaux résultant d'interactions entre plusieurs aléas peuvent ainsi être plus importants que la simple addition des dommages de chaque aléa pris individuellement (Gill et al., 2016). On nomme ce phénomène "effet cascade" ou "effet domino".

Un aléa comme les incendies de forêt est particulièrement susceptible de produire des effets cascades car en plus d'endommager directement les enjeux humains, un feu peut aussi réduire l'effet régulateur des écosystèmes vis-à-vis d'autres aléas naturels. Ainsi, l'accentuation des processus d'érosion consécutivement à des incendies de forêts a été démontrée dans les régions méditerranéennes (Fonseca et al., 2017; Inbar et al., 1998a). Il en va de même pour les aléas hydro-géomorphologiques (crues torrentielles et coulées de boues) post-incendies dans les montagnes portugaises (Nunes et al., 2017).
Enfin, la perte des capacités de protection contre les chutes de blocs de plusieurs hêtraies alpines situées en Italie et en Suisse suite à des feux de forêts a été soulignée par Maringer et al. (2016a).

CHAPITRE 2

Problématique

2.1 Besoins des praticiens et manque d'information scientifique

Les guides de sylvicultures de montagne fournissent des clés afin de juger qualitativement la capacité d'une forêt à diminuer l'aléa chute de bloc. Cependant, en France, ils ne concernent qu'un nombre de peuplements restreint : essentiellement les futaies des étages montagnards et subalpins. Les forestiers sont ainsi en demande d'informations et de méthodes plus précises pour passer d'une analyse qualitative à une analyse quantitative s'appliquant à n'importe quel type de forêt. Une meilleure quantification du rôle de protection pourrait aussi permettre la mise en place de mesures compensatoires auprès des propriétaires forestiers pour limiter le déficit économique lié à la réalisation d'interventions sylvicoles nécessaires au maintien de la fonction de protection.

Du côté des gestionnaires du risque, le rôle de la forêt est rarement pris en compte lors d'un dimensionnement d'ouvrages de protection (filets, merlon) car les informations qualitatives sont insuffisantes lorsqu'une protection maximale est recherchée. Des indicateurs quantitatifs précis permettant de juger de la diminution de la fréquence et de l'énergie des blocs liée à la présence de la forêt pourraient permettre de dimensionner des structures qui viendraient en complément de la forêt et non indifféremment de celle-ci ce qui réduirait considérablement les coûts d'installation et de maintenance.

Le lien entre l'accentuation de certains aléas naturels suite au passage d'un incendie est constaté en région méditerranéenne, notamment en ce qui concerne les chutes de blocs (Fig. 1.2c). Cependant, bien que quelques cas existent dans les Alpes, cet effet cascade reste très méconnu du fait de la faible fréquence de feux dévastateurs. À ce jour, une seule étude scientifique (Maringer et al., 2016a) s'est penchée sur la question mais elle se limite aux peuplements de hêtre, particulièrement vulnérables aux incendies. L'absence d'information sur les autres peuplements présents dans les Alpes apparaît ainsi comme une lacune auprès des forestiers et des acteurs locaux.

Cela est d'autant plus le cas depuis les feux impressionnants de l'été 2003 qui ont suscité beaucoup de questions et d'inquiétudes de la part des acteurs locaux et des services de l'État. La question de réglementer l'accès aux massifs forestiers en cas de conditions météorologiques défavorables comme cela se fait en région méditerranéenne s'est notamment posée plusieurs fois depuis 2003, avec, à chaque fois, très peu d'informations objectives pour appuyer la décision.

L'augmentation prévue des périodes favorables aux incendies liées aux changements climatiques accentue ces craintes et la demande d'informations spécifiques aux territoires alpins est ainsi forte. Ce besoin est aussi formulé par les services de lutte contre les incendies, qui, en l'absence d'enjeux directement menacés par un incendie, ont ordre de ne pas mettre tous les moyens de lutte en œuvre afin de limiter les risques encourus par les pompiers lors de leur progression sur des terrains très accidentés. Ainsi, si le rôle de protection d'une forêt n'est pas identifié, tous

les moyens de lutte pour limiter les dommages au peuplement peuvent ne pas être mis en œuvre. Afin de limiter ce cas de figure, une requête a été émise par ces services pour identifier les forêts de protection facilement, notamment celles étant particulièrement vulnérable au feu.
Enfin, au plan national, cibler les nouvelles zones vulnérables aux incendies est aussi une priorité afin d'adapter les moyens de lutte et de prévention des incendies.

2.2 Problématique scientifique

L'état de l'art et les demandes des praticiens soulignent des limitations majeures de (1) l'état actuel des connaissances sur l'aléa incendie de forêt dans les Alpes françaises et (2) des méthodes d'évaluation du rôle de protection des forêts de montagne contre l'aléa chutes de blocs. Partant de ce constat, ce travail de thèse répond pas à pas aux questions scientifiques suivantes :

1. Comment évaluer quantitativement l'effet protecteur d'une forêt contre les chutes de blocs ?

2. Quels sont les peuplements forestiers offrant la meilleure protection contre les chutes de blocs ?

3. Quel est le niveau d'exposition des Alpes françaises aux conditions climatiques favorables aux feux de forêt ?

4. Quels dégâts sur les principaux types de peuplements forestiers alpins peut-on prévoir suite au passage d'un feu de forêt ?

Les résultats successifs de ces quatre points contribuent à répondre à la problématique scientifique centrale de ce travail de thèse qui consiste à **évaluer la dégradation de la capacité de protection contre les chutes de blocs des forêts des Alpes françaises suite au passage d'un incendie de forêt**.

CHAPITRE 3

Objectifs et structure de la thèse

3.1 Objectifs de la thèse

Ce travail de thèse a pour objectif général l'**évaluation de la dégradation de la capacité de protection contre les chutes de blocs des forêts des Alpes françaises suite au passage d'un incendie**.

Cet objectif nécessite, au préalable, de **définir des indicateurs de référence pour quantifier l'effet protecteur des forêts contre les chutes de blocs**. Ces indicateurs sont dans un premier temps construits à partir de résultats de simulations de propagations de blocs sur plusieurs milliers de placettes forestières des Alpes françaises. Ils sont ensuite utilisés afin d'identifier les paramètres forestiers prépondérants pour assurer une bonne protection, puis pour comparer l'effet protecteur des principaux types de peuplements des Alpes françaises. En parallèle de cette analyse fonctionnelle, une analyse spatiale avec pour finalité la **cartographie des forêts de protection et l'identification des enjeux exposés à l'aléa chute de bloc** est conduite sur l'ensemble du territoire alpin français.

Pour ce qui concerne l'aléa incendie, le premier objectif est d'**identifier les évolutions spatiales et temporelles des conditions climatiques favorables aux incendies dans les Alpes françaises** afin d'identifier précisément les zones où cet aléa progresse ainsi que la nature de cette progression (en intensité, fréquence et/ou saisonnalité).
Le second objectif consiste à **évaluer la probabilité de mortalité des arbres après plusieurs scénarios de feux de forêts** en fonction des principaux types de peuplements alpins et des conditions climatiques observées à la phase précédente.

Enfin, en calculant les indicateurs définis précédemment suite au passage d'un incendie, le dernier objectif de ce travail de thèse est d'**identifier les peuplements forestiers les plus susceptibles de connaître des effets cascades**. Ce faisant, un sous-objectif est alors d'identifier des seuils critiques dans les caractéristiques forestières (surface terrière, distribution des diamètres...) au-delà desquels des effets cascades importants sont possibles sur les enjeux situés à l'aval.

3.2 Structure de la thèse

Ce manuscrit prend la forme d'une thèse sur article. De ce fait, suite à cette introduction générale, le manuscrit de thèse a été organisé en trois parties (Fig.3.1) chacune précédée d'un chapitre introductif et suivie d'une conclusion partielle.

- La première partie s'intéresse à l'évaluation de la capacité de protection contre les chutes de blocs des forêts des Alpes françaises. Elle se décompose en deux chapitres, chacun correspondant à un article publié (Dupire et al., 2016a; Dupire et al., 2016b). Le premier vise à définir des indicateurs quantitatifs afin d'évaluer l'effet protecteur des forêts. Le second chapitre porte sur les effets de la structure et de la composition des peuplements forestiers sur la capacité de protection contre les chutes de blocs.

- La seconde partie analyse l'aléa incendie dans les Alpes françaises. Elle est aussi divisée en deux chapitres correspondant à un article publié (Dupire et al., 2017) et un article en préparation (Dupire et al., In Prep. (a)). Le premier étudie les évolutions spatiales et temporelles des conditions climatiques favorables aux incendies sur l'ensemble du territoire Alpin français. Le second chapitre s'intéresse plus particulièrement aux dégâts sur les écosystèmes forestiers après plusieurs scénarios de feux en évaluant la mortalité à l'échelle de l'arbre puis à celle des principaux types de peuplements forestiers des Alpes françaises.

- La troisième partie concerne le croisement des deux aléas et l'évaluation des effets cascades potentiels résultant du passage d'un feu dans une forêt de protection contre les chutes de blocs. Un seul chapitre la compose correspondant à un article en préparation (Dupire et al., In Prep. (b)). L'analyse est réalisée à deux échelles : celle du peuplement forestier et celle de quatre sous-régions climatiquement homogènes des Alpes françaises.

Ce manuscrit se termine par une partie synthétisant l'ensemble des résultants et énumérant un certain nombre de perspectives associées à chacun des champs disciplinaires abordés dans ce travail de thèse.

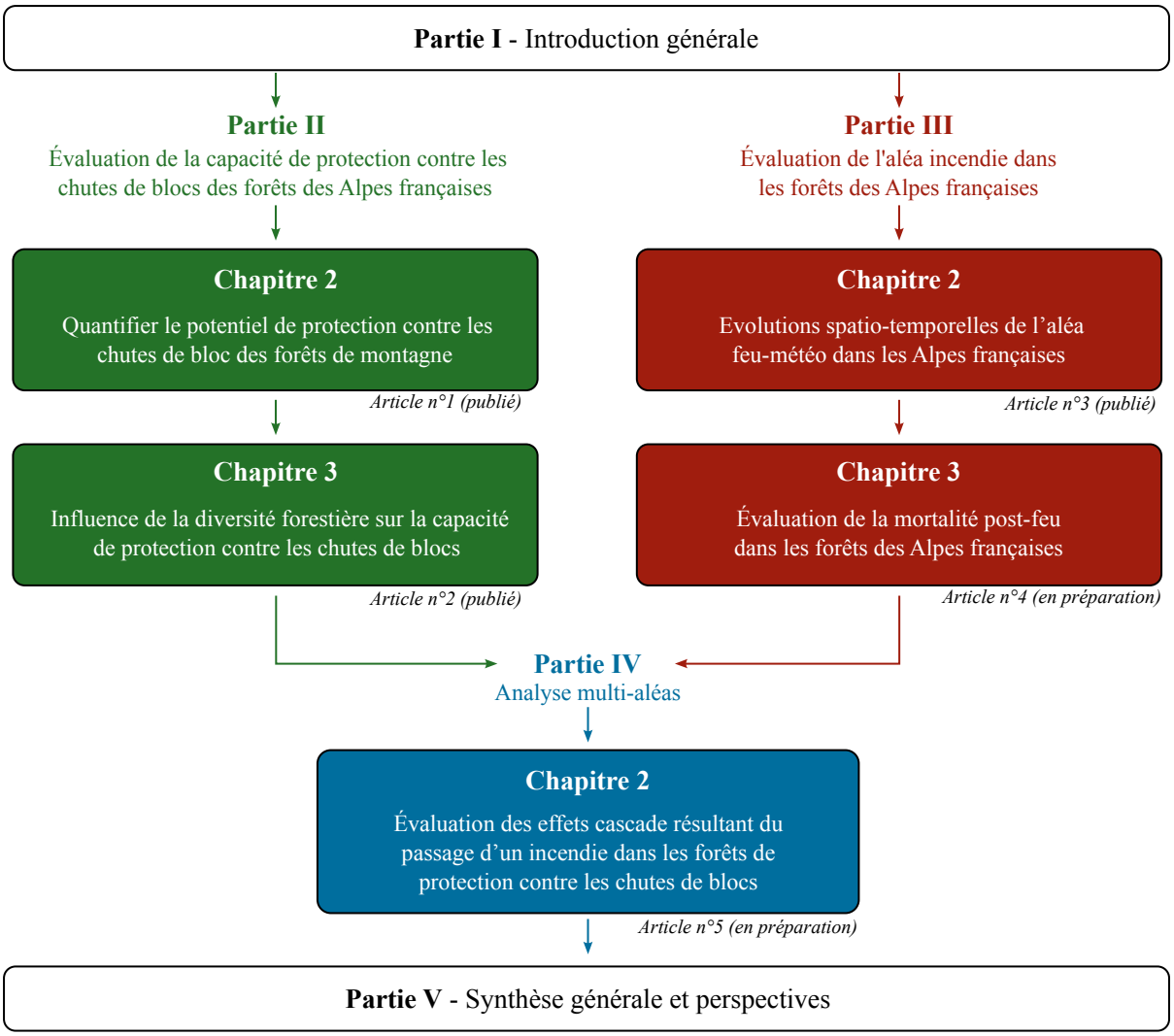

Figure 3.1 – Structure du manuscrit.

CHAPITRE 4

Démarche méthodologique

La figure 4.1 présente les étapes de la démarche méthodologique générale suivie dans ce travail de thèse.

La mise en place d'expérimentations grandeur nature est difficile voire impossible lorsqu'on s'intéresse à des phénomènes aussi destructeurs et dangereux que les deux aléas naturels étudiés dans ce travail. Ainsi, la démarche suivie repose en grande partie sur des travaux de modélisation numérique et statistique à partir de quatre sources de données principales.

Le modèle Rockyfor3D (Dorren, 2015) a été choisi pour évaluer la capacité de protection contre les chutes de blocs des forêts alpines. Une analyse de sensibilité a tout d'abord été conduite afin de choisir des paramètres de sol conservateurs tout en restant réalistes. Le modèle a ensuite été modifié et adapté aux besoins de cette étude, notamment la nécessité d'être intégré dans une chaîne de modélisation automatique capable de traiter rapidement les 4438 placettes forestières alpines de l'inventaire forestier national utilisées.

Le modèle FlamMap (Finney, 2006) a été choisi pour évaluer le comportement de feux se déclarant sur ces mêmes placettes sous différentes conditions climatiques. Les données de hauteur de flamme, vitesse de propagation et intensité du front de flammes ont ensuite été utilisées pour estimer la mortalité des arbres selon différentes méthodes empruntées dans la littérature (Bauer et al., 2010; Bova et al., 2005; Peterson et al., 1986; Spalt et al., 1962).

Afin d'intégrer au mieux la topographie particulièrement accidentée du territoire alpin, toutes les analyses spatiales réalisées dans ce travail ont été conduites à une résolution de 25 m qui est la résolution native du modèle numérique de terrain (BDAlti®) le plus précis disponible sur la zone d'étude.

Outre des compétences en programmation, en géomatique et en statistiques, ce travail de thèse fait aussi appel à diverses disciplines scientifiques. Des connaissances en biologie et en écologie sont tout d'abord requises tant pour appréhender le fonctionnement des écosystèmes forestiers que pour évaluer leurs réponses vis-à-vis d'une perturbation comme les feux de forêts. De plus, des connaissances en physique sont requises pour comprendre les processus impliqués dans les phénomènes de chutes de blocs (mécanique) et les incendies (thermodynamique). Dans une moindre mesure, ce travail fait aussi appel à des connaissances en climatologie notamment pour apprécier l'effet des conditions climatiques sur l'aléa incendie.

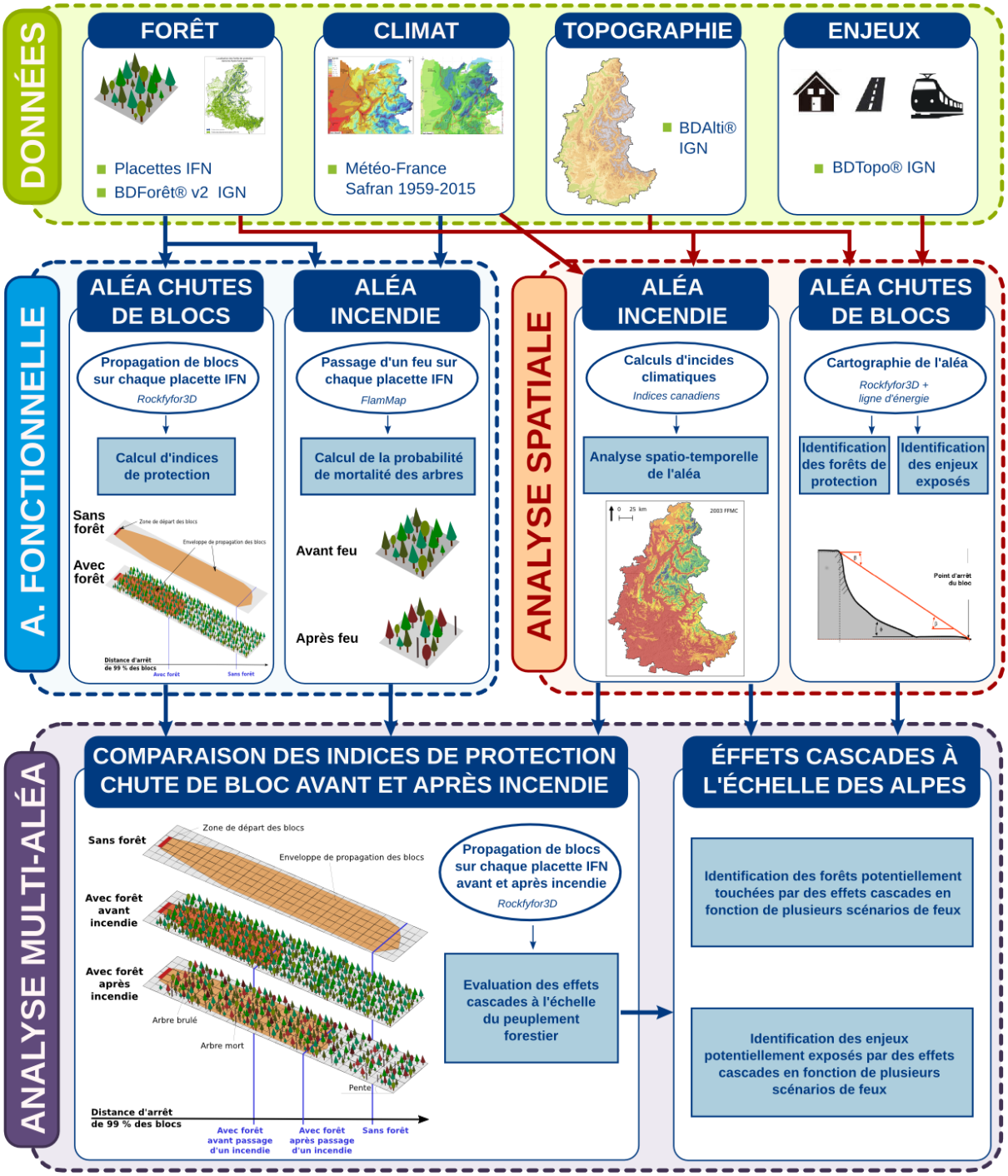

Figure 4.1 – Données utilisées et démarche méthodologique générale du travail de thèse.

Deuxième partie

Évaluation de la capacité de protection contre les chutes de blocs des forêts des Alpes françaises

CHAPITRE 1

Introduction

Contexte et objectifs

La présence d'arbres sur un versant contribue à réduire la fréquence et l'intensité des chutes de blocs (Dorren et al., 2006b). Le nombre de blocs arrêtés en forêt (réduction de la fréquence), nommé "effet barrière" dans la suite de ce travail, a été plusieurs fois utilisé pour caractériser l'effet protecteur d'une forêt (Radtke et al., 2014; Stoffel et al., 2006). En revanche, la réduction de l'énergie des blocs lors de chaque impact contre un arbre, nommée "effet tampon" dans la suite de cette étude, a très peu été exploitée. En pratique, l'évaluation quantitative de la capacité de protection consiste à comparer une grandeur obtenue pour un scénario sans forêt avec la même grandeur obtenue pour un scénario avec forêt (Radtke et al., 2014). Jusqu'à présent, il s'agit principalement du nombre de blocs parvenant jusqu'à une certaine distance. Une approche numérique est ainsi indispensable pour modéliser la propagation de blocs en l'absence et en présence de forêt. Rockyfor3D (Dorren, 2015) est aujourd'hui le seul modèle de propagation des blocs permettant de prendre en compte explicitement la forêt. Il nécessite cependant quelques modifications pour permettre d'analyser finement l'effet tampon comme notamment le suivi complet de la trajectoire (vitesses, positions) d'un bloc de son départ à son arrêt.

Jusqu'à présent, l'évaluation de la capacité de protection des forêts contre les chutes de blocs a concerné un nombre très restreint de forêt différentes. Les futaies de sapin/épicéa/hêtre de l'étage montagnard ont ainsi fait l'objet de plusieurs études (Fuhr et al., 2015; Stoffel et al., 2006; Dorren et al., 2006a) tout comme les taillis (Toe, 2016; Radtke et al., 2014). Très peu de données existent dans la littérature concernant les autres types de peuplements présents dans les Alpes. De plus, les méthodes utilisées et les sites d'études diffèrent généralement trop pour comparer les capacités de protection d'une forêt à l'autre. Il est donc nécessaire de mettre en place une méthodologie permettant d'évaluer uniquement la capacité de protection des forêts en maîtrisant les autres facteurs influençant la propagation des blocs comme la rugosité et le type de sol ou encore la topographie.

L'objectif principal de cette première partie est de définir des indicateurs de référence pour quantifier toutes les composantes de l'effet protecteur des forêts contre les chutes de blocs. Dans un deuxième temps, il s'agit de calculer ces indicateurs pour un nombre conséquent de forêts différentes afin de faire ressortir les caractéristiques forestières prépondérantes et comparer la capacité de protection des principaux types de peuplements forestiers des Alpes françaises.

Démarche méthodologique

La première étude (Chapitre II.2) vise à définir la méthodologie générale et les indicateurs quantitatifs permettant d'évaluer la capacité de protection d'une forêt. Une étude de sensibilité est conduite sur le modèle Rockyfor3D pour identifier la meilleure combinaison réaliste de paramètres de sol et de topographie pour assurer une propagatio nmaximale des blocs. Le même type de sol est ainsi appliqué pour simuler la propagation des blocs sur 3886 forêts différentes réparties sur l'ensemble des Alpes. Les indicateurs sont ensuite calculés pour chaque forêt à partir des résultats de simulation pour identifier les paramètres forestiers qui influencent le plus la capacité de protection.

La seconde étude (Chapitre II.3) utilise les indicateurs calculés au Chapitre II.2 sur les 3886 forêts pour évaluer la capacité de protection au niveau du peuplement forestier et comparer les principaux types de peuplements des Alpes françaises. L'influence de la structure du peuplement (notamment de la distribution des diamètres des arbres) et de la biodiversité (essentiellement au niveau des arbres) est aussi plus spécifiquement étudiée.

CHAPITRE 2

Quantifier le potentiel de protection des forêts de montagne contre les chutes de blocs

Novel quantitative indicators to characterize the protective effect of mountain forests against rockfall

Dupire S., Bourrier F., Monnet J.-M., Bigot S., Borgniet L., Berger F., Curt T.

Article published in *Ecological Indicators* Volume 67, Pages 98-107, August 2016.
DOI :10.1016/j.ecolind.2016.02.023

Abstract : Natural hazards are frequent in mountain areas where they regularly cause casualties and damages to human infrastructures. Mountain forests contribute in mitigating these hazards, in particular rockfalls. Assessing the protective effect of a forest against rockfall is a difficult task for both forest managers and rockfall experts. Accurate and simple tools are therefore required to efficiently evaluate the level of protection that results from the presence of forest.

This study defines three novel indicators to quantify the protective effect of forests against rockfalls, regarding 1) the reduction of the frequency of rockfalls, 2) the reduction of their maximum intensity, and 3) the combination of the reduction of the frequency and the energy of the rocks. The first two indicators are relevant for rockfall experts whereas the third is mostly interesting for foresters as it summarizes the protective effect of forest. The Rockyfor3D model was adapted and used to simulate rockfalls propagation on 3886 different forest stands located in all the French Alps. The results of the simulations were used to calculate the three indicators for each forest stand. Finally, the relations between the forest structures and compositions and the indicators values were investigated.

Our principal result shows that only three forest characteristics are required to accurately predict the indicators and evaluate the protective level of a forest against rockfall. The two first variables correspond to the basal area and the mean diameter at breast height (DBH) of the forest stand which are two parameters commonly used by forest managers. The third characteristic is the length of forest in the maximum slope direction which can be computed with a geographic information system (GIS). The method proposed in this study is easily reproducible and is suitable to evaluate the protective effect of European mountain forests at different scales. At local scale, the proposed indicators can enrich rockfall studies in which forests are usually set aside to simplify the evaluation. Moreover, the indicators may find direct applications with foresters by allowing them to identify the protective level of their forest and consequently to adapt their management. Finally, the indicators are convenient to perform spatial analysis and

produce maps of the protective effect of mountain forests that could find many applications in land settlement or evaluation of ecosystem services.

Keywords : Indicators · Protection forest · Rockfall · Ecosystem services · 3D simulation model · Mountain forest

2.1 Introduction

Forests have a prominent place in the mountain areas of the world. Mountain forests represent 23% of the global forest cover with over 9 million km^2 (Price et al., 2011). They provide many goods and services essential to human life and activities. In addition to the wood resources they represent, mountain forests also constitute a reserve of biodiversity and contribute to the landscape attractiveness and the environmental quality. A significant proportion of mountain forests also protect human beings and infrastructures against natural hazards such as rockfall, snow avalanches, flash floods and soil erosion (Brang et al., 2001). For instance, in France, about 25% of the Alpine forests are located between rock release areas and human infrastructures and may contribute to reduce rockfall damages and casualties (Toe et al., 2015).

An increasing number of studies have demonstrated that forests can be an efficient and cost-effective rockfall protection structure (Notaro et al., 2012; Wehrli et al., 2006; Wehrli et al., 2005), especially for small mass events (< 5 m^3) (Berger et al., 2002). On forested slopes, a falling rock can impact or break a tree with two responses after the contact : the rock is either stopped or deviated (Dorren et al., 2006a). Each time an impact occurs, the total energy of the rock is partially reduced (Bertrand et al., 2013; Dorren et al., 2006b). Therefore, forests contribute to reduce both the energy and the number of rocks that threaten human lives and infrastructures (Stoffel et al., 2006).

In mountain areas, optimizing forest management to mitigate natural hazards while maintaining other ecosystem services is a long-term fundamental objective. For this purpose, several empirical target values for stand parameters (mainly tree density, basal area, tree diameter and spatial distribution) have been proposed to optimize the protective effect of forests (Perret et al., 2004; Wasser et al., 1996; Gsteiger, 1993). These approaches have the advantages of being simple and directly practicable by forest managers. However they are mainly based on expert observations and are therefore insufficient to characterize and understand in details the functional processes involved in the interaction between forest and rockfalls. Recent studies proposed to use process-based rockfall modelling approaches that precisely describe rockfall trajectories including impacts against trees (Fuhr et al., 2015; Radtke et al., 2014; Stoffel et al., 2006). For instance, the RockyFor3D model has accurately predicted different rockfall patterns for several forested and non-forested sites in mountainous terrain (Dorren et al., 2006a).

Until now, numerical methods have only been used on a restricted number of sites and forest stand structures. Moreover, few studies propose to use quantitative indicators to characterize the protection provided by forest (Radtke et al., 2014). However, both forest managers and civil protection agents need quantitative indicators in order to accurately assess the protective effect of a particular forest and decide whether additional civil engineering measures are needed.

The aims of this study are (1) to define novel indicators allowing practitioners to characterize the protective effect (PE) of a forest and (2) to apply them to quantify and compare the PE of the main forest structures and compositions existing in the French Alps. For this purpose, we first evaluated the importance of non-forest inputs on the propagation of the rocks simulated with Rockyfor3D. Second, we applied the model on 3886 forest plots of the French National Forest Inventory (NFI). Third, we proposed and calculated new indicators to quantify both the rockfall frequency and the rock energy reduction for each forest plot. Finally, we introduced a

new practical method, based on the results of the simulations, to rank and predict the PE of the different forest structures and compositions in the French Alps.

2.2 Materials and Methods

Figure 2.1 shows the different steps of the methodology followed in this study. The different processes are detailed hereafter.

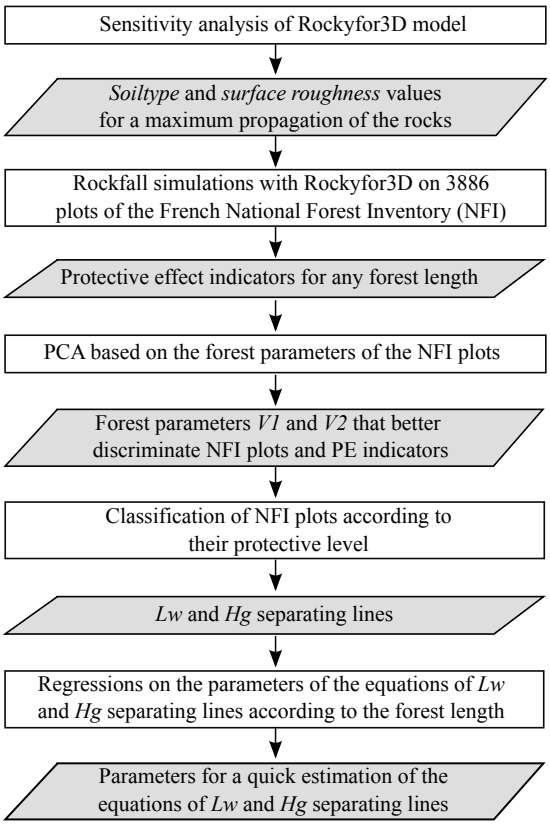

Figure 2.1 – Steps of the study. White rectangles correspond to processes. Grey-coloured parallelograms are results.

2.2.1 Rockfall simulation settings

The RockyFor3D software is one of the few rockfall simulation models (Dorren, 2015; Woltjer et al., 2008) which explicitly takes into account the protective effect (PE) of forests. Moreover, Rockyfor3D source code was made available for this study which made it possible to add new functionalities and to run the model in batch mode on a computing centre. RockyFor3D calculates trajectories of single, individually falling rocks, in three dimensions (Dorren et al., 2006a). The model simulates the propagation of rocks down a slope on a rasterized digital terrain model by successive sequences of free flights through the air, rebounds on the slope surface, and impacts against trees. When a rock impacts a tree, it loses part of its kinetic energy depending on the tree type (broadleaves versus conifers), on the vertical and horizontal locations of the impact on the tree, and on the rock trajectory before impact (Dorren, 2015). Rockyfor3D uses raster maps as input files that define slope surface, topography and characteristics of forest and rock. The *calculation screens* option allows the collection of detailed data on rockfall kinematics (mainly

energy, passing height and velocity) of each rock arriving on a certain line (i.e. *calculation screen*) positioned along the slope surface.

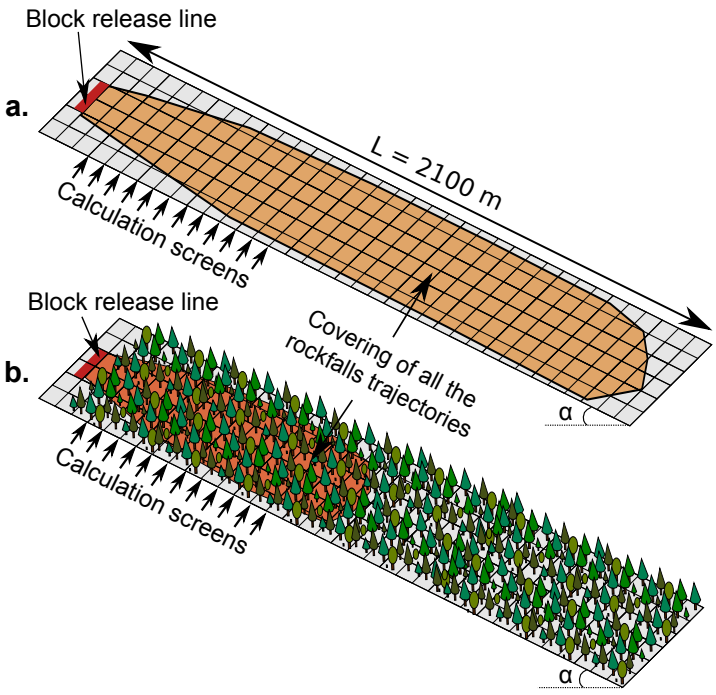

Figure 2.2 – Virtual terrain with uniform slope α and length L. Calculation screens are located every 5 m along the non-forested (a) and forested (b) profiles.

In order to identify the best settings of Rockyfor3D model, a first set of simulations was run to understand the relative importance of the surface roughness and *soiltype*. These parameters were tested on virtual digital terrain models (DTM) with 2-m resolution, a regular slope α and a length L of 2100 m (Fig. 2.2.a). Surface roughness was tested in the range [0 - 80] cm with a 1-cm increment. In Rockyfor3D, *soiltype* is directly linked to the normal coefficient of restitution R_n used in the rock rebound calculation. *soiltypes* 1 to 6 were tested which corresponds to R_n values in the range [0.21 - 0.58]. Each (*soiltype*, surface roughness) combination was also tested on the slope range [20 - 50] ° and with three rock volumes {0.5, 1, 5} m^3. For each simulation, 15000 spherical blocks with a density of 2600 $kg{\cdot}m^{-3}$ were released on a contour line situated at the top of the virtual terrain. To ensure identical initial conditions for all simulations, we modified Rockyfor3D model to allow the parametrisation of an initial velocity and direction of the rock. Initial velocity was set to 12 $m{\cdot}s^{-1}$ and initial direction was chosen to have a normal incidence angle of 25° for the first soil rebound. Those values are commonly observed in field experiments on forested slopes (Bourrier et al., 2009). Calculation screens were located every 5 meters along the slope surface in order to record the number of passing blocks depending on the distance to the release line. The ground distance from departure where 90% of the blocks were stopped (d_{stop}) was used as indicator in order to compare the results of the simulations.

2.2.2 Source and selection of forest data

Mountain forests present a wide diversity in terms of stand structures and composition (Price et al., 2011). Using accurate and standardized forest description for quantifying and comparing their protective effect is therefore of major importance. Since 2004, the French National Forest Inventory (NFI) is based on a systematic grid of 1 km × 1 km permanent plots designed to cover the whole national forested area. Each year, 10% of the plots are measured. From 2005 to 2013,

nine fractions are available with approximately 6700 forest plots each year. NFI data are collected on a system of concentric circle plots (Robert et al., 2010). Stand properties and topographic data are assessed in a 25-m radius. Tree characteristics are inventoried over a countable threshold at a diameter at breast height (DBH) of 7.5 cm.

NFI plots contain sufficient information for rockfall modelling regarding forest inputs. However, even though soil surveys are carried out on each NFI plot, soil data are not sufficient for a faithful description of the ground surface which has to be accurately qualified in term of roughness and hardness (Bourrier et al., 2009).

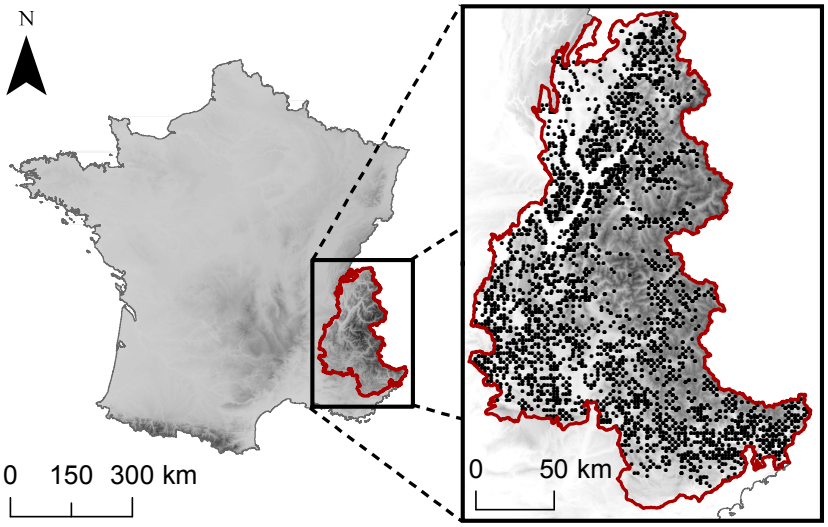

Figure 2.3 – Map of the 3886 selected NFI Alpine plots (black dots). French Alpine region is delimited by the red line.

Our study used NFI plots for the description of both terrain slope and forest stands and structures. Only the plots located in the Alpine region (Fig. 2.3) with a terrain slope gradient greater than or equal to 20° were used. For slope values less than 20°, rocks have a rolling mode of motion and their velocity decreases quickly (Dorren, 2003). This resulted in the selection of 3886 NFI plots measured from the period 2005-2013. Statistics about forest and slope parameters are shown in Table 2.1.

	Min	**25^{th}Pc**	**Median**	**75^{th}Pc**	**Max**
Terrain slope [°]	20	25	30	35	57
Basal area [$m^2 \cdot ha^{-1}$]	0.4	12.8	23.6	36.1	116.8
Mean DBH [cm]	7.6	13.7	17.3	23.1	76.7
Number of stems [ha^{-1}]	15	400	750	1200	5400

Table 2.1 – Statistics of terrain slope and forest stand parameters for the 3886 Alpine plots of the NFI. 25^{th}Pc and 75^{th}Pc are the 25^{th} and the 75^{th} percentiles respectively.

2.2.3 Rockfall simulations on NFI plots

A similar method as in section 2.2.1 was used for rockfall simulations on the NFI plots. For each plot, a new virtual terrain was generated and used for both forested and non-forested simulations. Each virtual terrain had a regular slope α corresponding to the NFI plot slope and a total length L of 2100 m in the slope direction (Fig. 2.2). Calculation screens were located every 5 meters along the slope surface to register both kinetic energy and number of passing blocks according

to the distance to the release line. The rock properties and initial conditions exposed above were also used for NFI plot rockfall simulation.

In order to compare and emphasize differences in the protection provided by the different stand structures and compositions, we used the same (surface roughness, *soiltype*) combination for all NFI plots. The sensitivity analysis carried out at section 2.2.1 allowed us to identify a combination that ensures a complete propagation of all the released blocks on the 2100 m long virtual terrain for all non-forested simulations. This combination presents two advantages. It emphasizes the protective effect of the forest and it corresponds to the worst plausible scenario where rocks cover a long distance down the slope.

Integration of forest characteristics in Rockyfor3D is done using the exact locations (x,y coordinates) and the diameters of all trees on the slope surface. When a rock impacts a tree, its energy is reduced due to both energy transfer and dissipation. Equation 3.1 is used to determine the maximum energy reduction of the rock during an impact on a tree (Dorren et al., 2006b).

$$max.Ered = Coeff(treetype) \times 38.7 \times DBH^{2.31} \tag{2.1}$$

In its original version, Rockyfor3D uses only two values for the *Coeff(tree type)* : one for all broadleaves species and one for all conifers species. Moreover, tree type (i.e. broadleaf or conifer) is assigned randomly during the simulation according to the proportion of conifers present in each raster cell.

For the purpose of this study, Rockyfor3D was modified in order to use species values (published in Dorren et al. (2006b)) instead of broadleaves / conifers values for *Coeff(tree type)*. Those values were made explicit for each tree to avoid random attribution. For each NFI plot, the forest was generated following two steps. First, the location of the trees in the slope surface were sampled with uniform probability until the tree density is equal to the measured one. Second, diameters and species of each tree were randomly attributed but respecting the diameter and species distributions observed on the NFI plot.

Finally, a total of six simulations per NFI plot were tested : one without forest and one with forest for each rock volume {0.5, 1, 5} m^3. All the 23316 (3×2×3886) simulations were computed on the Grenoble University high performance computing centre (CIMENT).

2.2.4 Definition of indicators for the protective effect of forests against rockfall

Three indicators were defined to characterize the PE of forests against rockfall. Each of them is a function of a distance x corresponding to the length of the forested slope in the maximum slope direction.

First of all, forests act as a natural barrier against rockfall and trees contribute to stop some of the falling blocks in a way similar to civil engineering devices (i.e. nets or embankments) (Lambert et al., 2013). We called this first effect the “barrier effect" and quantified it as shown in equation 2.2.

$$BARI(x) = 100 \times \left(1 - \frac{Nrock_{forest}(x)}{Nrock_{noforest}(x)}\right) \tag{2.2}$$

The BARrier effect Index *BARI(x)* of a forest of x m length along the maximum slope direction is related to the number of passing rocks at distance x for the simulation with forest $Nrock_{forest}(x)$ divided by this same quantity for the simulation without forest $Nrock_{noforest}(x)$. Therefore, *BARI(x)* is an indicator of frequency reduction of the rockfall hazard as it directly gives the percentage of rocks stopped due to the presence of forest on x m along the maximum

slope direction.

A second indicator was used to define the reduction of the rockfall maximum intensity under a forested slope of x m along the maximum slope direction (equation 2.3).

$$MIRI(x) = 100 \times \left(1 - \frac{E95_{forest}(x)}{E95_{noforest}(x)}\right) \tag{2.3}$$

The rockfall Maximum Intensity Reduction Index *MIRI(x)* is related to the 95^{th} percentile of the energy of all the passing rocks at distance x m along the maximum slope direction for the simulation with forest $E95_{forest}(x)$ divided by the same quantity for the simulation without forest $E95_{noforest}(x)$.

These two indicators give an objective information about the residual rockfall risk relative to a forested slope in term of frequency *BARI(x)* and maximum intensity *MIRI(x)*. These two elements are especially important for civil protection agents when deciding whether a civil protection structure has to be built in complement of forest.

The third indicator integrates both the proportion of stopped rocks and the total energy reduction of rocks due to the presence of forest. We called this effect the “overall rockfall protection" and quantified it with a third indicator as shown in equation 2.1.

$$ORPI(x) = 100 \times \left(1 - \frac{Ecum_{forest}(x)}{Ecum_{noforest}(x)}\right) \tag{2.4}$$

The Overall Rockfall Protection Index *ORPI(x)* of a forest of x m length along the slope direction is related to the total energy of all the blocks passing at distance x with forest $Ecum_{forest}(x)$ divided by this same quantity without forest $Ecum_{noforest}(x)$.

Presently, foresters mostly use indicators similar to *BARI(x)* which, by definition, only regards the reduction of the rockfall frequency due to forests. Therefore, they overlook a significant effect of forest which is the reduction of the energy of the rocks each time they impact a tree. *ORPI(x)* presents the advantage of combining both effects in one indicator. It can therefore be especially interesting for foresters that would like to take into account the protective effect of their forests in its entirety.

The three indicators have a range of values from 0 (no protective effect) to 100 (high protective effect). The calculation screens located every 5 m along the slope surface (Fig. 2.2) were used to collect the values with and without forest of *Nrock*, *Ecum* and *E95*. The three PE indicators were then calculated using these values on each NFI plot and for each rock volume. This resulted on 11658 (3×3886) simulations where values of the three PE indicators are known for $x \in [50 - 2100]$ m.

2.2.5 Classification and prediction of the PE indicators from forest characteristics

The previous work led us to the calculation of each PE indicator according to the forest length and the rock volume for all the NFI plots (Fig. 2.1).

Starting from the previous results, we first investigated the effect of the forest length along the slope direction x on each PE indicator. A principal component analysis was then conducted to identify the forest parameters that better discriminate both NFI plots and PE indicators. These parameters were used to elaborate a simple classification of the NFI plots into three levels of protection. Finally, we proposed a method to predict the level of protection for each PE indicator and for any European mountain forest directly from forest characteristics.

2.2.5.1 PCA on the NFI plots

A principal component analysis (PCA) was conducted in order to compare PE indicators with forest stand characteristics. The basal area, stem density, mean DBH, mean *Coeff(tree type)* and terrain slope of the 3886 NFI plots were used for the PCA. PE indicators for different rock volumes and forest length x were fitted afterwards.

The PCA was used to identify the two forest stand variables (*V1* and *V2*) that allow the best discrimination of both the NFI point cloud and the PE indicators. A Cartesian coordinate system with *V1* as abscissa and *V2* as ordinate was defined to perform the prediction of the protective effect and the classification of the NFI plots.

2.2.5.2 Classification of NFI plots according to their protective effect

NFI plots were divided randomly into two equivalent samples A (calibration) and B (validation) of 1943 NFI plots each. Plots of samples A and B were projected in the reference system defined by *V1* and *V2*.

PE values of each plot of the sample A were transformed in three levels of protection for each PE indicator. The first level corresponds to plots with PE value ≤ 50. We qualified the PE of those forests as “Low PE" as rockfall hazard is hardly reduced. Second level corresponds to plots with PE value from 50 to 90. We qualified the PE of those forests as “Medium PE". In this case, rockfall hazard is a least reduced by a factor 2. Last level gathers plots with a PE value ≥ 90. Those forests have a “High PE" as the rockfall component is at least reduced by a factor 10.

For each PE indicator and each forest length x, we computed the equations of the straight lines *Hg* that best separate the plots of sample A with PE levels equals to “Medium" and “High". Equations of the straight lines *Lw* that best separate the plots of sample A with PE levels equals to “Low" and “Medium" were also computed. These equations are of type :

$$V2 = slope \times V1 + intercept \tag{2.5}$$

To facilitate the use of the prediction method by the practitioners, the computation was chosen to keep the same value for the intercepts of the two separating lines *Lw* and *Hg* for each couple (PE indicator, forest length). Once all the equations of the separating lines were computed, it was possible to predict the PE level of any forest type and length by locating it in the reference system defined by *V1* and *V2*. For example, a forest located between the separating lines *Lw* and *Hg* will get a “Medium" PE.

To evaluate the quality of this classification, NFI plots from the sample B were projected in the reference system. Their calculated PE values were transformed into PE levels and compared with the PE level obtained according to their location relatively to the separating lines *Lw* and *Hg*. A contingency table was build for each PE indicator and forest length x and used to calculated the accuracy of the classification. Four statistics were used to evaluate the accuracy (Congalton, 1991):

- Total accuracy : obtained by dividing the total number of correctly classified plots by the total number of plots.
- User accuracy : obtained by dividing the total number of correctly classified plots in a category by the total number of predicted plots in that category. It measures the commission error by category. In this study, we present the average user accuracy.
- Producer accuracy : obtained by dividing the total number of correctly classified plots in a category by the total number of observed plots in that category. It measures the omission error by category. In this study, we present the average producer accuracy.

- Cohen Kappa coefficient (Cohen, 1960): it reflects the difference between actual agreement and the agreement expected by chance. Kappa is always less than or equal to 1. The agreement is generally qualified as good from 0.6 to 0.8 and very good when it is greater than 0.8. A value of 1 indicates a perfect agreement.

2.2.5.3 Prediction of the PE indicators from forest characteristics

Linear regressions between the forest length x and the *slope* and *intercept* values for both lines *Hg* and *Lw* of each PE indicator were computed. The resulting coefficients were used to draw both *Hg* and *Lw* separating lines and predict the PE levels of four different sites where empirical data on rockfall protection were available.

The process to predict the PE levels from the separating lines is done by (1) calculating the *slope* and *intercept* values at a given forest length for both *Hg* and *Lw* lines from the coefficients of the linear regression and (2) locating the forest in the reference system defined by forest characteristics *V1* and *V2* (define at section 2.2.5.1) where *Hg* and *Lw* are drawn with the values previously found.

This process was applied for a first validation of the predicted PE indicators with empirical data. Predicted PE indicators were compared to PE values observed during three different rockfall experiments (Dorren et al., 2006a; Doche, 1997; Jahn, 1988) and one numerical study where Rockyfor3D was calibrated according to the impact on trees observed on the field (Stoffel et al., 2006).

2.3 Results

2.3.1 Importance of soil and surface parameters in Rockyfor3D

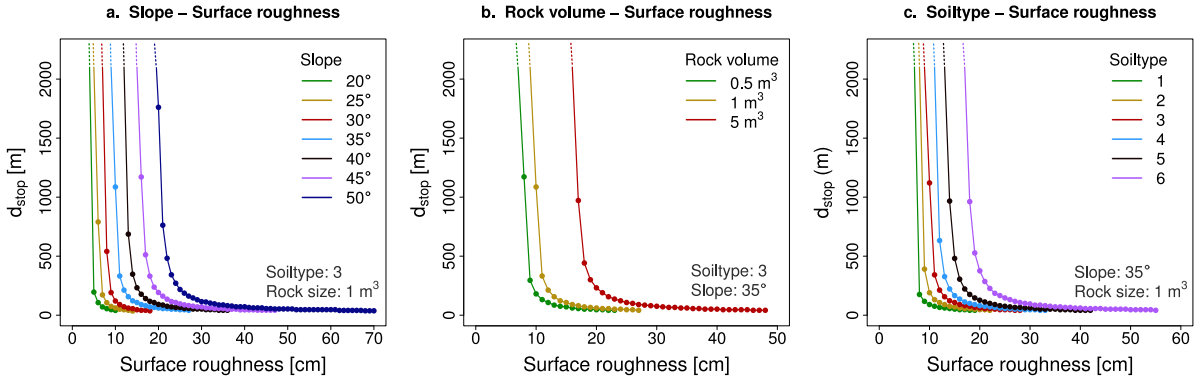

Figure 2.4 – Distance from departure where 90% of the released blocks are stopped (d_{stop}) in function of surface roughness (abscissa) and slope (a), rock volume (b) or soiltype (c).

Fig. 2.4 shows the influence of the surface roughness on the d_{stop} value. For each combination tested, a minimum value of surface roughness exists below which none of the released block is stopped on the 2100 m long virtual terrain. At the opposite, a maximum value of surface roughness exists above which all the released block are stopped in the first 50 m of the virtual terrain. Between these minimum and maximum values, d_{stop} decreases when surface roughness increases. These first simulations show that Rockyfor3D model is sensitive to surface roughness with a presence of two threshold values corresponding respectively to a complete propagation and a total stop of all the blocks. Increasing the slope, rock volume or *soiltype* (i.e. R_n) only enlarges the values taken by these two thresholds.

2.3.2 Effect of the length of forested slope on the PE indicators values

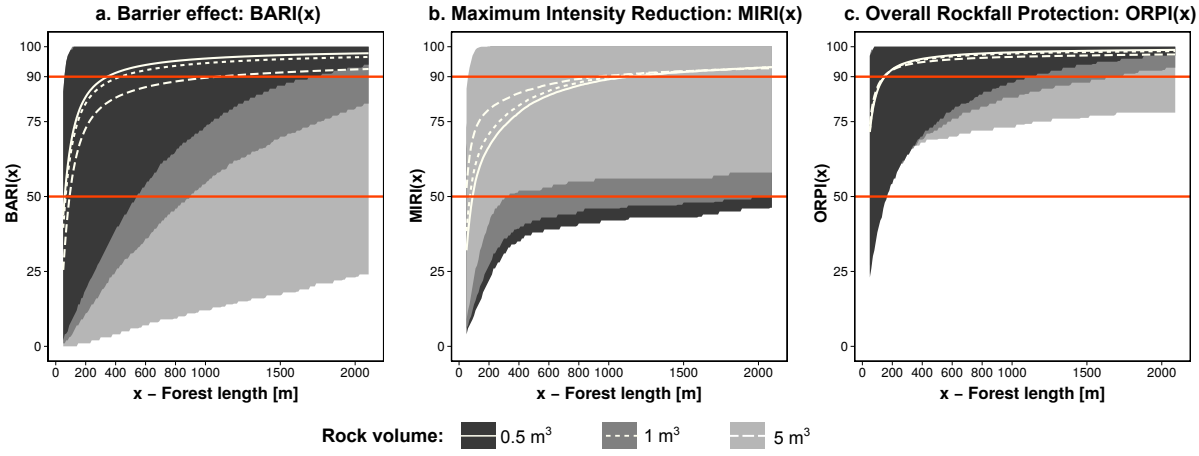

Figure 2.5 – Effect of the forest length along the slope on the three indicators for the 3886 NFI plots. White lines show the average values for each rock volume. Gray-colored areas are placed on top of each other and represent the possible indicators values taken from the 5^{th} percentile to the 95^{th} percentile for each rock volume. Red lines represent the separating lines Lw (50) and Hg (90) between the three levels of protection used in this study.

The effect of the forest length along the slope on the three PE indicators is displayed in Figure 2.5. The barrier effect index *BARI(x)*, the maximum intensity reduction index *MIRI(x)* and the overall rockfall protection index *ORPI(x)* evolve following an increasing curve to a horizontal asymptote for the long forested slopes. The range of values taken by *BARI(x)* is very wide. This range slightly decreases for *MIRI(x)* and significantly decreases for *ORPI(x)*. *BARI(x)* and *ORPI(x)* are higher for small rock volumes unlike *MIRI(x)* which is higher for big rock volumes.

2.3.3 Principal component analysis

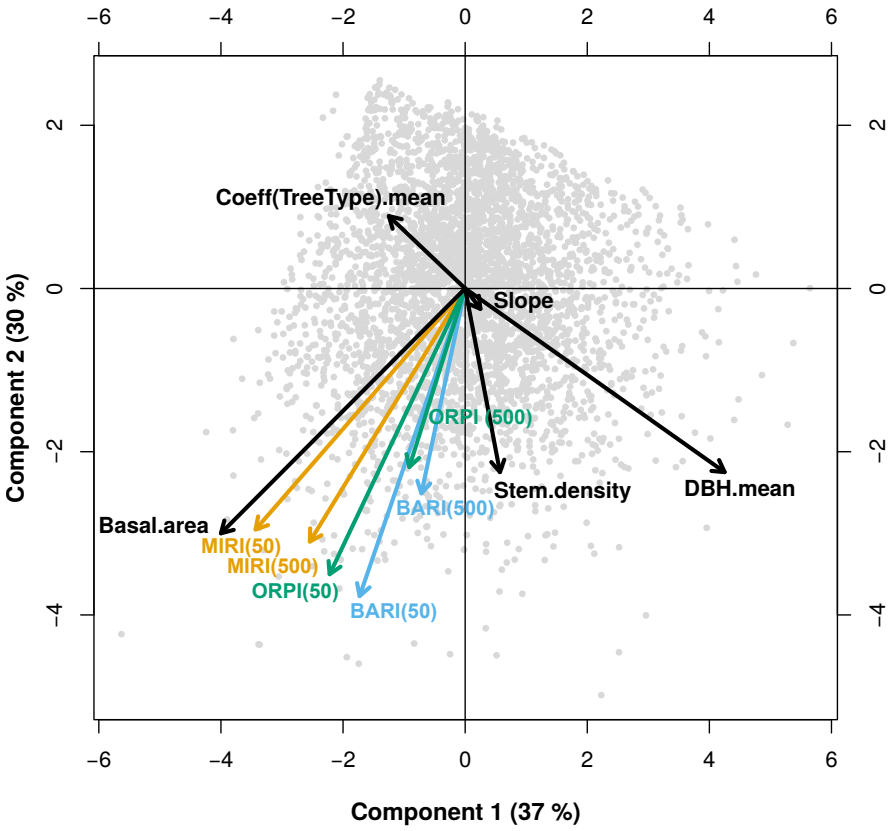

Figure 2.6 – Biplot of the principal component analysis (PCA) based on the basal area, stem density, mean DBH, mean coefficient for tree types and terrain slope (black arrows) of the 3886 NFI Alpine plots. PE indicators (coloured arrows) at x=50m and x=500m were fitted post hoc.

The biplot of the PCA (Fig. 2.6) described in section 2.2.5 shows the relative importance of the terrain slope and forest stand parameters of the NFI plots. PE indicators values after different forest lengths are also shown. According to the PCA, the slope of the terrain has a very low contribution to the PCA (0.2% and 0.3% on component 1 and 2 respectively). The mean value of *coeff(TreeType)* observed on each NFI plot has a medium contribution to the PCA (4.3% and 3.9% on component 1 and 2 respectively). It is slightly higher for the stem density with 0.9% on component 1 and 25.3% on component 2. Finally, the basal area and the mean DBH observed on NFI plots are the variables that best contribute to component 1 (44.4% and 50.2% respectively) and component 2 (45.1% and 25.4% respectively). PE indicators were fitted post hoc, the biplot shows that all of them are located between basal area and mean DBH. These points led us to keep as variables *V1* and *V2* (introduced at section 2.2.5) the basal area and mean DBH respectively.

2.3.4 Classification of NFI plots

NFI plots were projected in the Cartesian coordinate system defined by the basal area as abscissa and the mean DBH as ordinate (Fig. 2.7). In this reference system, PE values evolve following a clockwise motion, this regardless of the PE indicator and the forest length x. PE levels “Low",“Medium" and “High" were separated with two lines called *Lw* and *Hg* as shown in Figure 2.7.

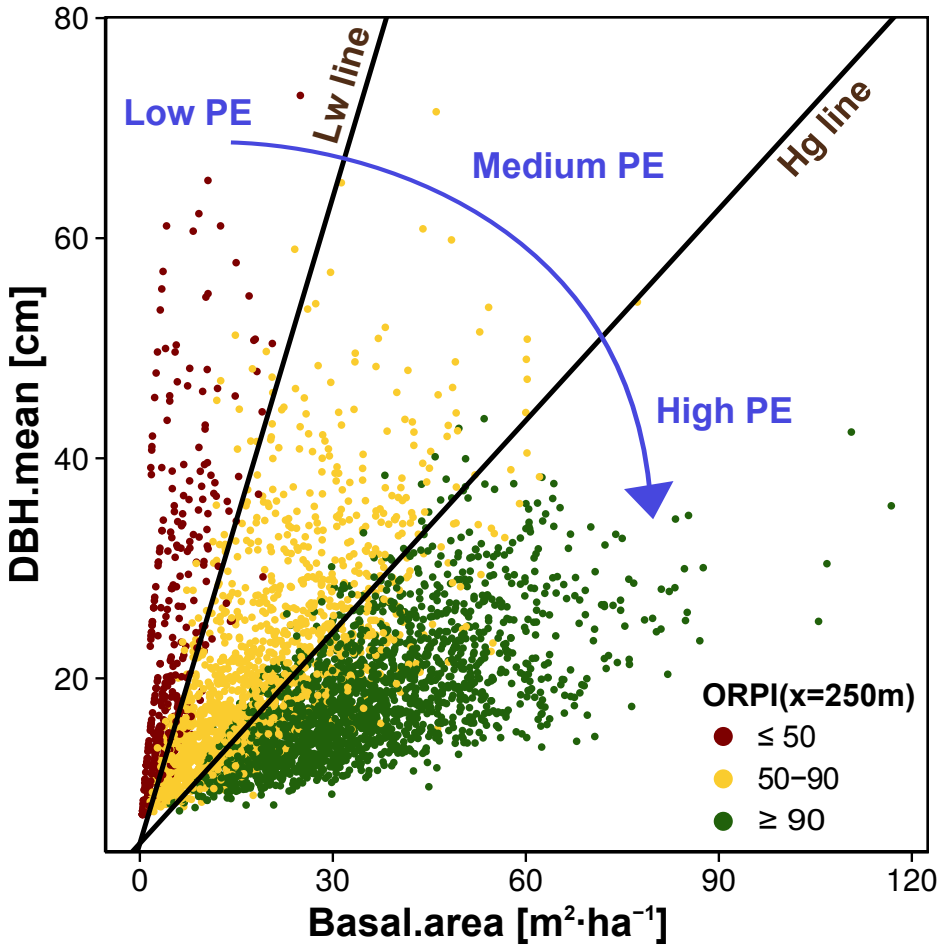

Figure 2.7 – Illustration of the separation in three PE levels by *Lw* and *Hg* separating lines. NFI plots are projected in the Cartesian coordinate system defined with basal area as abscissa and mean DBH as ordinate. Points are coloured according to the PE levels for *ORPI(x)* indicator at x=250 m and a rock volume of 1 m^3.

The quality of the partition of NFI plots with these two lines is illustrated in Figure 2.8. The values taken by the Cohen Kappa indicate a good agreement between observed and predicted PE level for *ORPI(x)* and a very good agreement for *MIRI(x)* and *BARI(x)*. Total accuracy oscillates between 0.75 and 0.95 which shows a good correlation between observed and predicted PE levels. The total accuracy is however lower for *BARI(x)*. User accuracy vary from 0.7 to 0.9 which indicates a fairly good prediction. *BARI(x)* and *ORPI(x)* have a better user accuracy than *MIRI(x)*. Finally, producer accuracy has the widest range of variation (0.62-0.95) for *MIRI(x)* and *ORPI(x)*. Producer accuracy for *BARI(x)* is high with a value of 0.96.

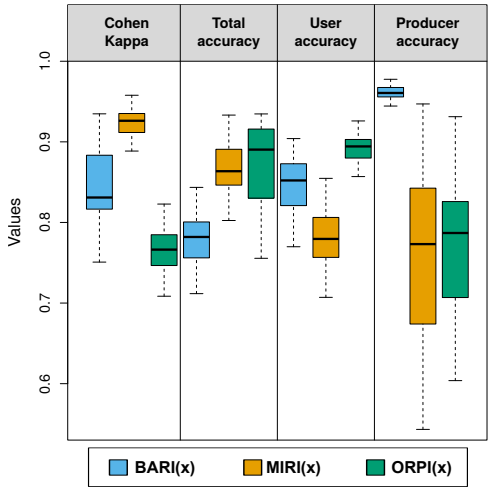

Figure 2.8 – Quality of the partition of NFI plots in three classes of protection level for the three PE indicators. Cohen Kappa and total, user and producer accuracies were calculated from the NFI plots of sample B. This represents 615 observations for each PE indicators (205 values of $x \in [50\text{ m} - 2100\text{ m}] \times 3$ rock volumes).

2.3.5 Influence of the forest length on the equations of the separating lines

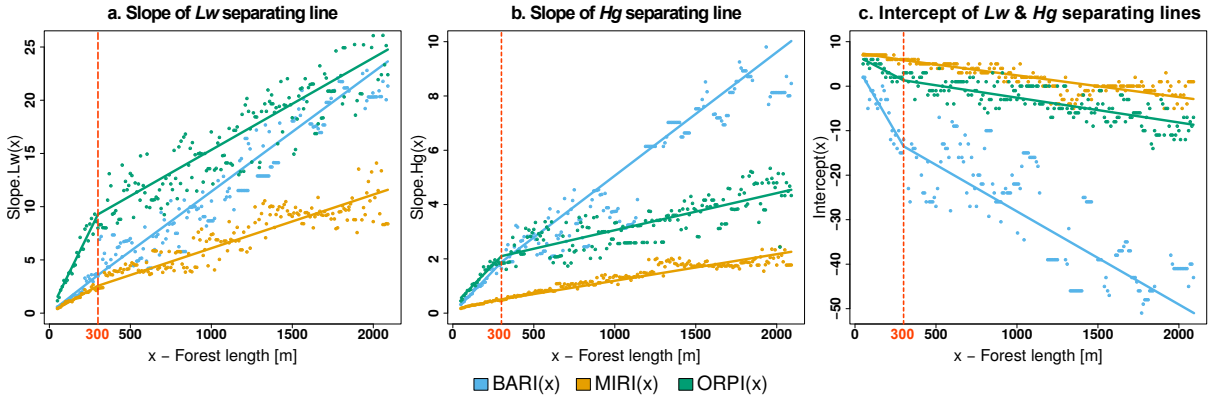

Figure 2.9 – Influence of the length on the slopes and intercept of separating lines Hg and Lw and for a rock volume of 5 m^3. The vertical dashed red line indicates the separation between short and long forest lengths.

Figure 2.9 shows the values of the slopes and intercept for Hg and Lw separating lines according to the forest length x and for the three PE indicators. The slopes of Lw and Hg lines increase when the forest length increases, this regardless of the PE effect. In contrast, the common intercept value of Lw and Hg decreases when the forest length increases. A break can be observed around a forest length of 300 m which lead us to consider two classes of forest lengths : short forest length ($x \leq 300$ m) and long forest lengths ($x > 300$ m).

Table 2.2 gives the equations for the slopes of Lw and Hg lines and their common intercept according to both the forest length x and the rock volume. Coefficients are given for short forest lengths and long forest lengths. Regressions for slope-Hg and slope-Lw present a better coefficient of determination R^2 (from 0.88 and 0.99) than for the intercept (from 0.53 to 0.89).

Rock volume	PE	Short Forest length (≤ 300 m)									Long Forest length (> 300 m)								
		Slope-Lw			Slope-Hg			Intercept			Slope-Lw			Slope-Hg			Intercept		
		a*	b	R^2	a*	b	R^2	a*	b	R^2	a*	b	R^2	a*	b	R^2	a*	b	R^2
0.5 m^3	BARI	132	0.00	0.99	57	0.00	0.99	-109	1.68	0.83	151	-0.57	0.98	37	0.61	0.91	-109	1.68	0.83
	MIRI	41	0.00	0.99	14	0.00	0.99	-35	7.57	0.53	14	0.81	0.94	8	0.17	0.98	-7	6.73	0.56
	ORPI	290	0.00	0.99	79	0.00	0.99	-93	5.11	0.73	187	3.11	0.92	48	0.93	0.87	-93	5.11	0.73
1 m^3	BARI	139	0.00	0.98	62	0.00	0.98	-356	4.70	0.74	179	-1.19	0.92	56	0.18	0.95	-174	-0.77	0.72
	MIRI	51	0.00	0.99	15	0.00	0.99	-46	7.69	0.54	20	0.93	0.89	8	0.19	0.97	-14	6.74	0.63
	ORPI	277	0.00	0.98	77	0.00	0.99	-119	5.35	0.53	159	3.56	0.95	50	0.81	0.83	-88	4.44	0.86
5 m^3	BARI	119	0.00	0.98	63	0.00	0.99	-372	0.00	0.82	112	0.21	0.92	45	0.51	0.90	-245	-3.81	0.81
	MIRI	86	0.00	0.99	13	0.13	0.95	-58	7.60	0.60	50	1.06	0.93	10	0.21	0.96	-49	7.31	0.89
	ORPI	309	0.00	0.99	74	0.00	0.99	-190	7.02	0.72	86	6.68	0.93	13	1.83	0.86	-56	2.99	0.84

a* : unit $\times 10^{-4}$

Table 2.2 – Coefficients of the linear regression $y = a{\cdot}x + b$ for the slopes and intercept of separating lines *Hg* and *Lw*. Intercept is common to the two lines. For a better estimation, regressions have been implemented for short (≤ 300 m) and long (> 300 m) forest lengths.

2.3.6 Comparison with real-size experiments

Table 2.3 shows the results of the comparison between PE levels predicted with our method and PE levels observed during real size experiments. For the four sites, the predicted PE levels are identical to the ones observed.

Source	Location	Site characteristics						Obserserved PE		Predicted PE	
		Slope gradient [°]	Forest length [m]	Stem density [ha^{-1}]	Basal area [$m^2.ha^{-1}$]	Mean DBH [cm]	Rock volume [m^3]	BARI	MIRI	BARI	MIRI
Dorren et al. (2006a)	Vaujany (FR)	38	190	294	31.6	36.9	0.5	Med (62)	Low (37)	Med	Low
Doche (1997)	Vailly (FR)	38	140	485	36.5	29.5	<0.5	Med (66)	Med (75)	Med	Med
Jahn (1988)	Liechtenstein	35.5	160	3400	45.1	13.0	<0.5	High (100)	-	High	-
Stoffel et al. (2006)	Diemtigtal (CH)	40	95	520	20.1	22.0	<0.5	Med (60)	-	Med	-

Table 2.3 – Comparison of empirical PE values and predicted PE levels on 4 different forests. The three first locations correspond to real size rockfall experiments, the fourth correspond to a site where Rockyfor3D has been calibrated according to rock impacts on trees observed on the field. For the observed protective effects both PE levels (e.g. Low, Medium and High) and PE values are given. For predicted protective effect only PE levels obtained with the equations of Table 2.2 are given.

2.4 Discussion

2.4.1 Interests and limitations of numerical modelling in rockfall assessment

Implementing rockfall field experiments in forested slope from different parts of the French Alps is not possible because of the implied financial and technical constraints. For these reasons, using accurate trajectory models for the rockfall hazard assessment is of major interest. Rockyfor3D has been calibrated and validated with real field experiments (Bourrier et al., 2012; Dorren et al., 2006a) and used in different countries and forest stands (Radtke et al., 2014; Bourrier et al., 2009; Stoffel et al., 2006). The sensitivity analysis carried out in this study allows a better understanding of the relative importance of the different non-forest inputs of Rockyfor3D. The threshold values observed have a consistent progression as the needed surface roughness to stop 90% of the released rocks increases when the slope or the rock volume increase or when the soil dissipative capacity decreases (Fig. 2.4). According to our study, the surface roughness is a very sensitive parameter, however it is very hard to measured it on the field. This point is especially interesting for the user community of the model when calibrating ground surface parameters on a new site.

Only one combination of ground roughness and *soiltype* (0 cm, 3) was used in this research. This choice was made to emphasize potential differences between forest plots while keeping a

ground description that is common in mountain forests. In Rockyfor3D, harder *soiltypes* necessarily go along with higher ground roughness as they correspond either to a compact soil with large rock fragments (*soiltype* 4) or to bedrock (*soiltypes* 5 and 6) (Dorren, 2015). On the contrary softer *soiltypes* imply a lower rock propagation as rocks loose more energy during each rebound. The combination used in this study corresponds to a conservative analysis of the rockfall hazard with a maximum propagation of the rocks on the non-forested slope.

In this study, the forest input file was modified to better take into account the species distribution and their relative capacities to absorb a part of the falling rock energy (see section 3.2.2). This improvement fixes a major limitation of the original version of the software that occurred when studying mixed forest. Until now, the coefficient *Coeff(tree type)* used to determine the maximum energy a tree can absorb (Equation 3.1) was assigned randomly during the simulation according to the proportion of conifers present in each raster cell. For heterogeneous mixed forests (for example composed of broadleaves with small DBH and conifers with high DBH), the random attribution of the *Coeff(tree type)* could produce a virtual forest quite different from the reality (i.e. small DBH for conifers and high DBH for broadleaves). In this research, this point was resolved and the usage of *Coeff(tree type)* improved with the inclusion of one value by tree species instead of one by tree type (i.e. broadleaf or conifer).

To our knowledge, this study is the first to propose a complete overview of the interactions between rockfalls and forest on a wide diversity of forests taken across the Alps. Previous studies were only focused on a specific forest structure or composition. Radtke et al. (2014) focused their work on coppice forests of Northern Italy, Cordonnier et al. (2008) aimed at evaluating the long term protection efficiency in Norway spruce forest stands and Stoffel et al. (2006) studied three different coniferous stands across Switzerland. The recent study carried out by Fuhr et al. (2015) is the only reference where the effect of maturity (and by extension structure) of mountainous uneven aged stands is related to the protective effect of forest against rockfalls.

Information about the spatial forest structure is not freely available in the French NFI database. Therefore, for each NFI plot, a forest stand had to be randomly generated on square areas with an equivalent size compared to the field plots. Although this issue has not been much investigated, previous studies showed that a random generation of the spatial forest structure can lead to a marginal overestimation of the PE against rockfall. Radtke et al. (2014) showed that a random spatial generation of coppice forests can lead to a small overestimation of the PE of about 10%. However, this result concerns only a particular forest structure and the PE indicator used cannot be related to one of those proposed in this study. Jancke et al. (2009) also studied PE of coppice forests with an indicator close to *BARI(x)*. Their results did not showed a significant difference between a random forest and a real forest. Recently, Monnet et al. (2017) focused on the influence of forest inputs on the estimation of the protective effect of three different forests : one coppice, one uneven-aged and one even-aged forest. They showed a marginal effect of using a randomly generated spatial forest structure compared to field inventory data.

For each NFI plot, the same stands characteristics was used on a regular virtual terrain of 2100 m length (Fig. 2.2). This produces a completely homogeneous forest stand on the entire mountainside which is not necessarily representative of the reality. Indeed, in mountain areas, forest structures and species compositions evolve following a gradient of altitude. This choice was made to emphasize PE differences between the 3886 NFI plots studied while controlling non-forest parameters. In further studies, it would be very interesting to apply the same methodology on forest structures and species distribution that evolves following an elevation gradient. However, for the smallest rock volumes (≤ 1 m^3), our results showed that a high protective level *ORPI(x)* was reached for the majority of NFI plot for forest length x along the maximum slope direction over 200 m (Fig. 2.5). Similarly, a high barrier effect level *BARI(x)* was reached after 400 m. These values are in the same order of magnitude as those observed in dendrogeomorphological studies carried out in France where the number of rock impacts on trees was measured along

the slope direction (Favillier et al., 2015). Therefore, consider a homogeneous forest stand on distances shorter than 400 m is realistic and the results presented in this study can directly be used in such conditions.

The comparison with empirical data presented in section 2.3.6 shows the difficulty of implementing real-size experiments with sufficient instrumentation to get accurate information about reduction of frequency and intensity. Only three real experiments were found in the literature and two of them have information about the energy of the rocks. For practical reasons, these experiments were conducted with small rocks on short distance forested slopes. With these site configurations, the comparison with empirical data showed a good agreement. However, it was not possible to compare our predicted PE levels with observed PE values for rocks bigger than 0.5 m^3 and slope longer than 190 m.

2.4.2 Interests and limitations of the protective effect indicators

The protective effect indicators provided in previous studies (Radtke et al., 2014; Jancke et al., 2009; Berger et al., 2007; Stoffel et al., 2006) are mainly focused on the reduction of the frequency of rockfall hazards and some of them can be related to *BARI(x)*. In this study, we completed the analysis of rockfall mitigation by forests with two completely novel indicators. First, *MIRI(x)* gives the reduction of the maximum intensity which is especially interesting for rockfall specialists. Second, *ORPI(x)* synthesizes the reduction of rockfall hazard (regarding both frequency and intensity) that can be attributed to the presence of forest. Their simple definition makes their accurate calculations possible for any new site with the use of Rockyfor3D as only pre-requisite. To get a first idea of the PE of a forest, they can also be estimated under three levels of protection without running Rockyfor3D when the three forest characteristics required are known.

The values the three PE indicators according to the forest length along the maximum slope direction reflects a combination of two mechanical aspects (Fig. 2.5). First, the protective effect of a forest is linked with the probability that an impact between the rock and a tree occurs. This probability increases with forest length, and this especially if the number of stems is important (Dorren et al., 2005). Therefore, the overall growing trend of the three indicators is a consequence of the impact probability. Second, the values taken by the PE indicators are linked to the capacity of the trees to reduce the rock energy. The reduction of rockfall intensity *MIRI(x)* is higher for big rocks than for smaller ones (Fig. 2.5). For small volumes, trees are usually resistant enough to stop or deflect the rocks because of their low energy values. Consequently, for small rocks, the dominant PE effect is the barrier effect as a substantial part of the rocks are stopped when an impact occurs. On the contrary, for big volumes, either rocks are deflected or trees break under the impact. In both cases, the impact slows down the rock that loses a part of its kinetic energy. For big rocks, a succession of impacts induces a loss of the kinetic energy, therefore, the dominant PE effect is the rockfall intensity reduction. The link between the protective effect of forest and the combination of impact probability and tree resistance has already been mentioned (Brauner et al., 2005; Gsteiger, 1993), however it is interesting to see that the PE indicators proposed in this study are closely related to it.

The terrain slope was expected to have a major importance on the protective effect of forest but it turned out to be negligible. Indeed, the three PE indicators are calculated by comparing a forested scenario with a non-forest scenario, both of them being totally similar in terms of slope and ground characteristics. Therefore, they correspond to the proportion of hazard reduction due to the presence of forests. This way of calculating the PE indicators omits that rocks cover a longer distance and have a higher energy on steepest slopes. Thus, these indicators allow focusing on the proportion of the hazard that is reduced, even if the absolute rockfall hazard is higher on steep terrains.

Finally, the major finding of this study is the capacity to predict accurately each of the three PE indicators from only three forest characteristics : the basal area, the mean DBH (both variables including all trees with a DBH $\geq$ 7.5 cm) and the forest length along the maximum slope direction. Moreover, the proposed transformation of PE indicators values to three PE levels allows a quick overview of the different components of the protective effect that can be expected from a particular forest without running a rockfall model. This result could be an interesting support to update and complement the online 2-D tool *RockforNET*. This empirical model, developed by Berger et al. (2007), allows a quick assessment of the residual risk of rockfall under a forested slope. Starting from forest and profile characteristics, the algorithm uses the energy lines principle (Toppe, 1987) to return an indicator of the rockfall frequency reduction. Our results, based on 3-D simulations realised on many different forests around the Alps, could enrich this online tool by simplifying the compulsory inputs and by returning the three PE indicators *MIRI(x)*, *BARI(x)* and *ORPI(x)*. With this update, users could benefit of additional information about both frequency and intensity of the rockfall hazard.

2.4.3 Implications for forest management and rockfall hazard assessment

Our research presents different applications for both forest managers and rockfall hazard mitigation. Rockfall specialists are not necessarily foresters and can therefore have difficulties to characterize a forest on a particular site. Our approach suggests to use only three forest variables to characterize the forest stand. The forest length can be easily measured with a map and an aerial photography. Basal area and mean DBH can be estimated with a relascope and a forestry tape on several plots distributed along a transect from the release area of the rocks to the deposit area. After this step, it is possible to locate the forest in the reference system defined by the basal area and the mean DBH (Fig. 2.7) and to plot *Hg* and *Lw* lines with equations of Table 2.2. If the forest has a high protective effect level, the civil engineering fences can be designed taking into consideration the hazard reduction due to the forest. For example, if both *BARI(x)* and *MIRI(x)* are higher than 90, the expected frequency and intensity of rockfall events is reduced by 10. Therefore, a small civil engineering fence can be considered which will have a cost significantly lower than if the fence were designed without taking into account the forest. The same process can be used for forest with a medium PE level. However, if the forest has a low PE level, it will be recommended to design civil engineering fences as if there were no forest.

The protective effect of a forest against natural hazards is one of the major input keys used in silviculture guides to adapt the management (Maroschek et al., 2014; Motta et al., 2000). However, foresters are not necessarily specialists of rockfall and need simple and accurate tools to manage their forest with the objective of maintaining the best level of protection as possible. Currently, foresters mostly use indicators similar to *BARI(x)* which concerns, by definition, only a part of the protective effect of forests (the reduction of frequency). Therefore, they overlook a significant effect of forest which is the reduction of the energy of the rocks each time they impact a tree. *ORPI(x)* presents the advantage of combining both effects in one indicator. Starting from an initial stand structure, our research allows a quick evaluation of this overall rockfall protection *ORPI(x)*. If the forest has a high PE level, its management must consider maintaining this high level of protection. The table 2.2 gives the equations of the *Hg* lines according to the forest length for each PE indicator. It provides an important support for foresters to know the threshold values they have to respect in order to keep a high PE level or to improve it in case of a medium or low initial PE level. Moreover, the indicators are convenient to perform spatial analysis and produce different maps of the protective effect of mountain forests against rockfall. Such maps could be very interesting for foresters and public stakeholders in order to prioritize their interventions according to the level of protection of the forests of the area.

2.5 Conclusion

This study focused on the definition of indicators to help professionals to assess the protective effect of mountain forests against rockfalls. The proposed indicators were calculated on 3886 different Alpine forests from rock trajectories simulated with the Rockyfor3D model. The relation between forest characteristics and PE indicators was investigated in order to propose a fast and simple method to predict the protective effect against rockfall of any Alpine forest without necessarily resort to rockfall simulations.

To validate our research at different scales, furthers studies could apply this method on different mountainsides subject to rockfall hazard and compare the PE levels predicted only with forest characteristics to real-size experiments or Rockyfor3D simulation results.

Finally, our study can find an application with the growing interest in the valuation of ecosystem services (Helfenstein et al., 2014). Indeed, the PE indicators proposed in this paper can be used to compare the costs of civil engineering fences when they are designed with or without taking into account the forest. The difference between the cost without forest and the cost with forest represents the (substitution) value of the protective effect of the forest against rockfall which is a good sample of ecosystem services.

Acknowledgement

This work was supported by the grant n°2101527657 of the Action 10 “Prévention des risques naturels et hydrauliques" of the Programme 181 “Prévention des risques" of the French Ministry of Ecology, Sustainable Development and Energy. It was also supported by the project ANR SAMCO (ANR-12-SENV-0004).

Most of the computations presented in this paper were performed using the CIMENT infrastructure (https ://ciment.ujf-grenoble.fr), which is supported by the Rhône-Alpes region (GRANT CPER07_13 CIRA : http ://www.ci-ra.org).

CHAPITRE 3

Influence de la diversité forestière sur la capacité de protection contre les chutes de blocs

The protective effect of forests against rockfalls across the French Alps : influence of forest diversity

Dupire S., Bourrier F., Monnet J.-M., Bigot S., Borgniet L., Berger F., Curt T.

Article published in *Forest Ecology and Management* Volume 382, Pages 269-279, December 2016.
DOI : 10.1016/j.foreco.2016.10.020

Abstract : The role of forests in the mitigation of natural hazards has been repeatedly demonstrated. The protective effect of mountain forests against rockfalls has especially been pointed out because it can constitute a natural and cost-effective protection measure in many situations. However, this particular ecosystem service may substantially differ according to the structure and the composition of the forest. Until now, the rockfall protection capability has always been studied at a local scale with only few forest types. Moreover, the comparison of the protective effect of the different forest types studied remains difficult because different methods and indicators were used. For the same reasons, it is not possible to draw conclusions about the influence of biological and structural diversities on the protection capabilities of forests from former works.

The aims of this study were (1) to quantitatively assess the protective effect of forests at the French Alps scale and build a classification based on the protection capability, (2) to compare the protective effect of the different forest types present in the French Alps and (3) to analyse the relations between the protective effect and the forest diversity in terms of stand structure and tree composition. For this purpose, the model Rockyfor3D was used to simulate the propagation of rocks on 3886 different forest plots spread over the whole French Alps. Quantitative indicators characterizing the protective effect of each forest plot were then calculated from the simulation results and used to perform the different analyses.

Our results emphasized the importance of taking into account the length of forest in the maximum slope direction for an accurate assessment of the protective effect. Thus, the minimum length of forest to get a reduction of 99% of the rockfall hazard was chosen as indicator to compare protective effect between forests. Using this indicator, half of the French Alpine forests presented a high level of protection after a short forested slope (190 m). A decreasing gradient in the protection capabilities was observed from forest types dominated by broadleaved species to those dominated by conifer species. Moreover, considering an equivalent proportion of conifers, stands dominated by shade-tolerant tree species showed better ability to reduce rockfall hazard.

Finally, our study highlighted that a high biodiversity and a structural heterogeneity within the forest have a positive effect on the reduction of rockfalls hazard.

Keywords : Mountain forest · Protection capability · Rockfall · Ecosystem services · Biodiversity · Alps

3.1 Introduction

Mountain forests represent a renewable wood resource and provide a wide range of ecosystem services (Briner et al., 2013). Among them, the protection of human beings and infrastructures against natural hazards is essential, especially in Alpine regions (Bebi et al., 2001). A significant part of the forested area in the Alps provides a natural protection against rockfall (Toe et al., 2015; Brang et al., 2001). On forested slopes located below a departure area, it is common to observe scars on trees resulting from one or several rockfall impacts (Favillier et al., 2015). Each impact against a tree reduces the energy of the block which results in a lower velocity or a complete stop (Bertrand et al., 2013; Dorren et al., 2006b). After a forested slope, both the energy (intensity) and the number of rocks (frequency) threatening human lives and infrastructures are reduced, especially in the case of small volume events ($\leqslant 5$ m^3) (Berger et al., 2002).

Quantifying the protective effect of a forest is of major importance to provide reliable recommendations to forest managers and enrich the argumentation concerning the consideration of forests in local or regional land use management strategies (Notaro et al., 2012). Although early studies were restricted to a qualitative assessment of the protective effect of forests (Wasser et al., 1996; Gsteiger, 1993), the quantitative evaluations have taken a prominent place since the development of reliable modelling tools such as Rockyfor3D (Dorren et al., 2006a). Maringer et al. (2016a) evaluated the protective capability of beech forests after a fire, Rammer et al. (2015) analysed the effect of forest management on rockfall protection and timber production in a mature spruce stand and Radtke et al. (2014) focused their work on coppice forests of Northern Italy. Fuhr et al. (2015) is the only reference based on many different mountainous uneven aged stands taken across Northern French Alps. Thereby, most of these works limited their analysis to a local scale or to only one forest type. Mountainous forest stands of *Abies alba*, *Picea abies* and *Fagus sylvatica* and more recently coppices have been particularly studied. Although these types of forests are very common, forests are much more diverse at the Alpine scale. Therefore, the current overview of the protective effect of Alpine forests remains incomplete. Even if common trends are noticeable, it is not possible to quantitatively compare the protective effect between the different forest stands as the methods and the indicators used in the previous studies were not standardized.

The aims of this study were (1) to quantitatively assess the protective effect of forests at the French Alps scale and build a classification based on the protection capability, (2) to compare the protective effect of the different forest types present in the French Alps and (3) to analyse the relations between the protection potential and the forest diversity in terms of stand structure and tree composition. For this purpose, we first used the model Rockyfor3D to simulate the propagation of rocks on 3886 different forest plots spread over the whole French Alps from the Mediterranean sea to the Swiss border. Second, quantitative indicators characterizing the protection potential of each forest plot were calculated from the simulation results and used to build the classification based on protection capabilities. The forest plots were then grouped according to their structure and composition in order to compare the protective effect between the different forest types. Finally, the interactions between forest diversity and protection capabilities were analysed.

3.2 Material and methods

3.2.1 Source and selection of forest data

Forest plots were extracted from the permanent sample plots of the French National Forest Inventory (NFI) based on a systematic grid of 1 km × 1 km covering the complete country. 10% of the plots are measured each year (approximately 6700 forest plots) resulting in nine fractions from 2005 to 2013. NFI data collection is based on circle plots (Robert et al., 2010) where stand properties and topographic data are assessed in a 25-m radius. On each plot, tree characteristics are inventoried for all trees with a diameter at breast height (DBH) greater than or equal to 7.5 cm.

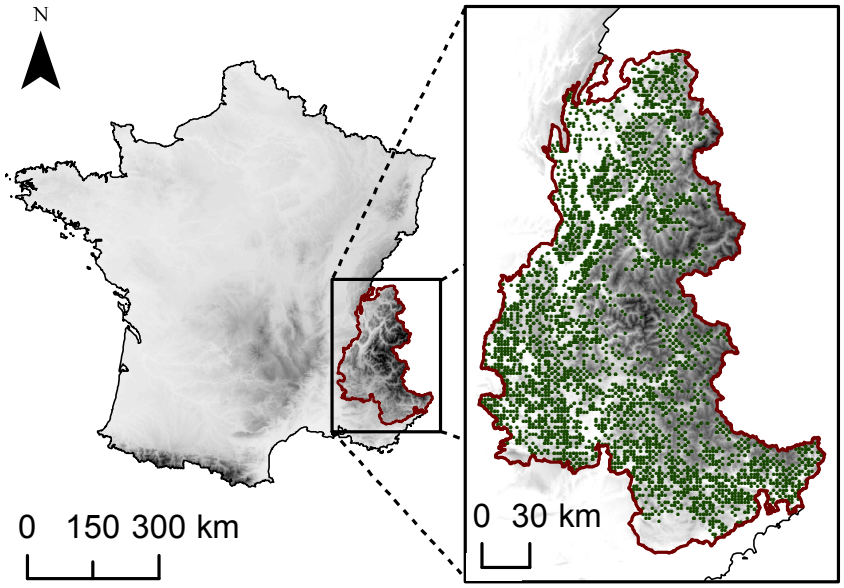

Figure 3.1 – Map of the 3886 selected NFI Alpine plots (green dots). French Alpine region is delimited by the red line.

This study used only the plots with a terrain slope greater than or equal to 20° and located in the Alpine region (Fig. 3.1). When the slope is lower than 20° rocks have a rolling mode of motion and their velocity decreases quickly (Dorren, 2003). Thus, the choice of a 20° threshold allows considering the protection potential of forests in both transit and deposition zones. This procedure resulted in the selection of 3886 NFI plots measured during the period 2005-2013.

3.2.2 Rockfall simulations on NFI plots

The RockyFor3D software (Dorren, 2015) is a rockfall simulation model taking explicitly into account the protective effect of forests. The trajectories of single, individually falling rocks are simulated in three dimensions (Dorren et al., 2006a). The propagation of rocks on a rasterized digital slope is modelled as a succession of sequences of free flights through the air, rebounds on the slope surface, and impacts against trees.

For each NFI plot, rockfall simulations were run on a virtual slope surface in order to focus on the protective effect of forests. Each virtual digital terrain model had a 2-m resolution, a regular slope α corresponding to the NFI plot slope and a total length L of 2100 m in the slope direction. Calculation screens were located every 5 meters along the slope surface to register both kinetic energy and number of passing blocks depending on the distance to the release line.

The protection potential of the forest was evaluated by comparing the results of simulations with forest and without forest on this virtual slope surface (Fig. 3.2).

In order to compare and emphasize differences in the protection provided by the different stand structures and compositions, we fixed the surface roughness to 0 cm and used a medium compact soil (*soiltype*=3) for all NFI plots (Dorren, 2015). This combination emphasizes the protective effect of the forest which corresponds to the worst plausible scenario with rocks covering a long distance down the slope.

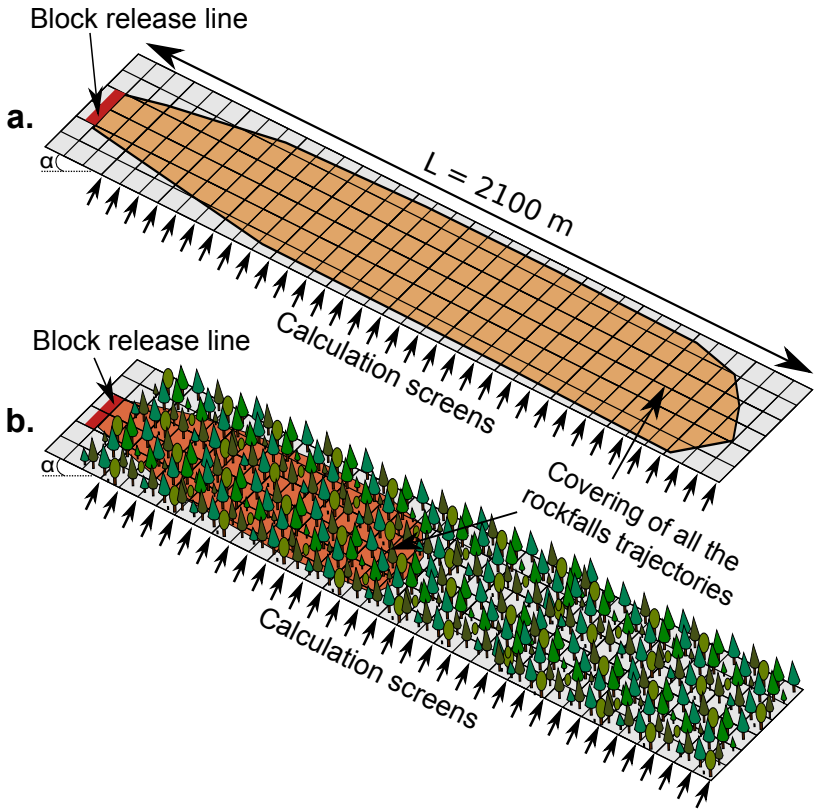

Figure 3.2 – Virtual terrain with uniform slope α and length L. Calculation screens are located every 5 m along the non-forested (a) and forested (b) profiles.

Integration of forest characteristics in Rockyfor3D is done using the locations and the *DBH* of all trees on the slope surface. When a rock impacts a tree, its energy is reduced due to both energy transfer and dissipation. Eq. 3.1 is used to determine the maximum energy reduction of the rock during an impact on a tree depending on the tree species and the *DBH* :

$$max.Ered = Coeff(species) \times 38.7 \times DBH^{2.31} \tag{3.1}$$

The original version of Rockyfor3D uses only two values for *Coeff(species)* : one for conifers and one for broadleaved species. For the purpose of this study, Rockyfor3D was modified in order to use species values of *Coeff(species)* (published in Dorren et al. (2006b)) instead of broadleaved / conifer values. For each NFI plot, the forest was generated following two steps. First, the location of the trees in the slope surface were generated following an uniform random distribution of trees coordinates. Second, diameters and species of each tree were attributed following the diameter and species distributions observed on the NFI plot.

Finally, a total of six simulations per NFI plot were tested : one without forest and one with forest for three rock volumes {0.5, 1, 5} m^3. All the 23316 (3 rock volumes × 2 (with / without forest) × 3886 plots) simulations were computed on the Grenoble University high performance computing centre (CIMENT).

3.2.3 Indicators for the protective effect of forests against rockfall

Dupire et al. (2016a) proposed three indicators to describe and quantify the protective effect of forests against rockfall. These indicators can be estimated with three forest characteristics : the basal area and the mean diameter of all trees with a DBH greater than or equal to 7.5 cm and the forested length in the maximum slope direction from the release area (L). Their main advantage is to be independent of the slope.

In this paper, we mainly focused on the overall rockfall protection index ($ORPI$) which integrates both the proportion of stopped rocks (frequency) and the total energy reduction of the rocks due to the presence of forest (intensity). This indicator is calculated as shown in Eq. 2.1 :

$$ORPI(L) = 100 \times \left(1 - \frac{\sum_{i=1}^{nfor} E_i(L)}{\sum_{k=1}^{nbare} E_k(L)}\right) \tag{3.2}$$

On the same slope surface, $ORPI(L)$ compares the sum of the energies of all the blocks that reached the distance L from the release line according to two configurations : (1) a forested slope surface ($\sum_{i=1}^{nfor} E_i(L)$) and (2) a bare slope surface ($\sum_{k=1}^{nbare} E_k(L)$). $nfor$ and $nbare$ correspond to the number of blocks that reached the distance L for the configurations (1) and (2), respectively.

Two other indicators were proposed by Dupire et al. (2016a). The first one traduces the ability of forests to stop some of the falling blocks. It is called the barrier effect index ($BARI$) which quantifies the reduction in term of frequency of the falling blocks. The second indicator quantifies the reduction of the maximum energy of the blocks and is called the maximum intensity reduction index ($MIRI$). In this study, these two indicators were only used for illustrative purpose.

The three indicators range from 0 (no protective effect) to 100 (high protective effect). They were calculated on each NFI plot and for each rock volume. This resulted on 11658 (3×3886) simulations where values of the three indicators are known for $L \in [50 - 2100]$ m.

3.2.4 Definition of classes for the rockfall protection capabilities of Alpine forests

In the Cartesian coordinate system defined by the basal area as abscissa and the mean DBH as ordinate, the three indicators evolve following a clockwise motion and straight lines can be computed to discriminate plots located above (or under) any ORPI value as shown in Fig. 3.3 (Dupire et al., 2016a).

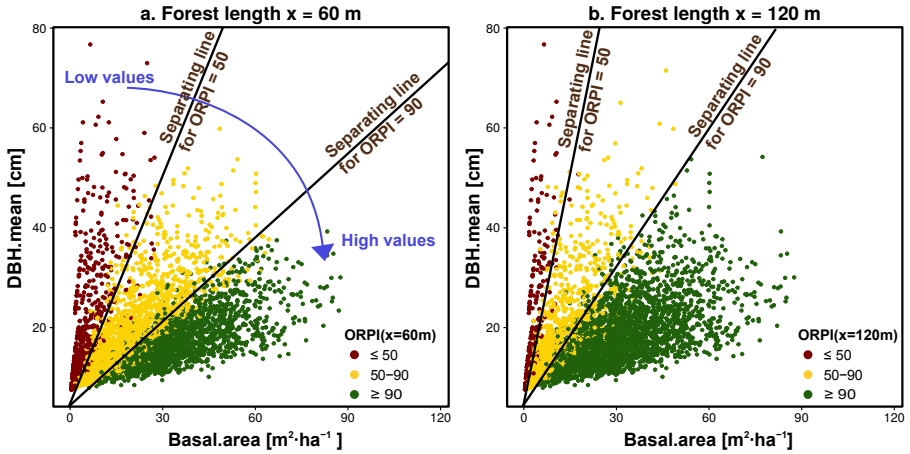

Figure 3.3 – Illustration of the clockwise motion of $ORPI$ values for a rock volume of 1 m^3 at forest lengths x=60 m (a.) and x=120 m (b.). Points are coloured according to $ORPI(x)$. The separating lines between plots were ORPI(x) < 90 (or 50) and plots were ORPI(x) ≥ 90 (or 50) are shown. (Figure adapted from Dupire et al. (2016a))

The classification proposed in this study follows three steps. First, for each NFI plot the minimum forest length L_{99} required to get an ORPI value greater than or equal to 99 (99% of the overall rockfall hazard reduced) were picked out from the results of Rockyfor3D simulations. Second, a k-medoids clustering was applied to define the optimal number of classes k that best separates the NFI plots according to their values of L_{99} (i.e. to their protection capabilities). Finally, the equations of the straight lines separating the k classes were computed.

3.2.4.1 k-medoids clustering

The k-medoids clustering is an adaptation of the k-means clustering. Rather than calculating the mean of the items in each cluster, a representative item, or medoid, is chosen for each cluster at each iteration. k-medoids is more robust to noise and outliers than k-means (Reynolds et al., 2006). Indeed, for each cluster, medoids are calculated by finding object within the cluster that minimizes a sum of pairwise dissimilarities instead of a sum of squared Euclidean distances. The k-medoids clustering can be summarized as follow : (1) choose k objects at random to be the initial cluster medoids, (2) assign each object to the cluster associated with the closest medoid, (3) recalculate the positions of the k-medoids and (4) repeat steps 2 and 3 until the medoids become fixed.

In this study, the aim of the k-medoids clustering is to find the optimal number of clusters (k) that allows the best partitioning of the NFI plots into k classes of rockfall protection capability. The *PAM* (Partitioning Around Medoids) algorithm of the *cluster* R-package (Reynolds et al., 2006; Kaufman et al., 1990) was applied on the dataset defined by three characteristics of the 3886 NFI plots : the basal area, the mean *DBH* and the minimum forest length L_{99} required to get ORPI $\geqslant$ 99 for a rock of 1 m^3.

Three criteria were used to determine the optimal number of clusters with $k \in [2 - 10]$. First, the gap statistic (Tibshirani et al., 2001) was calculated for each value of k. This method returns the optimal number of clusters defined as the smallest k such as *gap(k)* is not more than one standard error away from the first local maximum. Second, the average silhouette width s_i was calculated for each k. Only k satisfying $s_i > 0.5$ (partition qualified as "reasonable structure") were kept. Finally, the smallest number of NFI plots by cluster was checked and only k such as each cluster was composed with at least 5% of the NFI plots (i.e. 200 plots) were selected.

3.2.4.2 Computation of the separating lines between the k classes of protection

The k-medoids clustering was used to obtain the optimal number of clusters k as well as objective threshold values for the minimum forest length required to get ORPI $\geqslant$ 99 (L_{99}) for all NFI plots of each cluster. To evaluate the protection potential of a forest, the equations of the straight lines corresponding to each threshold value of L_{99} were computed as shown in Eq. 3.3 :

$$DBH = slope \times Basal.area + intercept \tag{3.3}$$

Finally, Kruskal-Wallis tests were performed on the NFI plots classified using the separating lines method for the three following stand characteristics : basal area, mean DBH and stem density. The tests were followed by a pair-wise comparisons between protection classes using the Dwass-Steel-Critchlow-Fligner post-hoc procedure (Hollander et al., 2013) only if the Kruskal-Wallis indicated significant differences in the means.

3.2.4.3 Validation of the classification method

Each NFI plot was assigned to one of the k protection classes according to its own coordinates and the locations of the different separating lines in the reference system defined by the basal area as abscissa and the mean DBH as ordinate. To evaluate the quality of this classification, the

predicted protection classes obtained with a rock volume of 1 m^3 were compared to the effective L_{99} values for the three rock volumes {0.5, 1, 5} m^3.

Four statistics were used to evaluate the accuracy (Congalton, 1991): (1) the total accuracy which gives the proportion of correctly classified plots, (2) the user accuracy which return the commission error, (3) the producer accuracy which measures the omission error and (4) the Intraclass Correlation Coefficient (ICC) (Bartko, 1966) which reflects the difference between actual agreement and the agreement expected by chance. The agreement is generally qualified as good from 0.6 to 0.8 and very good when it is greater than 0.8. A value of 1 indicates a perfect agreement.

The last step to evaluate the accuracy of this classification was to check that the values taken by L_{99} and $ORPI(L{=}L_{99})$ were correctly distributed between the k classes defined earlier.

3.2.5 Analysis of the protective effect against rockfalls by forest types

All the 3886 Alpine NFI plots were divided into 4 groups based on the forest composition and the stand characteristics as shown in Fig. 3.4.

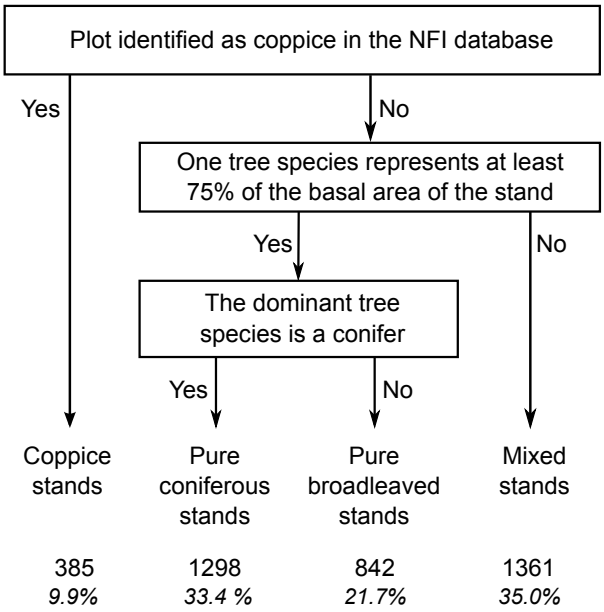

Figure 3.4 – Decision tree for the classification of the NFI plots into four groups. The number and proportion of plots are displayed below each group.

These four groups were used as basis for the forest typology of French Alps. Each group was split into different forest types according to the dominant species present on the NFI plot. The distributions of the L_{99} values of each forest types were then compared.

3.2.6 Forest biodiversity and rockfall protection

The influence of forest composition on the protective effect of Alpine forests against rockfalls was investigated at two levels. First, a comparison of the rockfall protection capacities between pure and mixed stands was performed using Wilcoxon rank sum tests (Hollander et al., 2013; Wilcoxon, 1945).

Second, three indexes were calculated on each NFI plot : two measuring biological diversity and one measuring structural diversity. The two first indexes are the tree species richness and the tree species evenness, both measuring the tree species biodiversity (Stirling et al., 2001). The

richness gives the number of tree species present on each plot while the evenness (Pielou, 1966) measures the relative abundance (number of stems) and the distribution of the different tree species. The third index is the Gini coefficient that measures the inequality of a variable within a set of observation (Weiner et al., 1984; Gini, 1921). Gini coefficient ranges from 0 (perfect equality) to 1 (high inequality). In this study, it was calculated on each NFI plot according to the DBH distribution, therefore it returns an index of the structural diversity of the stand. The distributions of these three indexes within the k rockfall protection classes were analysed and Kruskal-Wallis tests were performed to test for significant difference in the means. Finally, the tests were followed by a pair-wise comparisons between protection classes using the Dwass-Steel-Critchlow-Fligner post-hoc procedure in order to verify if lower forest diversities are observed in forests with lower protection capabilities.

3.3 Results

3.3.1 k-medoids clustering

Table 3.1 shows the values of three different statistics to choose the optimal number of clusters k. All of them converged to an optimal number k=6. It corresponded to (1) the highest number with an average silhouette width (s_i) greater than 0.5, (2) the optimal number according to the gap statistic and (3) the highest number with at least 200 NFI plots by cluster. Values for $k \in [8 - 10]$ are not shown as they did not fulfil the requirements for both average silhouette width and minimum number of plots by cluster.

	Number of clusters k					
	2	3	4	5	**6**	7
Average silhouette width	0.87	0.78	0.62	0.61	**0.60**	0.51
Gap statistic	0.63	0.70	0.76	0.80	**0.84**	0.84
Minimum number of plots by cluster	403	343	322	310	**303**	134

Table 3.1 – Statistics of the k-medoids clustering (PAM) according to the number of clusters k.

Using k=6, the ranges of values for the minimum forest lengths L_{99} to get ORPI $\geq$ 99 are shown for each cluster (i.e. each protection class) in Table 3.2.

Protection class	L_{99} range [m]	Number of plots
Class 1	$L_{99} \leq 110$	1037 plots
Class 2	$110 < L_{99} \leq 190$	1184 plots
Class 3	$190 < L_{99} \leq 320$	652 plots
Class 4	$320 < L_{99} \leq 600$	362 plots
Class 5	$600 < L_{99} \leq 2100$	373 plots
Class 6	$L_{99} > 2100$	278 plots

Table 3.2 – Ranges of L_{99} values and numbers of NFI plots for the six protection classes defined with the k-medoids clustering.

3.3.2 Equations of the partition lines into 6 classes of rockfall protection

Fig. 3.5 shows the partition of the NFI plots into 6 classes with the separating lines method for an intermediate rock volume of 1 m^3. The number of NFI plots and the distributions of the basal area, mean DBH and stem density are also displayed. Equations of the different separating lines are shown in Table 3.3.

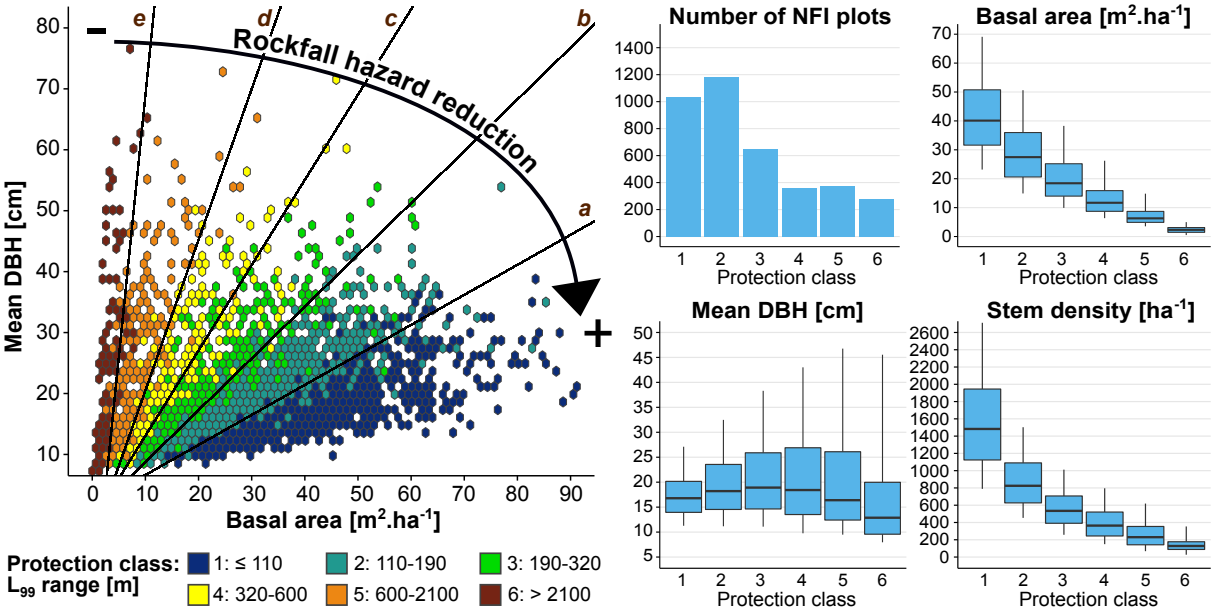

Figure 3.5 – Classification with the separating lines method (Dupire et al., 2016a) with a rock volume of 1 m^3. For a better visualization, NFI plots were grouped by hexagonal pixels, the colour represents the average value of the L_{99} of all the NFI plots contained in the pixel. The number of NFI plots per class and the distribution of the basal area, mean DBH and stem density are also shown.

Kruskal-Wallis tests indicated significant differences in the means for the three stand characteristics displayed in Fig. 3.5. The pair-wise comparisons between protection classes returned significant differences between all classes when considering the basal area or the stem density. However, only the protection class 6 significantly differed from the others when considering the mean DBH.

Separating line between classes	Equations
a : 1 - 2 at L_{99}=110 m	$y = 0.4927 \cdot x + 1.70$
b : 2 - 3 at L_{99}=190 m	$y = 0.8499 \cdot x + 0.26$
c : 3 - 4 at L_{99}=320 m	$y = 1.3999 \cdot x - 0.94$
d : 4 - 5 at L_{99}=600 m	$y = 2.4731 \cdot x - 4.24$
e : 5 - 6 at L_{99}=2100 m	$y = 8.5885 \cdot x - 16.96$

Table 3.3 – Equations of the 5 lines separating the 6 classes of protection for a rock volume of 1 m^3.

3.3.3 Validation of the partition into 6 classes of rockfall protection

The statistics to assess the quality of the partition of NFI plots with the 5 separating lines are shown in Table 3.4. Even if the partition lines were calibrated for a 1 m^3 rock volume, the partition give similar statistics for smaller rock volumes (0.5 m^3). However, regardless the statistic, the quality of partition is lower for largest rock volume (5 m^3). Total, user and producer accuracies oscillate around 0.7 which shows a good correlation between observed L_{99} and predicted protection classes. User and producer accuracies are close which indicates a similar level of commission and omission errors. The values taken by the intraclass correlation coefficient (ICC) indicate a very good agreement between observed L_{99} and predicted protection classes.

	Rock volume [m^3]		
	0.5	**1**	5
Total accuracy	0.74	**0.75**	0.62
User accuracy	0.71	**0.75**	0.62
Producer accuracy	0.73	**0.75**	0.58
ICC	0.91	**0.91**	0.89

Table 3.4 – Evaluation of the quality of the partition with the separating lines.

Fig. 3.6 shows the distribution of the minimum forest length L_{99} observed for the three indicators presented in this study (see section 3.2.3). Predicted protection classes obtained with the separating lines for a 1m^3 rock (abscissa) are compared to L_{99} observed in Rockyfor3D simulations (representing, by extension, the observed protection classes). About 75% of the L_{99} values observed for *ORPI* are distributed between the right protection classes for the rock volumes 0.5 and 1 m^3. For 5 m^3, L_{99} are well classified only for the three best protection classes. *BARI* (rockfall frequency reduction) and *MIRI* (rockfall maximum intensity reduction) are shown for informative purpose. We can observe a shift to one classes up for BARI and to 2 classes up for MIRI.

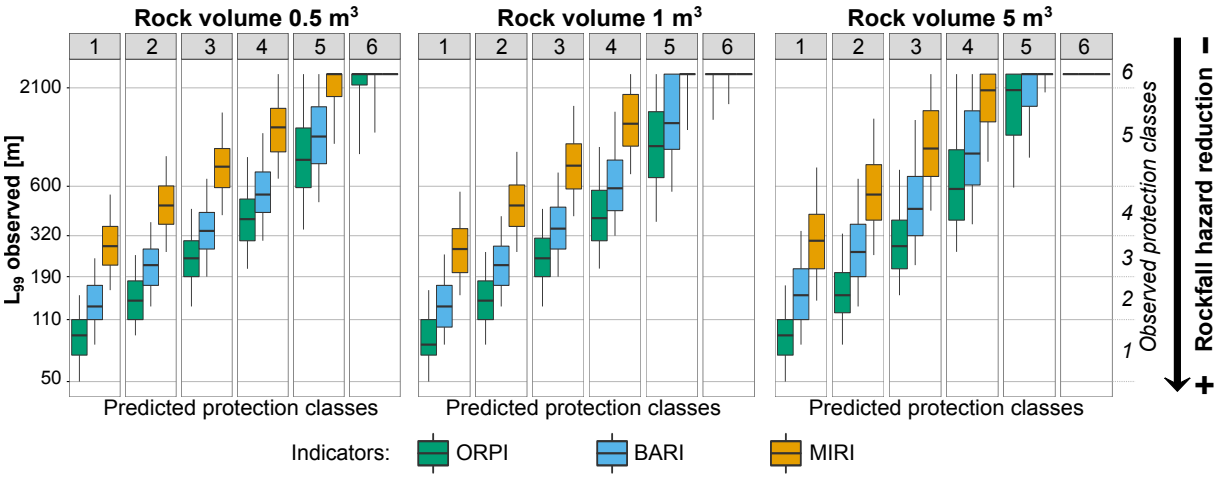

Figure 3.6 – Distribution of the minimum forest length L_{99} observed in Rockyfor3D simulations for the three indicators of rockfall hazard reduction according to the 6 classes of protection predicted with the separating lines obtained for a 1 m^3 rock. Ordinate axis has a logarithmic scale.

The same trends were observed for the distributions of the values taken by the three indicators according to the rock volume and the predicted protection classes (see Fig. A.1). Regardless the rock volume, *ORPI* values are always above 95 which indicates that 95% of the overall rockfall hazard is reduced after a forest length of L_{99}. *BARI* values are slightly shifted down compared

to *ORPI*, they are always above 90 for both rock volumes 0.5 and 1 m^3 but take a wider range of values for biggest rock volume. *MIRI* values are significantly lower. However, we can notice that, regardless the rock volume, the maximum intensity is reduced by at least 50% and even more when considering large rock volume on the best protection classes.

3.3.4 Distribution of the forest types into the 6 classes of rockfall protection

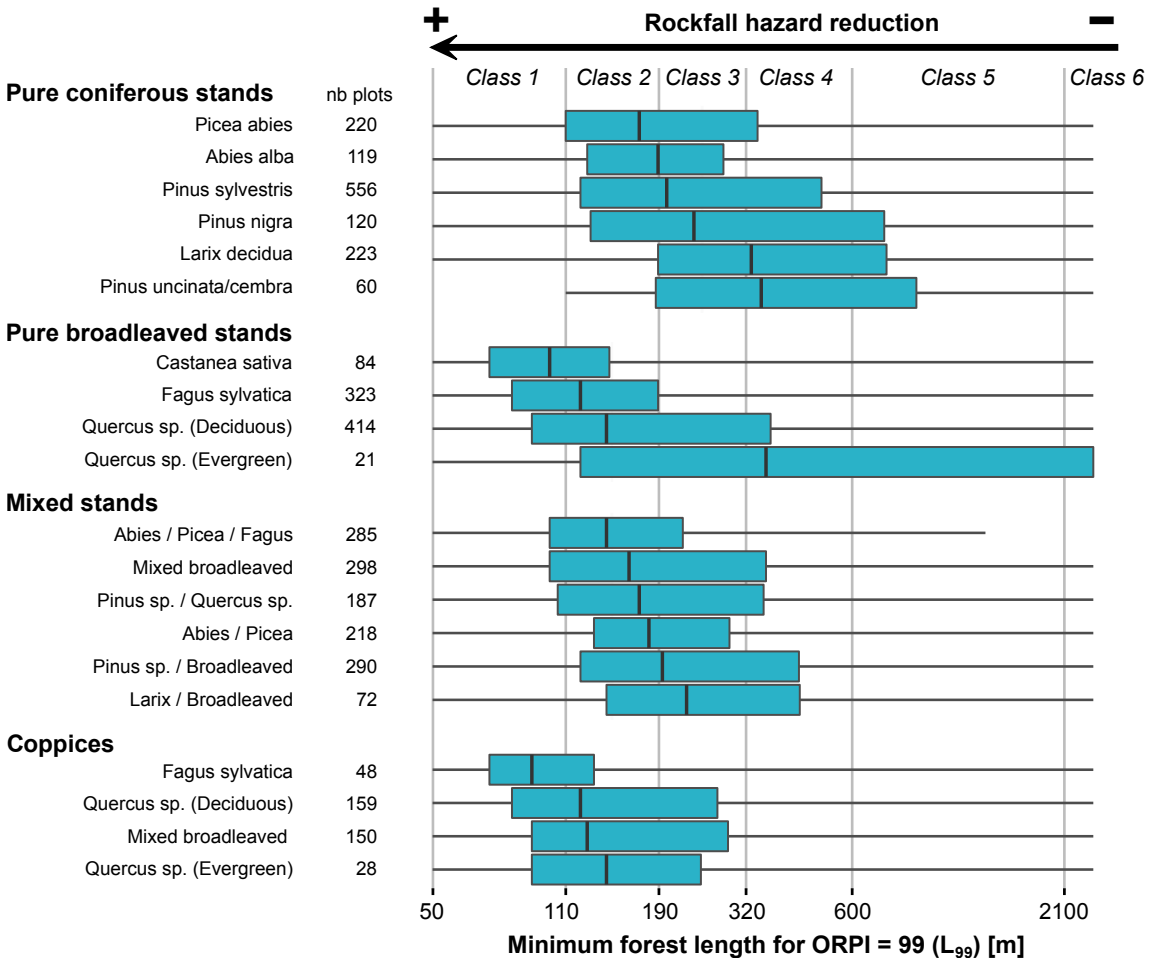

Figure 3.7 – Distribution of the minimum forest length L_{99} observed for each forest type of the French Alps (logarithmic scale). The number of NFI plots by forest type is also given.

Fig. 3.7 shows the distribution of the minimum forest length L_{99} required to get an ORPI value greater than or equal to 99 according to the different forest types. At the French Alps scale, coppices dominated by *Fagus sylvatica* and deciduous *Quercus sp.* present the best rockfall hazard reduction. They are followed by pure stands of *Castanea sativa* and *Fagus sylvatica* and mixed stand of *Abies/Picea/Fagus*. The lowest rockfall reduction rates are observed in pure coniferous stands of *Pinus sp.* and *Larix decidua*. More in details (Fig. A.2), in pure coniferous stands, forest types dominated by *Abies alba* and *Picea abies* present higher protective capabilities than forest types dominated by *Pinus sp.* or *Larix decidua*. In broadleaved stands (pure or coppice), forest types dominated by *Fagus sylvatica* present higher protective capabilities than those dominated by *Quercus sp.*. Finally, in mixed stands, this hierarchy between species is also observed and forest types dominated by *Abies alba*, *Picea Abies* and *Fagus sylvatica* present higher protective capabilities than those dominated by *Pinus sp.* and *Quercus sp.*.

3.3.5 Comparison of the protective effect against rockfall of pure and mixed stand

The comparison of the protection potential of pure stands and mixed stands dominated by the same species was performed using a Wilcoxon rank sum test. For each test, the alternative hypothesis "mixed stand have a higher protective effect than pure stand" was also tested. Results are shown in Table 3.5. In most case, mixed forests presented a higher protection capability, it was always verified when comparing pure coniferous stands with mixed stands dominated by the same species. However, no improvement of the protection capabilities is observed when two coniferous species are mixed or when comparing pure broadleaved stands with mixed stands.

A comparison of the proportion of NFI plots per forest group with a high protective effects according to the forest length in the slope direction is displayed in Fig. 3.8. Considering all NFI plots in each group independently of the forest type confirmed the hierarchy observed previously. Coppices had the highest protection capabilities followed by pure broadleaved stands and mixed stands. Pure coniferous stands came last.

Mixed stand > Pure stand

Pure stand	Mixed stand	Wilcoxon p-value
Picea abies	*Picea / Abies / Fagus*	$< 10^{-3}$
Abies alba	*Picea / Abies / Fagus*	$< 10^{-3}$
Larix decidua	*Larix / Broadleaved sp.*	0.004
Pinus sylvestris	*Pinus sp. / Broadleaved sp.*	0.045
Pinus sylvestris	*Pinus sp. / Quercus sp.*	0.014
Pinus nigra	*Pinus sp. / Broadleaved sp.*	0.050
Pinus nigra	*Pinus sp. / Quercus sp.*	0.009
Pinus unc./cem.	*Pinus sp. / Broadleaved sp.*	$< 10^{-3}$
Pinus unc./cem.	*Pinus sp. / Quercus sp.*	$< 10^{-3}$

Mixed stand ≤ Pure stand

Pure stand	Mixed stand	Wilcoxon p-value
Picea abies	*Picea / Abies*	0.628
Abies alba	*Picea / Abies*	0.403
Fagus sylvatica	*Picea / Abies / Fagus*	0.999
Quercus sp.	*Pinus sp. / Quercus sp.*	0.957

Table 3.5 – Results of the Wilcoxon Rank Sum test performed to compare pure stands against mixed stands. The alternative hypothesis tested is that mixed stands have a higher protective effect.

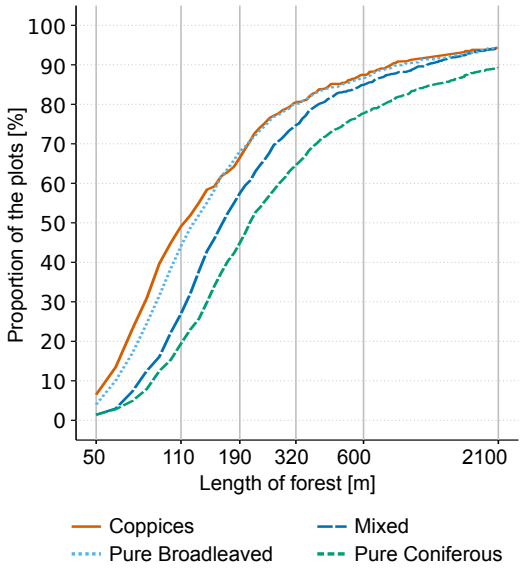

Figure 3.8 – Proportion of NFI plots by forest stand group such as $ORPI(x) \geq 99$ for $x \in [50 - 2100]$ m and for a rock of 1 m^3. Abscissa has a logarithmic scale.

3.3.6 Influence of tree species biodiversity and structural diversity on rockfall protection capability

Fig. 3.9 shows the distribution of NFI plots per protection class according to the Gini coefficient based on DBH and the tree species richness and evenness. For the three indexes, the highest values correspond to the highest diversity. Regardless of the index, the protection classes offering the best rockfall hazard reduction present the highest stand diversity.

Kruskal-Wallis tests indicated significant differences in the means for the three diversity indexes. The pair-wise comparisons between protection classes returned significant differences between all classes regarding the tree species richness and evenness. In addition, the pair-wise comparison underlined a gradual degradation of biological diversity indexes ranging from the highest classes of protection to the lowest. However, for the Gini coefficient based on DBH,

this trend was only observed for the last four protection classes (from 3 to 6), the result of pairwise-comparisons between the first two classes (1 and 2) being not significant.

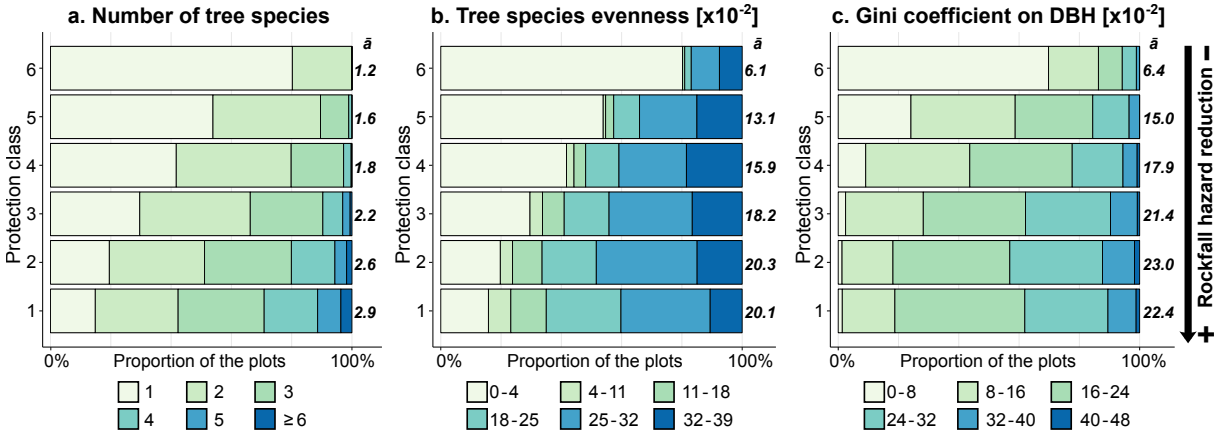

Figure 3.9 – Distribution of the tree species richness (a), evenness (b) and Gini coefficient based on DBH (c) according to the six protection classes. For each protection class, the average value of each diversity indicator ($\overline{a}$) is given.

3.4 Discussion and conclusion

Until recently, the evaluation of the protective effect of forests against rockfall was mainly assessed qualitatively. With the growing capabilities of numerical tools, efforts toward a quantitative assessment become more and more relevant and valuable (Trappmann et al., 2014; Straub et al., 2008; Corominas et al., 2005). This study worked in this direction by proposing a quantitative assessment of the protective effect of forests against rockfalls using only two forest parameters (basal area and mean DBH) taken from field inventories and the overall rockfall protection index ($ORPI$) derived from simulations results. Using $ORPI$ presents the advantage of combining both aspects of risk analysis, i.e. the frequency and the intensity of the hazard. Therefore, it brings added value to previous studies with quantitative assessments mainly focused on the reduction of the frequency (Jancke et al., 2009; Berger et al., 2007; Stoffel et al., 2006). The three parameters exposed before were used to evaluate the minimum length of forest to reach 99% of rockfall hazard reduction (L_{99}). L_{99} was finally adopted as main indicator to evaluate the protective effect of forests at the Alpine scale and to compare protection capabilities of the different forest types of the study area.

3.4.1 Protective effect of forests at the French Alps scale

The 3886 different forests studied in this paper are spread over the whole French Alps from the Mediterranean sea to the Swiss border. The quantitative assessment of the protective effect of forests had never been studied before on such forest diversity, whether in terms of forest structures or compositions. Therefore, this work provided a complete and reliable overview of the protection capabilities of the French Alpine forest which may be generalized to similar European mountain forests.

According to our results, half of the French Alpine forests presented a high ability to reduce rockfall hazard (see Table 3.2 and Fig. 3.5). Indeed, 27% of the forests were classified in the best protection class meaning that 99% of the hazard was reduced after 110 m of forest. This proportion grew up to 57% after 190 m of forest (i.e. considering protection classes 1 and 2).

These forests with a high protection capability were defined by an important growing stock (Fig. 3.5) with high stem density (> 800 stems.ha^{-1}) and high basal area (> 30 m^2.ha^{-1}). These results agreed with real size experiments which showed that, for effective protection, a large number of trees is more important than having thick trees only (Dorren et al., 2006a; Dorren et al., 2005). On the other hand, at the French Alps scale, there were still about 17% of the forests ranked in the two last protection classes meaning that 600 m of forested slope was not enough to reach a reduction of 99% of the rockfall hazard. Those forests were characterized by a stem density lower than 300 stems.ha^{-1} and a basal area lower than 15 m^2.ha^{-1} (Fig. 3.5) which mainly corresponded to sub-alpine stands of *Pinus sp.* or *Larix decidua* and open forests of evergreen *Quercus sp.* (Fig. 3.7).

3.4.2 Protective effect according to structural and biological forest diversities

The comparison of the protection potentials of the main forest types present in the French Alps returned interesting trends, particularly concerning the influence of the dominant tree species on the protection capabilities (Fig. 3.7). First, considering an equivalent proportion of conifers, the protection potential of the different forest types seemed independent of the *Coeff(species)* attributed to each tree species to determinate the maximum energy a tree can reduce (Eq. 3.1). For instance, for coniferous stands, *Pinus sp.* have a *Coeff(species)* of 1.12 which is higher than *Abies alba* and *Picea abies* : 1.0 and 0.9 respectively (Dorren et al., 2006b). Despite that, the protection capability of coniferous stands dominated by *Pinus sp.* was lower. The same trend was observed for broadleaved stands between *Quercus sp.* (2.18) and *Fagus sylvatica* (1.67). This finding underlined that stands dominated by shade-tolerant tree species such as *Fagus sylvatica*, *Abies alba* and *Picea abies* had a better protection potential than stands dominated by light-demanding species such as *Quercus sp.*, *Pinus sp.* or *Larix decidua*. Shade-tolerant species are known to be more competitive (Kunstler et al., 2012) and more susceptible to grow under high forest densities (Götmark et al., 2014; Rohner et al., 2012) which are favourable to reduce the rockfall hazard. This point agreed the recent findings of Toe (2016) and Dupire et al. (2016a) who showed that the structure (stem density, DBH and basal area) and composition of the forest stand were prevailing compared to the mechanical properties of the tree species.

Second, the analysis shown in Fig. 3.8 highlighted a decreasing gradient in the protection capabilities from forest types dominated by broadleaved species to those dominated by conifer species. This can be marginally explained by the values of *Coeff(species)* which ranged from 1.13 to 2.74 for broadleaved and from 0.66 to 1.13 for conifers. The main explanation is certainly in the historical silviculture of broadleaved forests in the Alps which were traditionally managed as coppice to produce firewood for the winter (Radtke et al., 2014). Coppices are generally characterized by a high density of small stems which is particularly efficient for rockfall protection as shown in our results and already mentioned in previous works (Toe, 2016; Jancke et al., 2009). Nowadays, many former coppice forests are undergoing natural succession or are progressively being converted into high forests. Thus, many of the plots classified as "pure broadleaved stands" are in the transition from coppice to high forest and present a high density of stems which explains their high capability in reducing rockfall hazard. Concerning coniferous forests, stands dominated by *Abies alba* and *Picea abies* are mostly uneven-aged with a high structural heterogeneity and a relatively high density, resulting in an interesting protective effect. Conversely, forests dominated by *Pinus nigra* (and to a lesser extend by *Pinus sylvestris*) are mostly plantations aged from 60 to 160 years (Burylo et al., 2011). Their structure is therefore homogeneous with a stem density that decreases with time resulting in a low protective effect. Finally, our study showed that the presence of other tree species (especially broadleaved) in any pure coniferous stand went along with a significantly higher ability to reduce rockfall hazard.

More generally, according to our results (Fig. 3.9), it seems worthwhile to promote heterogeneity and diversity within the forest stand in order to enhance its protective effect. Thus,

higher biodiversity indexes and structural heterogeneity index were observed in the most protective forests. Different studies carried out on European forests have shown that increasing species richness promotes growth ability and higher diversity in shade tolerance (Morin et al., 2011; Vilà et al., 2007), especially in broadleaved forests. This trend was also observed in our results with broadleaved forests and mixed forests showing higher growing stock resources than pure conifer stands resulting in an indirect positive effect on their protection capabilities (Table 3.5).

3.4.3 Implications for forest management

Several lessons can be learned from this study to improve the management of mountain forests. First, our study emphasized the influence of the length of the forested slope in the assessment of the protective effect of a forest. Currently, there are few mentions of the forest length in silviculture guides in Switzerland (Dorren et al., 2015), France (Ancelin et al., 2006) or Italy (Berretti et al., 2006) except that it should be greater than 250 m to ensure a significant protective effect. Although this value seemed correct for the most dense forests analysed in this study, our results demonstrated that 250 m are not always enough to ensure a high level of protection. Moreover, these guides give recommendations in terms of stem density and tree diameter to reach an optimal protective effect in the long term which are meant to be the best trade-off between stand regeneration and protection capability. However, considering these optimal values without taking into account the forest length can sometimes lead to nonsenses. For example, on long forested slopes, keeping a dense forest is not as important as on short slopes and a lower stand density could make the regeneration process easier without consequences on the protective effect against rockfall. Nevertheless, if the rockfall frequency is very high or the slope very steep the rate of broken trees after block impacts may increase significantly (Favillier et al., 2015). Therefore, in these configurations the stem density has to stay high enough to maintain a high protective effect even if the length of forest is important. This point has to be especially considered for forest types dominated by tree species presenting a moderate resilience to numerous rock impacts, i.e. tree species with thin bark such as *Fagus sylvatica* (Trappmann et al., 2013).

Second, our results showed that a high protective effect is compatible with a richer diversity within the forest stands, both in terms of biological diversity and structural heterogeneity. This result extends the findings of Fuhr et al. (2015) who demonstrated that the high biodiversity observed in mature forests with a lot of deadwood can counterbalance a low forest density and provide a satisfactory protection against rockfalls. It also complements the arguments in favour of preserving or even increasing the diversity within forests in order to provide a wide range of ecosystem services (Turner et al., 2007). In this way, a direct recommendation to forest managers would be to promote secondary tree species in their forests and particularly the shade-tolerant species. This is especially important in pure coniferous stands which are the most common forest ecosystems in the Alps.

3.4.4 Limitations and perspectives

The simulations on regular virtual slope and the settings of Rockyfor3D adopted in this study aimed at emphasizing potential differences between forests while keeping a ground description that is common in mountain forests. The combination of regular slope, soil type and soil roughness chosen leads to a maximum propagation of rocks down the slope which corresponds to the worst plausible scenario. Thereby, our results are conservative, meaning that, on rougher ground, on softer soil or on concave slopes, values of L_{99} are likely to be shorter (Monnet et al., 2017). Furthermore, information about the spatial structure of forests was unavailable in NFI database which forced us to use a random generation of the stand. This point can lead to a marginal overestimation of the protective effect of forest as discussed in Dupire et al. (2016a). The same stands characteristics and slope properties were used on a 2100 m slope. This produces homoge-

neous forest stand and slope surface on the entire mountainside which can be unrealistic. Indeed, in mountain areas, forest structures and species compositions evolve following a gradient of altitude. This choice was made to emphasize differences between forest structures and composition while controlling non-forest parameters.

The classification into 6 classes proposed in this study allows a fast evaluation of the protective effect of any Alpine forest with only the basal area and the mean DBH. This method returns a reliable but qualitative assessment of the protective effect of the forest which may be insufficient for a complete analysis with a monetary valuation of this particular ecosystem service. Providing an accurate quantitative assessment of the protective effect against rockfalls of any Alpine forest constitutes an interesting perspective to go further in this work. This could be done using a k-Nearest Neighbours algorithm (k-NN) (Mansuy et al., 2014; Eskelson et al., 2009) on the dataset containing the results of the rockfall simulations on the 3886 forests analysed in this paper. With such a tool, a forest manager could enter the mean DBH and basal area of a forest and instantly get the different quantitative indicators (see section 3.2.3) observed in the most similar forests of the dataset.

Finally, the results of this study could be used in order to identify the forested slopes with a high level of rockfall risk at a large scale. The protection forests could be first identified with a geographic information system by a simple method locating forests situated between rock release areas and human issues (Toe et al., 2015). Then, a rockfall risk level could be given according to the length of forest and the forest types present on the slope. If spatial information about DBH and basal area are known (for example on areas covered with Lidar), the process could even lead to a spatial quantitative assessment of the protective effect of forest against rockfall at a very large scale.

Funding

This work was supported by the French Ministry of Ecology, Sustainable Development and Energy [grant n° 2101527657] ; the ANR SAMCO [grant n° ANR-12-SENV-0004] ; and the Labex OSUG@2020 [grant n° ANR10 LABX56]. Most of the computations presented in this paper were performed using the CIMENT infrastructure supported by the Rhône-Alpes region [grant n° CPER07_13 CIRA].

Appendix A

See Fig. A.1 and Fig. A.2.

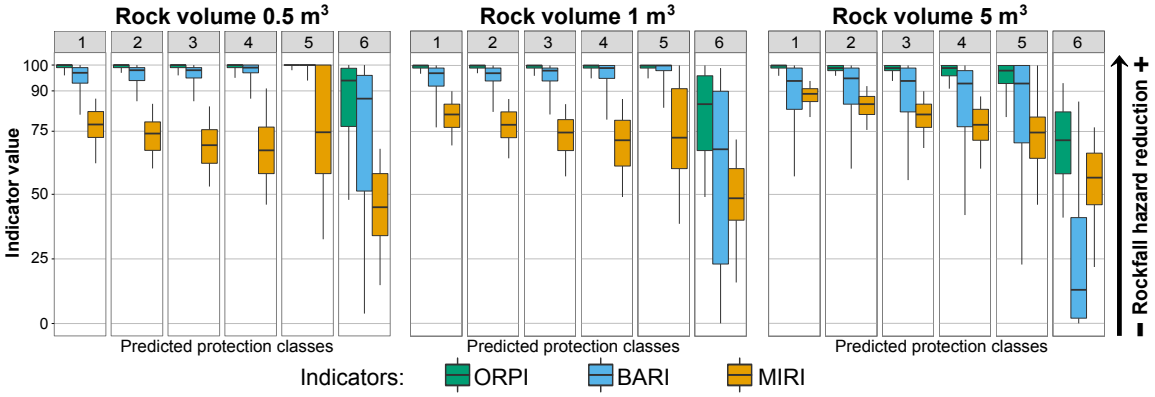

Figure A.1 – Distribution of the values of the three indicators according to the six classes of protection. Indicators values shown for classes 1 to 5 correspond to the values observed at L= 110, 190 320, 600 and 2100 m respectively. For the protection class 6, $ORPI \geqslant 99$ is never reached on the range of forest lengths tested, the indicators values are thus returned for L= 2100 m which corresponds to the maximum length tested.

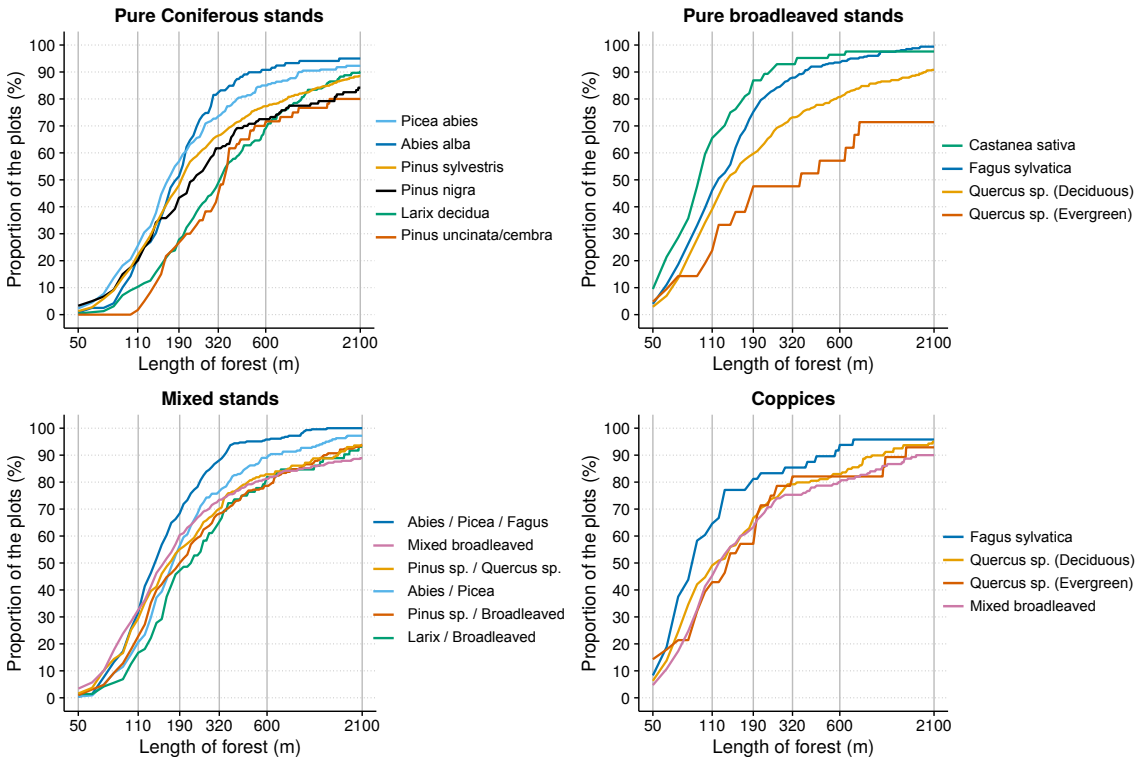

Figure A.2 – Proportion of NFI plots by forest type where $ORPI(x) \geq 99$ for a length of forest $x \in [50 - 2100]$ m and a rock volume of 1 m^3.

CHAPITRE 4

Synthèse de la partie II

Dans cette partie, nous avons cherché à évaluer la capacité de protection contre les chutes de blocs des forêts des Alpes françaises. Pour cela, deux études successives ont été conduites. La première a permis de développer une méthodologie d'évaluation fondée sur des simulations de propagations de blocs et de définir trois indicateurs pour quantifier à la fois la réduction de la fréquence et de l'intensité des chutes de blocs en présence d'une forêt (Chapitre II.2). La seconde reprend les résultats des simulations afin d'analyser dans le détail la capacité de protection au niveau du peuplement forestier et de comparer l'effet protecteur des principaux types de peuplements des Alpes françaises (Chapitre II.3). Les résultats principaux de cette partie sont détaillés ci-après.

Trois indicateurs quantitatifs.

Afin de détailler le plus précisément possible la capacité de protection d'une forêt, trois indicateurs quantitatifs ont été définis dans cette thèse en comparant les données de trajectoire des blocs enregistrées lors de simulations avec forêt et sans forêt. Le premier indicateur, *BARI*, évalue l'effet barrière et retourne la proportion de blocs arrêtés en forêt. Le second, *MIRI*, quantifie l'effet tampon et retourne la réduction de l'énergie maximale des blocs. Enfin, le dernier indicateur, *ORPI*, est une combinaison des deux premiers et renseigne sur la réduction globale de l'aléa en tenant compte à la fois de l'effet barrière et de l'effet tampon.
Comme ces trois indicateurs sont fonction de la longueur de forêt, un dernier indicateur dérivé de *ORPI* a été utilisé pour comparer l'effet protecteur des principaux types de peuplements forestiers des Alpes françaises. Il s'agit de L_{99}, la longueur de forêt nécessaire pour atteindre une réduction globale de l'aléa de 99% (c.-à-d. $ORPI \geq 99$).

Caractéristiques forestières prépondérantes.

Ce travail montre que trois caractéristiques suffisent pour évaluer précisément la capacité de protection d'une forêt. La longueur de forêt le long du versant est le paramètre le plus important. Viennent ensuite la surface terrière et le diamètre moyen, tous deux calculés pour les arbres de diamètre $\geq$ 7.5 cm. Une méthode fondée sur ces 3 grandeurs est proposée dans le Chapitre II.2 pour évaluer rapidement la capacité de protection d'une forêt.

Influence de la structure et de la composition forestière.

La comparaison de la capacité de protection effectuée au Chapitre II.3 a permis d'identifier les types de peuplements les plus protecteurs. Les peuplements dominés par des feuillus, en particulier les taillis, offrent ainsi un niveau de protection plus élevé que les peuplements conifères.

Par ailleurs, cette étude a démontré que les peuplements présentant des diamètres très hétérogènes et plusieurs espèces d'arbres offrent une meilleure protection que les peuplements réguliers monospécifiques.

Troisième partie

Évaluation de l'aléa incendie dans les forêts des Alpes françaises

CHAPITRE 1

Introduction

Contexte et objectifs

Dans les Alpes françaises, riches en biomasse, le départ et la propagation des feux de forêts sont principalement limités d'une part par les conditions climatiques et météorologiques, et, d'autre part, par les sources d'ignitions. Ces dernières sont bien connues dans la zone méditerranéenne (y compris les Alpes les plus méridionales) (Ruffault et al., 2017b; Curt et al., 2016), notamment en raison de disponibilité de la base de données Prométhée (2017) qui recueille tous les événements recensés depuis 1973 sur la zone. Un tel historique n'est pas disponible sur l'ensemble du territoire Alpin français. En effet, dans les Alpes du Nord, les événements ne sont recensés que depuis 2006 (BDIFF, 2017). En raison de l'absence d'informations homogènes sur le long terme sur l'ensemble de la zone d'étude, les sources d'ignition n'ont pas été étudiées dans ce travail de thèse. Ainsi, parmi les deux facteurs limitant les incendies, seules les conditions climatiques et météorologiques favorables aux incendies (désignées ci-après "aléa feu-météo") sont étudiées (Chapitre III.2).

Selon les observations de ces dernières décennies (Gobiet et al., 2014; Dumas, 2013) et les projections futures (Pachauri et al., 2014; Kohler et al., 2010), les Alpes sont particulièrement concernées par les changements climatiques. Ces changements induisent une modification de l'activité des incendies et du régime de feu (Harris et al., 2016) qui peuvent affecter les socio-écosystèmes alpins. Ainsi, l'augmentation de la température et l'extension des sécheresses devraient contribuer à un renforcement de la fréquence mais aussi de l'intensité des feux (Schumacher et al., 2006), tandis que des sécheresses exceptionnelles comme lors de l'été 2003 favorisent des incendies importants et intenses (Ruffault et al., 2016). L'évolution de l'aléa feu-météo au cours de ces dernières décennies a été étudiée à très large échelle en Europe (Venäläinen et al., 2014) et à échelle plus réduite dans la zone méditerranéenne (Moriondo et al., 2006) ou alpine (Wastl et al., 2012). Si ces études soulignent toutes une augmentation de l'aléa forêt-météo, leur échelle d'analyse ne permet pas de prendre en compte la complexité topoclimatique et les nombreuses influences climatiques des Alpes françaises. Le premier objectif de cette partie (Chapitre III.2) est ainsi d'étudier les évolutions spatio-temporelles de l'aléa feu-météo et des régimes de feu dans les Alpes françaises de 1959 à 2015.

La mortalité des arbres suite à un incendie de forêt résulte de processus directs (échauffement des méristèmes) ou indirects (physiologie altérée, attaques de parasites, etc.) (Michaletz et al., 2007). Dans les Alpes, les incendies de surface, qui se propagent principalement dans les combustibles de surface (litière, herbes et arbustes), sont les types de feux les plus communs (Valese et al., 2014). En fonction de leur intensité, les feux de surface peuvent affecter différentes parties de l'arbre : principalement le tronc en cas d'intensité faible, le tronc et le houppier en cas d'inten-

sité modérée à forte (Dickinson et al., 2001). Les feux de couronne sont plus rares dans les forêts alpines (Curt et al., 2016) et généralement concentrés dans la partie la plus méridionale. Les impacts potentiels des incendies sur les forêts des Alpes françaises sont peu connus. Plusieurs études ont porté sur les stratégies de résistance ou de résilience de différentes espèces alpines comme le hêtre (Maringer et al., 2016b) et le mélèze (Moris et al., 2017). Les traits écologiques influençant la résistance au feu des principales essences subalpine ont aussi été étudiés (Fréjaville et al., 2013). Bien que ces études soient très utiles pour comprendre l'impact des incendies sur les espéces étudiées, il est très difficile de les transposer à une approche prospective visant à évaluer la mortalité suite à un incendie se produisant dans des conditions climatiques données.
Le second objectif de cette partie (Chapitre III.3) est ainsi de proposer une méthode permettant d'appréhender la mortalité post-feu à l'échelle de l'arbre puis du peuplement forestier en fonction de différentes conditions climatiques.

Démarche méthodologique

La première étude (Chapitre III.2) vise à évaluer les tendances spatio-temporelles de l'aléa feu-météo dans les Alpes françaises. Les données quotidiennes de température, précipitations, humidité relative de l'air et vent, issues du modèle SAFRAN de Météo-France, ont été utilisées pour calculer deux indices climatiques caractérisant l'aléa feu-météo. Ces indices sont tirés de la méthode canadienne d'évaluation des dangers d'incendie de forêt (CFFDRS) (Van Wagner, 1987). Le premier indice est le *FFMC* (Fine Fuel Moisture Code) qui évalue l'humidité des combustibles fins (herbe, litière de surface, arbustes) et permet d'apprécier leur facilité d'ignition. Cet indice est particulièrement intéressant pour détecter les changements rapides de la teneur en eau des combustibles de surface qui sont les plus susceptibles de brûler dans les feux de surfaces. Le second indice est l'indice forêt-météo (*IFM*) ou Fire Weather Index (*FWI*). L'IFM est utilisé pour informer le public du risque d'incendie, il renvoie ainsi des informations tant sur la facilité d'ignition que sur l'intensité potentielle du feu.
Ces deux indices ont été calculés quotidiennement et spatialisés à haute résolution (25m) sur l'ensemble du territoire alpin. Ils ont servi à identifier les tendances spatio-temporelles des régimes de feu de 1959 à 2015. L'intensité moyenne, la durée de la fenêtre d'opportunité, la saisonnalité et la fréquence de l'aléa feu-météo ont ainsi été étudiées.

Le deuxième chapitre (Chapitre III.3) propose une méthode pour évaluer la mortalité post-feu dans les forêts des Alpes françaises. 112 placettes de descriptions du combustible réparties dans les Alpes françaises ont été utilisées pour simuler le comportement du feu le long d'un gradient de conditions climatiques allant de conditions hivernales à un été très sec et chaud (été 2003). Les simulations ont été réalisées avec le logiciel FlamMap 5.0 (Finney, 2006) qui renvoie des informations prépondérantes pour estimer la mortalité des arbres : intensité et vitesse de propagation du front de flammes et hauteur de flamme. Le comportement du feu selon trois conditions climatiques (feu d'hiver, feu d'été moyen et feu de l'été 2003) a ensuite été déterminé sur 4438 placettes forestières en fonction de la végétation et de l'aléa feu-météo calculé au chapitre III.2. 3886 placettes sur les 4438 sont les mêmes que celles utilisées pour la partie chute de blocs, les 552 placettes supplémentaires n'étaient pas disponibles initialement.
La mortalité post-feu a été estimée à partir du comportement du feu et des caractéristiques de chaque arbre (épaisseur d'écorce, hauteur totale et hauteur de base du houppier) selon différentes méthodes empruntées dans la littérature (Bauer et al., 2010; Bova et al., 2005; Peterson et al., 1986; Spalt et al., 1962).

CHAPITRE 2

Evolutions spatio-temporelles de l'aléa feu-météo dans les Alpes françaises

Spatio-temporal trends in fire weather in the French Alps

Dupire S., Curt T., Bigot S.

Article published in *Science of the Total Environment* Volume 595, Pages 801-817, October 2017.
DOI :10.1016/j.scitotenv.2017.04.027

Abstract : The Alpine area is particularly sensitive to climatic and environmental changes that might impact socio-ecosystems and modify the regime of natural hazards. Among them, wildfire is of major importance as it threatens both ecosystems and human lives and infrastructures. Wildfires result from complex interactions between available vegetation fuels, climate and weather, and humans who decide of the land use and are the main source of fire ignitions.

The changes in fire weather during the past decades are rather unknown in the French Alps especially due to their complex topography. Moreover, local institutions and managers wonder if the ongoing climate changes might increase fire risk and affect the environmental quality and the different ecosystem services provided by the mountain forests.

In this context, we used the national forest fires database together with daily meteorological observations from 1959 to 2015 to investigate the changes in wildfire danger in the French Alps. We analysed the spatial and temporal variations in terms of intensity, frequency, seasonality and window of opportunity of two fire weather indices : the fine fuel moisture code (FFMC) and the fire weather index (FWI) that measure the daily water content of vegetation and the potential intensity of fires, respectively.

Our results showed a major contrast between Southern Alps with a high fire weather danger on average and a significant increase in the past decades, and Northern Alps with low to moderate danger on average that increased only at low elevations. This study contributes to the understanding of the consequences of ongoings climate changes on wildfires in the French Alps. It produced high resolution results that account for the topographic and climatic variability of the area. Finally, the maps of the different fire weather components have practical implications for fire management and modelling and for preventing indirect effects of fires on ecosystems and human assets.

Keywords : Mountain forest · Wildfire · Fire weather · Climate Change · Alps

2.1 Introduction

Mountains environments are especially sensitive to climatic changes (Pachauri et al., 2014; Kohler et al., 2010; Beniston, 2005). The ongoing changes have already resulted in many impacts on natural hazards in the Alps (Einhorn et al., 2015) including snow conditions and avalanches (Castebrunet et al., 2014; Le Meur et al., 2007), rockfalls (Ravanel et al., 2011) or debris flows (Jomelli et al., 2004). Forest fires might also be a major hazard and a threat for many mountain ecosystems and human assets in the next decades. Wildfires may disturb plant and fauna communities (Gibson et al., 2016; Moretti et al., 2002) and alter soil stability with implications on water resources (Cerdà, 1998), soil erosion (Pardini et al., 2017; Shakesby et al., 2016) and runoff (Ebel et al., 2017). They may also affect Alpine forests which ensure protection against natural hazards (Dupire et al., 2016b), thus reducing their effectiveness in protecting human stakes which are generally located down slope (Maringer et al., 2016a).

Recent investigations have stated the main effects of climate changes in the Alps (Gobiet et al., 2014) and demonstrated an increase of temperature throughout the French Alps, especially since the 1980's (Dumas, 2013). Due to their extension and their topoclimatic complexity, the Alps experience many climatic influences and a strong regionalization of climate. In the French Alps (Fig. A.1) the overall annual increase in temperature is about +1°C on the period 1958-2002 (Durand et al., 2009). However, there are strong seasonal (Dumas, 2013) and spatial (Durand et al., 2009) variations. Mid elevations (1500-2000 m) and, in a lesser extent, low elevations, exhibited higher increases. Northern Alps showed a higher temperature increase than Southern Alps.

In the conceptual framework described by Bradstock (2010), climate is the only biogeographic factor that influences the four "switches" of fire regimes (e.g. biomass, availability to burn, fire spread and fire ignition). Thus, climate exerts a strong influence on fire activity in the Alps at different spatial and temporal scales. In the long term, it controls the vegetation composition and biomass (Blarquez et al., 2010). In the short term, it controls vegetation moisture content that drives flammability (Fréjaville et al., 2016) and weather conditions that control fire behaviour (Valese et al., 2014). In the classification of Meyn et al. (2007), the Alpine environments would mostly fit the "biomass-rich and rarely dry ecosystems" with favourable conditions to fuel growth. Therefore, in the French Alps, the fire regimes are mostly driven by fuel moisture and fire ignition. Thus, surface fires of low-to-moderate intensity are the majority (Valese et al., 2014), while intense crown fires are rare and mostly located in the Southern Alps (Curt et al., 2016). Fire size distribution is very asymmetric with many very small fires (< 1 ha) and few large fires, which generally develop during exceptional droughts like in 2003 (Poumadère et al., 2005; Luterbacher et al., 2004). Fires caused by lightning strikes are infrequent (only 15% of the fires) and mostly concentrated during the summer months (Arndt et al., 2013) at the highest altitudes where they primarily affect conifer forests, generally causing small to medium fires (Müller et al., 2015; Müller et al., 2013). In contrast, human-caused fires are prevailing and range from small to large fires. They mostly result from human activities (Reineking et al., 2010) and are predominant in winter and summer. In the last decades, new generation of intense wildfires are observed, they are linked to fuel accumulation due to both land abandonment, increase of the human stakes (Wildland-Urban Interfaces) and climate changes (Valese et al., 2014; Lahaye et al., 2014).

Climate-induced changes in wildfire activity and fire regime may affect Alpine territories and assets (Harris et al., 2016). The increase of temperature and droughts are hypothesized to increase fire frequency and intensity (Arpaci et al., 2013; Wastl et al., 2012), while exceptional droughts or heatwaves like in 2003 promote large and devastative wildfires (Gobron et al., 2005; Poumadère et al., 2005; Fink et al., 2004). Seasonal changes in weather conditions can also modify the fire regime in interaction with the use of fire by humans which are the main source of ignitions (Fréjaville et al., 2015).

Few studies exist concerning wildfire hazard in the Alpine region but none focused on the French Alps. Moriondo et al. (2006) included the Mediterranean Alps in their analysis and indicated that global warming would increase the length of the fire season and the probability of extreme meteorological events. In Switzerland, Reinhard et al. (2005) indicated that long episodes without rain and sunshine duration increased since 30 years, thus potentially decreasing the fuel moisture. Reineking et al. (2010) also depicted the increase in the severity and intensity of droughts and of lightning fires. In a study of 25 meteorological stations located throughout the Alps, Wastl et al. (2012) demonstrated that fire danger increased on average since 1951, but with high regional differences.

The overall aim of this study was to bridge the knowledge gaps on climate-fire relationships in the French Alps by jointly analysing fire weather and fire activity. Detecting hotspots of fire weather danger and spatial-temporal trends becoming more conducive to fire is of paramount importance for fire risk assessment and sustainable management of mountain socio-ecosystems. We investigated the climatic changes over the period 1959–2015 in order to determinate : (i) the fire weather hotspots with high fire weather frequency and intensity ; (ii) the changes in fire weather along seasons ; (iii) the hotspots where fire weather danger is increasing on average and for extreme conditions which promote large and destructive fires.

This approach has scientific and practical implications. First, it enhances knowledge of changing weather conditions on different components of fire weather at the regional scale which is a key scale for operational guidelines on the adaptation of forest management to ongoing climate changes and fire impacts. Second, it provides useful information and maps for a better prevention and suppression of fires.

2.2 Material and methods

2.2.1 Study area

The study area corresponds to the French Alpine area (Fig. A.1) as defined by the French Institutions (Decree n°2016-1208). Located at the South-East of France, it represents about 40600 km^2 with an elevation ranging from 15 m to 4809 m (Mont-Blanc). This territory is divided into Northern and Southern Alps representing respectively 41% and 59% of the total area. Southern French Alps are marked by a mountain climate with a strong Mediterranean influence (dry summer and wet autumn and winter). Northern Alps are characterized by a mountain climate with degraded oceanic influences (rainfall distributed all the year with summer thunderstorm). Moreover, in both areas, the climate undergoes a strong continental component in the Eastern part (inner Alps) (Joly et al., 2010).

The threshold of 800 m of elevation was chosen in order to differentiate the ecosystems from the sub-montane elevation level (low elevation) with those from the montane and Alpine elevation levels (high elevation) (Ozenda et al., 1975). It resulted in a sub-division of the Northern and Southern Alps with low elevation representing 36% of the total area and and high elevations 64%.

2.2.2 Climatic data

The climatic data used in this study were taken from the Safran analysis system implemented by Météo France (Vidal et al., 2010). Safran had initially been designed to provide atmospheric forcing data in mountainous areas for avalanche hazard forecasting and was then used to develop a long-term meteorological reanalysis over the French Alps (Durand et al., 2009). A detailed description of Safran and its application over France is given by Quintana-Segui et al. (2008).

Safran computes, for each climatically homogeneous zone, the vertical profiles of precipitation, temperature, humidity, wind speed and cloudiness every day at noon (precipitation) or every 6 h

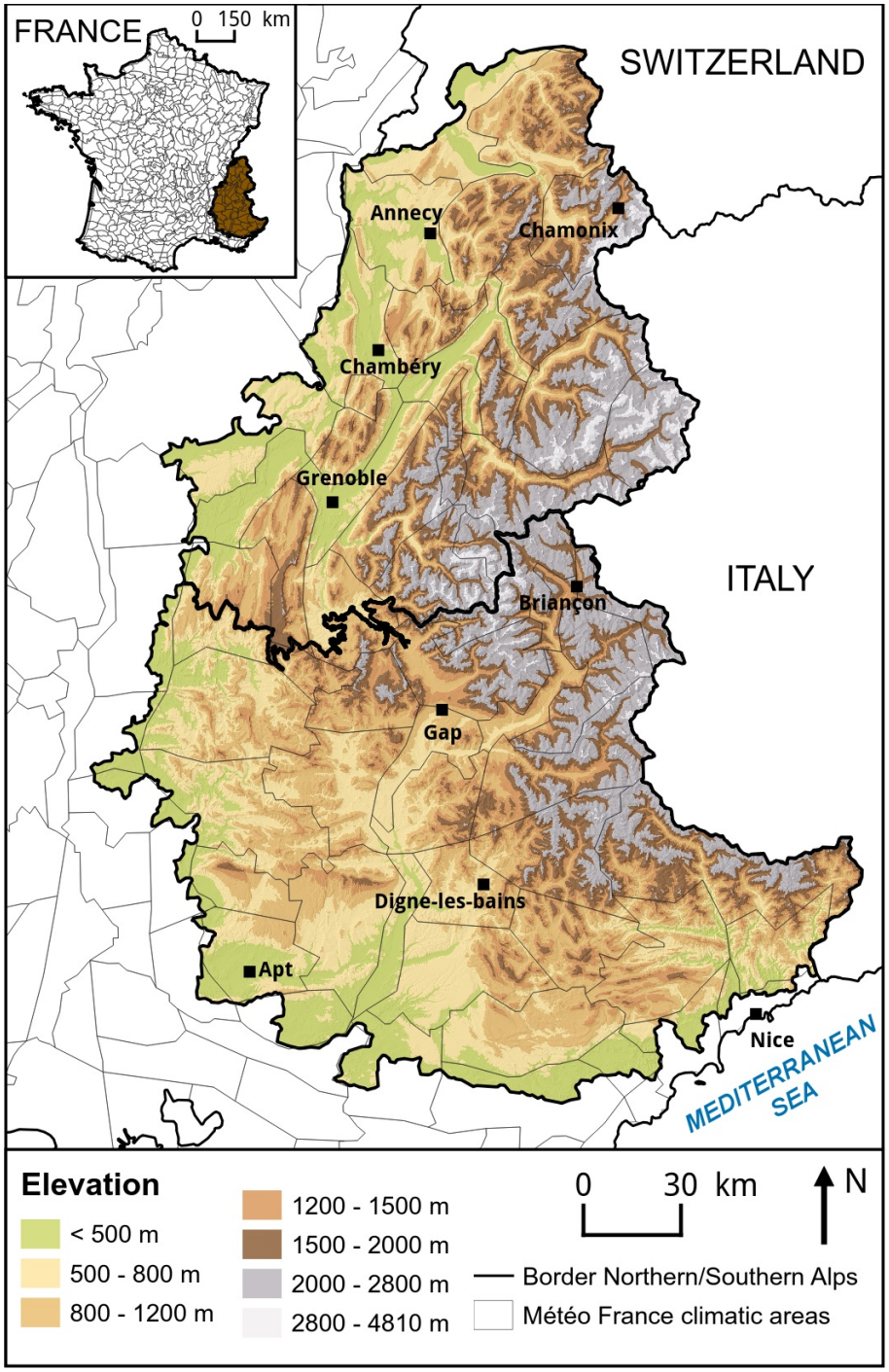

Figure A.1 – Map of the French Alpine area. The border between Northern French Alps and Southern French Alps is delimited with a thick black line. The contours of the Météo France Safran homogeneous climatic zones are shown with a thin black line.

(others variables). For each variable, a first guess of the values along the vertical profiles is predicted from large-scale operational weather prediction model and it is then refined according to surface observations from the Météo France weather stations network. These vertical profiles were available for 57 complete years (1959–2015) and for 615 climatically homogeneous zones covering France (65 zones for the Alpine area) as shown in Fig. A.1. The daily vertical profiles return the values of the different weather variables with an elevation step of 300 m for each

Safran zone.

2.2.3 Fire weather indices

At local scale and on a daily basis, weather controls the moisture of fuels thus their potential for ignition and propagation of fire. Consequently, many methods and indices have been produced to assess the daily wildfire risk based on meteorological data (Amatulli et al., 2013; Van Wagner, 1987).

In this study, we used the Canadian Fire Weather Danger Rating System (CFFDRS) (Van Wagner, 1987) defined by six daily meteorological-based indices, each one measuring a different aspect of fire danger. CFFDRS uses three weather variables measured daily at solar noon (temperature, relative humidity and wind speed) together with the precipitation sum of the last 24 h. The first three indices estimate the daily moisture content of vegetation fuels with specific drying rates. The fine fuel moisture code (FFMC) rates the moisture of live fine fuels including grass, fine shrubs and the surface litter (5-10 cm depth). It ranges from 0 to 101, and it evaluates the ease of ignition of these light fuels. FFMC is especially fitted for detecting rapid and short-duration changes in fine fuel moisture, which often occur in mountains. The duff moisture code (DMC) rates fuel moisture in medium sized surface fuels and in loosely compacted duff (10-20 cm depth). It evaluates the ease of ignition of the light duff and medium fuels (range 0 - ∞). The drought code (DC) is for the deep and compact organic layers, in which fire can smoulder. It estimates if deep duff can ignite, and the mop-up difficulty (range 0 - ∞). Strong increase of DC indicates that severe droughts and heats were established for weeks. As these indices have specific drying rates, they have specific time-lag constants : 16 h for FFMC, 12 days for DMC, and 52 days for DC.

The other three indices indicate the potential fire behaviour. The initial spread index (ISI) combines FFMC and wind speed to estimate the fire spread rate in light fuels in case of ignition. The build-up index (BUI) is a weighted combination of DMC and DC which indicates the total amount of fuel available for consumption. Finally, the fire weather index (FWI) is a combination of ISI and BUI which evaluates the fire-front intensity, and is generally used for public information about fire danger conditions (Van Wagner, 1987).

As recommended in Lawson et al. (2008), the presence of snow has to be taken into account for the calculation of CFFDRS indices in mountain areas. Safran dataset provides the total daily amount of precipitations as well as the distribution between the solid (snow or hail) and liquid (rain) phases. Therefore, in this study, the total amount of precipitation (including snow) was used to calculate FFMC, DMC and DC and FWI values were set to zero in presence of snow.

All CFFDRS indices were computed and their ranges of variation and statistical links with fire activity were compared. We finally focused on FWI and FFMC that performed better than the others indices, thus fitting with the results of Viegas et al. (2000) in Southern Europe and Schunk et al. (2017) in German forests. Moreover, the two indices are complementary as FWI is very integrative and indicates well the overall fire danger and the potential intensity of fire. FFMC detects minor changes in fuel moisture content of surface fuels which are the first most likely to ignite in the Alpine environments and to burn in the predominant surface fires.

2.2.4 Analysis of the national forest fire databases and fire danger assessment

Fire recording practices are heterogeneous in France which led us to use two different fire databases. In the Mediterranean area, subjected to many fires, the authorities launched in 1973 the Prométhée (2017) database. It includes all the Southern Alps area and gathers the wildland and forest fires with an indication of the date, hour, size, and location on a 2×2 km grid.

In other parts of France, the authorities started to record wildland and forest fires much later in the national forest fire database called BDIFF (2017) which has exactly the same structure

as Prométhée. The fire recording history is therefore much more recent. In Northern Alps, the oldest record dates back to 2006.

The objectives of the analysis of the national forest fire databases were first to study the spatial and monthly distributions of the fire records across the French Alps and second to define different fire weather danger from the weather observations on fire days. The annual fire density was first computed for all the French Alps with a resolution of 2 km × 2 km taking into account the two different fire recording periods. The average number of fires registered per month was then analysed distinguishing Northern Alps and Southern Alps.

Several thresholds of fire weather indices have been proposed initially in Canada to indicate the level of fire danger and the potential intensity of fire. These thresholds are commonly acknowledged as correct and are used worldwide in boreal (Flannigan et al., 2016), tropical (Groot et al., 2005) or Mediterranean regions (Bedia et al., 2013). However, they generally need to be fine-tuned to adapt to local conditions (Venäläinen et al., 2014). For this reason, we calculated both FWI and FFMC based on the weather observations from Safran for each fire record according to their date, elevation and location. The empirical distribution function for both FWI and FFMC values observed on fire days were then computed at the Northern Alps and Southern Alps levels.

Four fire weather dangers were then defined for each index according to the mean value of the 50^{th}, 75^{th} and 90^{th} percentiles of the two regions. Values below the 50^{th} percentile were defined with a low fire weather danger, those in the range 50^{th}-75^{th} percentiles with a moderate danger, 75^{th}-90^{th} with a high danger and above 90^{th} with an extreme fire weather danger. These threshold values were used in the following steps of the study in order to address different fire weather dangers.

2.2.5 Fire weather components

For each elevation step (300 m) of each 65 Safran zone, we calculated the daily values of the different CFFDRS indices from 01 January 1959 to 31 December 2015. It resulted in 11.2 millions of daily values covering 57 complete years. The main components of fire weather danger were derived from these daily values and investigated in both space and time (Fig. A.2).

2.2.5.1 Intensity of fire weather

The intensity of fire weather is hereafter called the fire weather danger. It was assessed using the annual absolute values taken by FWI and FFMC for three different percentiles of annual values (95^{th}, 75^{th} and 50^{th}). For each percentile, the average value observed on the period 1959–2015 was calculated in order to determinate the fire weather danger on average climatic conditions. The annual values observed on the year 2003 were also extracted in order to determinate the fire weather danger during exceptional drought year (Poumadère et al., 2005). Finally, the linear temporal trends for the three percentile levels were investigated.

2.2.5.2 Length of the fire weather window

The fire weather window (FWW) is defined by the number of consecutive days with a defined fire weather danger. It indicates the annual maximum duration of the period according to a gradient of favourable meteorological conditions (from moderate to extreme fire weather danger). A high FWW value indicates a long time period during which there is a greater likelihood that multiple fires occur, thus increasing the difficulty of suppression for firemen. The FWW was investigated for both FWI and FFMC and for the three highest fire weather dangers defined at section 2.2.4. As for the fire weather intensity, we calculated the FWW for average climatic conditions and

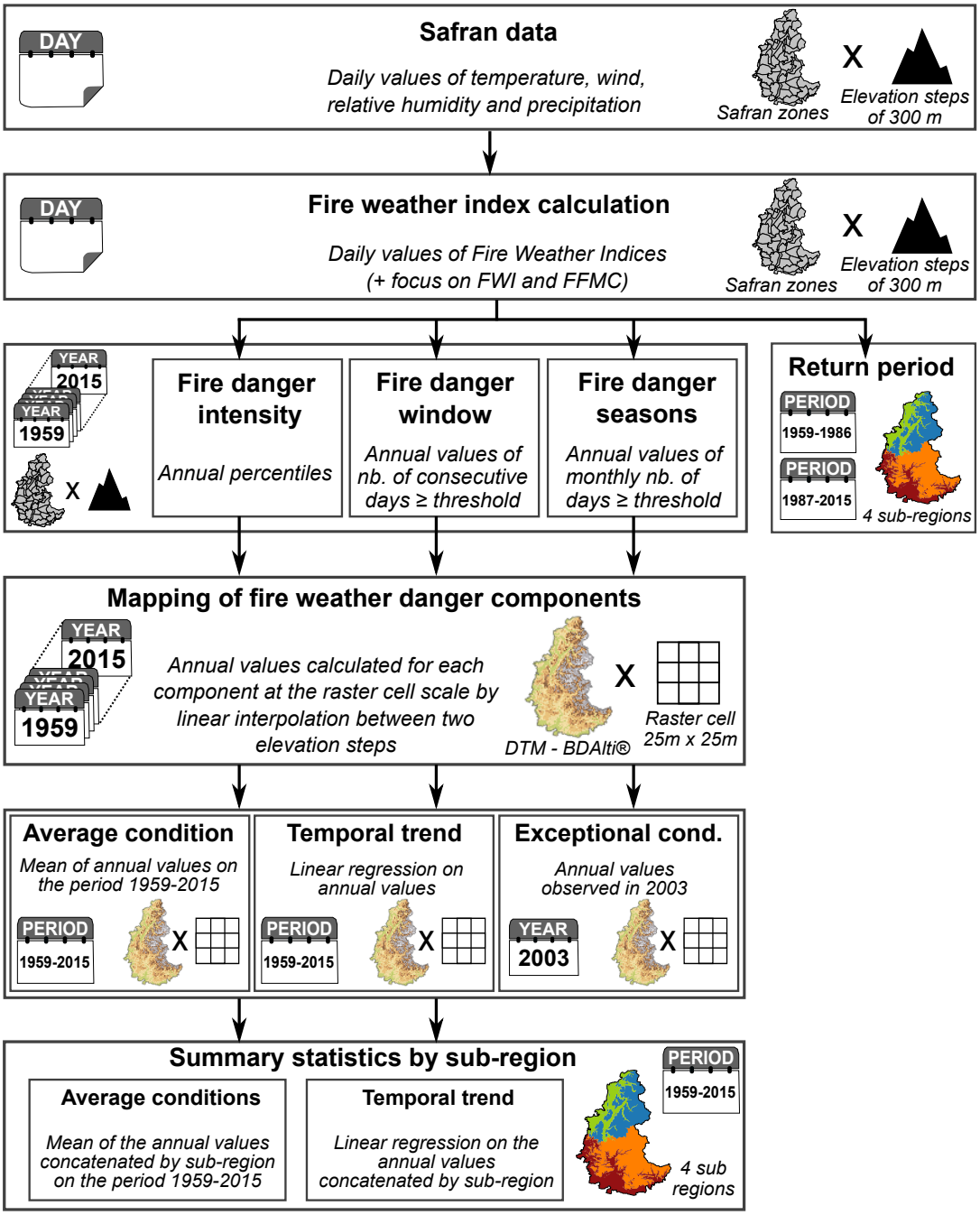

Figure A.2 – Workflow chart of the spatio-temporal analysis. Calendar icons and map icons indicate respectively the time and the spatial scales of analysis for each step of the work.

exceptional climatic conditions and we investigated the linear temporal trend over the period 1959–2015.

2.2.5.3 Monthly analysis of the fire weather

Wildfires can be ignited throughout the year by humans or lightening strikes in the Alps and it is of importance to know what is the period with favourable meteorological conditions for the fires. This point was investigated following the number of days (not necessarily consecutive) per month with a defined fire weather danger. As for the *FWW*, the thresholds corresponding to the

three highest fire weather dangers defined at section 2.2.4 were used. The number of days per month was first computed for each year of the period 1959–2015 before calculating the mean number of days per month observed considering the whole time period.

Finally, the linear temporal trends over the period 1959–2015 in the monthly number of days of each one of the fire weather danger were analysed.

2.2.5.4 Return period

The return period, or the recurrence interval is an estimate of the likelihood of an event to occur which is commonly used in natural hazard assessment (Jomelli et al., 2004). It estimates the frequency of different fire weather danger. In our study, the return period was calculated using the generalized extreme value (GEV) distribution (Coles et al., 2001) as proposed by Wastl et al. (2012). For both FWI and FFMC, the time series of daily values were used to compute the probability distribution of extreme events using the R package extRemes (Gilleland et al., 2016). The computation gave the return level (e.g., a FWI or FFMC value) associated to a given return period, e.g. the number of years to wait to observe the same or a greater index value. To investigate temporal trends in the return period we divided the observations into two sub-periods of 28 (1959-1986) and 29 (1987-2015) years.

2.2.6 Mapping and statistical analysis

In mountain areas, the fire weather danger may be spatially heterogeneous, especially due to variation of elevation (Moriondo et al., 2006) and to topoclimates (Wastl et al., 2012). The Safran dataset used in this study already integrates topoclimates by dividing the French Alpine area into 65 homogeneous climatic zones. The elevation issue was dealt combining the elevation step of 300 m of Safran zone with the BD Alti®, a digital elevation model (DTM) provided by the French National Institute of Geographic and Forest Information (IGN) with a 25m × 25m resolution.

2.2.6.1 Fire weather component mapping

Each fire weather component was first annually calculated for each Safran zone and each elevation as described in section 2.2.5. These annual components were then computed for each raster cell of 25m × 25m according to the elevation and the Safran zone of the cell. The component value of the cell was calculated by linear interpolation between the values with a 300 m step of elevation given by the Safran zone. As example, if a raster cell had an elevation of 700 m, we did a linear interpolation between the two component values of the Safran zone corresponding to 600 m and 900 m.

The mean fire weather danger component observed on the period 1959–2015 were then calculated for each raster cell from the annual rasters in order to produce a map of the component on average climatic conditions. The raster maps corresponding to the year 2003 were used to illustrate exceptional climatic years. Finally, the linear temporal trends were computed for each raster cell using a linear regression over annual values of the fire weather component.

2.2.6.2 Regional statistics

To facilitate and summarize the analysis over the French Alps, we divided the area into four regions according to the latitude (Northern Alps / Southern Alps) and the elevation (Low / High). The border between Northern and Southern Alps was used for the latitude splitting. The threshold value for the elevation was 800 m as explained in section 2.2.1.

The summary statistics by region were obtained with the following steps. First, the annual fire weather component values were calculated by averaging the values observed for each raster

cell corresponding to the region. Second, the mean component value over the period 1959–2015 (average climatic conditions), was calculated from annual values. Finally, the linear temporal trends were computed for each region using a linear regression over mean regional annual values of the fire weather danger component.

2.3 Results

2.3.1 Analysis of fire records

5731 fires (since 1973) have been recorded in the South and 413 fires (since 2006) in the North, although, for both areas, the recordings might not fully exhaustive. Once normalized to the same time period and the same area, we observed five times as many fires in the South ($7{\cdot}10^{-3}$ fires·year^{-1}·km^{-2}) as in the North ($1.4{\cdot}10^{-3}$ fires·year^{-1}·km^{-2}). The mean annual burnt area was 80 ha·year^{-1} (55% in summer) in the North and 938 ha·year^{-1} (70% in summer) in the South.

Fig. A.3 shows the location and density of the forest fires recorded in the National databases across the French Alpine area. Independently of the latitude, 75% of the fires were located at low elevations ($\leq$ 800 m). Both areas showed a bimodal repartition of fire frequency with two peaks of fire activity rather similar : one centred on March, and one centred on July/August (Fig. A.4.a). The first period is mostly characterized by small vegetation fires due to agriculture and management of vegetation (shrub clearing and burning of vegetation residues). These winter fires burning during periods with moderate FFMC and low FWI values generate low-intensity surface fires. The second period corresponds to the summer with fires covering larger areas. These summer fires happen with low fuel moisture and dry weather that promote high-intensity fires.

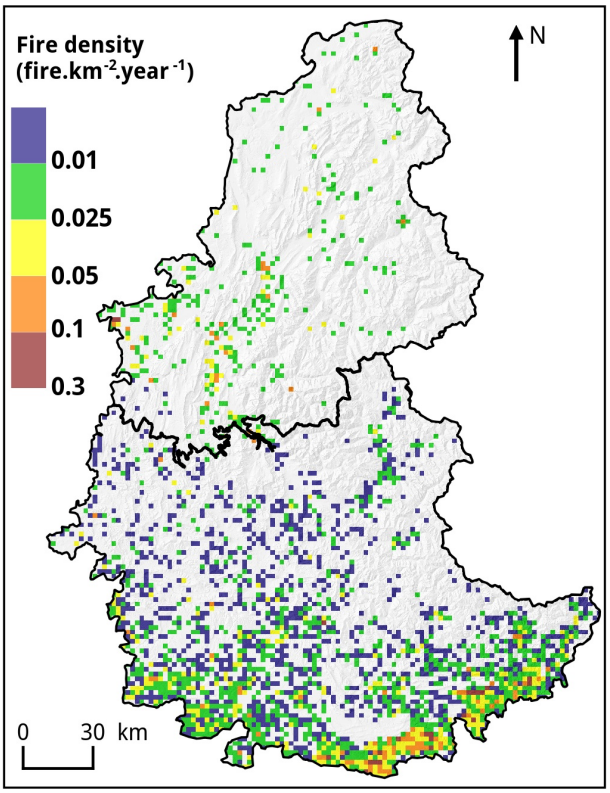

Figure A.3 – Map of the fire density computed from BDIFF and Prométhée fire databases. Resolution : 2 km × 2 km.

The fire weather indices were calculated for each historical fire record in order to determinate different fire weather danger. Fig. A.4.b and Fig. A.4.c shows the Empirical Cumulative Density Functions (ECDF) according to the values observed for FWI and FFMC on fire days. Lower FWI values were observed on the fire days in the Northern Alps compared to Southern Alps while FFMC values were quite similar for both areas. Three different thresholds indicating four fire weather dangers were calculated from the ECDF curves. They were characterized by the average values of each index corresponding to the 50^{th}, 75^{th} and 90^{th} percentiles, standing respectively for moderate (FWI $\in$ [10.5-21.5[; FFMC $\in$ [88.1-90.5[), high (FWI $\in$ [21.5-34.5[; FFMC $\in$ [90.5-92.3[) and extreme (FWI $\geq$ 34.5 ; FFMC $\geq$ 92.3) fire weather dangers. These values are similar to FFMC and FWI values encountered in literature for the Mediterranean area (Bedia et al., 2013; Moriondo et al., 2006).

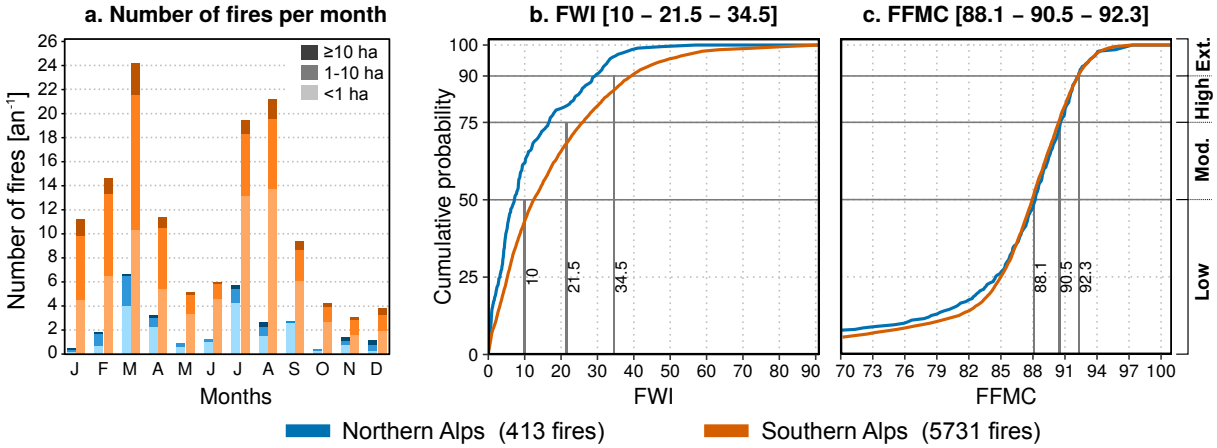

Figure A.4 – Distribution of the average annual number of fire records per month observed in the databases (a.) and Empirical Cumulative Density Function (ECDF) of FWI (b.) and FFMC (c.) values measured at the different dates and locations of the fire records. Figures between hook brackets in the title of (b.) and (c.) indicate the thresholds values for moderate, high and extreme fire weather danger.

2.3.2 Intensity of fire weather

Fig. A.5 shows the intensity of the fire weather danger (annual 95^{th} percentile) and the linear temporal trends of the fire weather indices during the period 1959–2015. In the Northern Alps, mean index values indicated a moderate fire weather danger at low elevations ($\leq$ 800 m) and a low fire weather danger at higher elevations. In average conditions, the fire weather danger regarding any index was therefore low to moderate. In exceptional conditions (year 2003), it increased significantly at any elevation. A high fire weather danger was reached in the foothills (+100-150%) and a moderate danger between 800 m and 1800 m (+50-100%). Above 1800 m the rise was in the same range, although the fire weather danger remained low. Finally, FFMC and, to a lesser extent FWI, showed a positive linear trend in most of the low elevations of Northern Alps indicating an increase of the average fire weather danger. Non-significant trend was observed at higher elevations except for some Prealps mountains such as Chartreuse and Belledonne where a light negative trend was detected.

In the Southern Alps, mean index values indicated high to extreme fire weather danger at low elevations ($\leq$ 800 m) and moderate at higher elevations. In average conditions, the fire weather danger regarding any index was therefore moderate to high. In exceptional conditions, it increased significantly at any elevation to reach a high or extreme danger in most of the area. Average raise was between +20% and +50% on extreme year except for the South-East with an increase between +50% and +100%. Finally, in most of the Southern Alps, positive temporal

trends were observed on the period 1959–2015 regarding the 95th percentile annual values of FWI and FFMC with a positive gradient from North-West to South-East.

Average values and linear temporal trends were also analysed for the annual 50^{th} and 75^{th} percentiles for both FWI and FFMC indices Table 2.1. The same areas appeared with non-significant trends independently of the percentile. However, when significant, the trends were more pronounced for higher percentiles.

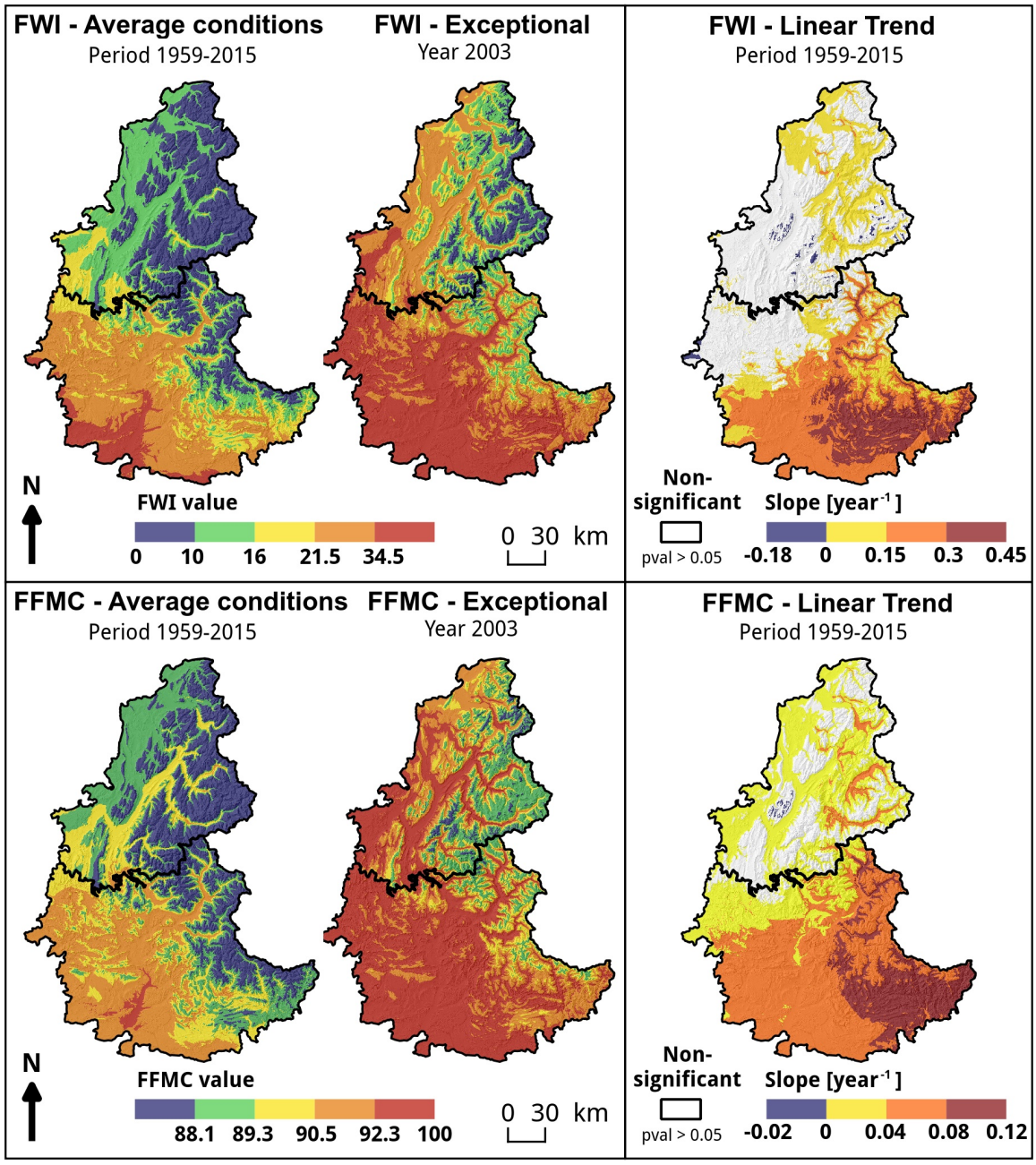

Figure A.5 – Maps of the intensity of the fire weather observed during the period 1959–2015. The annual values considered in these maps were annual 95th percentile values observed for each raster cell. Average conditions stand for the average of the annual values observed on the period 1959–2015. Exceptional values correspond to the annual values observed in the dry year 2003. The temporal trends observed on the period 1959–2015 were mapped on the right column for each index. Significant trends (p-value ≤ 0.05) are shown using colors, non significant trends are shown in white.

	Percentile	North Elevation ≤ 800 m		North Elevation > 800 m		South Elevation ≤ 800 m		South Elevation > 800 m	
		M ± Sd	Trend	M ± Sd	Trend	M ± Sd	Trend	M ± Sd	Trend
FWI	95^{th}	14.1 ± 4	**57***	7.8 ± 2.2	13	31 ± 6.4	**202****	17.2 ± 4.9	**163****
	75^{th}	4.3 ± 1.8	20	1.7 ± 0.8	5	15.1 ± 4	**103****	6.7 ± 2.5	**77****
	50^{th}	0.6 ± 0.3	3	0.3 ± 0.1	0	4.9 ± 1.8	**34***	1.7 ± 0.9	**25****
FFMC	95^{th}	89.2 ± 1	**26****	87.7 ± 0.9	14	91.3 ± 1.2	**55****	89.2 ± 1.2	**59****
	75^{th}	84.1 ± 1.6	21	80.5 ± 2.5	-8	88.4 ± 1	**43****	85.7 ± 1.5	**49****
	50^{th}	70.5 ± 4.8	31	61 ± 5.9	-58	83.6 ± 1.9	**37***	76.5 ± 3.9	**72***

M and Sd are without unit. Trend unit is 10^{-3}·year^{-1}

Signif. codes : ** : p-value≤0.001, * : p-value≤0.05

Table 2.1 – Average period value (M), standard deviation (Sd) and linear temporal trend of FWI and FFMC observed during the period 1959–2015 for different percentiles of annual values and for the 4 sub-regions of the French Alps.

2.3.3 Length of the fire weather window (*FWW*)

The *FFW* was studied for both FWI and FFMC indices (Fig. A.6 and Table 2.2).

The *FWW* for a moderate to extreme fire weather danger (Fig. A.6) was relatively short in Northern Alpine low elevations (about 10 days for both indices) and very short at higher elevations (about 5 days for both indices) during an average year. This partly explained the low occurrence of big fires in this part of the area. In the Southern Alps, the *FWW* was much longer with at least 20 consecutive days at low elevations (29 days for FWI) and 10 consecutive days at highest elevations (14 days for FWI). During an extreme year such as 2003, the *FWW* increased by 4 to 8 days regardless of the area.

	Fire weather danger	North Elevation ≤ 800 m		North Elevation > 800 m		South Elevation ≤ 800 m		South Elevation > 800 m	
		M ± Sd	Trend	M ± Sd	Trend	M ± Sd	Trend	M ± Sd	Trend
FWI	Moderate (≥10)	11.2 ± 5	37	4.9 ± 3	18	29.3 ± 8.7	**110***	14.4 ± 5.6	**124***
	High (≥21.5)	2.8 ± 2.9	34	0.7 ± 0.9	**22***	16.5 ± 7.1	**161****	5.3 ± 3.6	**118*****
	Extreme (≥34.5)	0.4 ± 0.8	**14*****	0.1 ± 0.2	**3***	5.4 ± 3.9	**123*****	1.4 ± 1.3	**47*****
FFMC	Moderate (≥88.1)	9.7 ± 3.8	**49***	6 ± 2.4	21	19.9 ± 5.7	**141****	10.8 ± 4	**156*****
	High (≥90.5)	3.7 ± 2.6	**58****	1.9 ± 1.4	**42*****	11.7 ± 5	**183*****	4.5 ± 3	**157*****
	Extreme (≥92.3)	1.1 ± 1.4	**39*****	0.5 ± 0.6	**19*****	5.2 ± 3.7	**180*****	1.7 ± 1.5	**63*****

M and Sd units are days. Trend unit is 10^{-3}·day·year^{-1}

Signif. codes : *** : p-value ≤ 0.001, ** : p-value ≤ 0.01, * : p-value ≤ 0.05

Table 2.2 – Fire weather windows for three different fire weather danger. Mean (M), standard deviation (Sd) and linear temporal trends (Trends) are given for the period 1959–2015 and for each subregion of the French Alps. Bold values indicate significant temporal trends.

The linear temporal trends of *FWW* for FFMC over the period 1959–2015 (Table 2.2) were positive in all parts of the French Alps, and so independently of the fire weather danger, except for moderate danger at high elevations of the North. The trend was however more pronounced in Southern Alps especially for high fire weather danger. This indicates an increase of the period favourable to surface fire in all the French Alps. The temporal trends regarding FWI were non-significant in Northern Alps for moderate to high fire weather danger. They were lightly positive for extreme fire weather danger although the *FWW* for such events remained very short. However in Southern Alps, the temporal trends were marked for all fire weather dangers.

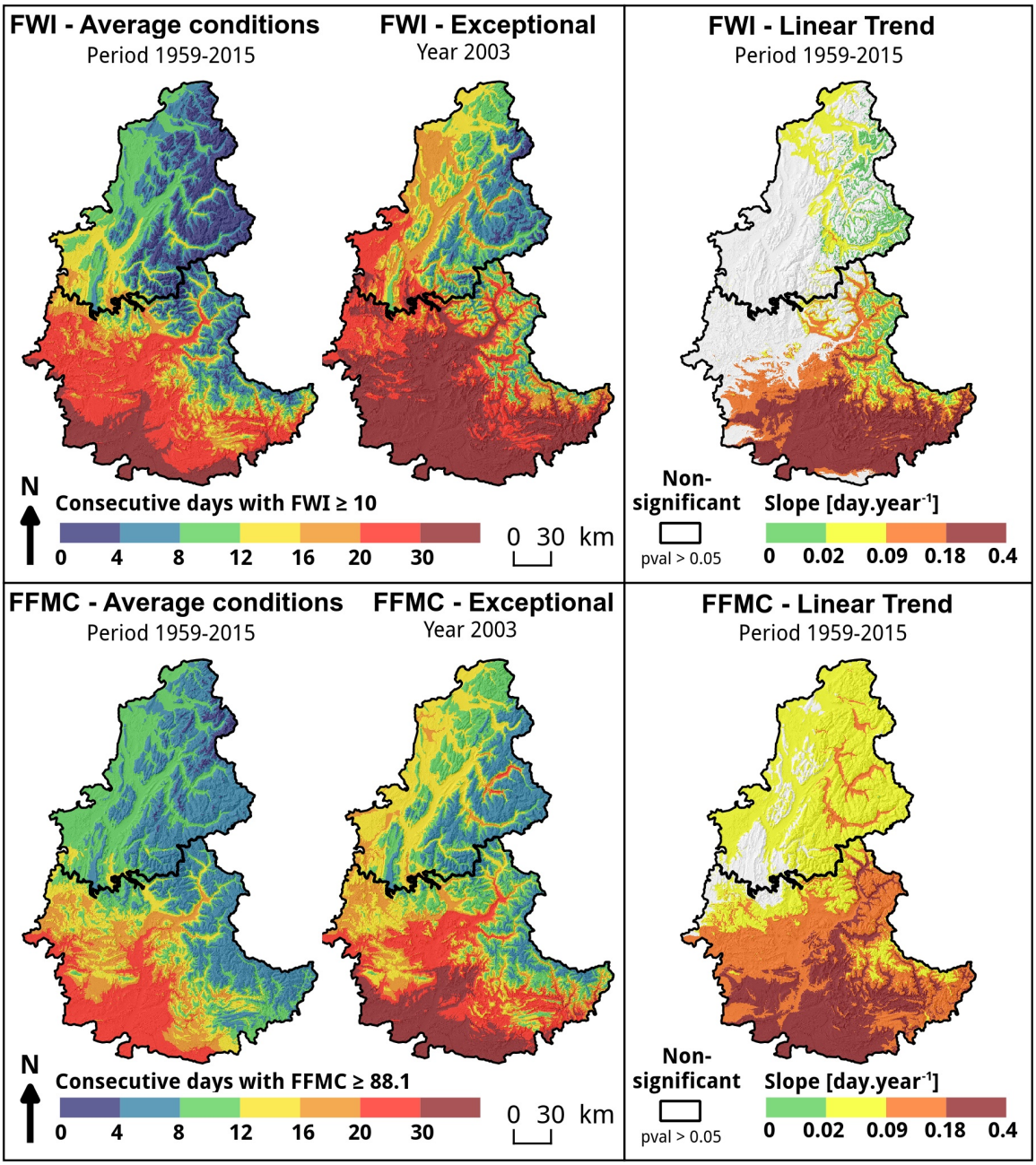

Figure A.6 – Maps of the average fire weather window *FWW* for moderate to extreme fire weather danger (FWI≥10 and FFMC≥88.1) observed during the period 1959–2015. Average conditions stand for the average number of days above the threshold observed on the period 1959–2015. Exceptional values correspond to the dry year 2003. The temporal trend of the annual *FWW* values observed on the period 1959–2015 is mapped on the right column for each index. Significant trends (p-value ≤ 0.05) are shown using colors, non significant trends are shown in white

2.3.4 Seasonal variations of fire weather

The seasonal variations of fire weather were analysed regarding the number of days per month with a moderate to extreme fire weather danger, for each month of the year and for FWI and FFMC (Fig. A.7 and Annexes B.1, B.2, B.3 and B.4). The linear temporal trends considering the number of days by month for each year of the period 1959–2015 were also analysed.

Regarding FWI (Fig. A.7 and Annexes B.1, B.2), the first days with moderate or higher fire

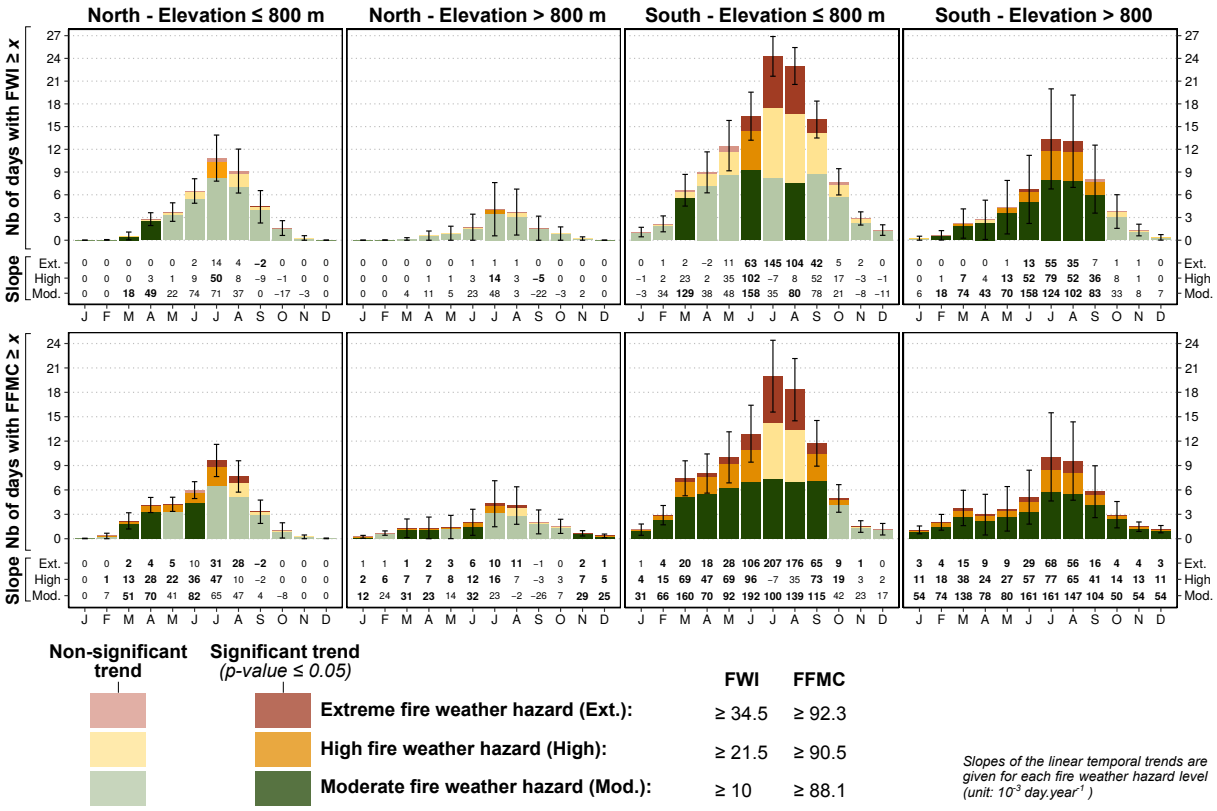

Figure A.7 – Average monthly number of days according to the fire weather danger regarding FWI and FFMC on the period 1959–2015. Dark color indicates a significant trend over the period, light color a non-significant trend. The slope of the linear trend for each fire weather danger are indicated under each barplot, bold values indicating significant trends (p-value ≤ 0.05). Slope unit is 10^{-3}·day·year^{-1}. Error bars correspond to the standard deviation for the monthly number of days considering moderate to extreme fire weather danger.

weather danger appeared earlier on average in the Southern Alps (March at low elevations, July in high) than in Northern Alps (April at low elevation, July in intermediate, no start in high elevations). In average, for the North and for high elevations of the South, the last days with moderate or higher fire weather danger were in October while they lasted one month more in intermediate elevation and two months more in low elevations in the South. The temporal trends underlined an earlier start of the fire weather danger in most of the Southern Alps and in some Northern valleys. However, the trend was not significant regarding the last day with fire weather danger for FWI regardless of the latitude except a negative trend in the Northern mountains in September. Summer fire weather presented a positive trend for the Southern Alps for all fire weather dangers.

Regarding FFMC (Fig. A.7 and Annexes B.3, B.4), the first days with moderate or higher fire weather danger started at the same time at low elevations in both areas (March) but earlier at high elevations in the South (April - June) than in the North (June - July). It lasted until October in Southern Alps and in the valleys in the Northern inner Alps while it ended in September for the rest of the Northern Alps. The temporal trends were characterized by an earlier start in most Alps and a later ending for all the inner Alps (Eastern Alps). More generally, the temporal trends regarding FFMC were more marked than for FWI especially in high elevations in the South where all months presented an increasing trend regardless the fire weather danger.

Both FWI and FFMC trends underlined a rise of the number of days with a moderate to extreme fire weather danger for almost all months in the French inner Alps (Eastern Alps) and especially from November to December.

2.3.5 Return period

Extreme values statistics were used to calculate return periods of extreme FWI and FFMC values in 4 sub-regions (Fig. A.8). Whatever the subregion or the index, the analysis underlined shorter return periods in the most recent time period. Regarding FWI, extreme fire weather danger (FWI>34.5) presented a return period lower than 1 year for low elevations in the South. Its return period for low elevations in the North and high elevation in the South were close, with respectively 3.5 years and 2.6 years for 1987-2015, 16.5 years and 13 years for 1959-1986. Therefore, in the recent period, the chance to have important crown fires increased by a factor 5 in these subregions. Finally in high elevations of the North, high fire weather danger was the most critical level reached with a return period of 3 years for 1987-2015 and 8 years for 1959-1986. Therefore, the chance to have a high danger increased by a factor 2.7 in this subregion.

Concerning FFMC, extreme fire weather danger (FFMC>92.3) presented a return period lower than 2 years for high elevations of the North and lower than 1 year for the others subregions for the recent period. This hazard level had a much longer return period in high elevations (> 100 years) and in low elevations of the North (> 5 years) in the period 1959-1987. This indicated drier moisture rates of fine fuel material in the recent years and by extension a higher probability of surface fires occurrence in these areas.

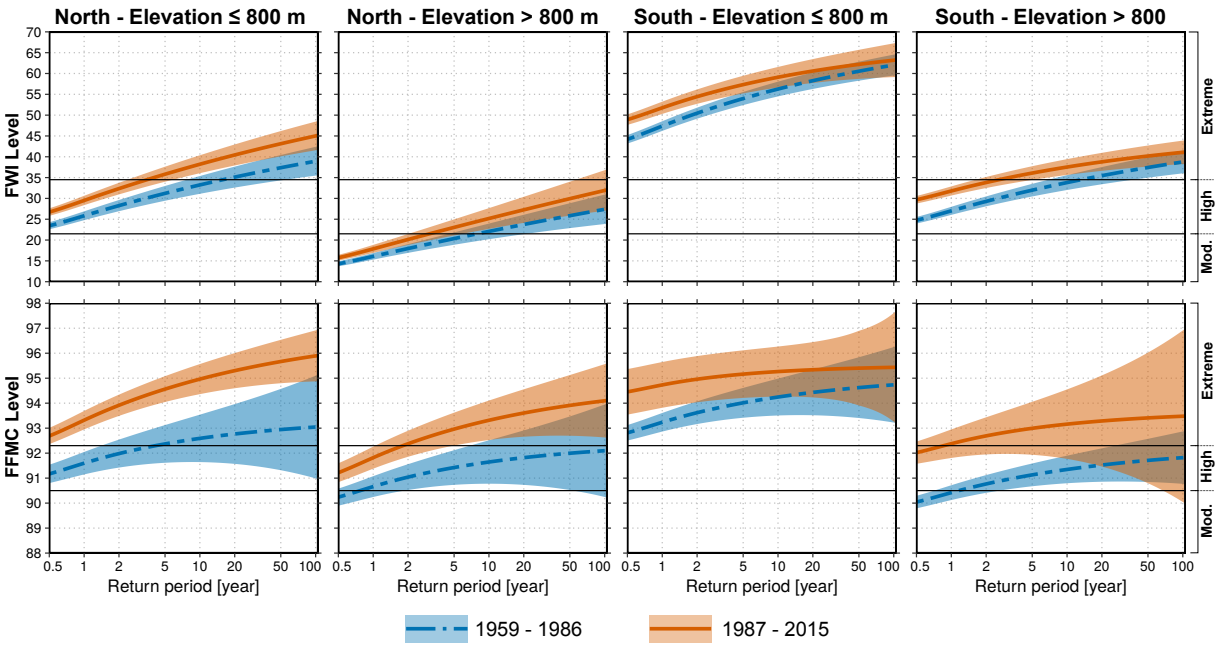

Figure A.8 – Generalized extreme value return level plots for FWI and FFMC in the 4 Alpine subregions. The solid orange line refers to the period 1987-2015, the dashed blue line to the period 1959-1986. Shading indicates the respective 95% confidence intervals. Black horizontal lines represent the threshold value for high (lower line) and extreme (upper line) fire weather danger.

2.4 Discussion

2.4.1 Ongoing changes in fire weather in the French Alps

This study highlighted several ongoing changes in fire weather in both spatial and temporal dimensions (summarized in Fig. A.9). Thus, three main hotspots of fire danger were identified across the French Alps but also some areas with low and stable fire weather danger. The most critical hotspot concerns the high elevations and inner valleys of Southern Alps which suffered a

significant increase for all components of fire weather over the past decades. In average climatic conditions, the fire weather danger was moderate in the 1960's and it is nowadays high. In addition, the *FWW* and the length of the period with a moderate or higher fire weather danger also increased significantly and extreme fire weather dangers are more and more common. Our results are consistent with previous studies (Ruffault et al., 2016; Durand et al., 2009) that demonstrated this part of France suffered one of the most important temperature increase in the past-decades with a trend that should continue during the 21^{st} century (Gobiet et al., 2014).

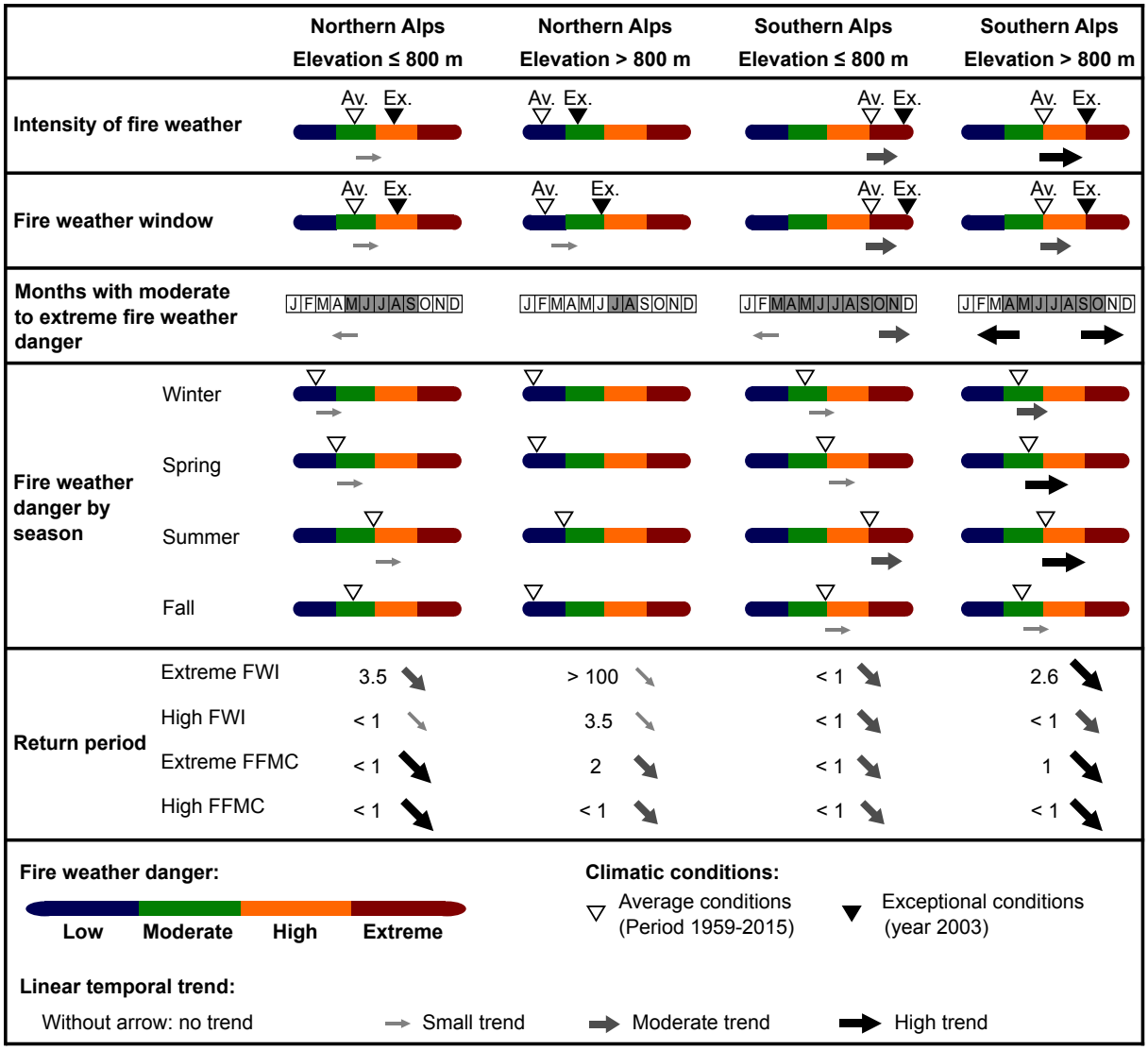

Figure A.9 – Summary table of the current fire weather danger and its temporal trend during the period 1959–2015 for each subregion of the French Alps.

The second hotspot corresponded to low elevations of Southern Alps which are the most prone to intense fires due to Mediterranean influence that combines high temperature and long summer period without rainfall. In this region, all fire weather components reached the highest values observed in the French Alps (Fig. A.9). However, this point has to be tempered given that the fire weather danger was already high and increased moderately in the past decade compared to the first hotspot. Moreover, in this area, people are used to forest fires and fire-fighting is quite developed and performing (Curt et al., 2016; Lahaye et al., 2014) which can mitigate the ongoing trends in fire weather.

The last critical hotspot was located in the low elevations of Northern Alps. In this area, on average climatic conditions, fire weather danger is low to moderate and wildfires are rare and generally small making fire suppression easy. Beside this “ordinary" fire activity, the fire weather reached a high danger during the 2003 exceptional drought which was marked by several large fires. The analysis underlined a rise in the frequency of such exceptional climatic conditions which might produce more large crown fires in the next decades. In addition to the frequency of extreme events, all other fire weather components showed a slight increase over the past decades in this area.

Despite these three hotspots, some parts of the French Alps remain with a low and stable fire weather danger. These areas are located in the high elevations ($>$ 800 m) of Northern Alps which are characterized by cool temperatures and precipitations well distributed along the year. Until now, this cool and relatively humid climate mitigated the effect of the global temperatures increase and allowed keeping a moderate fire weather danger even during exceptional drought. However, one may question about the future fire weather because it has been proved that significant increases in rainfall amounts are needed to maintain the current fuel moisture levels when mean temperature increase of 1°C (Flannigan et al., 2016).

Favourable climatic conditions alone are not sufficient to produce forest fires and an increase in fire weather danger does not necessary mean a direct rise in the number of fires (Curt et al., 2016). Indeed, the number of fires depends mostly on human-caused ignitions, thus on the density of human settlement and activities, and the burned area also depends on fuel types, landscape configuration, and the fire suppression capability. This is in line with the results of Wastl et al. (2012) which indicates that an increase in fire weather danger did not necessarily produced an increase in fire activity throughout the Alps. Therefore, future works should also consider land use, probability of ignition and fire management strategy to get a complete overview of the spatio-temporal trends of fire danger in the French Alps (Zumbrunnen et al., 2012). A first step could be to cross our analysis with a map of Wildland-Urban Interface areas (Modugno et al., 2016) to account for ignition caused by human activities (about 85% of the ignition) and a map of fuels that could be obtained using Lidar data (Skowronski et al., 2016).

Several works have used Safran to analyse observed fire weather in the South of France (Ruffault et al., 2017a; Fréjaville et al., 2015; Fréjaville et al., 2014). However, these works directly used a gridded outputs with a resolution of 8km $\times$ 8km which might suit relatively flat area but are not adapted to the complex topography found in the Alps. In this study, we proposed to use the raw Safran dataset has it as been already done for others natural hazards such as avalanches (Castebrunet et al., 2014). The main shortcomings of this dataset in the Alpine region were discussed in Quintana-Segui et al. (2008) and might affect the fire weather index calculation. In the Alps, an overall positive temperature bias was observed but it might be compensated by an under-estimation of wind speed in the calculation of FWI and FFMC. Recently, Safran system was used in Spain (Quintana-Seguí et al., 2016) and an over-estimation of precipitation was identified even if it does not seem to be the case in the Alps (Quintana-Segui et al., 2008).

2.4.2 Projected trends in a context of global changes

The results of this study are consistent with the climate changes observed and predicted for the French Alps. Models and simulations indicate higher temperature on average with +1.5°C at the mid-21^{st} century and between +2 and +4°C by the end of 21^{st} century with higher increases in the Southern Alps (Gobiet et al., 2014). Rainfall changes are not so obvious but increases are predicted mainly in spring and winter, and decreases during summer. These conditions might promote fire because spring and winter rainfalls allow accumulating fuel biomass in forests (Fréjaville et al., 2016) while higher temperatures and low rainfall in summer indicate lower fuel moisture (Flannigan et al., 2016). Severe droughts and heat waves are also predicted to be more

frequent, although their duration cannot be modelled (Gobiet et al., 2014). This study showed that exceptional meteorological years such as 2003 increase fire weather danger almost everywhere in the French Alps, thus reducing the regional contrasts that exist during "normal" years. All these prospects are made under the assumption that the future Alpine climate will evolve linearly and follow the trends observed since 1959. However, non-linear trends and uncertainties can modify the past-to-present changes (Flannigan et al., 2016).

To go further in the fire weather projection, it could be interesting to integrate regional climate change scenarios (Bedia et al., 2014) in the analysis. However, most climate change models have a much lower spatial resolution than the 25 m × 25 m used in this study. Therefore we could add a source of uncertainty by post-processing those low resolution projections with the DTM from BDAlti®.

2.4.3 Indirect consequences and practical implications for fire prevention policy

The identification of the three hotspots of fire danger might improve the fire prevention policy in the French Alpine area. Therefore, with a significant increase of all fire weather components, inner area and high elevations of Southern Alps might need a growing attention in the next decades. On the other hand, Northern Alps remain relatively unaffected by big fires but authorities must prepare for exceptional years such as 2003 which promote large and destructive wildfires.

Mountain forests provide a wide range of ecosystem services (Briner et al., 2013). Among them, the protection of human beings and infrastructures against natural hazards is essential, especially in Alpine regions (Bebi et al., 2001). In France, a significant part of the forested area in the Alps provides a natural protection against rockfall (Dupire et al., 2016a) or erosion (Stoffel et al., 2013). An increase of forest fires might degrade these important ecosystem services (Maringer et al., 2016a; De Graff et al., 2015). A better knowledge of the climatic component of the fire danger crossed with the map of protection forests (Toe et al., 2015) might also help the stakeholders in the allocation of fire fighting resources.

2.5 Conclusion

The ongoing climate changes lead to a major contrast between Northern Alps with low and slightly increasing fire danger, and Southern and inner Alps with high and increasing fire danger. The number of days days prone to fire slightly increased at spring in the North and significantly throughout the year in the South. Based on the increase of days with high fire weather danger, fires should also become more intense on average. These trends should reinforce in the next decades according to climate change predictions, due to increasing temperatures and higher variations in rainfall. The increasing frequency of heatwaves and severe droughts may generate large and intense fires, mostly in Southern and inner Alps, but also at low elevation in the North like in the year 2003. This study can help science-based decision for better alerting, prevention, suppression of wildfires and an adaptation of forests and French Alpine territories to wildfire risk.

Funding and acknowledgement

This work was supported by the French Ministry of Ecology, Sustainable Development and Energy [grant n° 2101527657] and the H2020 project NAIAD [grant n° 730497] from the European Union's Horizon 2020 research and innovation programme.

We acknowledge the DCSC-AVH and CEN from the Grenoble center of Météo France for providing us Safran data as well as useful advices for their manipulation.

Appendix B

See Figs. B.1, B.2, B.3 and B.4.

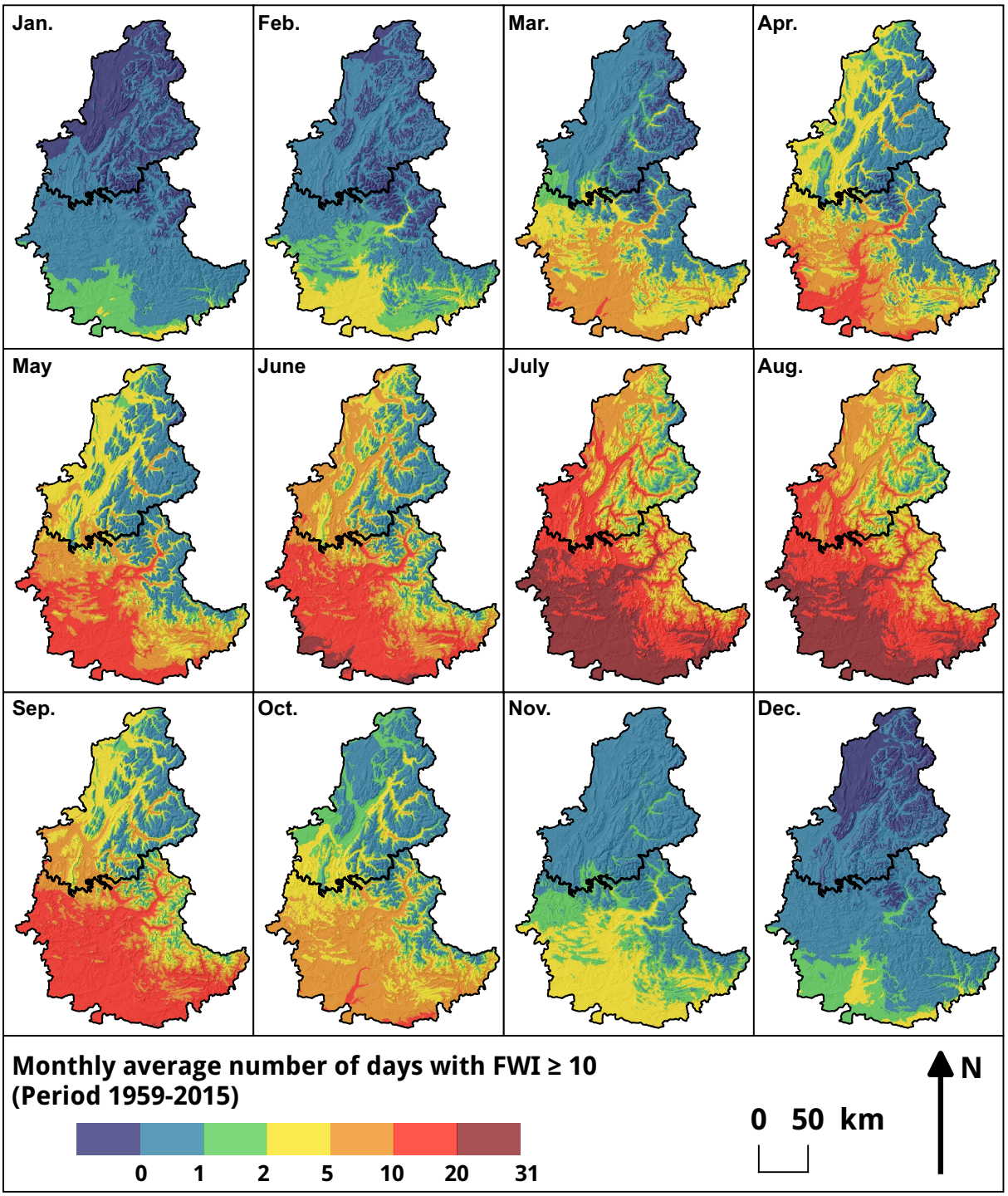

Figure B.1 – Maps of average number of days with FWI $\geq$ 10 for each month (period 1959–2015).

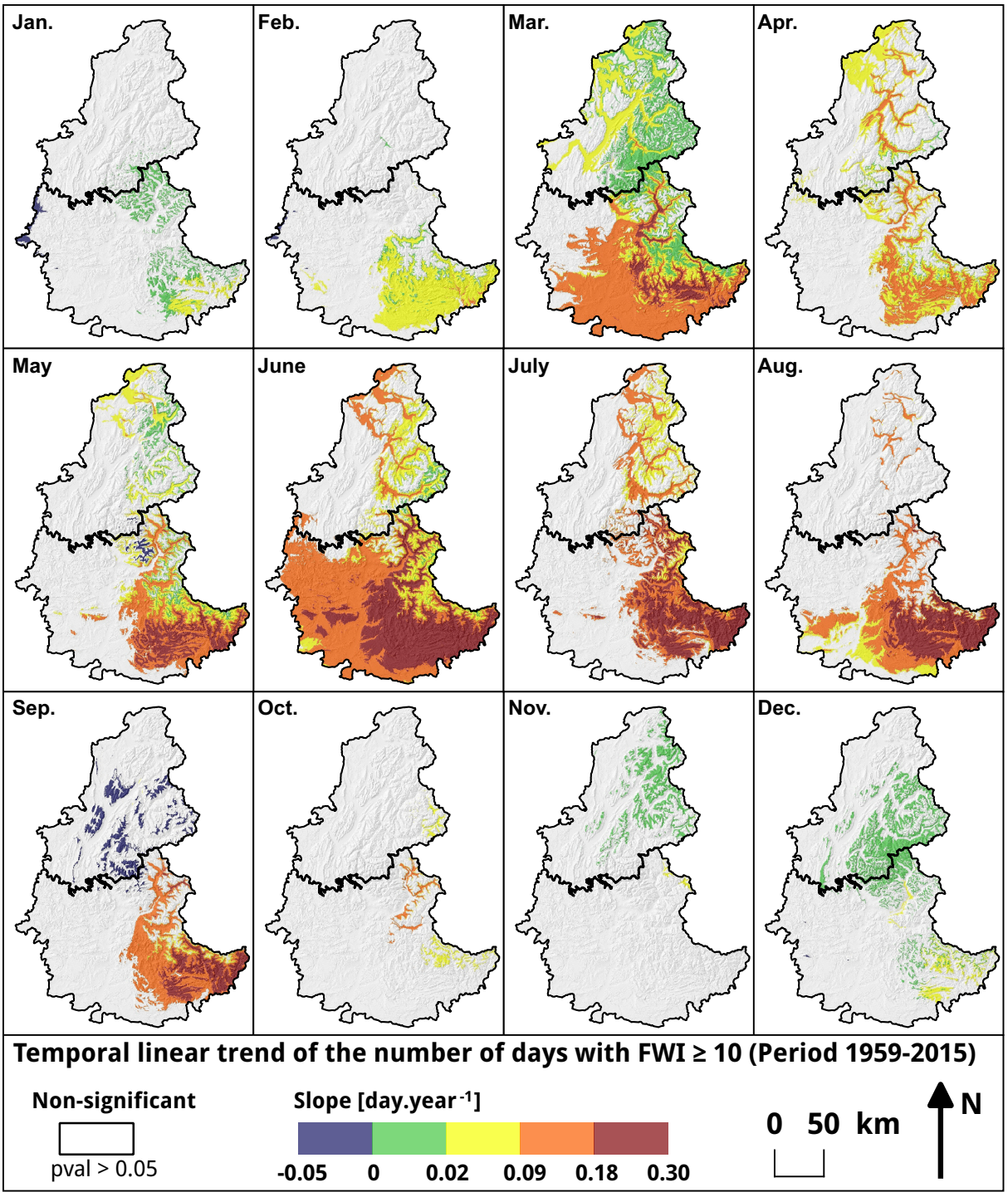

FIGURE B.2 – Maps of the temporal trend of number of days with FWI ≥ 10 for each month. Significant trends (p-value ≤ 0.05) are shown using colors, non significant trends are shown in white.

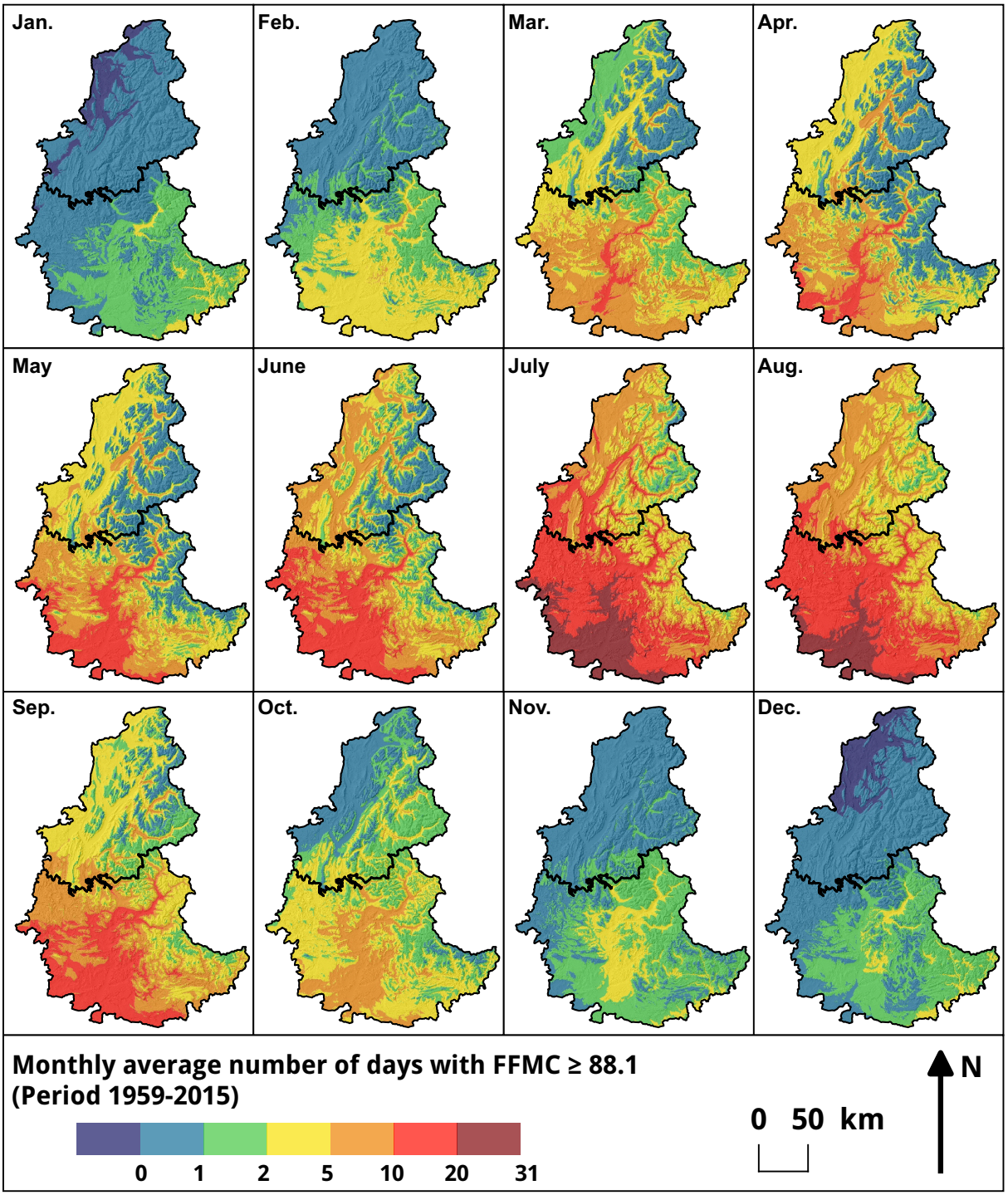

FIGURE B.3 – Maps of average number of days with FFMC $\geq$ 88.1 for each month (period 1959–2015).

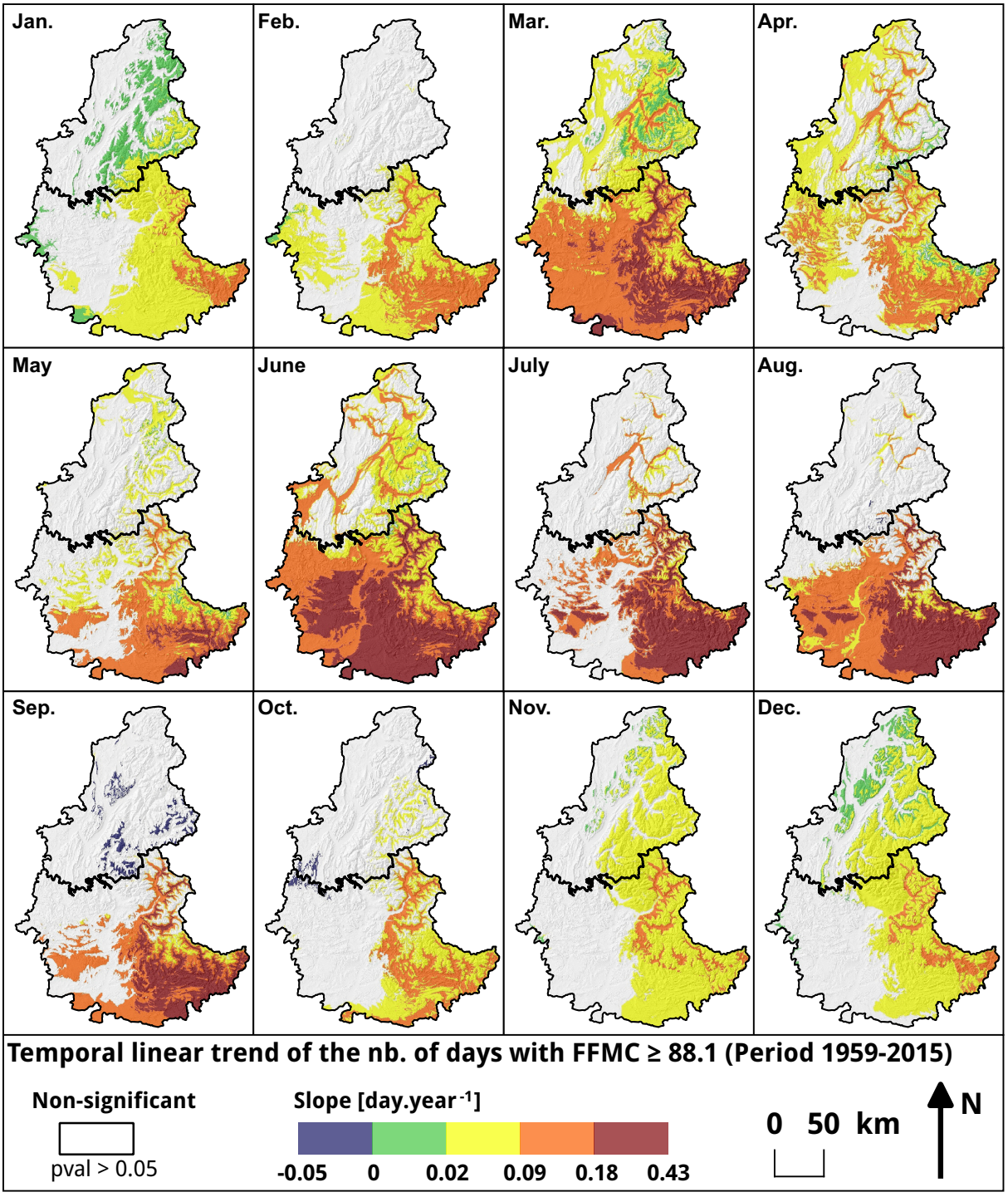

FIGURE B.4 – Maps of the temporal trend of number of days with FFMC $\geq$ 88.1 for each month. Significant trends (p-value $\leq$ 0.05) are shown using colors, non significant trends are shown in white.

CHAPITRE 3

Évaluation de la mortalité post-feu dans les forêts des Alpes françaises

Predicting potential post-fire tree mortality in the French Alps

Dupire S., Curt T., Bigot S., Fréjaville T.

Article in preparation

Abstract Predicting tree mortality after a forest fire is essential in order to enlighten forest management practices and fire fighting policy in a context of climate and societal changes. This is especially true in mountainous areas where forest provide many ecosystems services such as wood resource, biodiversity or protection of human lives and infrastructures against natural hazard. This paper aimed at describing and evaluating a method to assess tree mortality at different scales (tree level, stand level and French Alps level) from the outputs of fire simulations corresponding to three different climatic conditions (cold season, average summer condition and extremely dry summer conditions). Post-fire tree mortality was modelled at both tree and stand levels for 4438 forest plots located around the French Alps. Different methods were used and compared to real post-fire mortalities found in the literature in order to select the ones that most fit the local context. The results showed that fire occurring in the cold season (about 60% of the fires in the French Alps) have a limited impact on the forests. However, this study suggested that forests dominated by broadleaved species are the most susceptible to know high mortality rates after a summer forest fire, especially in extreme climatic conditions which are more likely to occur in the next decades. This study provides insights on the vulnerability of the main tree species and forest types of the French Alps that could be used in order to adapt the forest management practices and the fire fightings forces during severe fire danger episodes.

Keywords Mountain forest · Wildfire · Tree mortality · Alps · Climate · Fire simulations

3.1 Introduction

The impacts of climatic changes are especially perceptible in mountain areas (Pachauri et al., 2014; Kohler et al., 2010; Beniston, 2005). Since the 1960's, fire weather danger has increased almost in every parts of the French Alps (Dupire et al., 2017) in different ways such as longer fire seasons or more frequent extreme drought episodes. Forests of the Alpine area can be classified as "biomass-rich and rarely dry ecosystems" with favourable and non-limiting conditions to fuel

growth (Meyn et al., 2007). Therefore, fire regimes in the French Alps mostly depend on fuel moisture and fire ignition which are mainly human driven in this area.

Tree mortality following forest fires results from direct (damaged meristems due to heat transfers) or indirect (insect attack, altered physiology...) processes (Michaletz et al., 2007). In the Alps, surface fires, which burn and propagate only in the surface fuels (litter, herbs and shrubs), are the most common fire types (Valese et al., 2014). Depending on their intensity, surface fires can affect different tree components : mainly tree bole in low-intensity fires, bole and crown in moderate to high intensity fires (Dickinson et al., 2001). Roots can also be damaged if the duration of the fire is long enough. Crown fires occurred more rarely in Alpine forests (Curt et al., 2016) and are generally concentrated in the Southernmost part. Crown fires are generally devastating as they affect the organs of photosynthesis in addition to the vascular tissues.

Although wildfires have always been present in the Alpine areas (Power et al., 2008; Wick et al., 2006; Tinner et al., 1999), their potential impacts on the current forests and tree species are not so well known. Several studies focused on the resistance or resilience strategies of different Alpine species. Amongst them, Maringer et al. (2016b) investigated direct and indirect mortalities in beech forests, Fréjaville et al. (2013) focused on the ecological traits affecting the resistance to fire of the main subalpine species, Moris et al. (2017) studied the resilience of European Larch and Tinner et al. (2005) followed tree species responses to fires since the last ice age.

These studies are very useful to understand the impact of fires on the different tree species in the Alpine environment, however it is quite difficult to transpose them to a prospective prediction of post-fire mortality occurring in a given climatic condition. Yet, according to the ongoing and future climate changes it could be very interesting to assess the potential damage of wildfire occurring in different climatic conditions on the main Alpine forest ecosystems. This might also allow to identify potential cascading effects resulting from a fire event as, for sample, an increase of erosion, avalanches or rockfalls (Maringer et al., 2016a).

The aims of our study was to assess the immediate post-fire tree mortality on 4438 forest plots located across the French Alps according to different climatic conditions using outputs of fire behaviour simulations. Three different climatic conditions were first defined and corresponded to cold season (November to April), average summer and extreme summer. Fire simulations were then conducted using the fire behaviour program FlamMap on 112 plots with detailed fuel description. The outputs of these simulations were used to define the fire behaviour on each NFI plots. Different methods were tested to calculate individual post-fire tree mortality from the outputs of the simulations and for each climatic conditions. The resulting modelled mortalities were compared to observed mortalities after real fire events. Finally, direct post-fire tree mortality was detailed for the main tree species (tree level) and for the main forest types (stand level) of the French Alps.

3.2 Material and methods

3.2.1 Forest data and fuel characterization

This study focused on the forests of the French Alpine area (Fig. 3.1) as defined by the French Institutions (Decree n°2016-1208). The territory was divided into Northern and Southern Alps and low elevation ($\leq$ 800 m a.s.l.) and high elevation ($>$ 800 m a.s.l.) areas (Dupire et al., 2017).

Forest and fuel data were taken from two different sources (Fig. 3.1). Information on the fuel bed were measured in 96 plots (fuel plots) covering the French Alps (Fréjaville, 2015) + 16 complementary plots located only in the Northernmost part (measurements in 2017). On each fuel plot the horizontal cover, bulk density, height and load of litters, herbs and shrubs were measured. Tree characteristics (species, diameter, bark thickness, height and canopy base height) were also detailed.

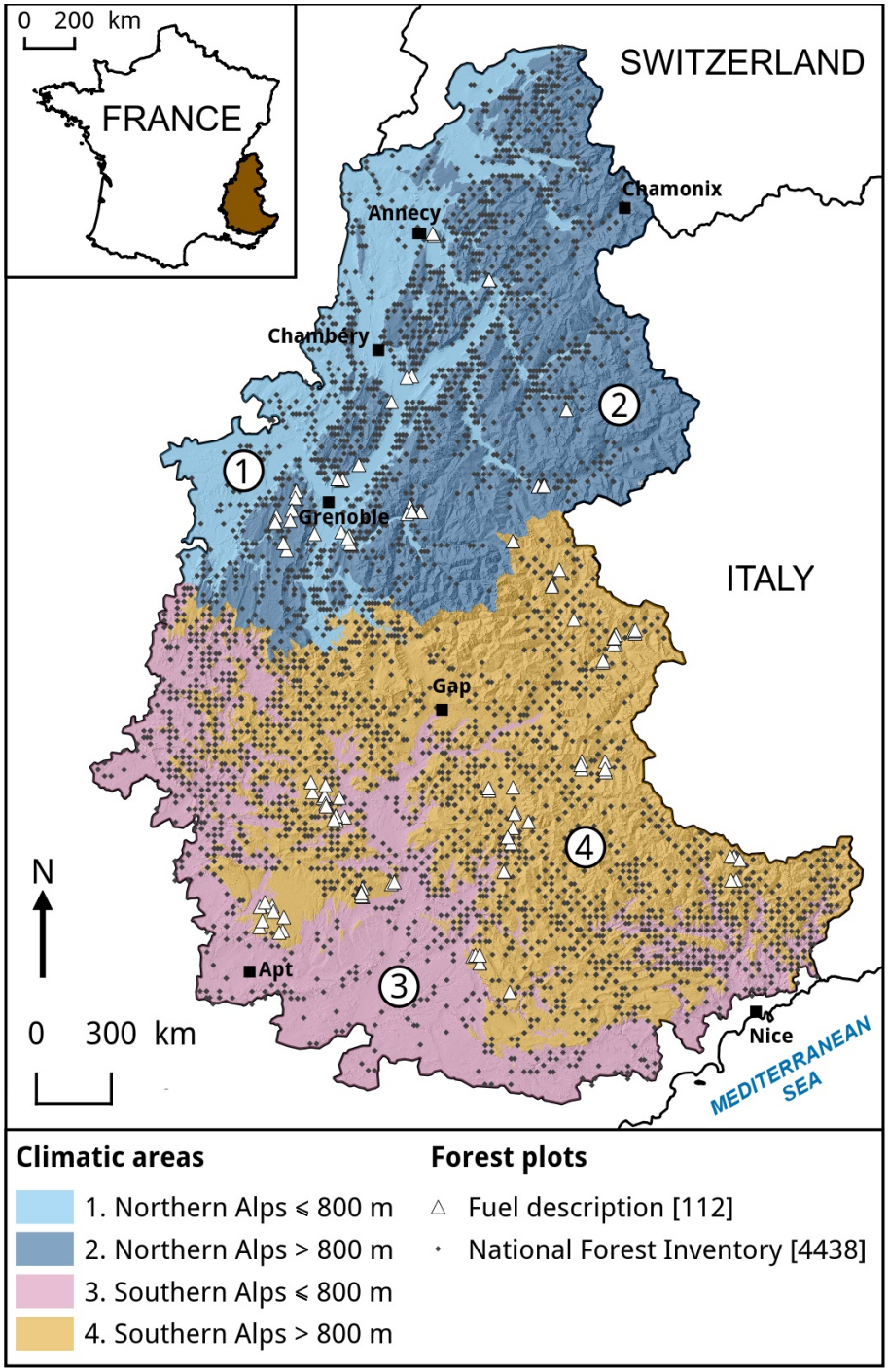

Figure 3.1 – Map of the French Alpine area and locations of the forest plots from the different sources. The four climatic areas used for analysing the results are also shown.

Forest plots were extracted from the permanent sample plots of the French National Forest Inventory (NFI) based on a systematic grid of 1 km × 1 km covering the complete country. A minimum slope threshold of 20° was applied in order to select only forests situated on moderate to steep slopes. 4438 plots measured from 2005 to 2015 are located in the French Alps and were used in this study. NFI data collection is based on circle plots (Robert et al., 2010) where stand properties and ecological and topographic data are assessed in a 25-m radius. On each plot, tree characteristics (species, total and first branch heights) are inventoried for all trees with a

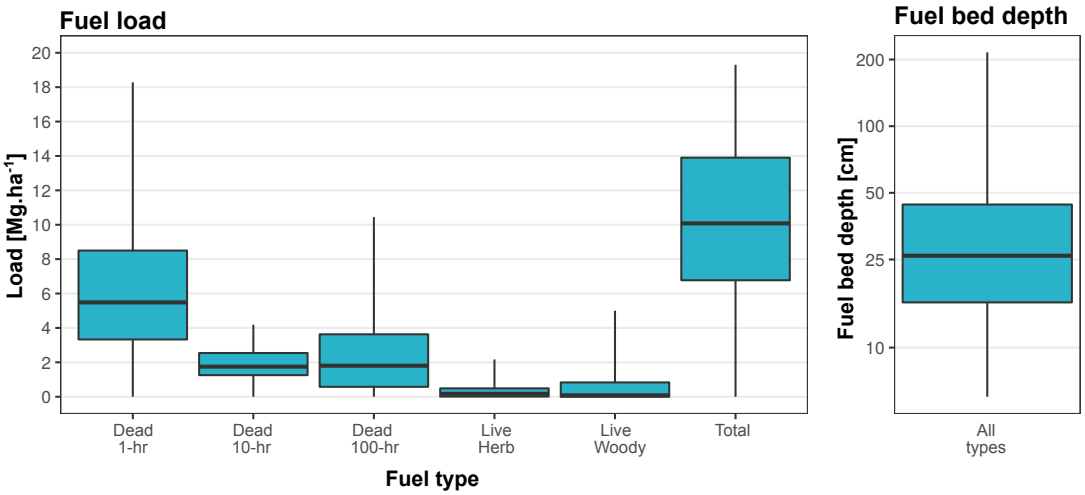

Figure 3.2 – Distribution of fuel load and fuel depth measured on the 112 fuel plots. Dead 1-hr fuels concern the dead leaves of the litter and dead pieces of wood with diameter < 6 mm. Dead 10-hr fuels concern dead pieces of wood with diameter from 6 to 25 mm. Dead 100-hr fuels concern dead pieces of wood with diameter from 25 to 75 mm. Fuel bed depth is the average height of surface fuels (litter, herb and shrubs) contained in the combustion zone of spreading fire front.

diameter at breast height (DBH) greater than or equal to 7.5 cm. Bark thickness of the NFI trees were estimated from allometric equations according to DBH and tree species (Fréjaville, 2015).

3.2.2 Climatic conditions

Climatic data came from the Safran analysis system implemented by Météo France (Vidal et al., 2010; Quintana-Segui et al., 2008) which computes vertical profiles of precipitation, temperature, humidity, wind speed and cloudiness every day at noon (precipitation) or every 6 h (others variables) on 615 climatically homogeneous zones covering France.

Safran data were used to calculate the daily fine fuel moisture code (*FFMC*) over the French Alps from 1959 to 2015 (Dupire et al., 2017). *FFMC* is one of the six meteorological-based indices of the Canadian Fire Weather Danger Rating System (Van Wagner, 1987) calculated on a daily basis from weather variables measured at solar noon (temperature, relative humidity and wind speed) together with the precipitation sum of the last 24 h. *FFMC* rates the moisture of live fine fuels including grass, fine shrubs and the surface litter (5-10 cm depth) and therefore evaluates the ease of ignition of these light fuels. *FFMC* can be related to the 10-hr fuel moisture content (mc) of the US National Fire Danger Rating System (see Eq. 3.1, Wotton (2009)) which is a key input of many fire simulation models.

$$mc = 147.2 \cdot \frac{101 - FFMC}{59.5 + FFMC} \tag{3.1}$$

Two periods of the year had been considered for the fire simulations. The first period included the months from January to April plus November and December. It corresponds to the cold season where 60% of the vegetation fires occur in the French Alps (Dupire et al., 2017). Those fires are mainly due to human activities (agriculture and forest cleaning) and generally have a low intensity and stay in the understory layer. The second period corresponded to the summer months (e.g. from June to September) where the most intense wildfires are observed. Finally the annual values observed during the summer 2003 were used to account for exceptional drought (Poumadère et al., 2005). The three climatic conditions derived from these different periods are presented in the Table 3.1.

Climatic condition	Months	Years	*FFMC* considered	Fire modelled
Average summer	Jun - Sep	1959 - 2015	$FFMC_{Summer} = \frac{1}{57} \cdot \sum_{y=1959}^{2015} P_{95}^{y}(FFMC_{Jun-Sep})$	Average summer fires
Exceptional summer	Jun - Sep	2003	$FFMC_{2003} = P_{95}^{2003}(FFMC_{Jun-Sep})$	Exceptional summer fires
Average cold season	Jan - Apr Nov - Dec	1959 - 2015	$FFMC_{Cold} = \frac{1}{57} \cdot \sum_{y=1959}^{2015} P_{95}^{y}(FFMC_{Jan-Apr,Nov-Dec})$	Average winter fires

Table 3.1 – Description of the climatic conditions and their associated *FFMC*. $P_{95}^{y}(FFMC_{Months})$ is the annual (year y) 95^{th} percentile of daily FFMC values for the months considered.

For each climatic condition and each forest and fuel plot we computed the associated *FFMC* ($FFMC_{clim-scen}$) as well as the average wind speed and air temperature taking into account only the days where $FFMC \geq FFMC_{clim-scen}$.

3.2.3 Fire behaviour simulations

Fig. 3.3 shows the general workflow followed for the simulation of the fire behaviour. Fire simulations were first computed on the 112 fuel plots. Then, fire behaviour on the NFI plots was estimated from the outputs of the fire simulations.

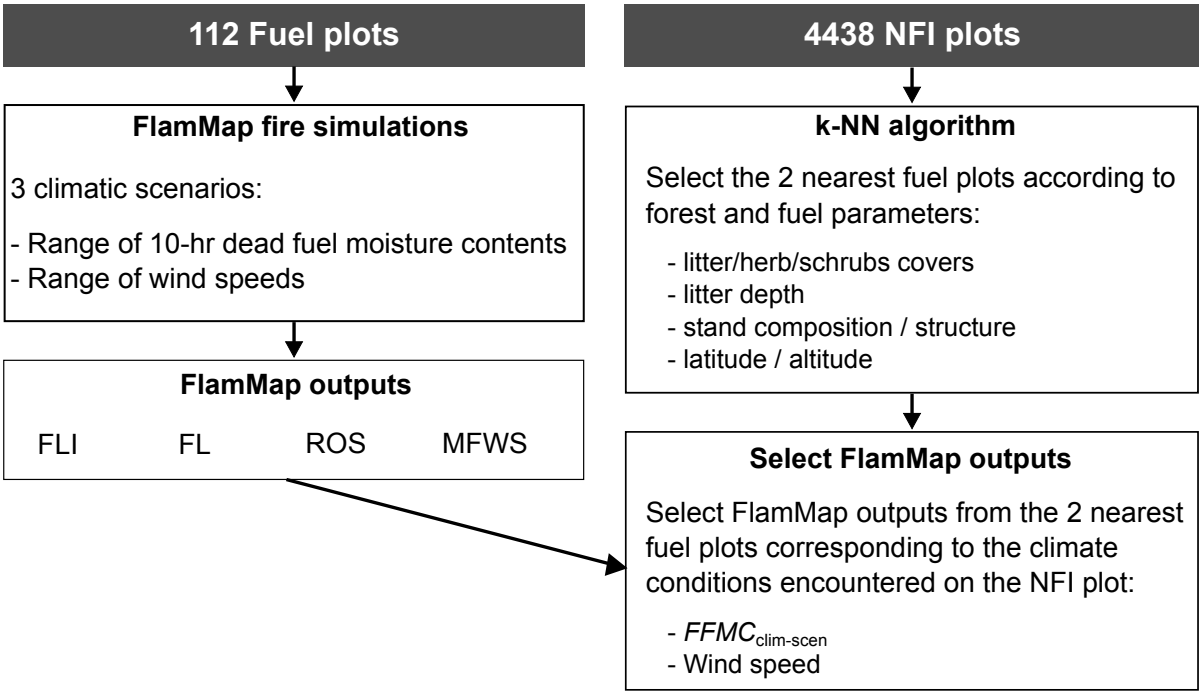

Figure 3.3 – Workflow chart of the fire modelling. The program FlamMap 5.0 (Finney, 2006) was used for the fire simulations. The fireline intensity (FLI), flame length (FL), rate of spread (ROS) and mid-flame wind speed (MFWS) were extracted for each fire simulation.

3.2.3.1 Fire simulation on the 112 fuel plots

The program FlamMap version 5.0 (Finney, 2006) was used to model the fire behaviour within the 112 fuel plots under a range of fuel moisture contents and wind speeds (Table 3.2). FlamMap simulates fire behaviour and propagation based on the fuel and weather data. Potential fire behaviour calculations include surface fire spread (Rothermel et al., 1972), crown fire initiation

(Van Wagner, 1987), and crown fire spread (Rothermel, 1991). FlamMap has extensively been used worldwide for simulating fires, both in Mediterranean environments (e.g. Mitsopoulos et al. (2016)) or in mountain environments (Ager et al., 2011).

Climatic condition	10-hr dead fuel moisture content	live herb moisture content	live woody moisture content	Wind speed	Slope
Average summer	5 - 14%	60%	90%	3 - 20 km·h^{-1}	20°
Exceptional summer	4 - 13%	40%	70%	3 - 20 km·h^{-1}	20°
Average cold season	9 - 17%	90%	120%	3 - 20 km·h^{-1}	20°

Table 3.2 – Fuel parameters used for FlamMap simulations for each climatic condition.

10-hr dead fuel moisture contents (mc) were obtained from Eq. 3.1 using the range of $FFMC_{clim-scen}$ values observed on both NFI and fuel plot. Moisture contents of other dead fuel classes were assumed to be $mc-1$ for 1-hr and $mc+1$ for 100-hr as recommended in Finney (2006). Live herb and live woody moisture content were fixed for each climatic condition according to fuel collection around the Grenoble region along the year 2016 as well as historical follow-ups in the South of France. The slope of the terrain was set to 20° which corresponds to the minimum slope of the NFI plots.

Four FlamMap outputs were used to assess post-fire tree mortality. The first is the fireline intensity (FLI, kW·m^{-1} Byram, 1959) which indicates the energy (heat) release per unit time per unit length of the fire front. The second is the flame length (FL, m) which accounts for the height of scorching in trees, and the possibility of flame transition to the tree crown. The third is the rate of spread (ROS, min·m^{-1}) or the speed of the fire front. ROS can be related to the flame residence time (τ_f) if the width of the burning strip (D) is known : $\tau_f = \frac{D}{ROS}$ (Alexander, 1982). Finally, the mid-flame wind speed ($MFWS$, km·h^{-1}) is used in the calculation of the fraction of crown volume killed.

3.2.3.2 Fire behaviour on the 4438 NFI plots

Fuel information on the NFI plots was insufficient to perform direct fire simulation with FlamMap. In order to get the potential fire behaviour according to the different climatic conditions we chose to use a k-nearest neighbors (k-NN) algorithm (Mucherino et al., 2009) to identify the nearest 2 (k=2) fuel plots in terms of fuel load and distribution as well as stand composition and structure. For each climatic condition, the outputs of the fire simulations concerning these 2 plots and corresponding to the weather conditions ($FFMC$ and wind speed) of the NFI plot were extracted and averaged.

3.2.4 Post-fire tree mortality

In this study only direct mortality processes were taken into account. Moreover we focuses on boles damages (vascular cambium) and crown damages (apical meristems) which are the most vulnerable tree components in surface fires. In practice, the different methods to assess post-fire tree mortality consist in estimating whether the lethal temperature of the different tree components (generally fixed at 60°C) is reached according to the fire behaviour and the tree characteristics (Dickinson et al., 2004; Gutsell et al., 1996; Brown et al., 1987; Peterson et al., 1986). This lethal threshold can theoretically be reached for any fire intensity if the flame residence time is long enough (Bauer et al., 2010). Thus, low intensity fires need a long flame residence time in order to damage the vegetative tissues while high intensity fires can produce the same damages in a shorter time laps (Bova et al., 2005). In this study, we tested different methods to estimate cambial mortality which is the most susceptible to occur in the Alpine surface fires. Van Wagner (1977) crown-fire transition criteria was used to assess crown-fire transition.

3.2.4.1 Modelling cambial mortality

Cambial mortality has been shown to be strongly linked to the insulation capability of the bark (Spalt et al., 1962) which mainly depends on its thickness and, to a lesser extent, on its moisture content and density (Bauer et al., 2010). Different approaches were used and compared to estimate the post-fire cambial mortality on the forest plots.

Cambial mortality from temperature gradient and heat duration A common method to estimate cambium necrosis was first proposed by Spalt et al. (1962) who modelled it as a one-dimensional conduction into a semi-infinite solid (Fourrier's law) as shown in Eq. 3.2 :

$$\frac{T_c - T_f}{T_a - T_f} = erfc\left(\frac{bthi}{2\sqrt{\alpha \cdot \tau_{min}}}\right) \tag{3.2}$$

where

T_c : lethal temperature of cambium [°C]
T_f : temperature of the flame [°C]
T_a : ambient temperature [°C]
$erfc$: complement of the Gauss' error function
$bthi$: bark thickness [cm]
α : bark thermal diffusivity [$cm^2 \cdot min^{-1}$]
τ_{min} : flame residence time [min]

According to this approach, cambium necrosis can be related to a temperature gradient and a heating duration. However, most of the classical fire behaviour model do not return information about temperature and give a rough estimation of the flame residence time. Therefore, flame temperature is generally assumed to be constant over time and equals to the maximum temperature of the flaming fireline. For sample, Peterson et al. (1986) derived Eq. 3.2 by fixing T_c=60°C, T_f=500°C, T_a=20°C and α=0.06 $cm^2 \cdot min^{-1}$; with these parameters the equation becomes :

$$t_{c-PR} = 2.9 \cdot bthi^2 \tag{3.3}$$

where t_{c-PR} is the time required to reach the lethal conditions in the cambium or, equivalently :

$$bthi_{c-PR} = \sqrt{\frac{\tau_{min}}{2.9}} \tag{3.4}$$

where $bthi_{c-PR}$ is the minimum bark thickness (or critical bark thickness) required to prevent reaching the cambium lethal temperature according to the fixed parameters. Peterson et al. (1986) equations are very convenient to use but assuming that surface fires always reach 500°C can lead to an overestimation of cambial mortality especially for low-intensity fires.

Cambial mortality from bark burning experiments Bauer et al. (2010) were particularly interested in the insulation capability of the bark under low-intensity fires. They designed an experiment to measure the time needed to reach the lethal cambial temperature ($t_{c-Bauer}$, s) for different European tree species (*Abies alba, Fagus sylvatica, Larix decidua,Pinus sylvestris*) with a constant flame temperature of 214°C and different bark moisture contents. They managed to produce a general equation that included all the tree species studied for wet and dry bark. Only the equation for the dry bark is presented here :

$$t_{c-Bauer} = 9.1 \cdot bthi^{1.401} \iff bthi_{c-Bauer} = 0.2068 \cdot \tau_s^{0.7138} \tag{3.5}$$

where $bthi_{c-Bauer}$ (mm) is the critical bark thickness required to prevent reaching the cambium lethal temperature according to the authors experiments.

Cambial mortality from heat flux Bova et al. (2005) were particularly interested in linking outputs of fire behaviour models with stem heating and tissue necrosis. They developed equations based on physical relationships between fire behaviour and surface heat flux, and between surface heat flux and tissue necrosis. Although only two tree species were studied (*Acer rubrum* and *Quercus prinus*), they produced an equation linking the depth of necrosis (or critical bark thickness : $bthi_{c-Bova}$, mm) with fireline intensity (FLI, kW·m^{-1}) and flame residence time (τ_s, s) independent of the tree species :

$$bthi_{c-Bova} = 0.21 \cdot FLI^{0.2} \cdot \tau_s^{0.64} \Longleftrightarrow t_{c-Bova} = 12.57 \cdot bthi^{1.56} \cdot FLI^{-0.31} \quad (3.6)$$

3.2.4.2 Comparison of cambium mortality approaches

In order to test the different approaches on low intensity surface fires we used the measurements done during litter flammability test (Curt et al., 2011) on samples collected between May and July during three consecutive years (2006 to 2008) into oak forests located in the South of France. For each experiment, 0.5 kg of litter was placed on a 40 cm diameter round tray equipped to monitor the mass loss during the burning phase ; temperature, rate of spread and flame length were also measured. Note that this litter loading corresponded to a dead 1-hr fuel load of 40 Mg·ha^{-1} which was much more than the average measured load on the fuel plots. Therefore, although the experiment have a reduce scale compared to a real surface fire, the fire behaviour variables measured are certainly conservative due to this fuel overloading (Curt et al., 2011). 81 experiments were kept and corresponded to situation where the flame lasted at least 20 s. For each experiment, the maximum flame temperature (T_f), flame residence time (τ) and the ambient temperature (T_a) were extracted from the temperature profile along time (Fig. 3.4). The fireline intensities were calculated according to Byram (1959) equation : $FLI = H \cdot w \cdot ROS$ where H is the fuel low heat of combustion (taken to be 15000 kJ·kg^{-1}, Bova et al. (2005)), w is the weight of fuel consumed during combustion and ROS the rate of spread (both measured during the experiments).

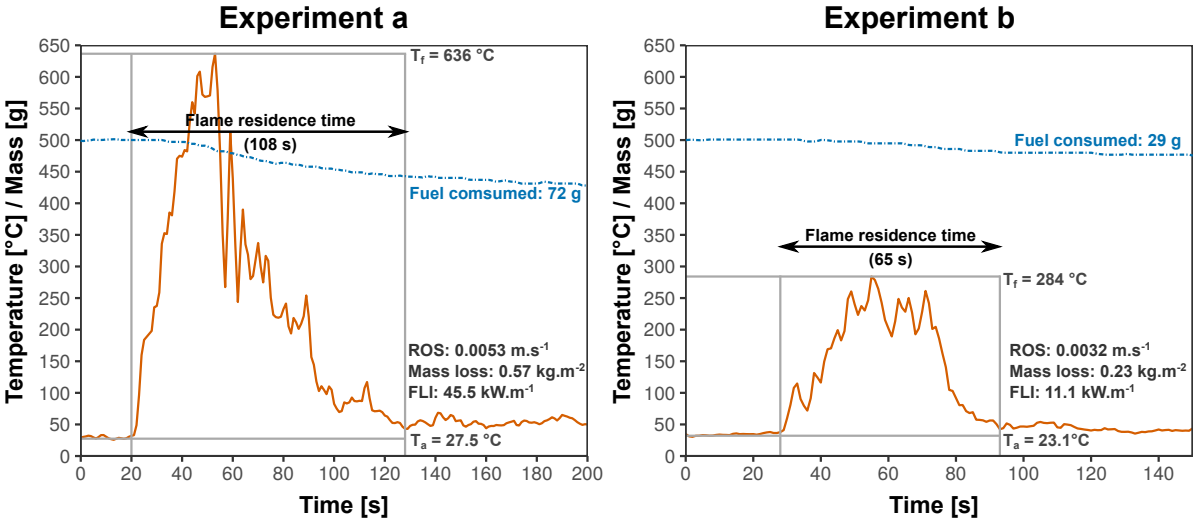

Figure 3.4 – Examples of temperature (orange solid line) and mass (dashed blue line) profiles measured along time during two different litter flammability experiments.

Method	Variables used	$bthi_c$ Experiment a	$bthi_c$ Experiment b
Eq. 3.2 (Spalt et al., 1962)	T_f, T_a, τ	8.8 mm	5.2 mm
Eq. 3.4 (Peterson et al., 1986)	τ	7.9 mm	6.1 mm
Eq. 3.5 (Bauer et al., 2010)	τ	5.9 mm	4.1 mm
Eq. 3.6 (Bova et al., 2005)	FLI, τ	8.6 mm	4.5 mm

Table 3.3 – Example of critical bark thickness calculated with the different approaches for 2 litter flammability tests.

For each experiment we calculated the critical bark thickness $bthi_c$ according to the different approaches mentioned above and the fire behaviours observed (Tab. 3.3). As the flame temperature is not an output of FlamMap, we computed a linear regression linking τ to $bthi_c$ from the results of the litter flammability experiments for Eq. 3.2 (Spalt et al., 1962) in order to apply it to post-fire mortality of the NFI plots.

3.2.4.3 Modelling crown mortality

Crown mortality was modelled according to Peterson et al. (1986) who estimated the fraction of crown killed from tree characteristics (tree height and crown proportion), fireline intensity and windspeed. This method presented the advantage of being directly compatible with the outputs of FlamMap simulation and the tree characteristics available.

$$C_k = \frac{(h_k - h_t + c_l) \cdot (h_t - h_k + c_l)}{c_l^2} \tag{3.7}$$

with :

$$h_k = \frac{3.94 \cdot FLI^{1.17}}{(T_c - T_a) \cdot (0.11 \cdot FLI + MFWS^3)^{0.5}} \tag{3.8}$$

C_k : fraction of crown volume killed ($0 \leq C_k \leq 1$)
h_t : tree height [m]
c_l : crown length [m]
h_k : height of crown kill [m]
$MFWS$: mid-flame windspeed [m·s^{-1}]

3.2.4.4 Overall post-fire tree mortality

The probability of post-fire mortality of a tree P_m was assessed by combining the critical time for cambial kill (τ_c) and the fraction of crown volume killed (C_k) as proposed in Peterson et al. (1986):

$$P_m = C_k^{\left(\frac{\tau_c}{\tau_f} - 0.5\right)} \tag{3.9}$$

where

P_m : Probability of mortality ($0 \leq P_m \leq 1$)
C_k : fraction of crown volume killed ($0 \leq C_k \leq 1$)
τ_c : critical time for cambial kill [min]
τ_f : flame residence time [min]

The probability of mortality strongly depends on the flame residence time which is difficult to get from fire simulations. For this reason we chose to mark off P_m by calculating it for two τ_f thresholds. The lowest threshold was fixed at 30 seconds which corresponds to a minimum time for a low-intensity surface fire to maintain itself (Peterson et al., 1986). The highest threshold corresponded to the theoretical maximum duration of lethal bole heating defined in Peterson et al. (1986) which depends on the moisture content and the loads of the different fuel size classes (1-h, 10-h, 100-h). For our data, it ranged from 1 min to 5 min depending on the fuel bed loading and moisture content.

Post-fire tree mortality of the main tree species was calculated at the French Alps scale with the four approaches to account for cambial mortality presented in section 3.2.4.1. The modelled post-fire mortality rate was compared, when available, to observed data taken in the literature or to field observations. As post-fire tree mortality studies often refer to fire severity (Moris et al., 2017; Maringer et al., 2016b; Catry et al., 2010), we assumed in our comparison that low, moderate and high fire severity corresponded to cold season, average summer and 2003 summer climatic conditions respectively.

Post-fire tree mortality in the main forest types was finally computed for the four climatic areas of the French Alps using the cambial mortality equation that best fitted the observed mortality. In France, the National Forest Inventory attributes a weight to each tree according to the distance between the tree and the center of the plot (Robert et al., 2010). These weighs were used to calculate the mortality rate at the NFI plot level as described in Eq. 3.10.

$$Stand\ mortality\ rate = \frac{\sum_{i=1}^{n} w_i \cdot P_m(i)}{\sum_{i=1}^{n} w_i} \tag{3.10}$$

where

$P_m(i)$: Probability of mortality of the tree i ($0 \leq P_m \leq 1$)
w_i : weight attributed to the tree i
n : number of trees measured on the NFI plot

3.3 Results

3.3.1 Fire simulations

The results of the fire simulations according to the main forest types (Dupire et al., 2016b) and climatic areas of the French Alps are presented in Fig. 3.5, Fig. 3.6 and Fig. 3.7. As expected an increase of fireline intensity and rate of spread was observed from cold season to summer 2003. Decreasing gradients of *FLI*, *FL* and *ROS* were generally observed from Southern Alps to Northern Alps and from low elevation to high elevation.

Forest fires occurring during the cold seasons showed very low intensity (often < 100 kW·m^{-1} in the Northern Alps and < 200 kW·m^{-1} in the Southern Alps) as well as low *ROS* which indicates a slow fireline speed due to a high fuel moisture which implies a longer preheating phase (Michaletz et al., 2007). Nonetheless, some forest types might have more severe fire behaviour in the cold season. They are mainly composed of broadleaved species (pure or mixed) which may present a high litter load in the cold season due to the falling leaves. Such fire behaviour levels mainly corresponds to low intensity surface fires.

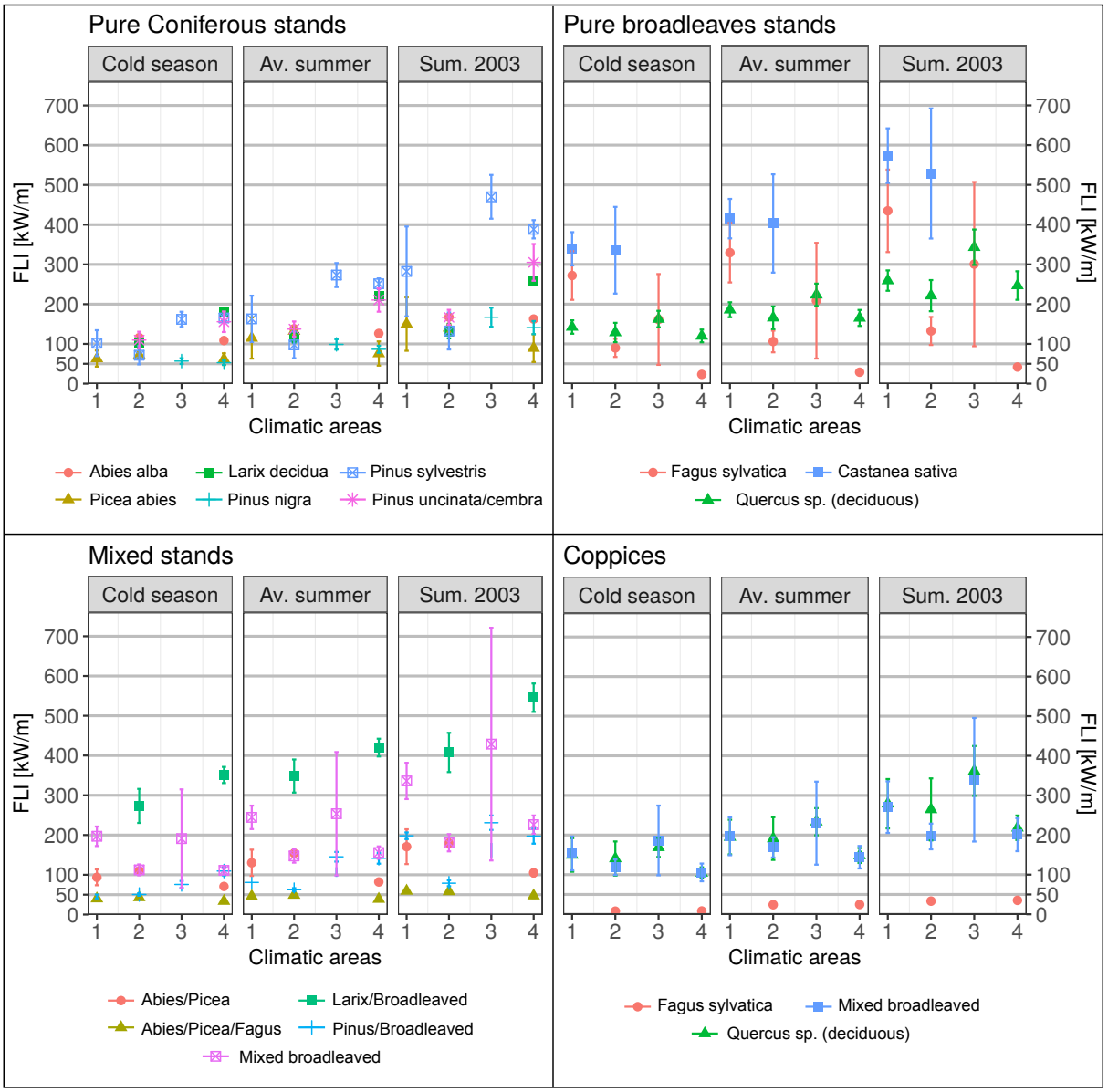

Figure 3.5 – Fireline intensity modelled on the NFI plot according to forest type, climatic condition (Tab. 3.1) and climatic areas (Fig. 3.1) : 1-Northern Alps $\leq$ 800 m, 2-Northern Alps $>$ 800 m, 3-Southern Alps $\leq$ 800 m, 4-Southern Alps $>$ 800 m. The points indicate the mean value, error-bars indicate the 95% confidence interval. Forest types are shown only if at least 10 plots in the climatic area are present.

In average summer conditions, the modelled forest fires presented a low to moderate intensity generally in between 100 and 400 kW·m^{-1} with an accentuated difference between low elevations and high elevation locations and Northern and Southern Alps. The fire front also had a greater speed (mostly between 0.5 and 1.5 m·min^{-1}) than in the cold season. The forest types that already showed higher fire intensities in the cold season also had greater values during average summer conditions. Amongst conifers, pure stands of *Pinus sylvestris* and *Pinus uncinata/cembra* and mixed stands of *Pinus sp. + broadleaved* and *Larix decidua + others sp.* were characterized by higher values of *FLI*, *FL* and *ROS*. Although, most of the fire behaviour variables are typical to surface fires with low to moderate intensity, some forests characterized by a small stand height or presenting a vertical continuity of the vegetation may experience crown fires especially at low elevation in the Southern Alps.

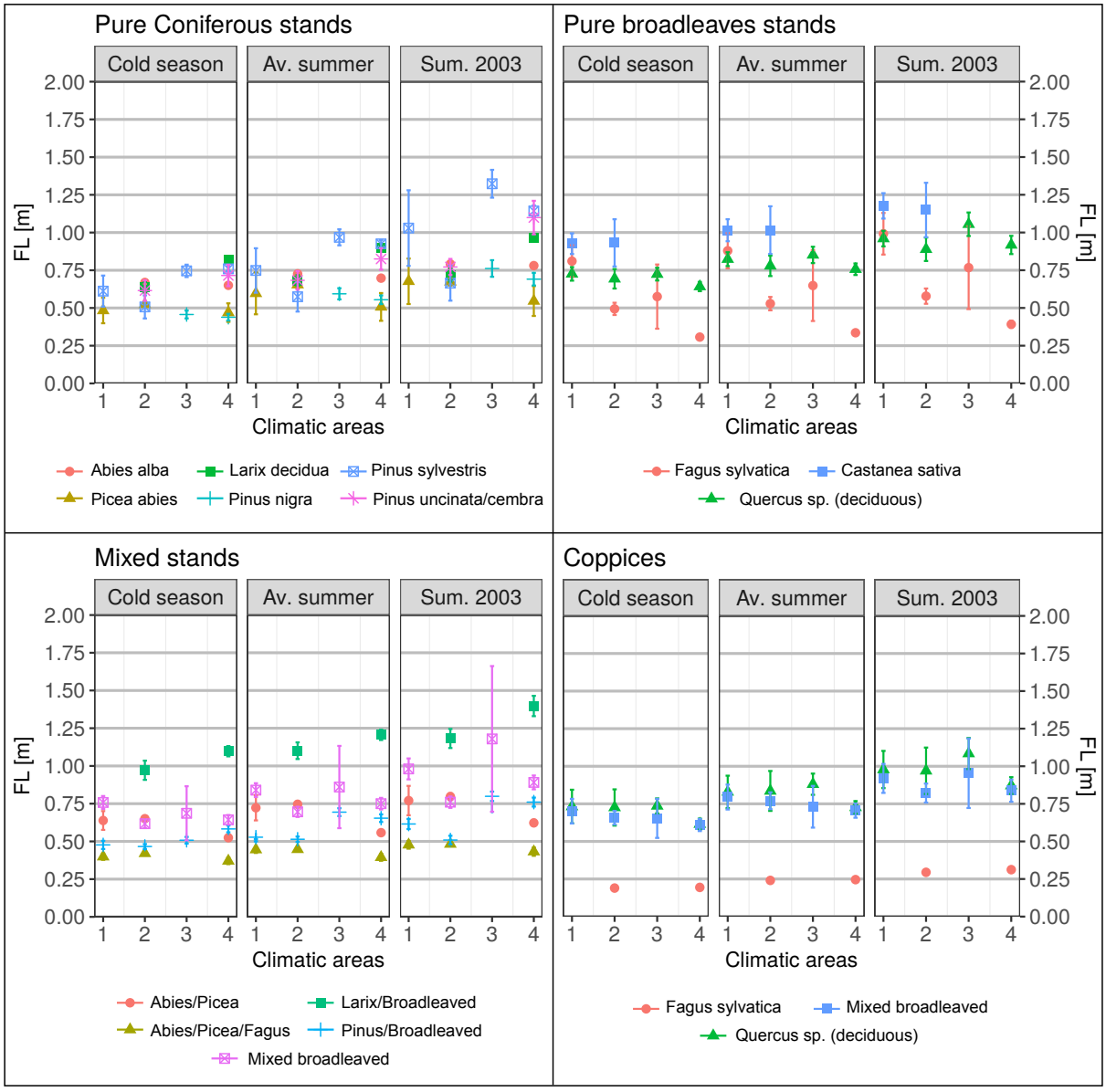

Figure 3.6 – Flame length modelled on the NFI plot according to forest type, climatic condition (Tab. 3.1) and climatic areas (Fig. 3.1) : 1-Northern Alps $\leq$ 800 m, 2-Northern Alps $>$ 800 m, 3-Southern Alps $\leq$ 800 m, 4-Southern Alps $>$ 800 m. The points indicate the mean value, error-bars indicate the 95% confidence interval. Forest types are shown only if at least 10 plots in the climatic area are present.

In extreme summer conditions like summer 2003, simulated forest fires presented moderate intensity from 150 to 600 kW·m^{-1} with a significant difference according to the climatic areas. The hierarchy observed between forest types for average summer was emphasized and the probability of crown fires increased with several forest stands showing $FLI > 500$ kW·m^{-1}.

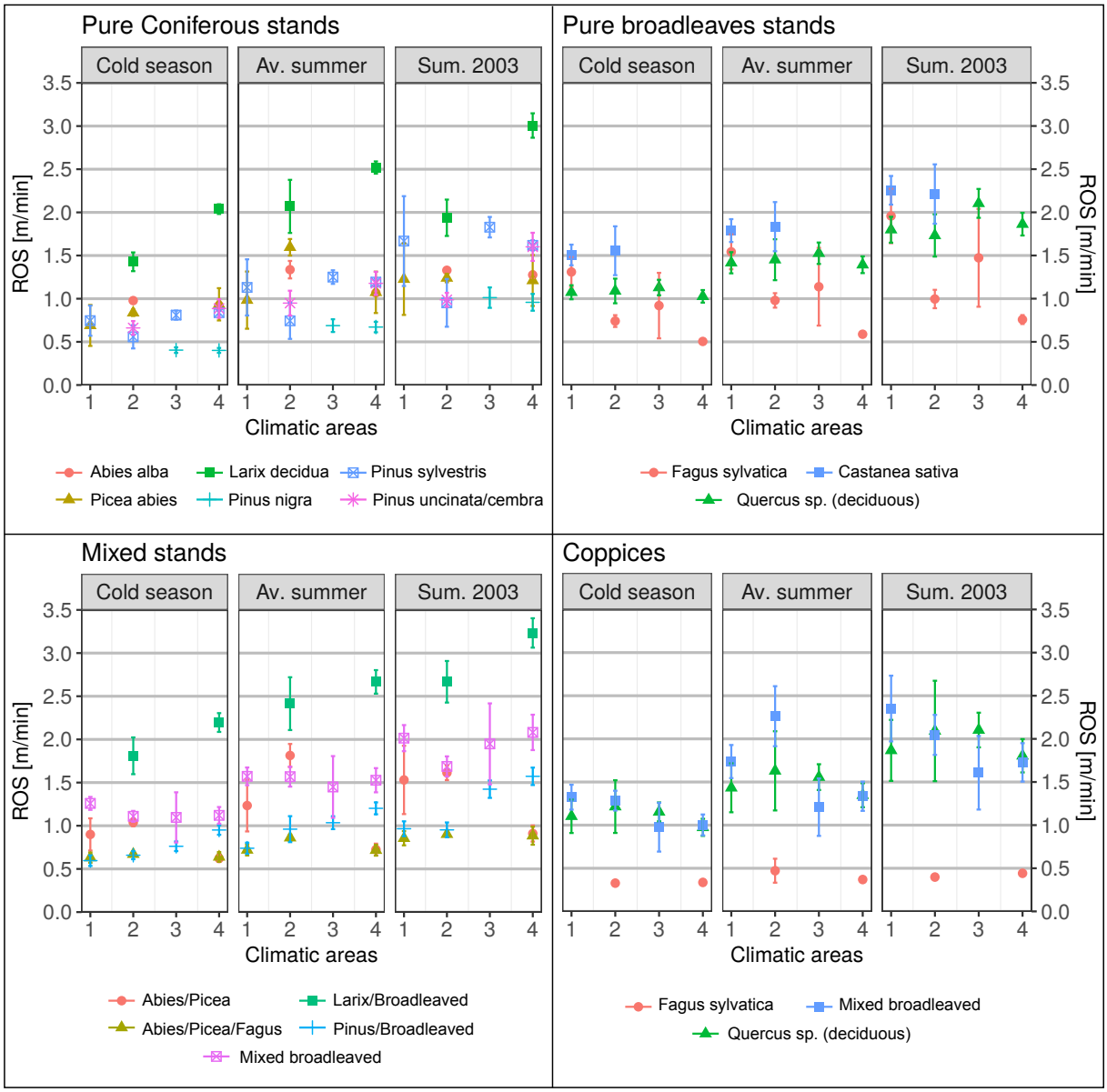

Figure 3.7 – Rate of spread modelled on the NFI plot according to forest type, climatic condition (Tab. 3.1) and climatic areas (Fig. 3.1) : 1-Northern Alps $\leq$ 800 m, 2-Northern Alps $>$ 800 m, 3-Southern Alps $\leq$ 800 m, 4-Southern Alps $>$ 800 m. The points indicate the mean value, error-bars indicate the 95% confidence interval. Forest types are shown only if at least 10 plots in the climatic area are present.

3.3.2 Comparison of cambial mortality equations on litter flammability experiments

Fire behaviour variables measured during litter flammability experiments are shown in Fig. 3.8. The observed flame residence times ranged between 20 s and 255 s with half of the values from 60 s to 150 s which are classic times for surface fires (Bauer et al., 2010).

The maximum flame temperature measured ranged from 100°C to 850°C with a median value at 300°C. According to these experiments, we can already say that Bauer et al. (2010) equation (Eq. 3.5) should produce low mortality rate as it was calibrated with a flame temperature of 214°C. Conversely, Peterson et al. (1986) equation (Eq. 3.4) should produce higher mortality rate with a fire temperature fixed at 500°C.

The observed *FLI*, *FL* and *ROS* ranges corresponded to low intensity fires which is certainly an inherent consequence of the laboratory experiments with small scale fires.

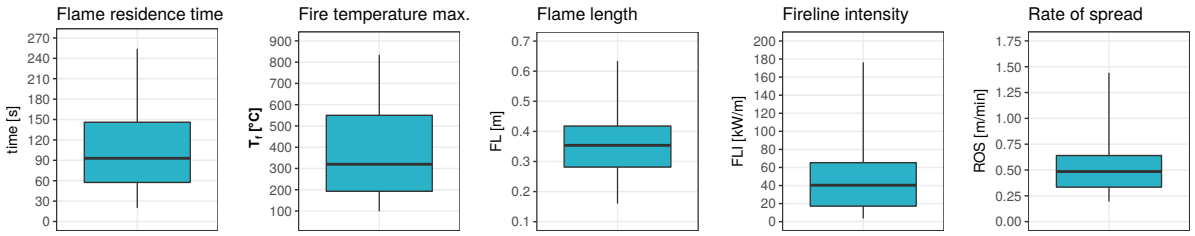

Figure 3.8 – Distribution of the main fire behaviour variables calculated from the laboratory measurements done during the 81 litter flammability experiments. The boxplots show the percentiles 1%, 25%, 50%, 75% and 99%.

Fig. 3.9 returns the distribution of the values of *FLI* and flame residence time according to the measured maximum flame temperatures. Both *FLI* and flame residence time increased with flame temperature. According to this observation, Bauer et al. (2010) equation (Eq. 3.5) should certainly be adapted for very low intensity fires ($< 25 \text{kW}\cdot\text{m}^{-1}$). Moreover, Peterson et al. (1986) equation (Eq. 3.4) might be suitable when $FLI > 50 \text{kW}\cdot\text{m}^{-1}$.

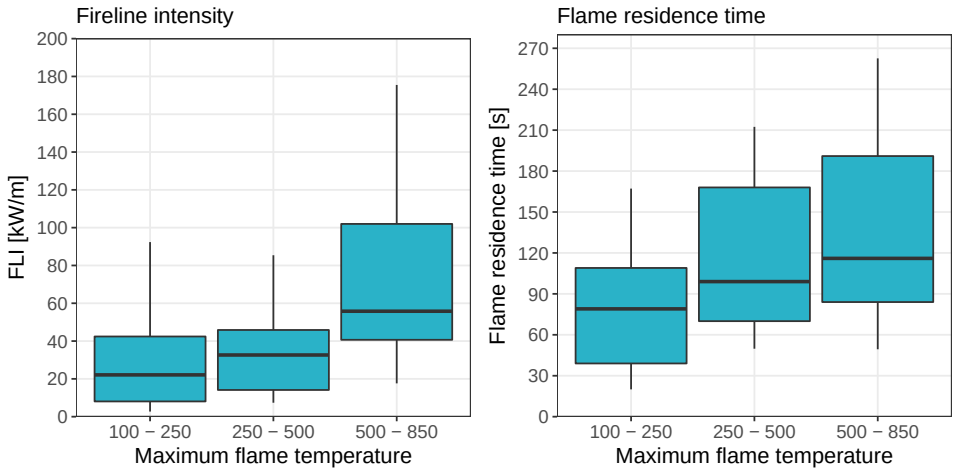

Figure 3.9 – Distribution of *FLI* and flame residence time values according to the maximum flame temperature [°C] measured during litter flammability experiments.The boxplots show the percentiles 1%, 25%, 50%, 75% and 99%.

Critical bark thickness calculated from litter flammability measurements are shown in Fig. 3.10. Bauer et al. (2010) equation (Eq. 3.5) returned significant lower critical bark thickness than others equations independently of the flame residence time. This is consistent with the hypothesis assumed by the authors ($T_f = 214$°C) which might not be adapted for the highest fire intensities.

The three other equations returned fairly similar distributions of critical bark thickness with slightly lower values for Spalt et al. (1962). However, some differences were underlined when critical bark thickness is related to the flame residence time (τ). Thus, we can observed three configurations :

- for $\tau \in [0-60]$ s : Peterson et al. (1986) $\geq$ Bova et al. (2005) $>$ Spalt et al. (1962)
- for $\tau \in [60-180]$ s : Bova et al. (2005) $>$ Peterson et al. (1986) $>$ Spalt et al. (1962)
- for $\tau \in [180-480]$ s : Bova et al. (2005) $>$ Spalt et al. (1962) $>$ Peterson et al. (1986)

In order to use Eq. 3.2 (Spalt et al., 1962) to assess post-fire tree mortality we computed the linear regression liking the critical bark thickness to the flame residence time.

$$bthi_{c-Spalt} = 0.25 \cdot \tau^{0.72} \Leftrightarrow \tau_{c-Spalt} = 11.468 \cdot bthi^{1.109} \tag{3.11}$$

with $bthi$ in mm and τ in second.

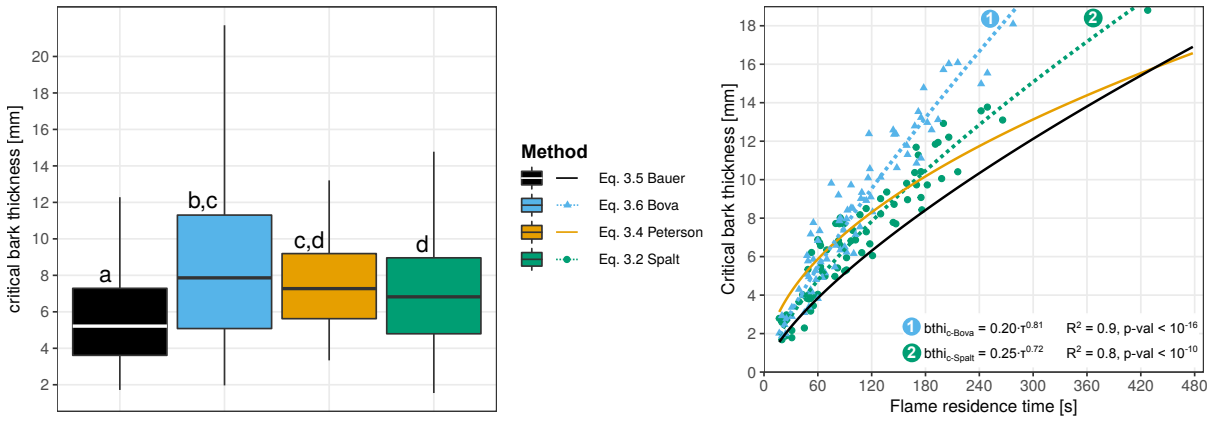

Figure 3.10 – Comparison of the critical bark thickness calculated with the different methods. All calculation are based on the variables of fire behaviour observed during the 81 litter flammability experiments. The boxplots show the percentiles 1%, 25%, 50%, 75% and 99%. Letters (a,b,c,d) on the boxplots indicate the results of Tukey honest significant difference (different letters = significant difference). Dotted lines on the right plot are the linear trend lines for Bova (1) and Spalt (2) methods, equations of the lines are given at the right-bottom of the plot. Peterson and Bauer methods are direct functions of the flame residence time so only the curves corresponding to their respective functions are shown.

3.3.3 Post-fire tree mortality of the main species

3.3.3.1 Detail per tree species

Fig. 3.11 to 3.18 present the post-fire mortality rate per species according to *DBH*, cambial mortality method of calculation and climatic conditions. For each tree species, post-fire mortality is bounded between two flame residence time (τ). The bounds were assumed to correspond to a τ of 30 s for the lowest and to the maximum theoretical flame residence time t_{max} for the highest ($t_{max} \in [60-300]$ s according to fuel load and fuel moisture content).

Abies alba is often characterized as a "fire intolerant" species (Tinner et al., 2000) due to its relatively small bark thickness (Fréjaville et al., 2013) but especially because of its low resilience ability several years after fire (Tinner et al., 2005). It has even been assumed that its extinction in the mid-Holocene in the Southern Alps was due to an increase of forest fires frequency (Wick et al., 2006; Tinner et al., 2005; Tinner et al., 1999).

According to our simulations, the immediate post-fire mortality was not so severe especially for short flame residence time. However for long flame residence time, the majority of the trees under 20 cm *DBH* were modelled as dead. Bigger tree were affected only for the most extreme climatic conditions and for long flame residence time. Unfortunately, no field observations nor post-fire study were found concerning this species.

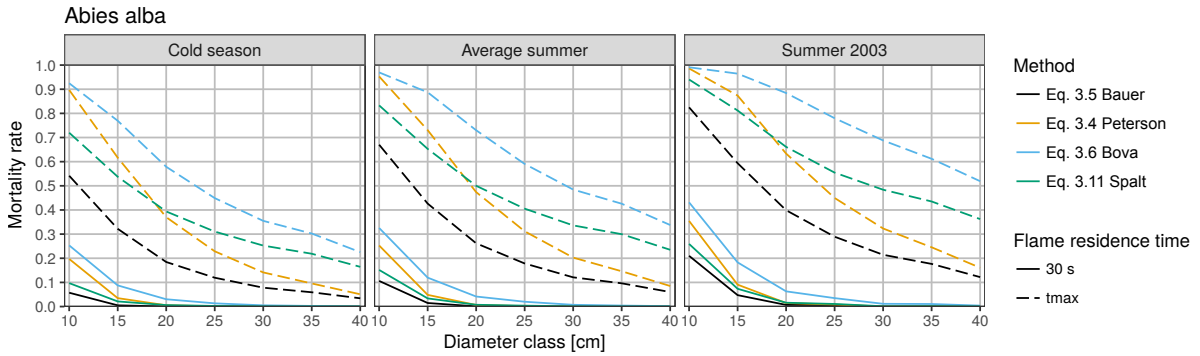

Figure 3.11 – *Abies alba* mortality rate by diameter and according to different climatic conditions.

Picea abies has a similar behaviour than *Abies alba* (Tinner et al., 2000). In Sweden, it has been shown that forest fires can reach high mortality rates in young stands (Wallenius et al., 2005).

According to the fire simulations, the immediate post-fire mortality is quite similar to the one of *Abies alba*. The post-fire mortality following a forest fire that occurred in August 2003 in Champagny-en-Vanoise, Savoie, France (1600-1900 m a.s.l.) was added to the plot of extreme climatic conditions. It followed the mortality rates calculated according to Bova et al. (2005) for the maximum theoretical flame residence time. Two studies were found with reference of post-fire mortality of small diameter *Picea abies*, the first one concerned summer prescribed burnings in Sweden (Linder et al., 1998) with moderate fire intensity and the second one a summer surface fire in Finland (Kolström et al., 1993).

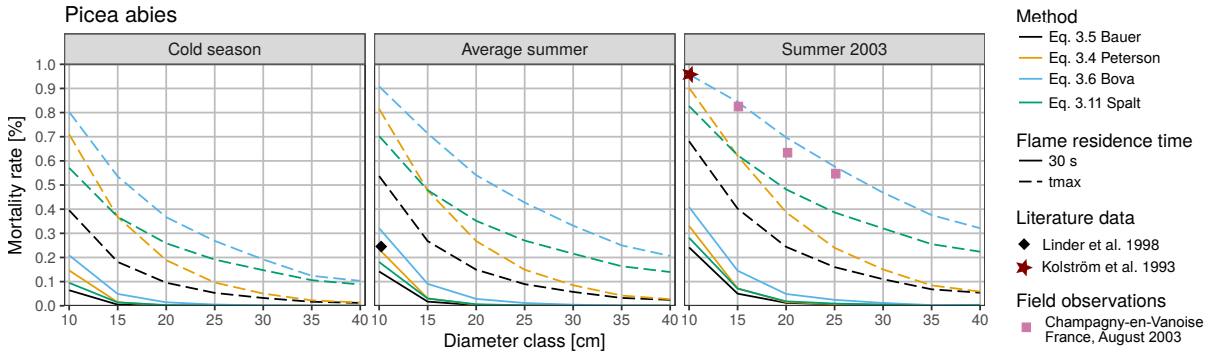

Figure 3.12 – *Picea abies* mortality rate by diameter and according to different climatic conditions.

Fagus sylvatica is classified as a "fire sensitive" species (Tinner et al., 2000) due to its very thin bark (Fréjaville et al., 2013). High fire frequency generally lead to a considerable decreases (Tinner et al., 2000) of the species.

According to the fire simulations, the immediate post-fire mortality is the highest observed amongst the species studied. Its thin bark makes the species especially sensitive even for the biggest trees. Our results were compared to the post-fire observations carried out by Maringer et al. (2016b) in Swiss and Italian Alps. We assumed that the low, moderate and high fire severities of the pre-cited authors were applicable to cold season, average summer and 2003 summer respectively. Low fire severity followed the mortality rate as calculated by Bauer et al. (2010) and Spalt et al. (1962) for a flame residence of 30s. Moderate fire severity was in in the middle of the bounded mortality rates for average summer. Finally, high fire severity were consistent with the maximum flame residence time in summer 2003 conditions independently of the method of calculation of the mortality used.

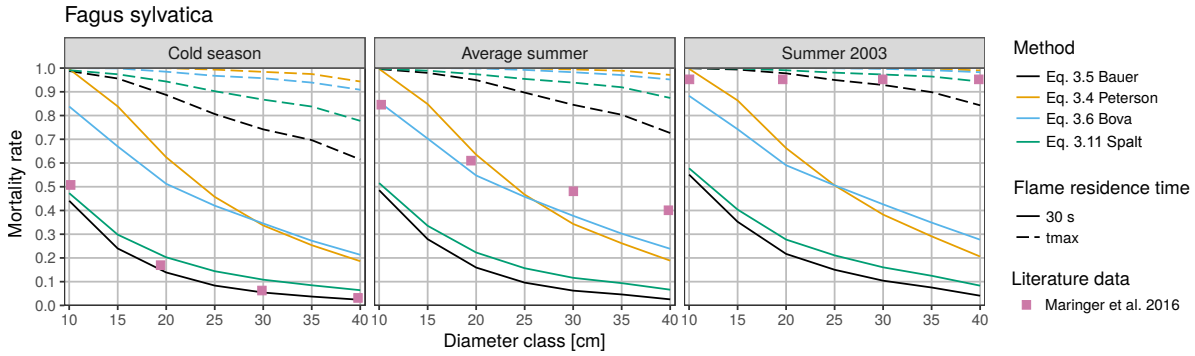

Figure 3.13 – *Fagus sylvatica* mortality rate by diameter and according to different climatic conditions.

Larix decidua is a "fire-indifferent" species (Tinner et al., 2000) due to its thick bark, especially for the biggest trees (Fréjaville et al., 2013), but especially because of its high post-fire resilience (Moris et al., 2017). Nonetheless, high mortality rates can be observed in low-density stands which are characterized by a low crown height or in young stands defined by thinner bark (Moris et al., 2017).

According to the fire simulations, the immediate post-fire mortality can be relatively high in the lowest diameter ($DBH < 20\ cm$) especially for the upper flame residence time bound. However, the mortality rate quickly decreased for bigger DBH which is consistent with the quick increase of bark thickness with diameter observed in this species (Fréjaville, 2015).

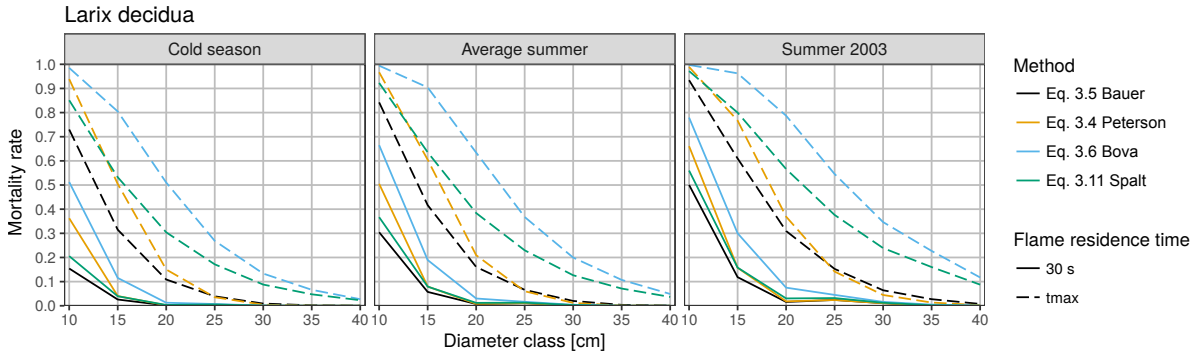

Figure 3.14 – *Larix decidua* mortality rate by diameter and according to different climatic conditions.

Pinus nigra* and *Pinus sylvestris have a similar behaviour toward fires (Fernandes et al., 2008). They are "fire-resistant" tree species which means that they can survive several surface fires from low to moderate intensities (Granström, 2001) especially when the trees *DBH* exceed 20 cm. *Pinus sylvestris* is however less resistant than *Pinus nigra* (Valor et al., 2017) partly due to its lower crown base height for a same *DBH* (Fernandes et al., 2008), but also because its tissues are less protected from heat (Valor et al., 2017). Comparisons of the post-fire mortality obtained from fire simulations with different post-fire mortality studies are shown in Fig.3.15 and Fig.3.16.

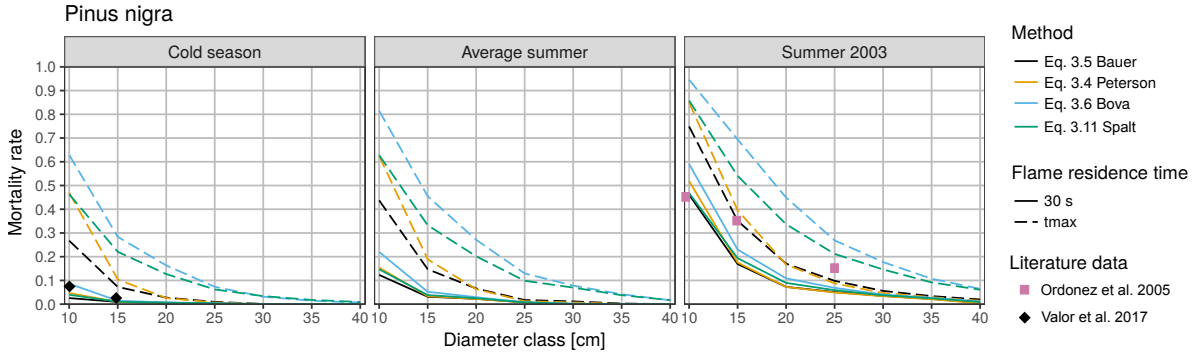

Figure 3.15 – *Pinus nigra* mortality rate by diameter and according to different climatic conditions.

Ordóñez et al. (2005) investigated post-fire mortality of *Pinus nigra* in NE of Spain after a large summer fire. According to the intensity of this fire, we assumed that their results could be compared to modelled mortality rate during the summer 2003 climatic conditions in the French Alps (Fig.3.15). Their observations were located in between the two bounds of flame residence time.

Valor et al. (2017) investigated post-fire mortality of both species for spring and fall fires in the foothills of the Pyrenees in Spain. Therefore, we compared their findings to the modelled mortality rate in the cold season. Their observations appeared to follow the mortality rate calculated with the Bova et al. (2005) method for short flame residence time.

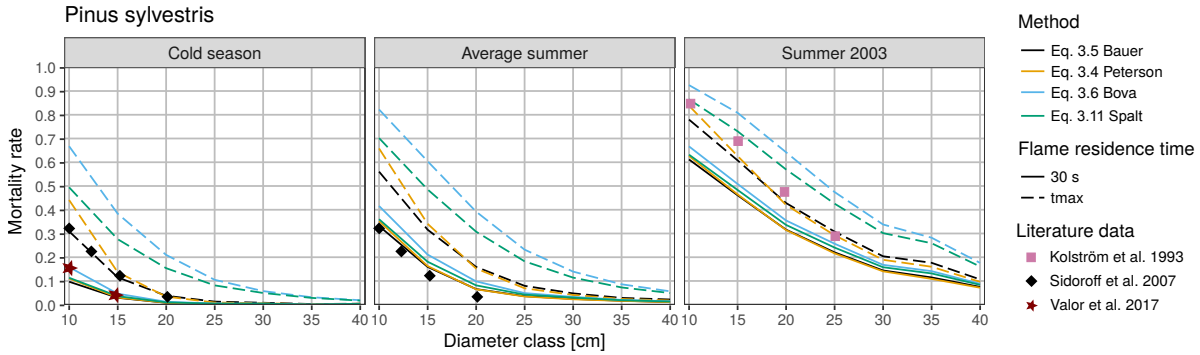

Figure 3.16 – *Pinus sylvestris* mortality rate by diameter and according to different climatic conditions.

Sidoroff et al. (2007) investigated post-fire mortality of *Pinus sylvestris* in Southern Finland after summer prescribed burnings. The values of *FL* and *ROS* observed during these fires are between the values modelled in our fire simulations for cold season and average summer season. Thus, we assumed that we can compare mortality rate measured in Finland to our modelled mortality for both climatic conditions (Fig. 3.16). The measured post-mortality followed Bauer

et al. (2010) mortality rate calculated for the maximum flame residence time in the cold season and was slightly lower than the modelled mortality for a flame residence of 30s in the average summer conditions.

Kolström et al. (1993) proposed the following logit model (Eq. 3.12) to estimate the probability of mortality of *Pinus sylvestris* based on field observation of a summer surface fire that occurred in summer in Finland.

$$P_{m-Kolstrom} = 1 - \frac{e^{\alpha+\beta \cdot DBH}}{1 + e^{\alpha+\beta \cdot DBH}} \quad with \quad \alpha = -3.4655 \quad and \quad \beta = 0.178 \tag{3.12}$$

Because the fire was characterized with moderate to high intensity, the results of this equation are plotted in the summer 2003 climatic conditions. the equation was. Eq. 3.12 was only applied for $DBH \in [0 - 25]\, cm$ which corresponds to its calibration range. The points are located between the two bounds of flame residence time.

Pinus uncinata* and *Pinus cembra are fire sensitive species due to their thin bark and low crown base height compared to others *Pinus* species (Fernandes et al., 2008). Fréjaville et al. (2013) conduced bark flammability tests on the main subalpine tree species and noticed that the bark of *Pinus cembra* was significantly more flammable than the other species studied.

The modelled mortality rates (Fig. 3.17) are in agreement with these specific traits with higher values than in others *Pinus sp.* Unfortunately, no field observations nor post-fire study were found concerning this species.

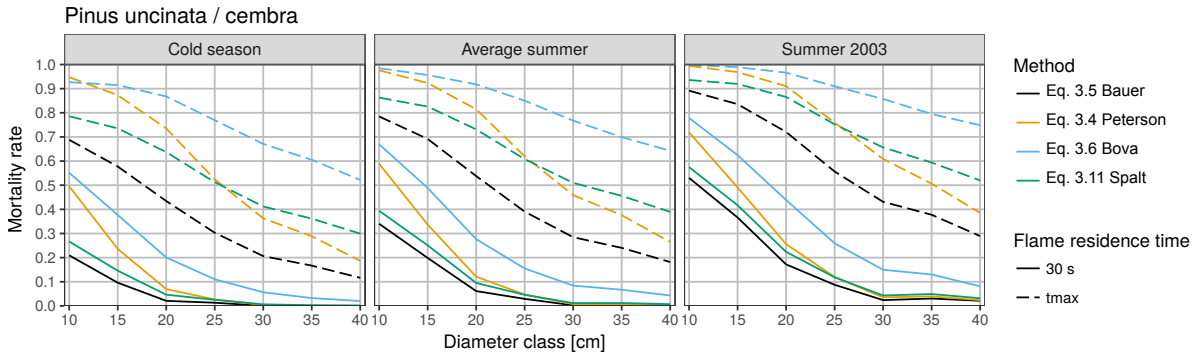

Figure 3.17 – *Pinus uncinata / cembra* mortality rate by diameter and according to different climatic conditions.

Deciduous Quercus sp. (e.g. *Quercus pubescens*, *Quercus robur* and *Quercus petraea*) are fire-indifferent species such as *Larix decidua* (Tinner et al., 2000). Conedera et al. (2010) described *Quercus robur* and *Quercus petraea* as highly resistant to low-fire intensity but sensitive to moderate fire intensity especially because of a high foliage loss and significant bark failures.

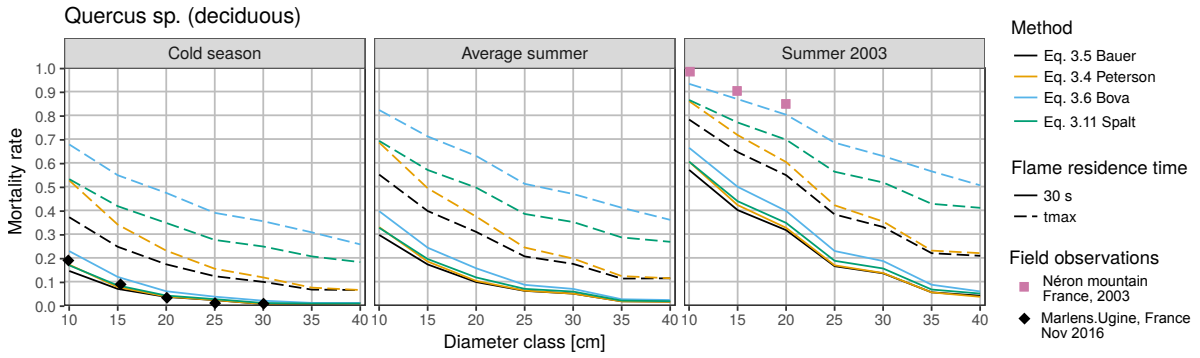

Figure 3.18 – Deciduous *Quercus sp.* mortality rate by diameter and according to different climatic conditions.

The modelled mortality rates agreed with this description with low values in the cold season and moderate to high values in extreme climatic conditions. Mortality rates observed after two events are displayed in Fig. 3.18. The first event burned about 100 ha of mixed coppices in November 2016 near Ugine, Savoie, France (450-900 m a.s.l.). Tree-mortality one year after fire are plotted in the cold season graph and followed the curves for flame residence time of 30s. The second event burned about 380 ha of shrubs and oak coppices on the Néron mountain near Grenoble, France in August 2003 (250 - 1300 m a.s.l.). Almost all trees died and the observed mortality follow the most extreme modelled curve for summer 2003.

3.3.3.2 Lessons from literature, field observations and modelled post-fire tree mortality

Different points can be emphasized from the preceding section 3.3.3.1. First, the modelled tree mortality agreed with the different sources and field observations especially because they are surrounded between two extreme flame residence times. Therefore, it seems important to confine modelled tree mortality between two bounds especially, in our case, for the average summer conditions. For the two others climatic conditions this point can be moderated. Thus, it appeared that mortalities from the different sources or field observations tend to follow the 30s flame residence in the cold season and the maximum theoretical flame residence time during the summer 2003.

Second, it is important to detail the tree mortality according to the size of the trees. This is not new but but we can see that the same tree species can be vulnerable at the young age but very resistant at the mature age (such as *Larix decidua*). At the contrary some species are vulnerable at almost all maturing stages (such as *Fagus sylvatica*). Here, only mortality rate as function of *DBH* is shown but a similar result could be obtain regarding the height of the trees (Rigolot, 2004).

According to the section 3.3.3.1, we selected one method of tree mortality calculation for each climatic conditions and each bound of the flame residence time range (see. Tab. 3.4). Those method were applied to calculated the mortality rate at the stand level range.

Climatic condition	Lower bound, flame residence = 30s	Upper bound, flame residence time = τ_{max}
Cold season	Eq. 3.11 (Spalt et al., 1962)	Eq. 3.11 (Spalt et al., 1962)
Average summer	Eq. 3.6 (Bova et al., 2005)	Eq. 3.11 (Spalt et al., 1962)
2003 summer	Eq. 3.6 (Bova et al., 2005)	Eq. 3.6 (Bova et al., 2005)

Table 3.4 – Selected methods for the post-fire mortality modelling at the stand level.

3.3.4 Post-fire mortality in the main forest types and climatic areas of the French Alps

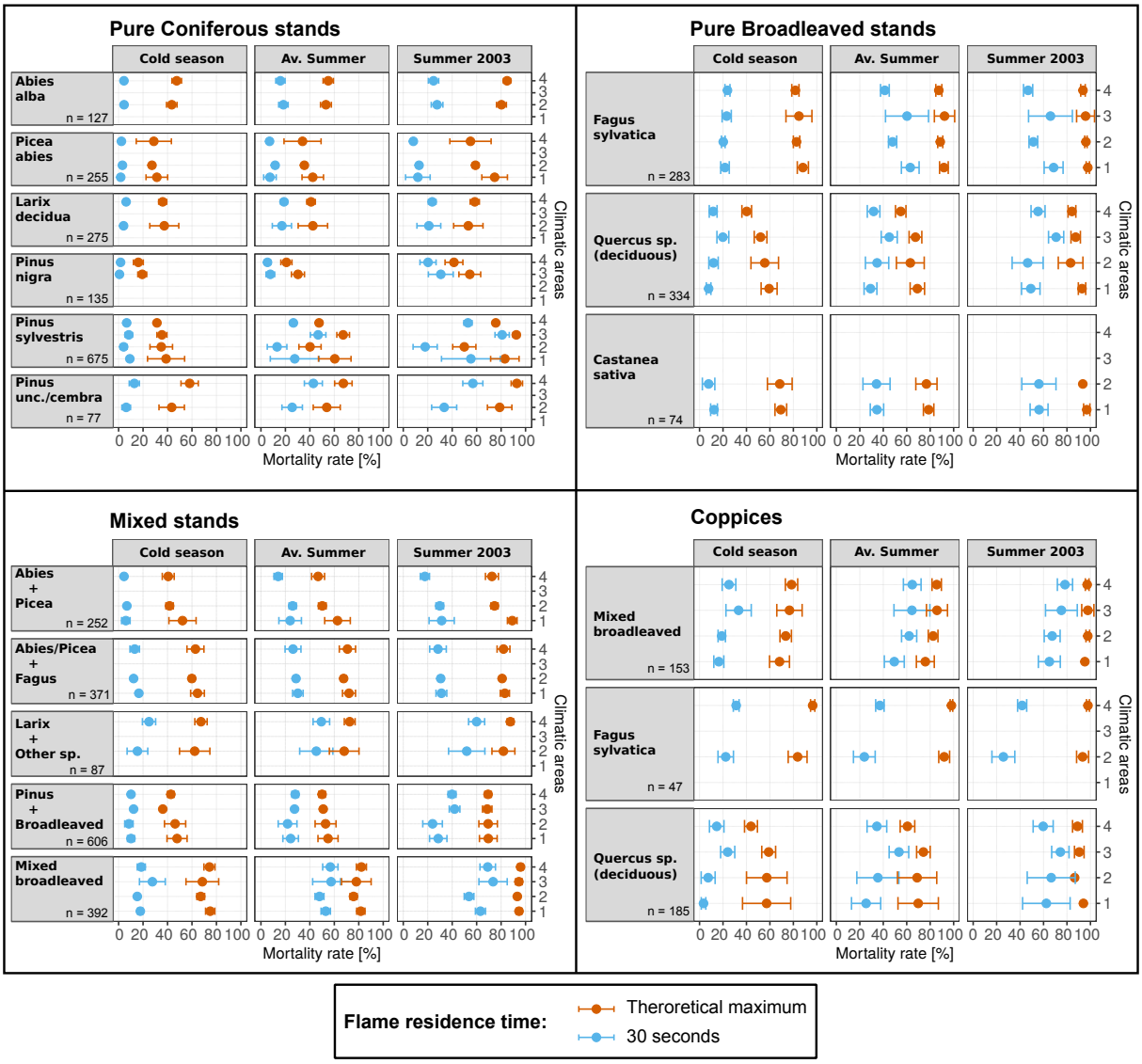

Figure 3.19 – Mortality rate modelled on the NFI plot according to forest type, climatic condition (Tab. 3.1) and climatic areas (Fig. 3.1) : 1-Northern Alps $\leq$ 800 m, 2-Northern Alps $>$ 800 m, 3-Southern Alps $\leq$ 800 m, 4-Southern Alps $>$ 800 m. The points indicate the mean value, error-bars indicate the 95% confidence interval. Forest types are shown only if at least 10 plots in the climatic area are present. Blue and orange colors correspond to short and theoretical maximum flame residence time respectively.

The modelled post-fire mortality at the forest stand level is displayed in Fig. 3.19 for the main forest types of the French Alps, the three climatic conditions and the four climatic areas. For

each configuration, the mortality rate was confined according to two flame residence times as defined in Tab. 3.4. The symbolic threshold of 50% was used in order to compare the mortality rate of the different forest types.

In the pure coniferous stands (see Dupire et al. (2016b) for definition), the mortality rates modelled in the cold season were quite low ($< 50\%$) even for upper limit except for pure stands of *Pinus uncinata / cembra* in the Southern Alps (60%). In average summer conditions, only pure stands of *Abies alba*, *Pinus sylvestris* (only at low elevations) and *Pinus uncinata / cembra* showed mortality rate above 50% for the highest bound. Finally, in extreme summer conditions, all stands except *Pinus nigra* showed upper limit of mortality above 50%. *Abies alba* and *Picea abies* stands returned the widest range of mortality rates.

In the pure broadleaved stands, modelled mortality rates were higher. In the cold season, all stands reached 50% for upper limit. *Fagus sylvatica* even reached 80% of mortality for the upper bound. In average summer conditions, pure stands of *Fagus sylvatica* showed mortality rate above 50% also for the lowest bound. Finally, in extreme summer conditions, all stands showed a lower limit of mortality above 50%.

In the mixed stands, modelled mortality rates were in between pure coniferous ans pure broadleaved stands. In the cold season, 3 forest types reached 50% for upper limit (*Abies/Picea/Fagus*, *Larix/Others sp.* and *Mixed Broadleaved*), the 2 others stayed just below. In average summer conditions, mixed stands of *Larix/Others sp.* and *Mixed Broadleaved* reached 50% of mortality even for the lowest bound while the others had their lower limit below the threshold of 50% and their upper limit above. Finally, in extreme summer conditions, the same trend is observed with a shift to greater values for both bounds.

Coppices showed the highest mortality rates just before pure broadleaved stands. This is certainly due to the small sizes of the tree compared to high stands dominated by the same species. All coppices reached the threshold of 50% in the cold season. In the summer, mixed coppices showed high mortality rate in average summer ($> 60\%$ for lower limit) and very high mortality in extreme summer condition ($> 80\%$ for lower limit). Values for *Quercus sp.* coppices are lightly lower but also reached very high level in summer 2003 conditions. Finally, *Fagus sylvatica* coppices presented a very wide range of mortality rate with relatively low lower bound and very high upper bound. This can be partly explained by the fact that *Fagus* coppices are mainly located at high elevations (from 900 to 1700 m a.s.l. in NFI plots) with a moderate fire-weather hazard which produce low intensity fires (see Fig. 3.5) that necessitate a long flame residence time to produce high mortality rates.

3.4 Discussion et conclusion

This work aimed at assessing post-fire tree mortality in the French Alpine forests from outputs of fire simulations based on different climatic conditions. It provided a complete method that returns the immediate post-fire tree mortality at both tree and stand levels. Uncertainties inherent in any modelling work are taken into account by returning mortality rates confined between two extreme scenarios represented by two flame residence times.

It is important to notice that we returned mortality rates independently on the probability of fire ignition. However, in the Western Europe, about 85% of wildfires result from human activities (Curt et al., 2016; Reineking et al., 2010) and only 15% from natural ignitions such as lightenings (Arndt et al., 2013). The spatial distribution of fire ignitions is also heterogeneous as most of the fire occur near human infrastructures and populated areas (Ganteaume et al., 2013; Moreira et al., 2011) which are mainly located in the foothills in mountain areas. Therefore, forest stands the most likely exposed to a fire ignition are also those that showed the highest mortality rates as, for sample, downhill coppices and high stands with broadleaved stands.

The predicted ranges of post-fire mortality can sometimes be quite wide (for sample for pure stands of *Abies alba* and coppices of *Fagus sylvatica*). This point is linked with the choice to confine the mortality between two extreme scenarios but also to the lack of information concerning the real fire behaviours that occurred in the different post-fire mortality studies. In fact, most of post-fire studies speak in terms of fire severity, e.g. the percentage of trees killed and not in fire intensity (Keeley, 2009). Most of the time, no information are given concerning the fire behaviour that caused a certain fire severity. It is therefore hard to have a direct link between modelled fire behaviours (which depends on climatic conditions and fuel properties) and fire impacts.

This shortcoming could be improved with a better documentation on the wildfire. In France, at the moment, the fire databases Prométhée (2017) and BDIFF (2017) only provide information about the date of ignition, the location, the burnt surface and sometimes the cause. It would be very interesting to have more information (even rough) on fire behaviour such as flame length, speed of the fire front, width of the flaming area and on the type of fire (surface, intermediate or crown fire). These basic informations do not required special material but would be very useful for the scientific community in order to better predict the effect of fire on trees.

In this study, we focused on the immediate post-fire tree mortality. Therefore, only direct mortality processes were taken into account, i.e. damages to the vegetative tissues resulting from their exposition to a heat source. However, indirect mortality (e.g. fungus or insects attacks, soil degradation...) might sometimes cause more damages to burnt forests in the long term (Varner et al., 2009; McHugh et al., 2003; Swezy et al., 1991). Furthermore, we did not account for the resilience abilities of the different tree species. For example, Conedera et al. (2010) showed that coppices of *Castanea sativa* can experiment high mortality levels after low to moderate fire intensity but also a quick response consisting in a strong vegetative resprouting activity few years after the fire. Moris et al. (2017), demonstrated that *Larix decidua* had a strong recruitment after fire, all the more so the fire intensity is high. At the opposite, several studies suggested that *Fagus sylvatica* lack of both resistant and resilient strategies (Maringer et al., 2016b; Conedera et al., 2010).

This point could be improved with the follow-up of several pilot forests across the Alps that were touched by a fire. A common method could be applied for the main forest types inspired by the pre-cited existing works. Doing so, the knowledge about both direct and indirect mortality together with the resilience ability of the main tree species of the Alps could be significantly improved. Such a network would also allow provide useful information for the adaptation of mountain forests to climate changes.

Finally, this work could find different applications in the quantification of ecosystem services loss due to different levels of fire intensity (Maringer et al., 2016a; Inbar et al., 1998b) in relation with climate changes. It can also provide useful information to forest managers and local stakeholders for the fire prevention by pointing out the forest stands and tree species the most vulnerable to wildfires.

CHAPITRE 4

Synthèse de la partie III

Dans cette partie, nous nous sommes intéressés à l'aléa incendie dans les forêts des Alpes françaises. Pour cela, deux études ont été conduites. La première s'intéresse à l'évolution spatio-temporelle de l'aléa feu-météo dans les Alpes françaises (Chapitre III.2) afin d'améliorer les connaissances actuelles sur l'occurrence de conditions météorologiques favorables aux incendies de forêt. La seconde étude concerne les effets des incendies sur les principales essences et les principaux types de peuplements (Chapitre III.3) : il s'agit de prédire le niveau de dommages produit par un feu sur les types de peuplements et les espèces. Les résultats principaux de cette partie sont détaillés ci-dessous.

Une cartographie à haute-résolution de l'aléa feu-météo.

Lors du travail exposé au Chapitre III.2 de nombreuses cartes à haute résolution (25m) ont été produites sur diverses composantes de l'aléa-feu météo : intensité du phénomène, longueur de la fenêtre d'opportunité pour le départ et la propagation des feux, nombres de jours par mois concernés par différents niveaux d'aléas... Outre leur intérêt scientifique, ces cartes représentent un outil d'aide à la décision important pour alimenter les décisions politiques dans le domaine de la lutte et de la prévention des incendies de forêts dans le contexte des changements climatiques en cours.

Trois types d'espaces connaissent une hausse significative de l'aléa feu-météo.

Les résultats de la première étude (Chapitre III.2) suggèrent que trois zones sont particulièrement concernées par une hausse significative de l'aléa feu-météo. L'augmentation la plus importante a été observée aux hautes altitudes ($>$ 800 m) des Alpes du Sud avec un aléa qui évolue dans toutes ses composantes (intensité, longueur de la saison feu, fréquence d'épisodes extrêmes...). La seconde zone concerne les basses altitudes des Alpes du Sud où les indices feu-météo sont les plus élevées des Alpes françaises. Cependant, la tendance à la hausse est moins marquée qu'aux hautes altitudes. Enfin la dernière zone marquée par une hausse de l'aléa se situe aux basses altitudes des Alpes du Nord ($\leq$ 800 m). Dans cette zone, l'aléa feu-météo reste modéré excepté lors de périodes de fortes chaleurs, comme lors de l'été 2003. La fréquence de telles périodes, favorables à des incendies intenses, a significativement augmenté au cours des dernières décennies.
Enfin, il faut souligner que les hautes altitudes des Alpes du Nord n'ont pas connu de hausse significative de l'aléa feu-météo de 1959 à 2015.

Mortalité post-feu à l'échelle du peuplement forestier.

La seconde étude (Chapitre III.3) permet d'évaluer la résistance des principaux types de peu-

plements forestiers à trois types de feu. Ainsi, les feux d'hiver, peu intenses, semblent très peu causer de dommages aux peuplements. Les feux d'été moyen en revanche peuvent entraîner des taux de mortalité modéré à élevés. Enfin, les mortalités potentielles observées après des feux d'été très sec et chaud (2003) sont généralement très élevées. Au sein d'un même peuplement, un incendie va avoir un effet très asymétrique en endommageant principalement les arbres de plus faible diamètre et/ou hauteur. De plus, certaines essences sont particulièrement vulnérables en raison d'une épaisseur d'écorce très fine (hêtre, sapin, pin à crochets, pin cembro...) et seront plus affectées que d'autres présentant des écorces plus épaisses (mélèze, pin noir, pin sylvestre, chênes décidus). Les peuplements les plus sensibles sont ainsi composés d'arbres de faible diamètre et/ou de faible hauteur. Cela concerne principalement les peuplements de type taillis, où les diamètres sont souvent faibles ainsi que les futaies feuillues et mixtes qui présentent une structure relativement irrégulière. Ces peuplements sont aussi ceux qui sont exposés au plus fort aléa feu-météo, car situés à basse altitude, en comparaison des futaies résineuses qui sont cantonnées en altitude et donc moins exposées à des conditions très sèches et chaudes.

Manque de relevés post-feu dans la zone alpine.

La seconde étude (Chapitre III.3) souligne le manque de relevés post-feu pour suivre la mortalité des arbres dans le temps. En effet, ces informations sont essentielles afin de calibrer les méthodes d'estimation de la mortalité et affiner les résultats de cette étude. Pour limiter les erreurs, la mortalité a été estimée par une borne basse correspondant à un temps de résidence du front de flammes court (30 secondes), et une borne haute correspondant à un temps maximum théorique (fonction de la charge en combustible et de sa teneur en eau).

Quatrième partie

Analyse multi-aléas

CHAPITRE 1

Introduction

Les milieux montagnards sont soumis à de multiples aléas liés au climat, à la topographie et à la géologie. Les méthodes présentées en partie II et III de ce mémoire permettent d'appréhender l'aléa chutes de blocs et l'aléa incendie individuellement ainsi que d'étudier leurs interactions avec les écosystèmes forestiers des Alpes françaises. L'objectif de cette thèse est de prendre en compte des aléas multiples et d'évaluer les effets de leur combinaison sur les risques encourus par différents enjeux humains et écologiques. En effet, les incendies peuvent profondément affecter la capacité de protection des forêts contre les chutes de blocs, comme cela a été démontré sur plusieurs hêtraies des Alpes suisses et italiennes (Maringer et al., 2016a). Hormis cet exemple, cet effet cascade reste peu étudié alors que la demande de connaissances et de méthodes sur ce sujet augmente chez les décideurs publics et les gestionnaires du territoire. L'objectif principal de cette partie est ainsi de quantifier l'effet d'un incendie sur la capacité de protection des forêts alpines françaises qui protègent les enjeux situés en aval. Les mortalités des arbres estimées pour chacun des trois scénarios de feu (Chapitre III.3) sur 4438 placettes forestières sont ainsi utilisées pour quantifier l'effet protecteur de ces forêts avant et après feu en s'inspirant de la méthode présentée aux chapitres II.2 et II.3.

En parallèle de ce travail conduit à l'échelle des principaux types de peuplement forestier, une analyse spatiale a été effectuée sur tout le territoire alpin français. Le premier objectif de cette analyse est d'identifier et de localiser les forêts de protection contre les chutes de blocs ainsi que les enjeux humains (routes, voies ferrées, bâtiments) qu'elles protègent. Le second objectif est d'évaluer les potentiels effets cascades après incendie en fonction de l'aléa feu-météo (Chapitre III.2) et de la vulnérabilité des peuplements aux incendies.

Démarche méthodologique

L'analyse multi-aléas a tout d'abord été menée à l'échelle du peuplement forestier. Pour cela, la mortalité post-feu obtenue au chapitre III.3 pour les arbres de 4438 placettes forestières réparties dans les Alpes françaises a été introduite dans la chaîne de modélisation de la capacité de protection contre les chutes de blocs (Chapitres II.2 et II.3). Ainsi, pour chaque placette forestière, des simulations de propagation de blocs ont été réalisée avec Rockyfor3D pour chacun des scénarios de feu (feu d'hiver, feu d'été moyen, feu d'été extrême). Pour prendre en compte l'effet du feu sur le peuplement initial, les arbres présentant une probabilité de mortalité après feu supérieure à 50% ont été retirés des simulations. Cela a ainsi pour effet de réduire la probabilité d'impact contre les arbres et donc l'effet protecteur de la forêt.
L'indicateur *ORPI* défini précédemment, ainsi que la longueur de forêt nécessaire pour réduire l'aléa chutes de blocs de 99% (L_{99}) ont ensuite été calculés à partir des résultats de simulations

afin de comparer la capacité de protection avant et après feu pour chaque scénario. Ces indicateurs ont dans un premier temps été utilisés afin d'identifier les peuplements susceptibles de connaître une baisse de leur capacité de protection. Ensuite, l'influence des variables forestières et topoclimatiques sur la baisse de la capacité de protection a été étudiée pour chaque type de peuplement en utilisant des algorithmes de forêt aléatoire (Random Forest).

L'analyse a ensuite été conduite à l'échelle des Alpes françaises. Une méthode de cartographie des forêts de protection contre les chutes de blocs a été élaborée. Cette méthode se divise en deux étapes. Tout d'abord, des simulations de propagations de blocs sont réalisées avec Rockyfor3D à large échelle pour identifier les zones potentielles de propagation des blocs. Ensuite, les profils en long reliant chaque zone de départ de blocs aux enjeux humains situés dans la zone de propagation en aval sont analysés. Si une partie du profil contient des forêts, celles-ci sont cartographiées comme forêt de protection potentielle.
Pour chaque forêt de protection cartographiée, la capacité de protection initiale contre les chutes de blocs est estimée en comparant la longueur boisée du versant avec les valeurs de *ORPI* observée pour la même longueur au sein des placettes forestières (parmi les 4438) appartenant au même type de peuplement que celui de la forêt considérée (Chapitre II.2). Pour évaluer les effets cascades après chaque scénario de feu, les indices d'aléa feu-météo (Chapitre III.2) sont, dans un premier temps, extraits pour chaque forêt. En fonction du niveau de l'aléa feu-météo observé, du type de peuplement et de la longueur boisée, la capacité de protection post-feu est estimée en utilisant la même méthode que pour l'estimation de la capacité de protection initiale. Enfin, la capacité de protection des forêts, et le niveau d'exposition des enjeux humain sont analysés pour chaque scénario de feu en fonction des 4 zones d'analyses utilisées lors des chapitres précédents (Alpes du Nord / du Sud, altitude $\leq$ 800 m / $>$ 800 m).

CHAPITRE 2

Évaluation des effets cascade résultant du passage d'un incendie dans les forêts de protection contre les chutes de blocs

Forest fires in mountain forests with a protection function against rockfalls : assessing cascading effects

Dupire S., Curt T., Bigot S.

Article in preparation

Abstract : Natural hazards are frequent in mountain areas where they regularly cause casualties and damages to human infrastructures. Mountain forests contribute in mitigating these hazards, in particular rockfalls. However, some natural hazards such as wildfire can damage the protection forests and reduce their protective capabilities.

A multi-hazard analysis was carried out in order to assess the damaging of the protection capabilities against rockfall of the forests of French Alps. This cascading effect was first evaluated at the stand level from results of rockfall simulations on 4438 forest plots. For each forest plot, three wildfire scenarios were applied (cold season wildfire, average summer wildfire, extreme summer wildfire) and the loss of rockfall protection capability was quantitatively computed from the rockfall simulations. The spatial co-occurrence of both hazard was also investigated and the importance of the different forest types as well as the residual risk on human assets were documented.

The results at the stand level highlighted the high vulnerability to wildfire of the most protective forest types (coppices and high broadleaved stands) and the important resulting cascading effects in case of fire. Mixed stands and pure coniferous stands generally presented a lower loss of protection capability. The spatial analysis showed that the low elevation areas (< 800 m) are the more subject to high cascading effects in case of fire, especially in the Northern Alps where a high concentration of human assets is exposed to rockfall hazard.

Keywords Cascading effects · Forest fires · French Alps · Rockfalls · Mountain forests · Natural hazards · Protection forest · Multi-hazard

2.1 Introduction

Mountain areas are particularly concerned by a high concentration of natural hazards. In the Alpine region the main natural hazards can be classified according to four groups (Gill et al., 2014): geophysical (avalanche, landslide, rockfall), hydrological (flash-flood, debris flow, erosion, drought), atmospheric (wind storm, thunderstorm, lightening) and biophysical (wildfire, pests and pathogens attack). Long term trends highlight an increase of the number of disasters in the mountains over the last century (Hewitt, 1997) and a significant evolution of the natural hazard activities due to climate and societal changes (Einhorn et al., 2015).

Different hazards can co-occur on a same place and/or at the same time and the overall effects produced by these interactions may be greater than the simple addition of the effects of each individual hazard (Gill et al., 2016). However, if single-hazard analyses are well-established, the study of multiple hazards is much more challenging due to the different characteristics of each process and the evaluation of the potential cascading effect resulting from the hazard interactions (Gill et al., 2016; Kappes et al., 2012).

The role of mountain forests in mitigating natural hazards are well known (Brang et al., 2001). However, some natural hazards (e.g. avalanches, storms, drought, wildfire) can damage the forest itself and reduce its protective capabilities. Different studies were interested in multi-hazard in relation to European or Alpine forests. Vacchiano et al. (2016) crossed the maps of the different natural hazards in Aosta Valley (Italy) with the protection forest map and identified those prone to multi-hazard. Bebi et al. (2009) investigated the ecosystem disturbances in protection forests following snow avalanches in Switzerland. Fonseca et al. (2017); Inbar et al. (1998a) focused on the erosion processes following wildfires in Mediterranean areas. Nunes et al. (2017) studied the post-wildfire hydro-geomorphological hazards in Portuguese mountains. Finally, Maringer et al. (2016a) investigated the temporal evolution of the protective effect against rockfalls of burnt forests of *Fagus sylvatica* in Swiss and Italian Alps.

These examples highlight the growing interest in assessing the indirect effects of wildfires on others natural hazard through the damaging or destruction of the natural protection offered by the mountain ecosystems. It is especially important in a context of climate changes which favour the ignition and the propagation of forest fires in the Alps (Dupire et al., 2017; Wastl et al., 2012).

In this study, we focused on the cascading effects resulting from different wildfire scenarios in forests with a protective effect against rockfall. A functional analysis of this multi-hazard interaction was first carried out at the stand level on the main forest types of French Alps in order to quantitatively assess the loss of protection capability according to dominant tree species, location and wildfire severity. In a second phase, we investigated the potential spatial co-occurrence of both hazard at the French Alps scale. The spatial importance of the different forest types as well as the residual risk on human assets were then documented according to three wildfire scenarios and four climatic areas.

2.2 Materials and Methods

2.2.1 Functional analysis at the forest stand level

2.2.1.1 Forest data

Forest data were extracted from the permanent sample plots of the French National Forest Inventory (NFI) based on a systematic grid of 1 km × 1 km covering the complete country. A minimum slope threshold of 20° was applied in order to select only forests situated on moderate to steep slopes. This resulted in the selection of 4438 plots measured from 2005 to 2015. NFI data collection is based on circle plots (Robert et al., 2010) where stand properties and ecological and

topographic data are assessed in a 25-m radius. On each plot, tree characteristics (species, total and first branch heights) are inventoried for all trees with a diameter at breast height (DBH) greater than or equal to 7.5 cm.

2.2.1.2 Wildfire scenarios and associated post-fire tree mortality

Three wildfires scenarios were used in this study. They were defined according to the climatic conditions observed during the period 1959-2015 in the French Alps (see (Dupire et al., 2017; Dupire et al., In Prep. (a))). The first fire scenario corresponded to wildfire occurring in the cold season (January to April plus November and December) where 60% of the vegetation fires are registered in the French Alps (Dupire et al., 2017). Those fires generally have a low intensity and are limited to the understory vegetation. The second fire scenario represented forest fires occurring during summer with average climatic conditions (mean of 1959-2015 observations). Finally the last scenario corresponded to extreme summer climatic condition which were chosen as the 2003 summer in the French Alps according to climatic records (see Dupire et al. (In Prep. (a))).

The probability of post-fire mortality (P_m) was calculated for each tree of each NFI plot according to the wildfire scenario (fire intensity, flame residence time) and the tree characteristics (bark thickness, total height and base of the crown height). Individual tree mortality was marked out within two thresholds corresponding to two flame residence times (30 s and theoretical maximum duration of lethal bole which ranged from 1 to 5 min). For more information see Dupire et al. (In Prep. (a)).

2.2.1.3 Rockfall propagations at the stand level

For each NFI plot, rockfall propagations were simulated using the model Rockyfor3D (Dorren, 2015). Simulations were run on a virtual slope surface in order to focus on the protective effect of forests. Each virtual digital terrain model had a 2-m resolution, a regular slope α corresponding to the NFI plot slope and a total length L of 2100 m in the slope direction. In order to emphasize differences between forest stands, rock volume and surface roughness were respectively fixed to 1 m^3, and 0 cm. Moreover the same soil type (*soiltype*=3, medium compact soil) was used for all NFI plots. 30000 theoretical blocks were released for each NFI plot. The trajectory of each block was followed every 5 meters along the slope surface to register both kinetic energy and number of passing blocks depending on the distance to the release line. The protection potential of the forest was evaluated by comparing the results of simulations according to the three different scenarios : without forest, with forest before fire, with forest after fire (Fig. 2.1).

Integration of forest characteristics in Rockyfor3D was done using a *treefile* for each NFI plot. The *treefile* contained the locations and the *DBH* of all trees on the slope surface as well as their probability of mortality P_m according to the wildfire scenario. It was created following two steps. First, the location of the trees in the slope surface were generated following an uniform random distribution of trees coordinates. Second, diameters, species and probabilities of mortality of each tree were attributed following the diameter and species distributions observed on the NFI plot as well as the post-fire tree mortality calculated previously.

Most recent works on the effect of trees on rockfalls (Toe et al., 2017c; Dupire et al., 2016a) suggest that tree diameter is the preponderant parameter during the impact of a block on a tree far ahead intra-specific and inter-specific mechanical properties. For this reason instead of artificially reduce the mechanical properties of burnt trees, we adopted a conservative binary approach consisting in removing all trees with a $P_m > 0.5$ according to a wildfire scenario from the initial *treefile* for the post-fire rockfall simulations (see Table 2.1).

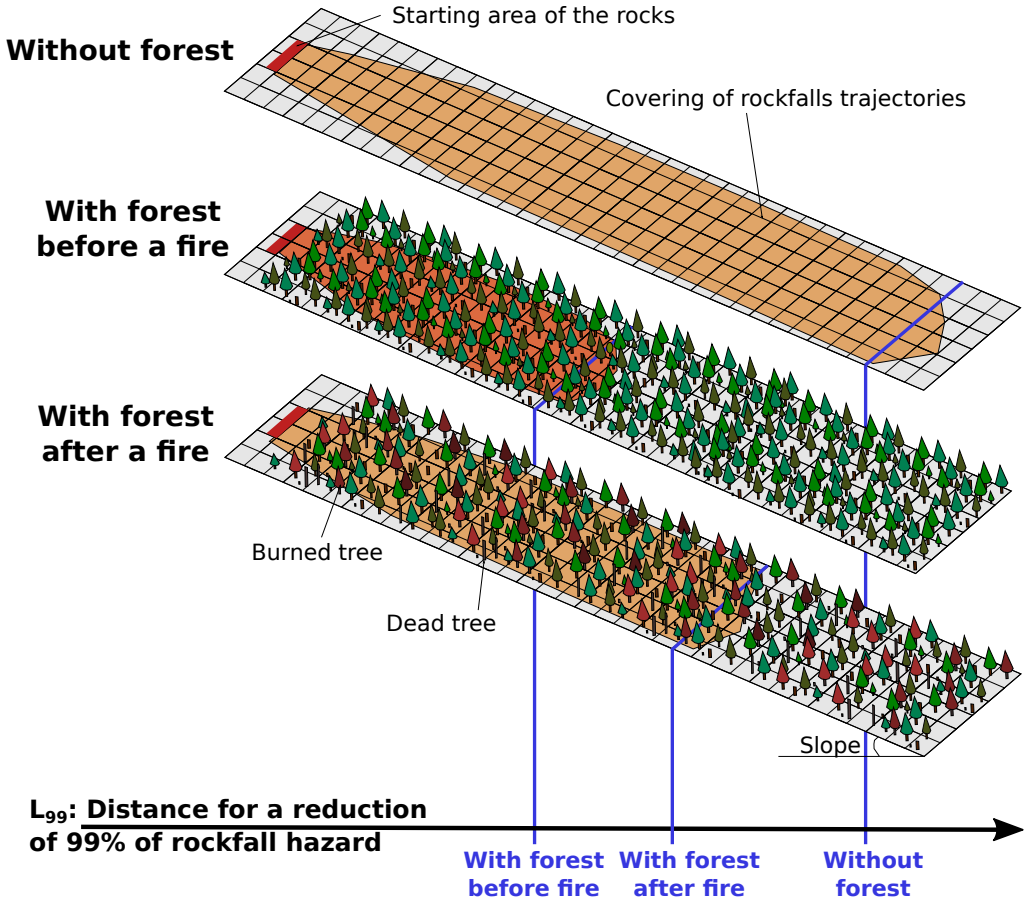

Figure 2.1 – Virtual terrain with uniform slope and length along the slope of 2100m. For each NFI plot, the same profile was used for the different scenarios. Calculation screens are located every 5 m along the different profiles in order to collect the rock energy and rock number distributions along the slope.

At the end, 8 simulations per NFI plots were tested as shown in Table 2.1. It resulted in 35504 (8 scenarios × 4438 plots) simulations that were computed on the Grenoble University high performance computing centre (CIMENT).

Simulation with forest	Wildfire scenario	Flame residence time	*treefile* taken
No	None	0	None
Yes (Reference)	None	0	initial *treefile*
Yes	Cold season	30 s	initial *treefile* without trees with $P_m(Cold\ season - 30s)$>0.5
Yes	Cold season	Max	initial *treefile* without trees with $P_m(Cold\ season - max)$>0.5
Yes	Av. Summer	30 s	initial *treefile* without trees with $P_m(Av.\ Summer - 30s)$>0.5
Yes	Av. Summer	Max	initial *treefile* without trees with $P_m(Av.\ Summer - max)$>0.5
Yes	2003 Summer	30 s	initial *treefile* without trees with $P_m(2003\ Summer - 30s)$>0.5
Yes	2003 Summer	Max	initial *treefile* without trees with $P_m(2003\ Summer - max)$>0.5

Table 2.1 – Description of the 8 rockfall simulations ran for each NFI plots. Two flame residence times are used for each wildfire scenarios.The minimum time is fixed to 30 s, the maximum time (Max) is the theoretical maximum flame duration which depends on the type, load and moisture of the fuel (see Dupire et al. (In Prep. (a))).

The rockfall protection capability was assessed using the minimum forest length L_{99} (Dupire et al., 2016b) required to get 99% of the overall rockfall hazard reduced. L_{99} is derived from the Overall Rockfall Protection Index ($ORPI$) introduced in Dupire et al. (2016a). $ORPI$ integrates both the proportion of stopped rocks (frequency) and the total energy reduction of the rocks due

to the presence of forest (intensity). It is calculated as shown in Eq. 2.1 :

$$ORPI(L) = 100 \times \left(1 - \frac{\sum_{i=1}^{nfor} E_i(L)}{\sum_{k=1}^{nbare} E_k(L)}\right) \quad (2.1)$$

On the same slope surface, *ORPI(L)* compares the sum of the energies of all the blocks that reached the distance L from the release line according to two configurations : (1) a forested slope surface ($\sum_{i=1}^{nfor} E_i(L)$) and (2) a bare slope surface ($\sum_{k=1}^{nbare} E_k(L)$). *nfor* and *nbare* correspond respectively to the number of blocks that reached the distance L for the configurations (1) and (2).

Therefore, L_{99} is the minimum L required to get an ORPI value greater than or equal to 99. This length was computed for the 7 simulations with forest (see Table 2.1) for each NFI plot.

2.2.1.4 Analysis of the cascading effect at the stand level

The distribution of L_{99} according to the different wildfire scenarios were compared for the main forest types encountered in the French Alps (Dupire et al., 2016b). Kruskal-Wallis tests were performed for each forest type in order to test differences in the L_{99} ranks observed for each scenario. The tests were followed by a pair-wise comparisons between the scenarios using the Dwass-Steel-Critchlow-Fligner post-hoc procedure (Hollander et al., 2013) only if the Kruskal-Wallis indicated significant differences.

In addition to this first analysis, we computed Random Forest (RF) regression (Breiman, 2001) for each wildfire scenario and forest type. RF presents several advantages : (1) it allows to estimate the importance of several predictor variables influencing the response variable, (2) it is robust in case of variable collinearity, and (3) it is possible to visualize the effect of predictors on the response variable (Cutler et al., 2007).

In this study, the response variable is the mean difference in L_{99} between a wildfire scenario and the reference scenario without fire. According to Dupire et al. (In Prep. (a)), we assumed the following weighting for the mean difference in L_{99} :

- Cold season : 0.75× 30s flame residence time + 0.25× Max. flame residence time
- Average summer : 0.5× 30s flame residence time + 0.5× Max. flame residence time
- Summer 2003 : 0.25× 30s flame residence time + 0.75× Max. flame residence time

Beside the response variable, 10 predictor variables were used for the RF regressions (see Table 2.2). They were selected amongst the available variables that describe (1) forest stand (basal area, mean diameter, diameter distribution, stand height, canopy base height), (2) vegetation layers (cover rates of herbaceous, shrubs and trees), and (3) climate and position (elevation, fire weather hazard, latitude, longitude). The selection was based on the pair-wise collinearity of the variables. If the correlation coefficient was less than -0.5 or greater than 0.5 only one variable was kept. This condition occurred three times. First, with mean diameter and diameter distributions, the diameter distribution was kept as it contains more information than only the mean diameter. Second with stand height and canopy base height, the stand height was selected as it is more common in forest management practices. Last, with elevation and FFMC, the FFMC was kept because it returns information about the fire weather danger.

Due to the stochastic component of RF, each new run can produce a slightly different rankings of predictor variables importance. For this reason, we computed 20 RF runs for each forest type and each wildfire scenario and classified the predictors according to their average ranks. The default parameters used for all RF runs were : number of trees = 1000, minimum terminal node size = 5, and number of variables tried at each split = 3. The variable importance was classified according to the indicator $\%IncMSE$ which returns the increase of the mean square error (MSE)

Variable	Description	Unit
G	Basal area of all trees with DBH $\geqslant$ 7.5cm	$m^2 \cdot ha^{-1}$
H	Mean height of all trees with DBH $\geqslant$ 7.5cm	m
Perche	Proportion of stems with DBH $\in$ [7.5-17.5[("Perche")	%
PB	Proportion of stems with DBH $\in$ [17.5-27.5[("Petit bois")	%
BM	Proportion of stems with DBH $\in$ [27.5-47.5[("Bois moyen")	%
%Shrubs	Cover rate of small wooden species (Height $<$ 2m)	%
%Herb	Cover rate of herbaceous species	%
FFMC	Fine Fuel Moisture Code (Van Wagner, 1987)	None
Lat	Latitude of the NFI plot (EPSG 2154)	1000 km
Long	Longitude of the NFI plot (EPSG 2154)	1000 km

Table 2.2 – Description of the 10 predictor variables used in the Random Forest regression.

when the variable is randomly permuted (i.e. same initial model with one variable less). Thus, if an important variable is randomly permuted, the predictions will significantly change which will produces a high value of $\%IncMSE$.

Partial dependence plots were also produced to interpret the effect of the four main predictors on the loss of rockfall protection capabilities, one of the predictor variable being preferentially the FFMC when it contributes significantly to the regression. Even if the objective was not to produce high performance models, we also showed the total variance explained by RF. All this modelling process was carried out using the R package *randomForest*.

2.2.2 Spatial analysis at the French Alps scale

2.2.2.1 Data source

Spatial data used in the analysis were taken from the French institute for geographic and forest information (IGN : http://professionnels.ign.fr/donnees) databases.

Forest cover was extracted from the BDForêt® version 2.0 which describes forest and natural plan formations obtained by photo-interpretation. Available as a shapefile (vector layer of polygons), it returns a basic description of stand type and dominant species for areas over 5000m^2. Forest types provided by this data source are therefore less detailed than those available in the NFI plots. For sample some of the forest types used in the functional analysis are merged in the forest cover (see. Table 2.3).

Name of the forest type in BDForêt® version 2.0	Concerned forest types in functional analysis
Abies / Picea	Pure Coniferous stands - Abies alba
	Pure Coniferous stands. - Picea abies
Mixed Broadleaved and Coniferous	Mixed stands - Pinus sp. / Broadleaves
	Mixed stands - Larix / Others
	Mixed Abies / Picea / Fagus
Mixed Coniferous	Mixed stands - Abies / Picea
	Mixed stands - Larix / Others

Table 2.3 – Correspondence between BDForêt® version 2.0 forest types and functional analysis forest types.

The relief was extracted from the BDAlti® which is a digital terrain model (DTM) with a raster cell definition of 25m available for the entire French territory. Terrain slope was derived from the DTM in order to identify the potential rock release areas according to Eq. 2.2 (Toe et al., 2015):

$$\alpha = 55 \times Resolution^{-0.075} \tag{2.2}$$

If the slope of a raster cell is greater than or equal to α (°), the cell was identified as potential release zone (e.g. α=43.2° for a 25m resolution).

Human assets were taken from the BDTopo® which is the database locating all topographical information in France. The assets used were of four types (see Table 2.4). Four layers were therefore used (shapefile format). For linear assets, the portions located inside a tunnel were removed from the analysis as they obviously cannot be subjected to rockfalls. No detailed information was available in the BDTopo® in order to distinguish the different types of buildings (e.g. houses, schools, industry, etc.). Thus, we assumed the same vulnerability to rockfall for all buildings. Moreover, there was no information about linear assets that are already protected from rockfall with permanent civil engineering fences such as embankments. Therefore, linear assets were assumed to be vulnerable to rockfall on their entire length.

Name	Description	Shape
Buildings	Houses, socio-economic complexes, infrastructures	Polygon
Railways	National or regional railway lines	Line
Main roads	Highways + national or regional roads	Line
Secondary roads	Local roads + passable tracks	Line

Table 2.4 – Description of the human assets used in the spatial analysis.

Fire weather hazard was taken from Dupire et al. (2017). Only the fine fuel moisture code (FFMC) maps were used, they were simplified in order to get 4 levels of fire weather danger : Low for FFMC<88.1, Moderate for FFMC$\in$ [88.1 − 90.5[, High for FFMC$\in$ [90.5 − 92.3[and Extreme for FFMC>92.3.

Protection capabilities according to wildfire scenario were calculated for each BDForêt® version 2.0 forest types from the results of the functional analysis. For each forest type, we computed the 75^{th} percentile of the length of forest needed to reach a given ORPI value from the rockfall simulation on NFI plots (see section 2.2.1). This length of forest was calculated for each wildfire scenario for ORPI in the range [1-99] with a step of 1.

2.2.2.2 Workflow of the spatial analysis

The spatial analysis was divided into three consecutive steps as presented in Fig. 2.2.

a. Rockfall hazard mapping was realized with the Rockyfor3D software (Dorren, 2015) on the entire French Alps using a raster cell resolution of 25m (native DTM resolution). The modelling parameters were chosen to produce the theoretical maximum propagation of the rocks. Surface roughness was set up to 0 cm, rock volume to 5 m^3 and soil type to medium compact (*soiltype*=3). In order to avoid non realistic rock propagation along the rivers, we fixed the soil type to "water" (*soiltype*=0, i.e. complete stop of the rocks) in rivers with a permanent water regime and surface roughness to 30 cm in rivers with non-permanent water regime. The propagations of 500 blocks per potential release raster cell (slope≥43.2°, see Eq. 2.2) were modelled.

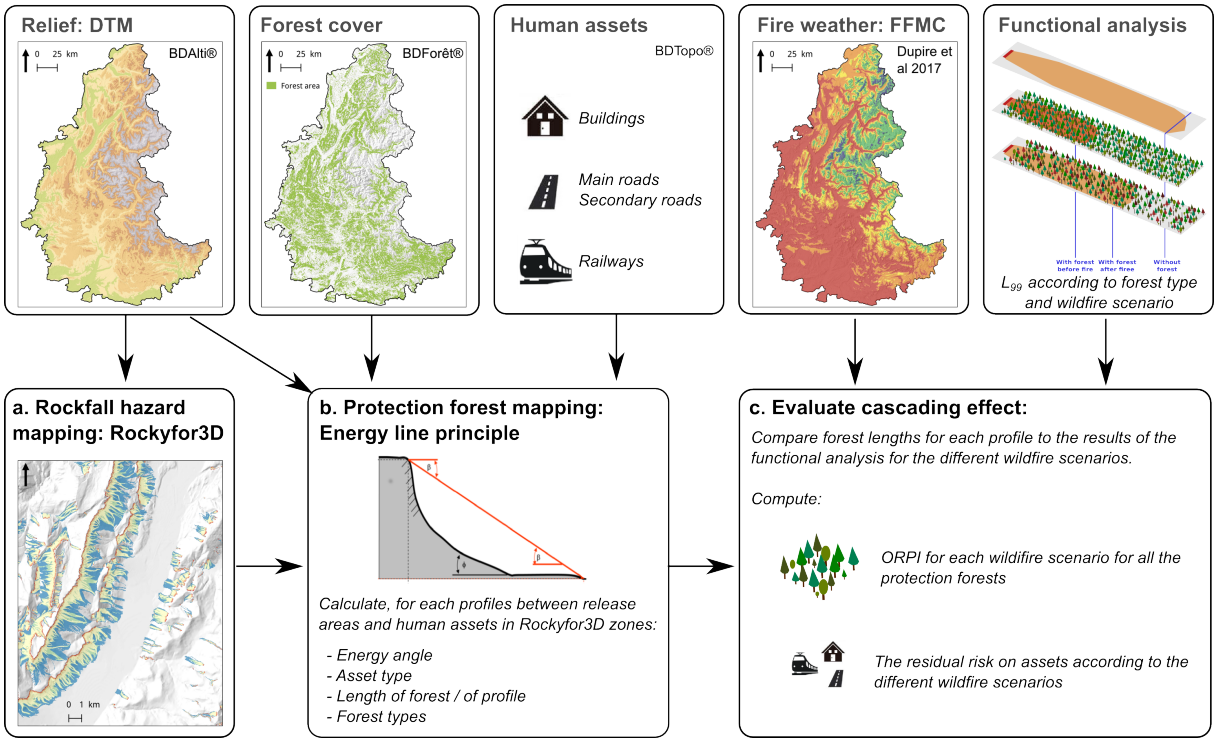

Figure 2.2 – Workflow of the spatial analysis.

b. Protection forest mapping was then completed using the energy line principle first described by Heim (1932) and then used by Berger et al. (2007) and Toe et al. (2015). The energy line is characterized by the angle β between the horizontal plane and a fictive line drawn between the top of a rockfall source to the stopping point (Fig. 2.3). β is easy to measure on the field and can provide a rough statistical estimation of the rockfall run-out distance. A classification of the rockfall danger has been proposed in France based on the distribution of β values measured for about 1000 events across the Alps (Table 2.5 from BRGM et al. (2014)).

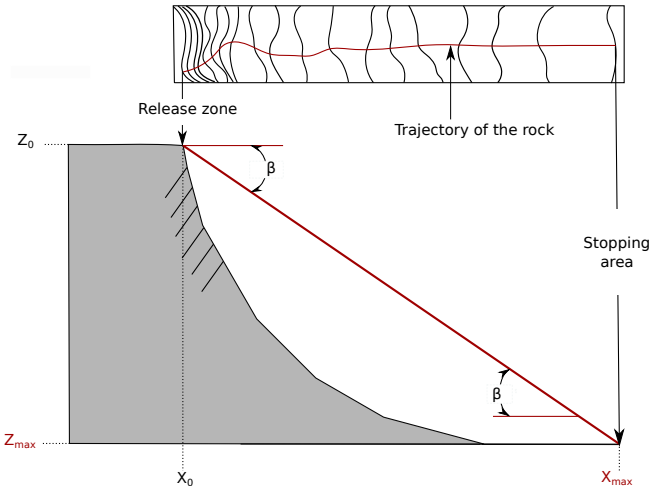

Figure 2.3 – Energy line principle adapted from Toe et al. (2015) on a theoretical ground profile. The energy angle β is given by the equation $\beta = atan\left(\frac{z_0 - z_{max}}{x_{max} - x_0}\right)$

β value	Rockfall hazard	% events
$\beta < 26°$	Extremely low	4%
$26° \leq \beta < 30°$	Low	9%
$30° \leq \beta < 33°$	Low to moderate	10%
$33° \leq \beta < 35°$	Moderate to high	10%
$\beta \geq 35°$	High	67%

Table 2.5 – Classification of rockfall danger according to the energy line angle (BRGM et al., 2014).

In order to map the protection forests we proceeded as follow :

1. Select all assets that intersect the rockfall propagation area computed with Rockyfor3D ;
2. Calculate β for all combinations between an asset and the release areas in a 5km radius
   if $\beta \geq 26°$ and ground profile always going down, save the profile characteristics :
   - Angle β
   - Total length (L_{tot}) and forested length (L_{for}) along the profile
   - Dominant forest type encountered on the profile
   - Type of the concerned asset (railway, building, main or secondary road)
   - x,y,z coordinates of asset and release area

At the end of this process we obtained a database containing all the potential ground profiles between release areas and human assets. With a simple rasterization of these profiles, we could eliminate the areas of rockfall propagation with no human asset from the Rockyfor3D outputs. Finally the forests with a potential protective function against rockfall were mapped by intersecting the new rockfall propagation area with the forest cover (BDForêt®).

c. The cascading effect at the French Alps scale was finally assessed combining the results of the previous steps with the fire weather data and the protection capabilities of the forests according to the different wildfire scenarios.

For each profile from the database created at the previous step we estimated the overall rockfall protection index (ORPI) according to the length of forest (L_{for}), the dominant forest type and the wildfire scenario (see 2.2.2.1). The FFMC value at the location of the asset was used in order to identify the fire weather danger. If the fire weather danger of a period (cold season, average summer or 2003 summer) was low (FFMC<88.1, (Dupire et al., 2017)), we used the ORPI value corresponding to the scenario without fire, otherwise the ORPI value of the period was used. Once the estimated ORPI of the different wildfire scenarios were computed, we rasterized it at the French Alps scale with a conservative objective. Thus, if a raster cell was concerned by different profiles, the lowest ORPI value was kept.

The four rasters of ORPI (without fire, cold season fire, average summer fire and 2003 fire) were then intersected with (1) the forest cover (BDForêt®) and (2) the different human assets layers (BDTopo®). This final step returned respectively the potential protection capability (ORPI) for each forest type and the residual risk on human assets (100−ORPI) for each wildfire scenario.

2.3 Results

2.3.1 Functional analysis

2.3.1.1 Increase of the length of forest to reach ORPI≥99 after a fire

Table 2.6 and Fig. 2.4 present the distribution of L_{99} according to the different wildfire scenarios and forest types. Independently of the wildfire scenario, we can already rank the stand types according to the increase of L_{99} after fire. Coppices suffered the highest loss of rockfall protection capability followed by pure broadleaved stands, mixed stand and finally pure coniferous stands. This ranking can be explained by several factors. First the more the initial protection capability is high, the more it is susceptible to decrease. When we observed this data (see Fig. 2.4) we can see that without fire the highest protection capabilities are observed in coppices and the lowest in pure coniferous stands (observation also highlighted in Dupire et al. (2016b)). Second, the loss of protection capability is strongly related to the mortality rate after fire which is higher in forest stands dominated by small trees (e.g. coppices) and tree species with a thin bark as for example *Fagus sylvatica*, *Pinus uncinata* and *Pinus cembra* (Fréjaville et al., 2013). Finally, a part of the protection capability loss is due to the degree of exposure to fire weather hazard. For example, *Abies alba* is a specie quite sensitive to fire (Tinner et al., 2000) but in its distribution area there are few cases where it is exposed to severe fire weather hazard. Therefore compared to others more fire-resistant species such as *Quercus sp.*, forest dominated by this specie did not suffer a strong loss of protection capability.

Stand type	**Main tree species**	**Cold season L_{99} inc.**		**Average summer L_{99} inc.**		**Summer 2003 L_{99} inc.**	
		τ_{30s}	τ_{max}	τ_{30s}	τ_{max}	τ_{30s}	τ_{max}
Coppices	Fagus sylvatica	0 (0)	2197 (163) ***	92 (101)	2197 (163) ***	170 (142) *	2197 (163) ***
	Mixed broadleaved	72 (56)	1079 (164) ***	588 (131) ***	1307 (162) ***	907 (155) ***	1819 (140) ***
	Quercus sp. (deciduous)	191 (80)	663 (142) ***	637 (138) ***	1101 (154) ***	1203 (156) ***	1915 (120) ***
Mixed stands	Abies - Picea	0 (0)	198 (41) ***	72 (25) *	281 (55) ***	99 (30) **	839 (95) ***
	Abies - Picea - Fagus	0 (0)	484 (58) ***	84 (20) ***	647 (65) ***	97 (22) ***	1080 (76) ***
	Larix - Others	138 (88)	616 (141) ***	340 (121) ***	716 (154) ***	478 (146) ***	1334 (183) ***
	Mixed broadleaved	33 (23)	1012 (96) ***	355 (61) ***	1288 (100) ***	558 (80) ***	1759 (88) ***
	Pinus sp. - Broadleaves	7 (5)	214 (33) ***	126 (25) ***	345 (45) ***	366 (52) ***	850 (68) ***
Pure broadleaved stands	Castanea sativa	8 (5)	958 (230) ***	57 (34) *	1564 (222) ***	440 (180) ***	2145 (145) ***
	Fagus sylvatica	10 (15)	1787 (92) ***	393 (81) ***	1993 (78) ***	516 (94) ***	2126 (64) ***
	Quercus sp. (deciduous)	65 (28)	390 (79) ***	281 (67) ***	671 (100) ***	689 (100) ***	1490 (106) ***
Pure coniferous stands	Abies alba	0 (0)	140 (39) ***	33 (14)	256 (67) ***	51 (24)	1495 (152) ***
	Larix decidua	18 (17)	256 (61) ***	111 (38)	308 (66) ***	156 (49)	602 (90) ***
	Picea abies	3 (4)	51 (15)	16 (7)	87 (23) *	25 (11)	421 (76) ***
	Pinus nigra	0 (0)	25 (16)	12 (14)	62 (43)	93 (54)	283 (104) **
	Pinus sylvestris	33 (14)	161 (31) ***	281 (46) ***	506 (60) ***	802 (74) ***	1114 (77) ***
	Pinus uncinata - cembra	45 (48)	793 (210) ***	256 (125)	1084 (229) ***	536 (183) ***	1456 (218) ***

Legend : Mean L_{99} increase (95% c.i.) p-value : ' ' : non significant, * : <0.05, ** : <0.01, *** : <0.001

Table 2.6 – Results of the pairwise comparisons between post-fire scenario and reference scenario without fire for the different forest types. τ_{30s} and τ_{max} stand respectively for flame residence times equal to 30 s and to the theoretical maximum time. Figures indicate the mean increase of L_{99} [m] after the fire scenario and figures in parentheses give the 95% confidence interval. The p-value level of the Dwass-Steel-Critchlow-Fligner procedure is also returned.

L_{99} increases were bounded between two flame residence times for each wildfire scenario. Wildfires with short flame residence time have limited impact on the protection capability. Thus, L_{99} increases were never significant for the cold season (season where short duration is more likely to occur) which means that short cold season fires do not degrade the protective effect of forest. L_{99} increases were only significant for broadleaved (coppices and high stands) and mixed stands for the summer wildfires scenarios. However, wildfire with the maximum theoretical flame duration are more devastating regardless of the wildfire scenario except for *Pinus nigra* and *Picea*

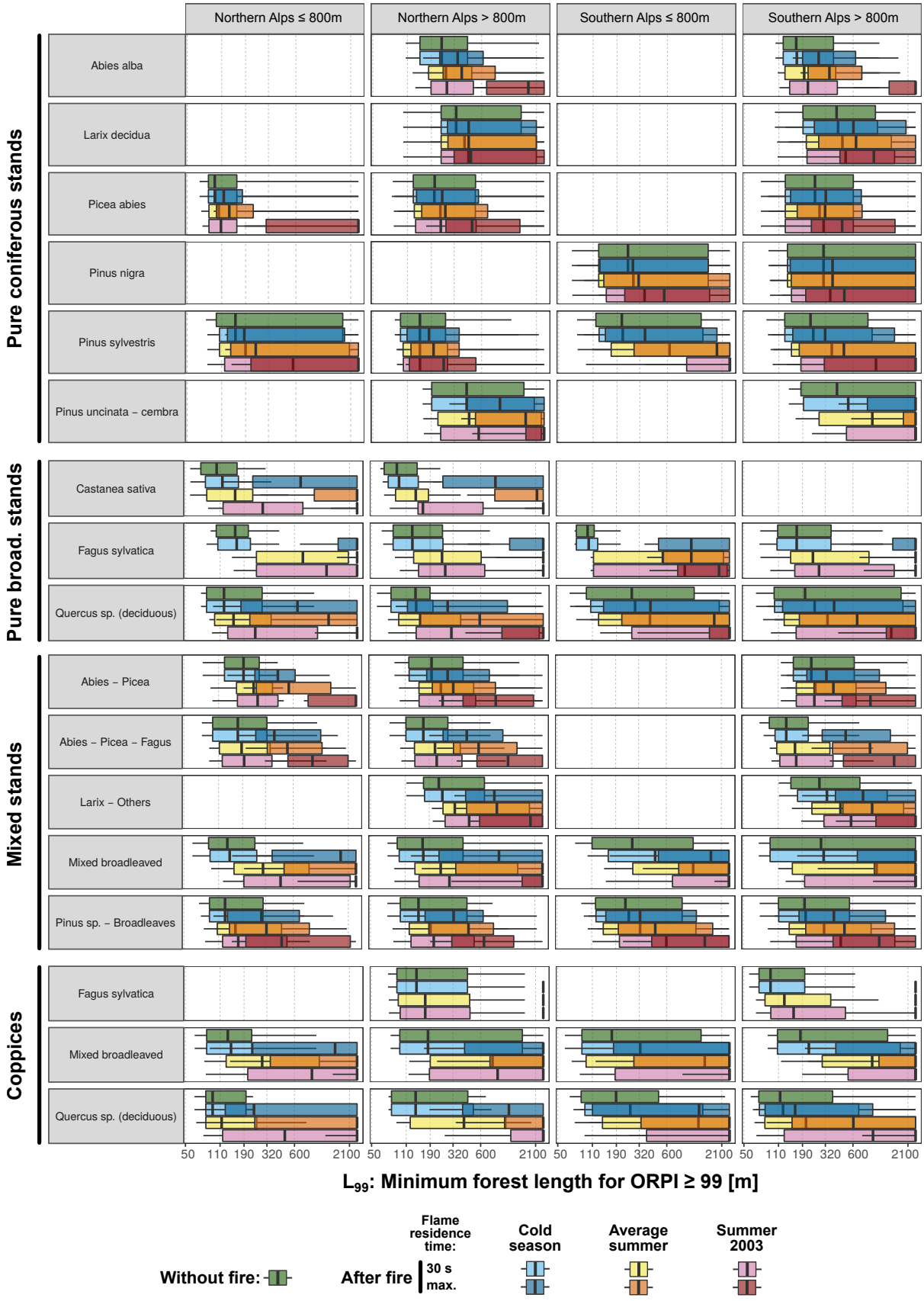

Figure 2.4 – Distribution of L_{99} for the main forest types of the French Alps according to different wildfire scenarios and climatic areas. The boxplots give the following percentiles : 5, 20, 50, 80, 95.

abies pure stands in the cold season.

Finally, it is interesting to notice a decreasing gradient in L_{99} increases after fire from high elevation to low elevation and from North to South when a forest type is present in the different climatic areas. It is particularly noticeable in *Quercus sp.* and *Pinus sylvestris* stands which present wide spatial distributions.

2.3.1.2 Determinant variables to evaluate the cascading effect at the forest stand level

The Table 2.7 summarizes the results of the RF realized for the main forest stands of the French Alps. Graphical detailed results per forest stands are available in Appendix B (Fig. C.1 to C.17).

Stand type	Main species	% of var. explained			Var. 1	Var. 2	Var. 3	Var. 4
		C. S.	Av. S	2003				
Coppices	Fagus sylvatica	32.4	12.3	27.9	BM : $^{0-10}\searrow_{25-65}$	%Herb : $^{0-20}\searrow_{100}$	G : $_{0}\nearrow^{25-60}$	H : $^{0-13}\searrow_{16-25}$
	Mixed broadleaved	29.4	22.9	61.3	G : $_{0}\nearrow^{10-20}\searrow_{25-70}$	Long : $^{8.5-8.7}\nearrow^{9.5-11.1}$	H : $_{0}\nearrow^{10-12.5}\searrow_{22.5}$	FFMC : $^{84-87}\nearrow^{95}$
	Quercus sp. (dec.)	15.2	25.7	44.4	G : $_{0}\nearrow^{10-15}\searrow_{25-50}$	%Herb : $^{0-10}\nearrow^{100}$	%Shrubs : $^{0-50}\searrow_{100}$	FFMC : $^{85-89}\nearrow^{96}$
Mixed stands	Abies - Picea	37.9	43.2	35.9	Perche : $^{0-40}\nearrow^{100}$	BM : $^{0}\searrow_{40-100}$	G : $_{0}\nearrow^{15}\searrow_{35-90}$	H : $^{0}\searrow_{17.5-35}$
	Abies-Picea-Fagus	11	22.3	20	G : $^{0}\searrow_{35-100}$	Perche : $^{0-60}\nearrow^{100}$	%Shrubs : $^{0}\searrow_{50-100}$	BM : $^{0}\searrow_{30-100}$
	Larix - Others	18.8	34.7	34.6	G : $_{0}\nearrow^{10-15}\searrow_{35-90}$	H : $^{5-7.5}\searrow_{12-25}$	BM : $^{0}\searrow_{40-100}$	Perche : $^{0-50}\nearrow^{100}$
	Mixed broadleaved	9.7	26.1	46.7	G : $_{0}\nearrow^{10-25}\searrow_{35-90}$	H : $^{3-7.5}\nearrow^{15-27.5}$	Perche : $^{0-60}\nearrow^{100}$	BM : $^{0}\searrow_{50-100}$
	Pinus sp.-Broad.	11	14.3	28	Perche : $^{0-40}\nearrow^{100}$	G : $_{0}\nearrow^{15-25}\searrow_{40-75}$	H : $^{3-12.5}\nearrow^{12.5-22.5}$	BM : $^{0}\searrow_{30-100}$
Pure broadleaved stands	Castanea sativa	23.6	28.4	35.3	G : $_{0}\nearrow^{25-70}$	BM : $^{0}\searrow_{30-100}$	Lat : $^{63.2-64}\nearrow^{64.5-66}$	Perche : $_{0}\nearrow^{30-100}$
	Fagus sylvatica	10.8	12.2	18.3	G : $_{0}\nearrow^{30-90}$	Perche : $_{0}\nearrow^{100}$	H : $_{5}\nearrow^{12.5-20}\searrow_{32.5}$	BM : $^{0}\searrow_{30-100}$
	Quercus sp. (dec.)	8.4	20.4	50.3	G : $_{0}\nearrow^{20-60}$	%Herb : $^{0}\searrow_{25}\nearrow^{80-100}$	H : $^{2.5}\searrow_{12.5-25}$	Perche : $^{0-30}\nearrow^{100}$
Pure coniferous stands	Abies alba	21.2	24.8	35	Perche : $^{0-20}\nearrow^{100}$	H : $^{5}\searrow_{17.5-32.5}$	G : $_{0}\nearrow^{7.5-20}\searrow_{40-90}$	BM : $^{0}\searrow_{30-100}$
	Larix decidua	35.6	54.5	59.7	G : $_{0-5}\nearrow^{10-15}\searrow_{30-75}$	H : $_{3}\nearrow^{5-7.5}\searrow_{15-30}$	Perche : $^{0-40}\nearrow^{100}$	FFMC : $^{85-87}\nearrow^{95}$
	Picea abies	*NR*	18	30.9	Perche : $_{0}\nearrow^{100}$	G : $_{0}\nearrow^{10-15}\searrow_{35-100}$	BM : $^{0}\searrow_{40-100}$	FFMC : $^{85-87}\nearrow^{94}$
	Pinus nigra	*NR*	*NR*	33.7	Perche : $^{0-60}\nearrow^{100}$	G : $_{0}\nearrow^{20-70}$	H : $^{3}\searrow_{12.5-22.5}$	BM : $^{0}\searrow_{50-100}$
	Pinus sylvestris	14.6	48.1	60.9	G : $_{0}\nearrow^{17.5}\searrow_{40-100}$	H : $_{2.5}\nearrow^{7}\searrow_{12.5-22.5}$	Perche : $_{0}\nearrow^{100}$	%Herb : $_{0}\nearrow^{40}\searrow_{100}$
	Pinus unci.-cemb.	26.9	35.2	59.8	G : $_{0}\nearrow^{20-70}$	FFMC : $^{84-86}\nearrow^{95}$	Perche : $_{0}\nearrow^{100}$	PB : $^{0}\searrow_{25}\nearrow^{100}$
All forest types		16.3	28.3	42.3	G : $_{0}\nearrow^{10-15}\searrow_{30-100}$	Perche : $_{0}\nearrow^{100}$	Lat : $_{62.7}\nearrow^{66}$	%Herb : $^{0-60}\nearrow^{100}$

NR : Non relevant (i.e. non significant L_{99} increase). Variation of L_{99} : – : stable, ↗ : increase, ↘ : decrease.

Table 2.7 – Summary of the RF regression for the different wildfire scenarios. The proportions of the total variance explained by the model are given for each wildfire scenario : (C.S. : Cold season, Av. S : Average summer, 2003 : Summer 2003). The four most important variables for the prediction of the L_{99} increase are also showed (Var. 1, Var. 2, Var. 3, Var. 4). The variations of L_{99} along the range of values of the predictor variables are summarized with the arrows and figures. The variable abbreviations are given hereafter. G :Basal area of all trees with DBH $\geqslant$ 7.5cm ; H :Mean height of all trees with DBH $\geqslant$ 7.5cm ; Perche :Proportion of stems with DBH $\in$ [7.5-17.5[; PB :Proportion of stems with DBH $\in$ [17.5-27.5[; BM :Proportion of stems with DBH $\in$ [27.5-47.5[; %Shrubs :Cover rate of small wooden species (Height $<$ 2m) ; %Herb :Cover rate of herbaceous species ; FFMC :Fine Fuel Moisture Code (Van Wagner, 1987) ; Lat :Latitude of the NFI plot (EPSG 2154 $\times$ 100000 m) ; Long :Longitude of the NFI plot (EPSG 2154 $\times$ 100000 m).

Among the 10 predictors variables used in the different RF, those that regularly stood out as the most important to explain the loss of the protection capabilities were the basal area, the proportion of trees with DBH$\in$[7.5-17.5[cm, the herbaceous cover and the stand height. Fire weather (FFMC) was not automatically among the four most important variables. This can be explained by the spatial distribution of forest type. For example, when a forest type is present in homogeneous topoclimatic areas (e.g. coppice of *Fagus sylvatica* mostly concentrated at the highest elevations), the fire weather will be quite similar from one site to another. On the contrary, when a forest type is widely distributed, we can encounter a widest range of fire

weather (e.g. mixed broadleaved, deciduous *Quercus sp.*). The predictor variables related to the location of the forest (Longitude, Latitude) had a similar trend. When a forest type is present in both External Alps (West) and Intern Alps (East) it is exposed to warmer and wetter climate in the first than in the second (e.g. coppice of mixed broadleaved). If it is distributed North/South it suffers stronger Mediterranean influences while going to South with driest summer and is then exposed to a more severe fire weather danger (e.g. *Larix decidua*, (Dupire et al., 2017)).

Even if we did not seek for model performance here, we can noticed that RF for the summer season, especially 2003 summer, generally present a higher rate of explained variance. This point is quite interesting in order to target the forests the most subjected to a high cascading effect in case of severe drought in the next decades where preventive forest management measures could be taken in order to reduce their vulnerability.

2.3.2 Spatial analysis

2.3.2.1 Importance of the forest with a potential protective effect against rockfall in the French Alps

Fig .2.6 and 2.5 return respectively the location and the degree of exposure to rockfall and fire weather hazards of the protection forests at the French Alps scale.

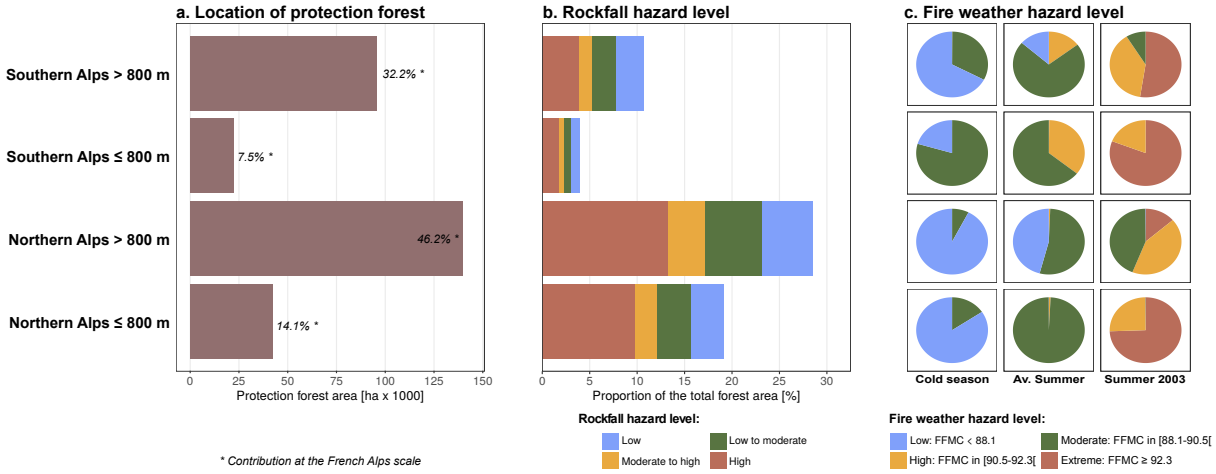

Figure 2.5 – Surface of forest with a protective effect against rockfall according to the different climatic areas (a.). Proportion of the forest area according to climatic area (b.) and rockfall hazard levels based on energy line angle : Low [26-30°[, Low to moderate [30-33°[, Moderate to high [33-35°[, High ≥35°. Proportion of the protection forest area according to fire weather hazard level and climatic conditions (c.).

296 500 ha of protection forests where identified which corresponds to 14% of the forest area of the French Alps. 60% of the protection forests are located in the Northern Alps where they represent between 18% and 28% of the total forest area. 40% are located in the Southern Alps with a lesser proportion of the total forested area (4% to 10%). 78% of the protection forests are located at elevation > 800m.

Independently of the climatic area, the forest exposed to a significant rockfall hazard (energy line angle ≥ 30°, see Table 2.5) represent 80% of the total area of protection forest. This proportion is of 40% while considering only high rockfall hazard.

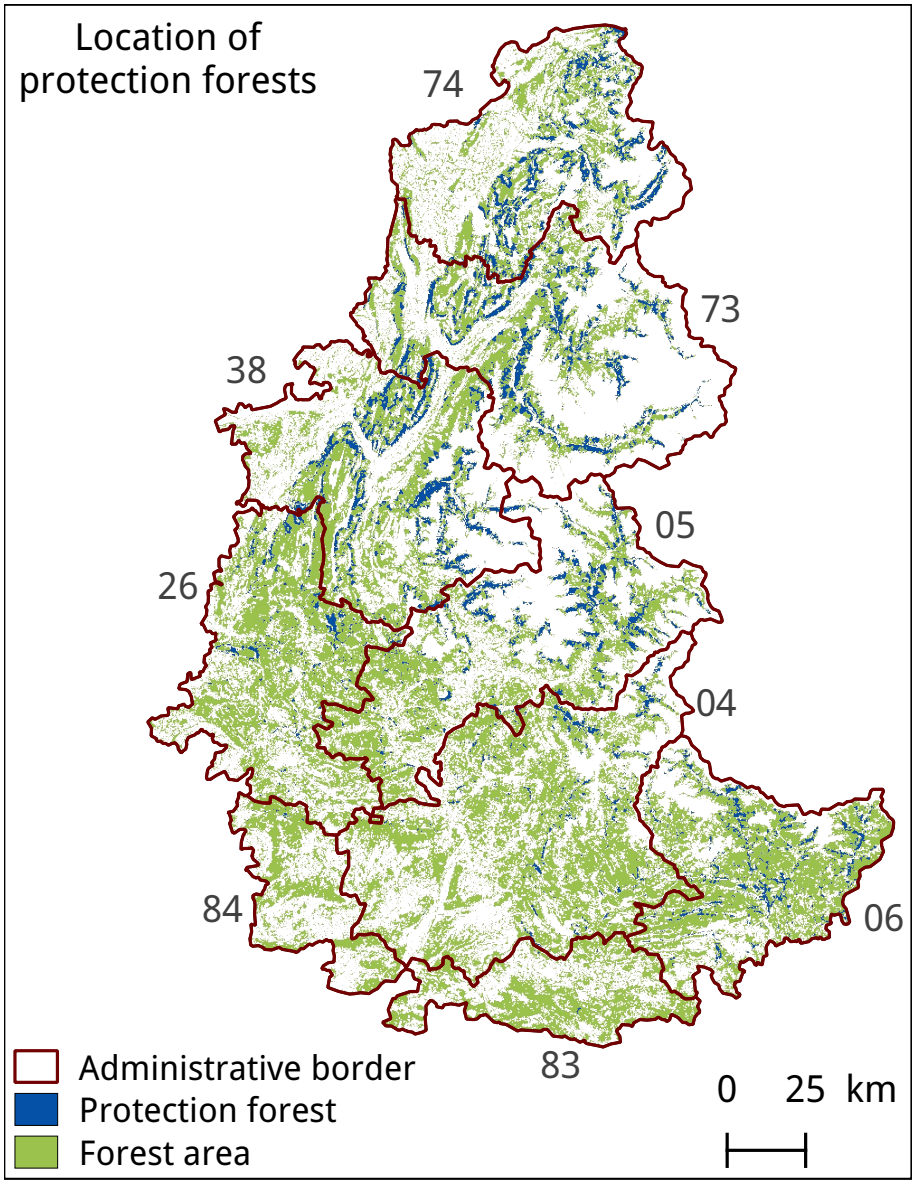

Figure 2.6 – Distribution of the protection forests against rockfall in the French Alps.

In the cold season, the fire weather hazard stay mostly low in all climatic areas except low elevations of Southern Alps where it is predominantly moderate. In average summer climatic conditions, it is low to moderate in the Northern Alps but it can reach a high level in the Southern Alps especially at low elevations. Finally, during the summer 2003 the fire weather hazard reached the extreme level in all climatic areas but with a lower extent for the high elevations.

2.3.2.2 Detail per climatic area

The detailed results per climatic area are presented in this section. For each climatic area, the main forest types and the evolution of their protection capabilities after fire are presented. A focus is also made on the human assets at risk and their level of protection before and after the different wildfires scenarios (see Fig. 2.7 to 2.10). For each plot, the main forest types present in the climatic area are classified according to their contribution to the protection forest area (a.). The estimated protection capabilities (ORPI) is showed for each forest type for the different wildfire scenarios (b.). Figures between (a.) and (b.) return the surface (green) and the proportion

of the total area of the forest type identified as protection forest (grey). The proportion of forest area that potentially protect the four different human assets is shown in (c.). Figures between (c.) and (d.) return the number or the distance (green) and the proportion of the total human assets identified as endangered (grey). The empirical cumulative distribution curves of the number of human assets according to the rockfall residual hazard and the wildfire scenario is shown in (d).

Northern Alps ≤ 800 m. The top three protection forest types in low elevations of Northern Alps are composed of mixed broadleaved (high stand and coppices) and mixed stands (broadleaved + conifers). All stands presented an initial (without fire) high protection capability (ORPI>90, i.e. 90% of the overall rockfall hazard reduced) which is lightly reduced in the cold season fire scenario. However, both summer fires reduced drastically the protection capability for 5 forest types out of 10 (ORPI < 10, i.e. only 10% of the overall rockfall hazard reduced). For the other half, the protection capability decrease to 70% at best and to 30% at worst during average summer conditions, and 55% at best and to 10% at worst during 2003 summer conditions. The less vulnerable forest types being those with a significant coniferous species proportion and the most vulnerable the coppices.

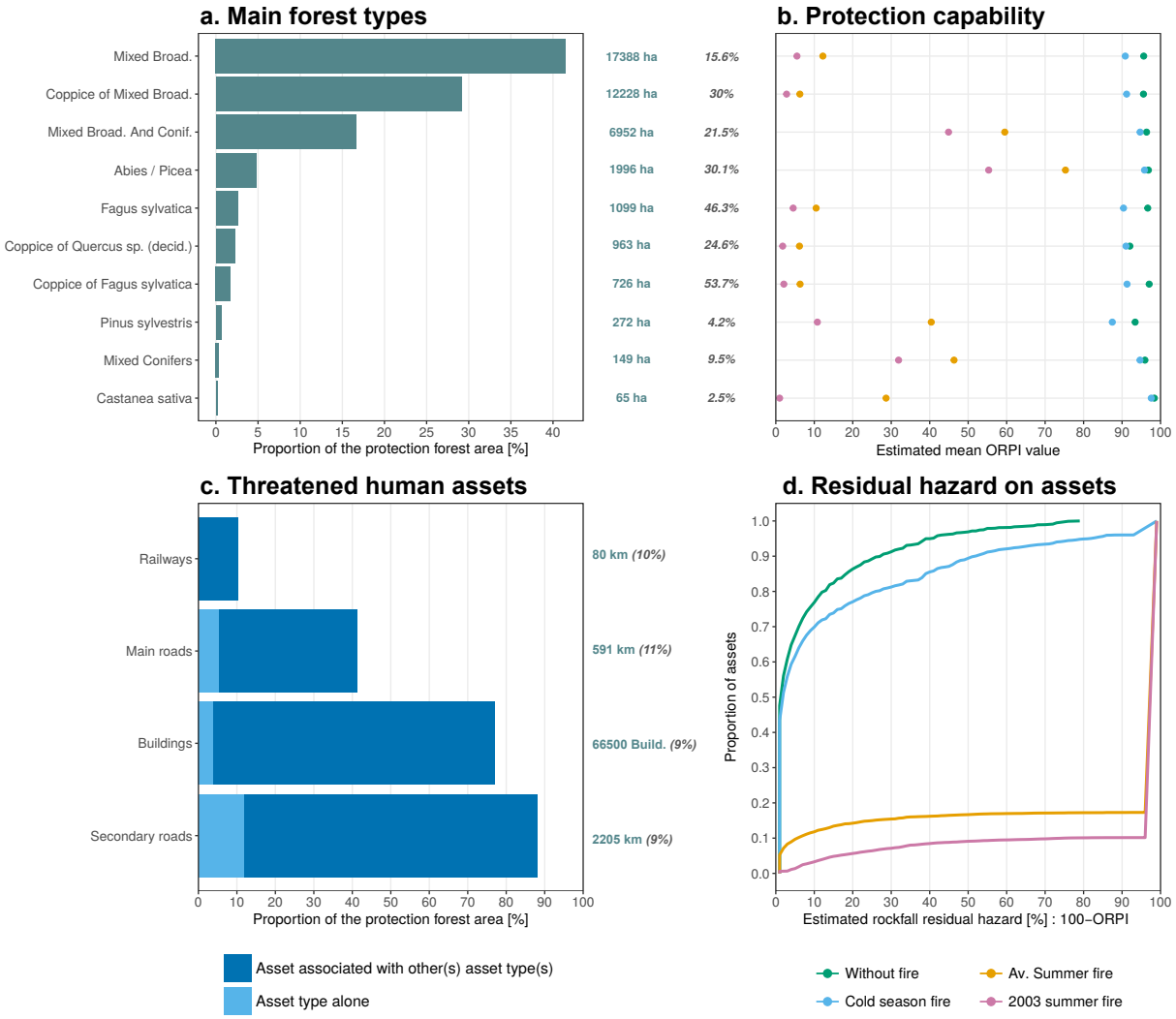

Figure 2.7 – Northern Alps with elevation ≤ 800 m.

In this area, about 10% of the human assets are at risk independently of their type. The forests mostly protect buildings and roads and in most of the case a combination of different

asset types. Without fire, 75% of the assets present a residual rockfall hazard < 10%. After fire, this proportion lightly decrease in cold season (70%) but shown a large decrease in case of summer fire (12%) and extreme fire (4%).

Northern Alps > 800 m. Most of the protection forests in the high elevations of Northern Alps are dominated by coniferous species (*Abies alba* and *Picea abies* in particular) alone or mixed to broadleaved (*Fagus sylvatica* and *Acer sp.*). All stands presented an initial high protection capability (ORPI>90) except coppices of deciduous *Quercus sp.*. Protection capability after average summer fires stayed above an ORPI value of 50 for the forest types dominated by coniferous species (71% of the protection forest area). For the others forest types, the protection capability was between 8% and 30% in average summer condition. The same trend was respected for summer 2003 scenario but with lower estimated ORPI values.

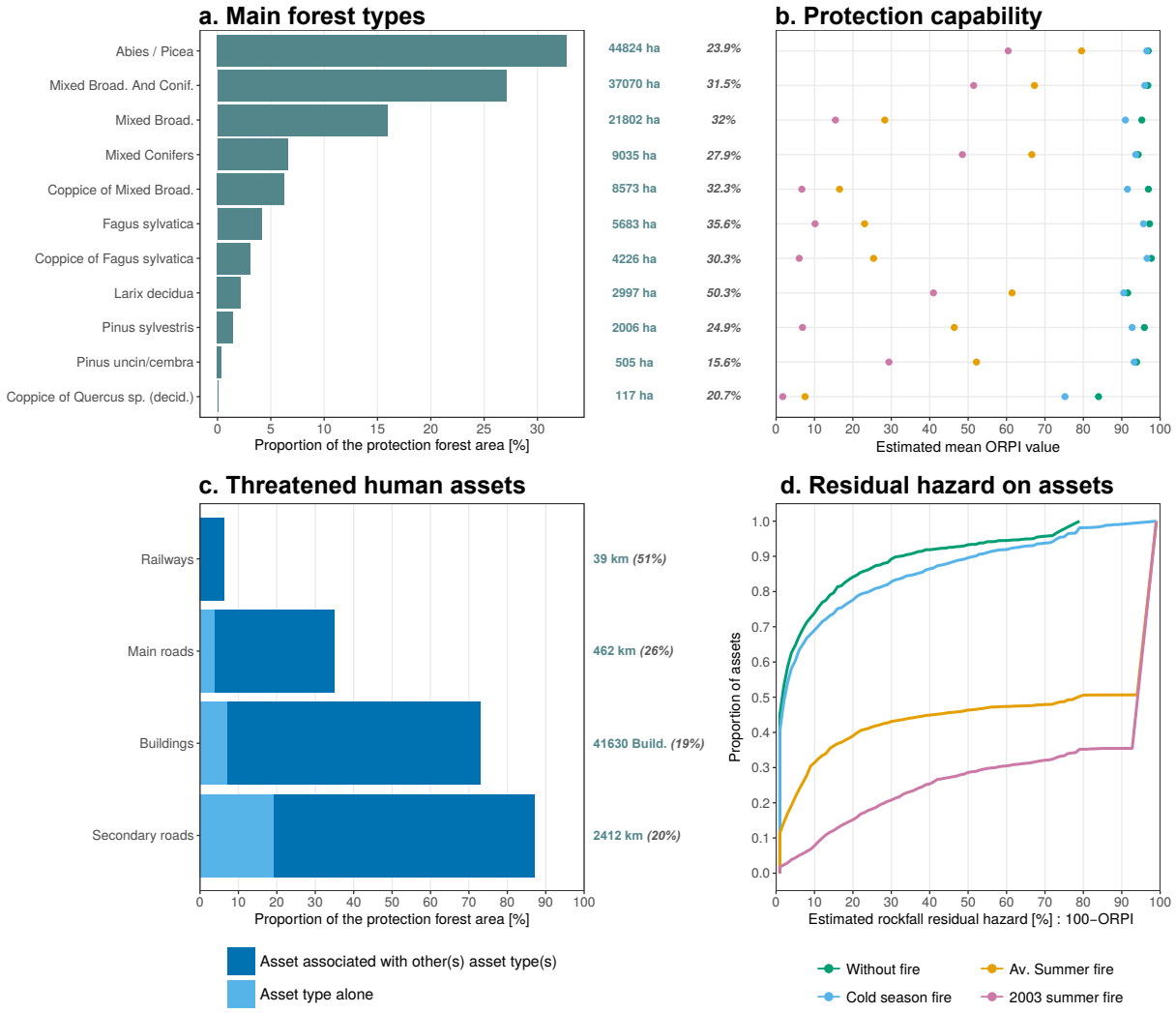

Figure 2.8 – Northern Alps with elevation > 800 m.

This climatic area presents the highest rates of human assets at risk of the French Alps (51% for railways ; between 19% and 26% for buildings and roads). The forests mostly protect buildings and roads and in most of the case a combination of different asset types. We can also notice that about 20% of the protection forest area only protect secondary roads which are the less important asset among those taken into account. Without fire, 75% of the assets present a residual rockfall hazard < 10%. After fire, this proportion lightly decreases in cold season (70%).

This proportion was divided by 2 in case of summer fire (32%) and by 7 in case of extreme fire (10%).

Southern Alps ≤ 800 m. is the area with the highest Mediterranean influence of the French Alps. Thus, most of the protection forest area is dominated by broadleaved species (80%). Protection capability without fire was generally high (ORPI>90) except for coppices of evergreen *Quercus sp.* and high stands of deciduous *Quercus sp.*. Unlike the two Northern climatic areas, the protection capability of forests after a cold season wildfire can suffer a significant decrease in the low elevations of Southern Alps especially in coppices. After summer fires the protection capability of all forest essentially composed of broadleaved species was very low (ORPI < 10). However, stands dominated by coniferous species showed an interesting resistance, especially those composed of *Pinus nigra*.

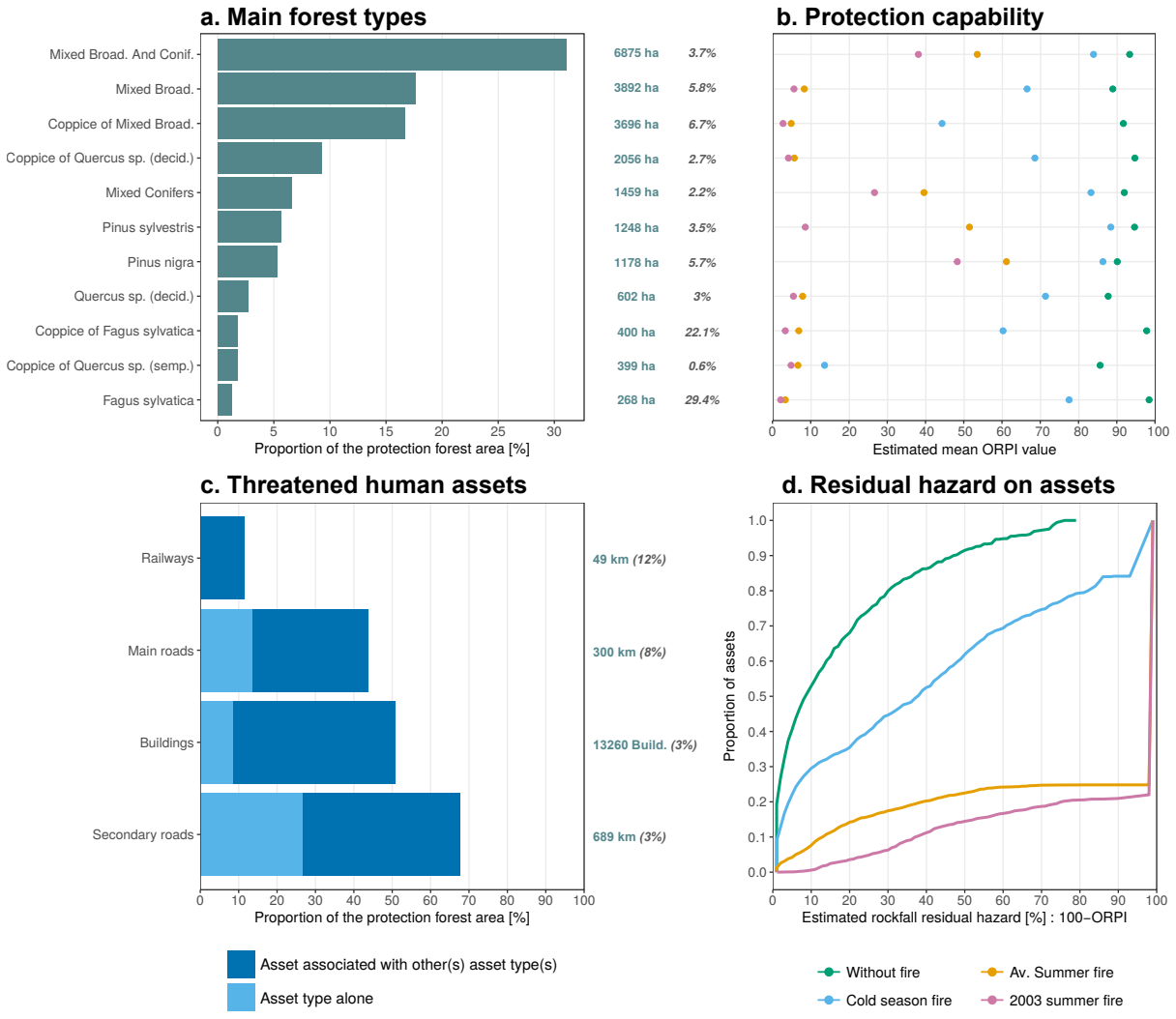

Figure 2.9 – Southern Alps with elevation ≤ 800 m.

This climatic area presents the lowest rates of human assets at risk of the French Alps (about 10% for railways and main roads and 3% for buildings and roads). The forests mostly protect buildings and roads and in most of the case a combination of different asset types. We can also notice that about 26% of the protection forest area only protect secondary roads which are the less important asset among those taken into account. The residual rockfall hazard in this area is the highest of the French Alps. Without fire, only 50% of the assets presented a residual rockfall

hazard < 10%. After fire, this proportion was of 30% in the cold season scenario, 10% in the summer fire scenario and 0% in case of extreme fire.

Southern Alps > 800 m. As in the Northern Alps, most of the protection forests in the high elevations of Southern Alps are dominated by coniferous species (85% of the area) but with others species(*Larix decidua* and *Pinus sp.*). All stands in this area presented an initial high protection capability (ORPI>90). Protection capability after cold season fires was slightly lower in forest dominated by coniferous species but it was significant lower in broadleaved stands ($70 \leq$ ORPI < 90). Protection capability after average summer fires stayed above an ORPI value of 50 for the forest types dominated by coniferous species except for *Pinus uncinata/cembra* stands. For the others forests types, the protection capability was between 8% and 20% in average summer condition. The same trend was respected for summer 2003 scenario but with lower estimated ORPI values.

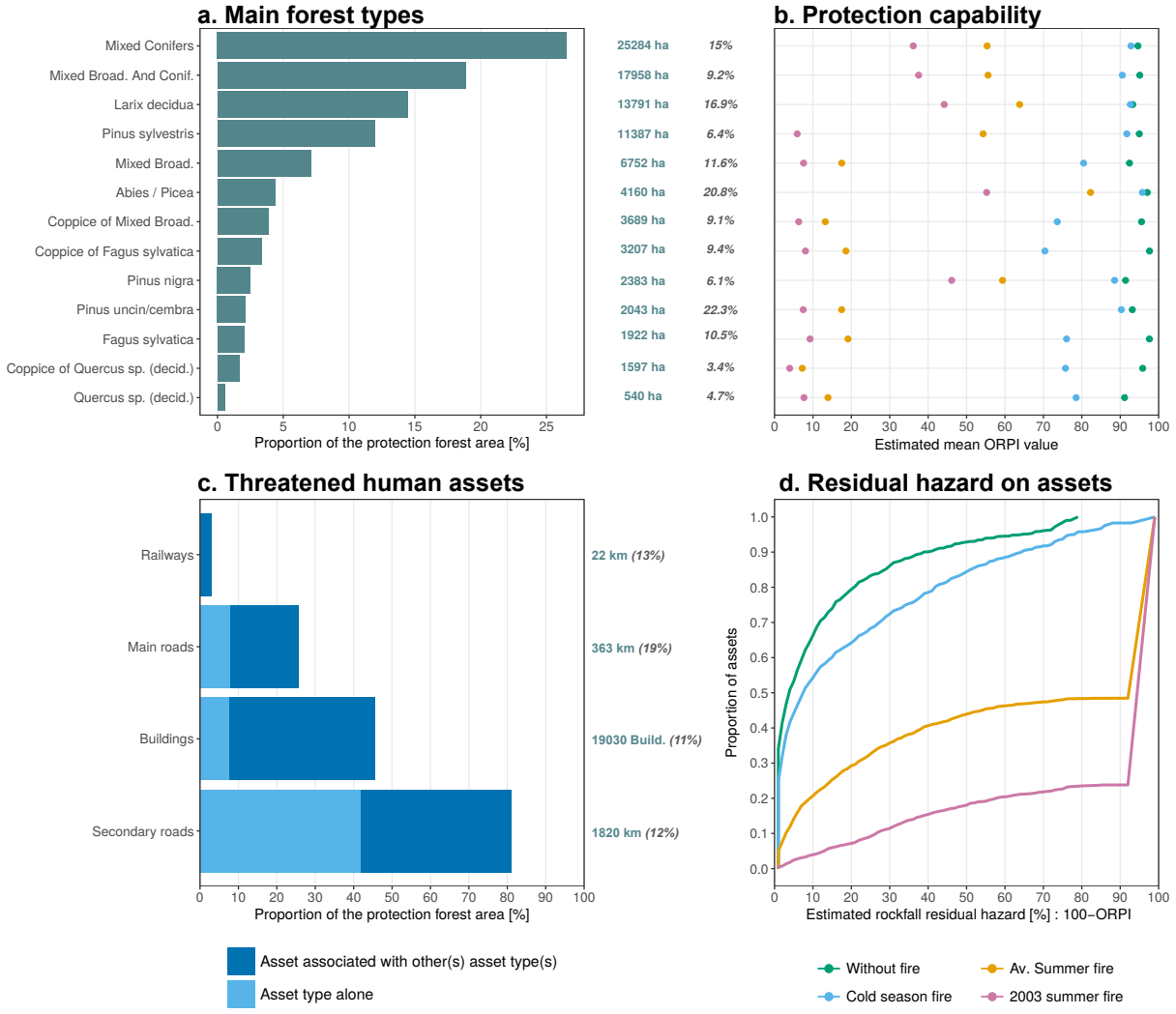

Figure 2.10 – Southern Alps with elevation > 800 m.

In this area, between 11% and 19% of the human assets are at risk. About 40% of the forests only protect secondary roads, 10% only main roads, 10% only buildings and 40% a combination of different asset types. Without fire, 70% of the assets present a residual rockfall hazard < 10%. After fire, this proportion decrease continuously according to the fire intensity : 55% for cold season fire, 20% for average summer fire and 5% for extreme fire.

2.4 Discussion and conclusion

This work aimed at evaluating the cascading effects in mountain forests with a protective effect against rockfalls after different wildfires intensities. It provided detailed results for two scales of analysis and decision making : the stand level and the regional level.

The forest types the most subjected to important loss of protection capabilities after fire were therefore identified. It mainly concerns coppices (about 42000 ha, 14% of the protection forest area) and to a lesser extent broadleaved stands (60000 ha, 20% of the protection forest area). Fires occurring in the cold season generally have a low effect on the protection capabilities of mountain forest. However, average summer fires and most importantly extreme summer fires can severely alter the protection capabilities especially in broadleaved stands. These results are consistent with the only reference existing (Maringer et al., 2016a) on the subject which focused on *Fagus sylvatica* stands. Cascading effects are also present in coniferous dominated stands, although to a lesser extent. Thus, the average protective effect is generally reduced by a factor between 2 and 3 in case of extreme wildfires. However, these results did not account for the resilience abilities of the different tree species several years after fire. For example, Conedera et al. (2010) showed that coppices of *Castanea sativa* can experiment high mortality levels after low to moderate fire intensity but also a quick response consisting in a strong vegetative resprouting activity few years after the fire. Moris et al. (2017), demonstrated that *Larix decidua* had a strong recruitment after fire, all the more so the fire intensity is high. At the opposite, several studies suggested that *Fagus sylvatica* lack of both resistant and resilient strategies (Maringer et al., 2016b; Conedera et al., 2010).

For conservative and modelling purposes, we opted for removing trees with a high probability of post-fire mortality from the initial forest without fire. Hopefully, the reality is not so binary and the burnt trees may still contribute to the protective effect according to the burn severity and the duration since the fire. Bortoletto et al. (2003) studied mechanical properties of *Pinus taeda* few hours after a surface fire and showed that the resistance to compression was slightly reduced (11%) for the logs with the highest burn severities. No significant differences were observed for lowest burn severities. Thus, dead trees may temporary have a similar effect than alive ones. In case of post-fire tree fall, they may have a similar effect than the management practice consisting in deliberately let trees on the ground to increase surface roughness and reduce rockfall hazard (Olmedo et al., 2015). However, we can expect a progressive decrease of the mechanical properties from the base to the top of the dead trees linked to the combination of the alteration of the tissues due to the fire and the biological decay mostly related to insect and fungal activity (Barré et al., 2017b; Barré et al., 2017c). The kinetic of this biological decay is quite difficult to predict but it has been shown that warm and wet climatic conditions promote a faster process (Barré et al., 2017a).

The spatial analysis carried out in this study provided a complete overview of the importance of protection forests in the French Alps as well as the proportion of human assets exposed. It completed the previous work initiated by Toe et al. (2015) which mapped the area subjected to rockfall for several Alpine districts of the French Alps but using only the energy line principle with a fixed β angle. Adding a first step with rockfall propagations modelled with Rockyfor3D allows to respect a certain catchment logic and to eliminate many areas where the rocks do not go through by simple gravitation. Two main improvements could be added to the proposed method. First, the automatic detection of the release areas only based on a slope threshold could be improved using information about the bedrock stability. Nonetheless, a study carried out in the Vercors mountain (Guirimand, 2013) showed that only 2% of the release areas were not detected applying the slope threshold from BDAlti® at 25m. Second, the workflow followed for the mapping of protection forest could be directly implemented in Rockyfor3D in order to build exact ground profiles and improve the informations on forest along the profile collected by our

method.

Several hotspots of potential cascading effects were identified. Low elevation of Northern Alps are the most subjected to important cascading effects in case of summer fires in protection forest. In this area, 10% of the human assets are at risk but in absolute value this area present the highest number of assets exposed. Without fire, the forest offers a high level of protection with 75% of the exposed assets presenting a residual rockfall hazard less than or equal to 10%. After an average summer fire, only 10% of the assets exposed still present this level of protection, this proportion is even lower in case of extreme fire (5%). It is the highest loss of protection observed among the 4 climatic areas. Hopefully, according to the records, summer fire ignitions in this area are relatively low compared to the Southernmost part of the French Alps (Dupire et al., 2017). The second area potentially the most subjected to cascading effect is the low elevation of the Southern Alps. In this area, the number of assets endangered by rockfall is relatively low but the fire danger is the highest of the Alpine area. The forests in this area offer a moderate rockfall protection but they are quite vulnerable to fire. Their protective effect in case of fire (especially summer fires) suffers a high decrease. The two areas at high elevation present a similar potential cascading effect in case of fire with low decrease of the protective capability in case of cold season fire, moderate in case of average summer fire and severe in case of extreme summer fire. However, they differs in the number of assets exposed to rockfall (higher in the North) and in the fire danger (higher in the South). Therefore it is more likely to see cascading effect in the South where fire ignitions are more numerous (Dupire et al., 2017).

Finally, this work can find practical applications for forest managers and natural hazard managements services. First, it provided many information on the vulnerability of the main forest types to fire. Above all, the regression forests return a range of values where the main forest parameters may have an influence on the loss of protection capabilities. For sample, in a pure stand of *Larix decidua*, it is recommended to limit the proportion of tree with DBH < 17.5cm below 40% and to avoid basal area from 10 to 17.5 $m^2 \cdot ha^{-1}$ (see Fig. C.5). Second, it is possible to identify the protection forests that need a special attention in case of extreme drought conditions such as summer 2003 from the result of spatial analysis. This can be done by coupling the fire weather hazard of the moment with the characteristics of the forest types in place (forested length along the slope and main species).

Funding

This work was supported by the French Ministry of Ecology, Sustainable Development and Energy [grant n° 2101527657] and the H2020 project NAIAD [grant n° 730497] from the European Union's Horizon 2020 research and innovation programme.

Appendix C : Detail of cascading effect for the main forest stands of the French Alps

All the figures from Fig.C.1 to Fig.C.17 present the results of the regression forest for the main forest stands of the French Alps. They are always organized in the same way. On the top line, the left figure present the L_{99} distribution taking into account all the NFI plots corresponding to the forest type, the three figures at the right present the importances of the predictor variables according to the different wildfire scenarios. Finally the four figure in the bottom line show the partial plots for the four main important predictor variables. The blue, orange and pink curves correspond respectively to cold season, average summer and 2003 summer.

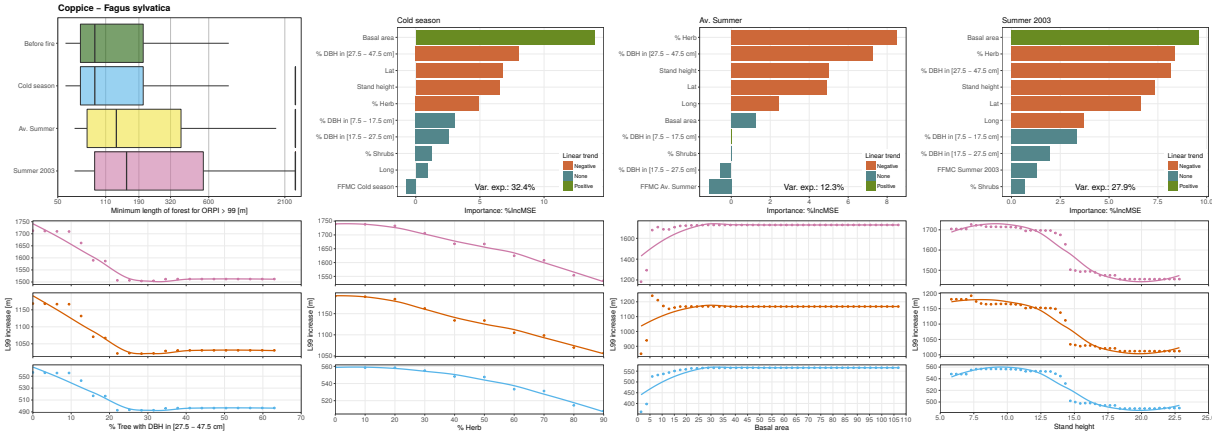

Figure C.1 – Result of regression forest for coppice of *Fagus sylvatica*.

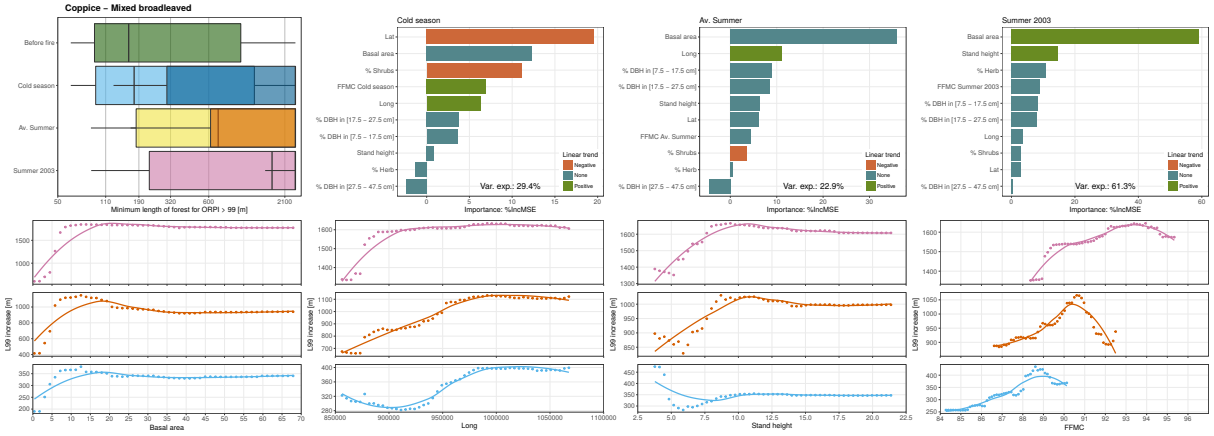

Figure C.2 – Result of regression forest for coppice of mixed broadleaved.

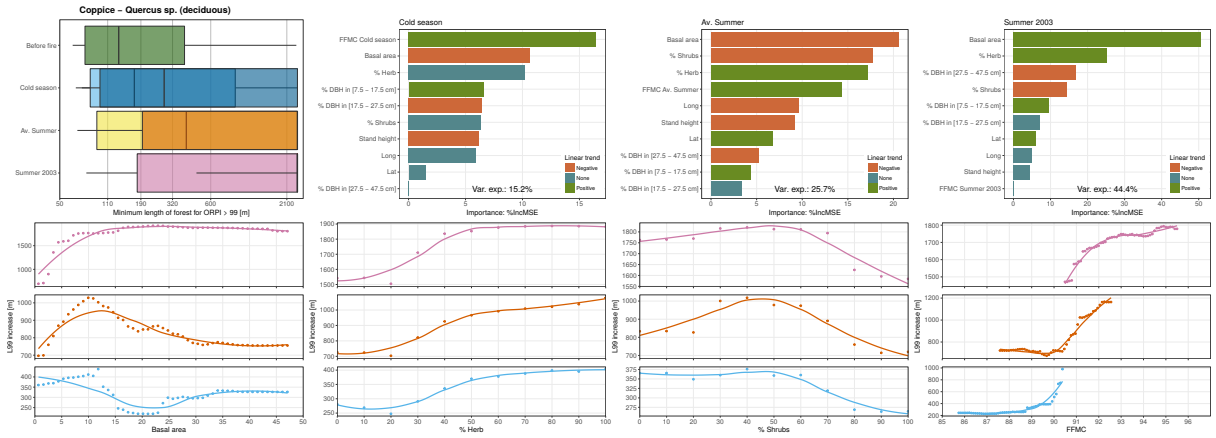

Figure C.3 – Result of regression forest for coppice of deciduous *Quercus sp.*.

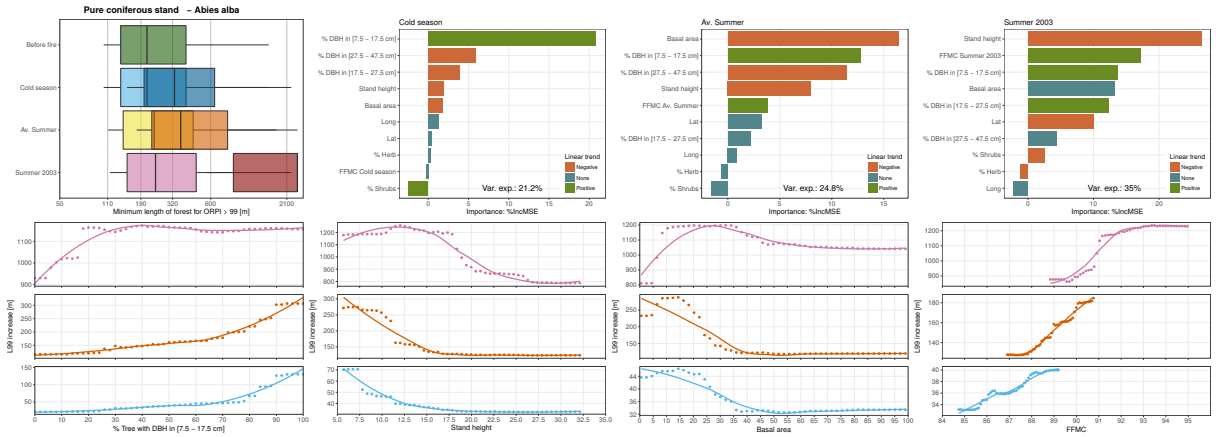

Figure C.4 – Result of regression forest for pure coniferous stands of *Abies alba*.

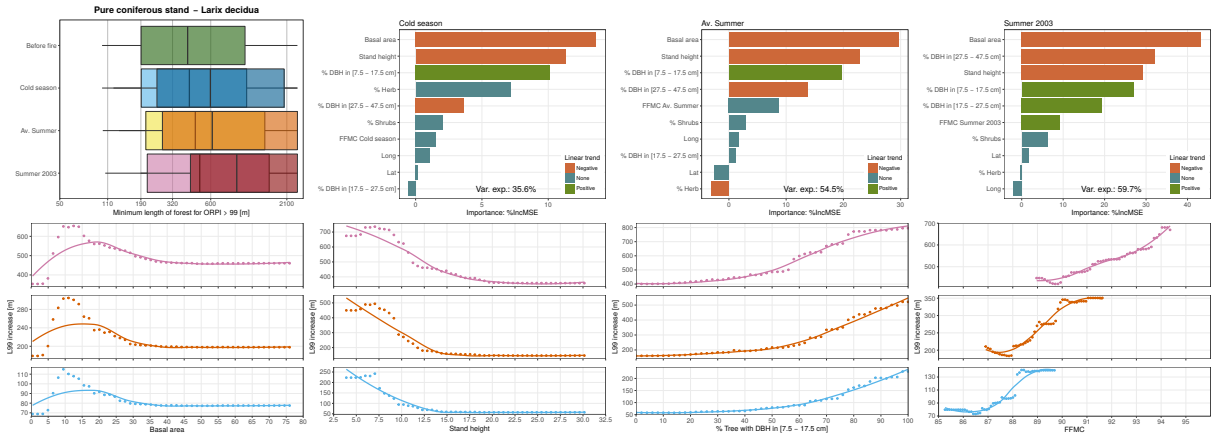

Figure C.5 – Result of regression forest for pure coniferous stands of *Larix decidua*.

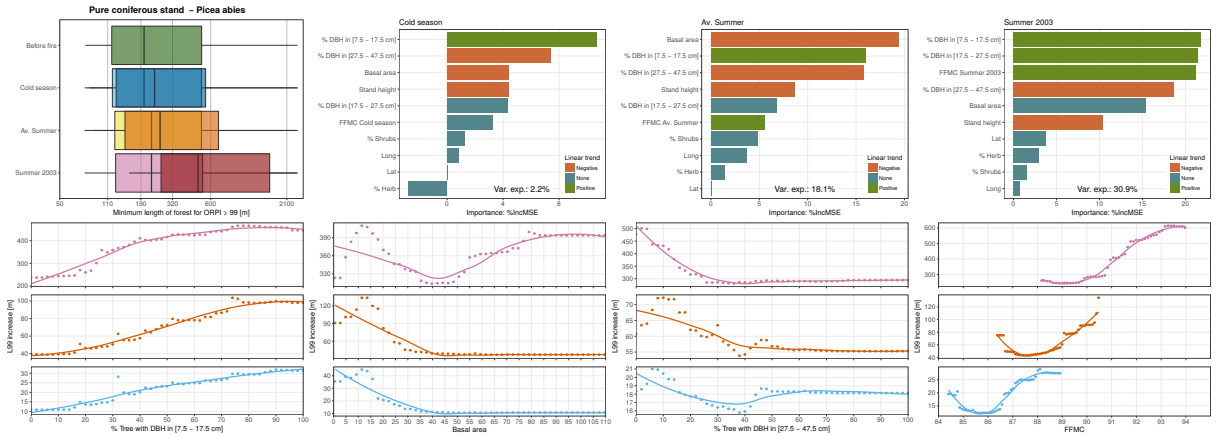

Figure C.6 – Result of regression forest for pure coniferous stands of *Picea abies*.

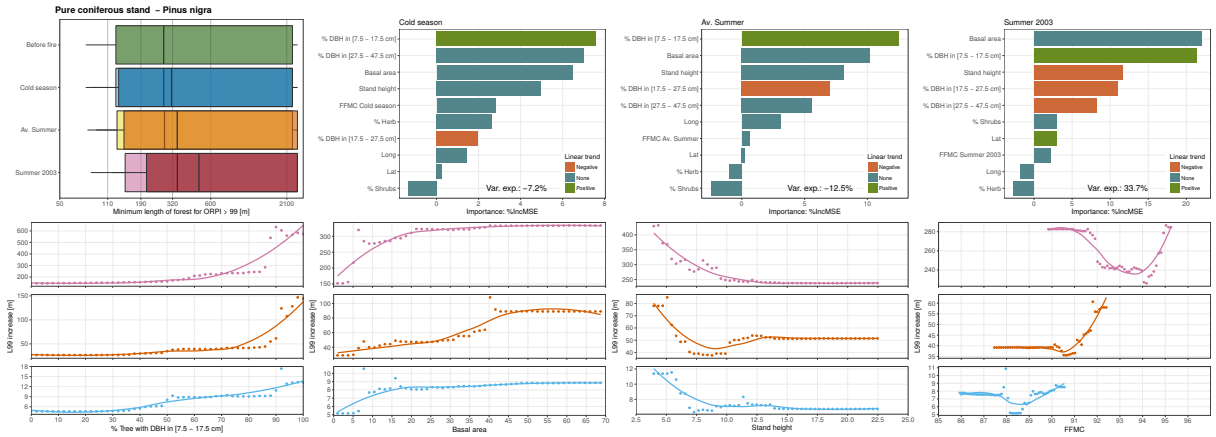

Figure C.7 – Result of regression forest for pure coniferous stands of *Pinus nigra*.

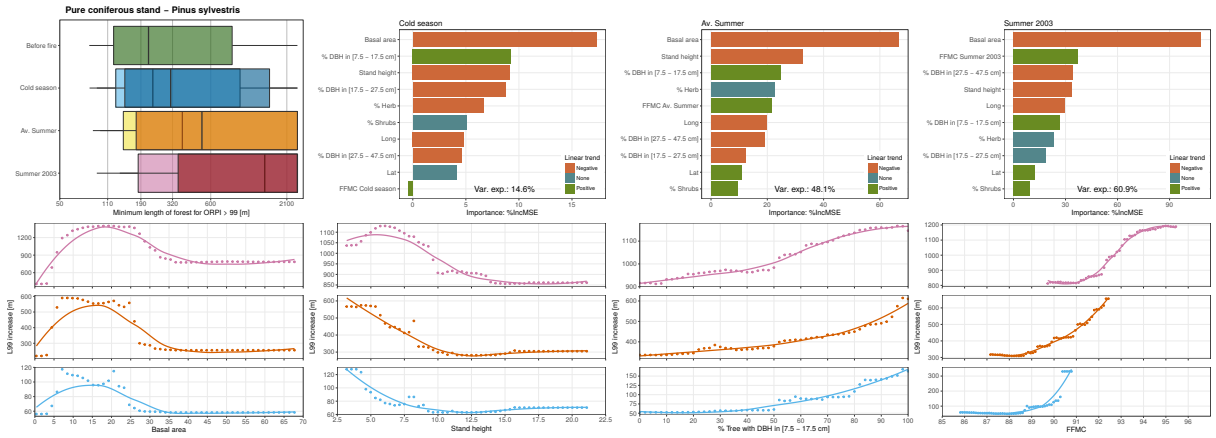

Figure C.8 – Result of regression forest for pure coniferous stands of *Pinus sylvestris*.

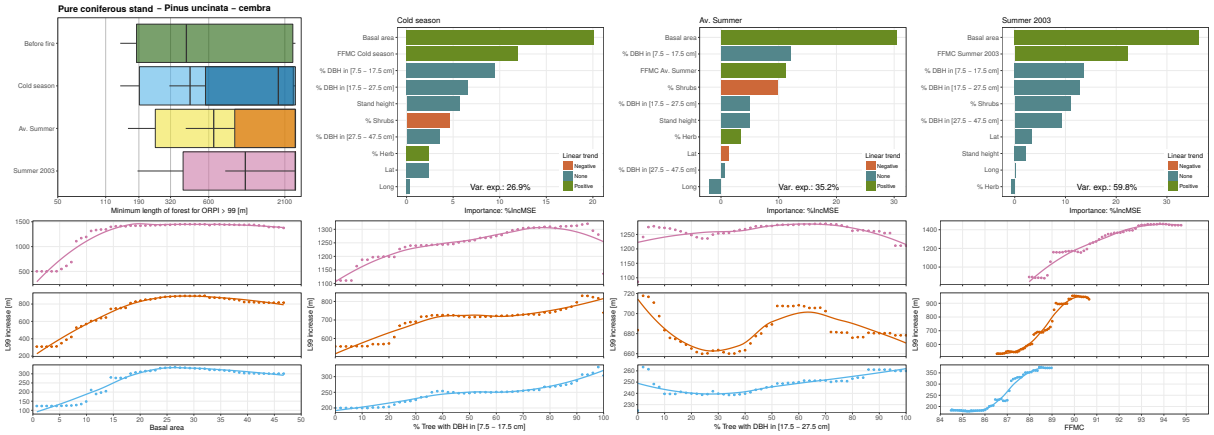

Figure C.9 – Result of regression forest for pure coniferous stands of *Pinus uncinata* or *Pinus cembra*.

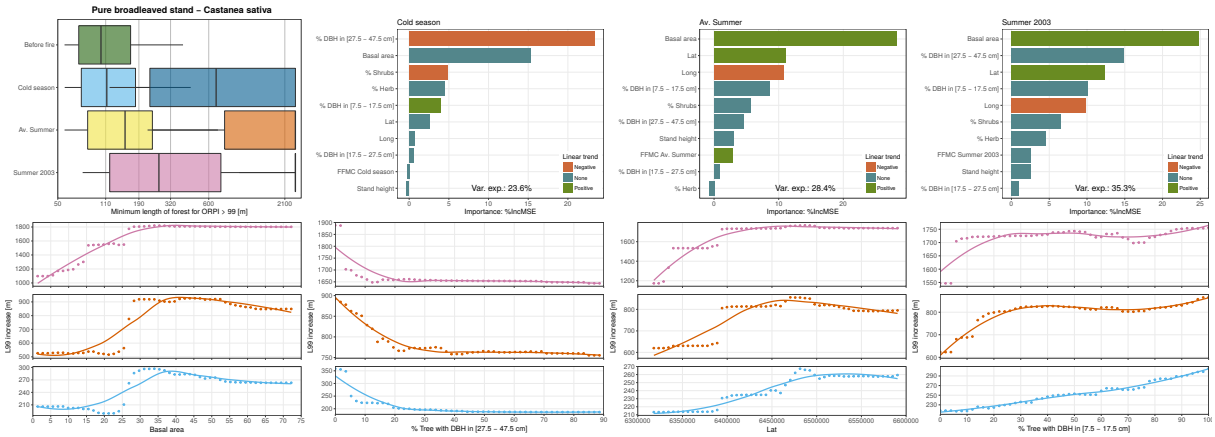

Figure C.10 – Result of regression forest for pure broadleaved stands of *Castanea sativa*.

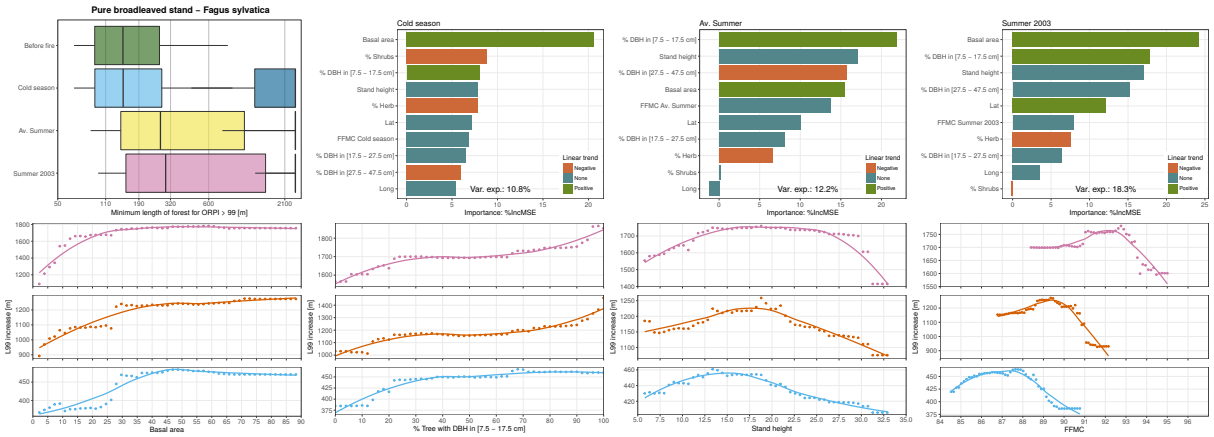

Figure C.11 – Result of regression forest for pure broadleaved stands of *Fagus sylvatica*.

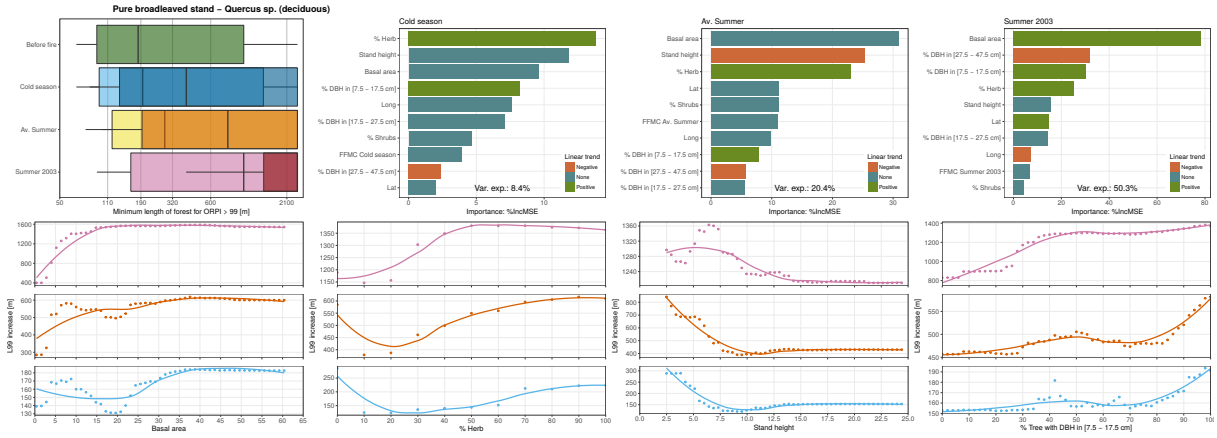

Figure C.12 – Result of regression forest for pure broadleaved stands of deciduous *Quercus sp.*.

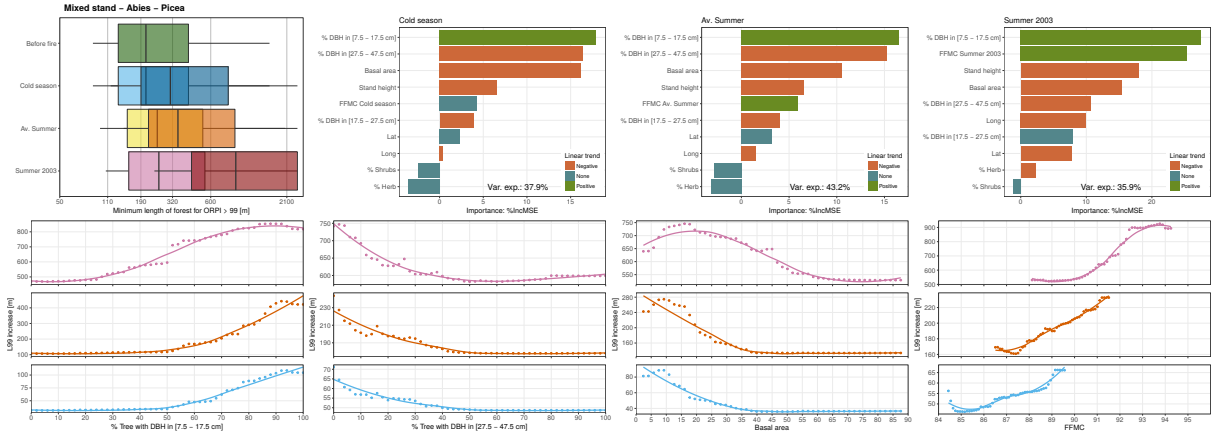

Figure C.13 – Result of regression forest for mixed stands dominated by *Abies alba* and *Picea abies*.

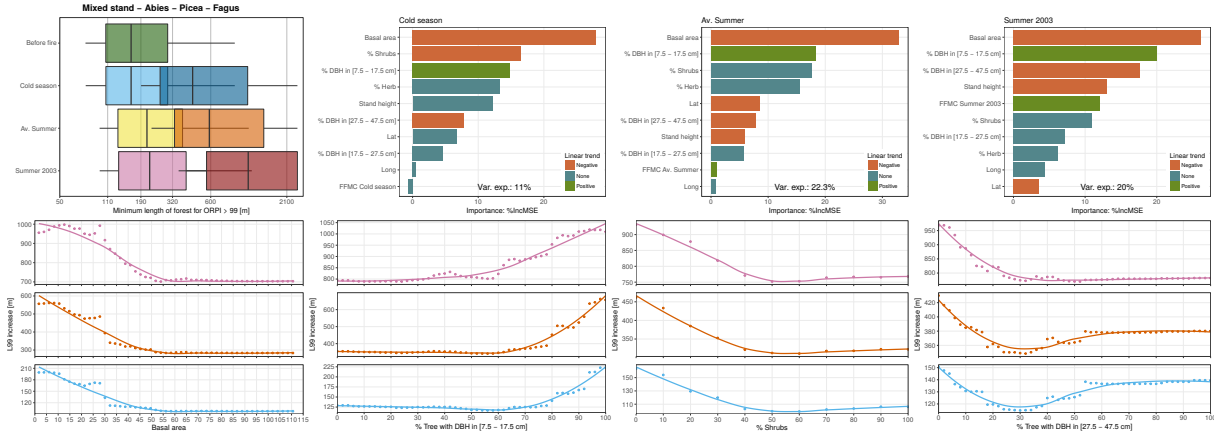

Figure C.14 – Result of regression forest for mixed stands dominated by *Abies alba*, *Picea abies* and *Fagus sylvatica*.

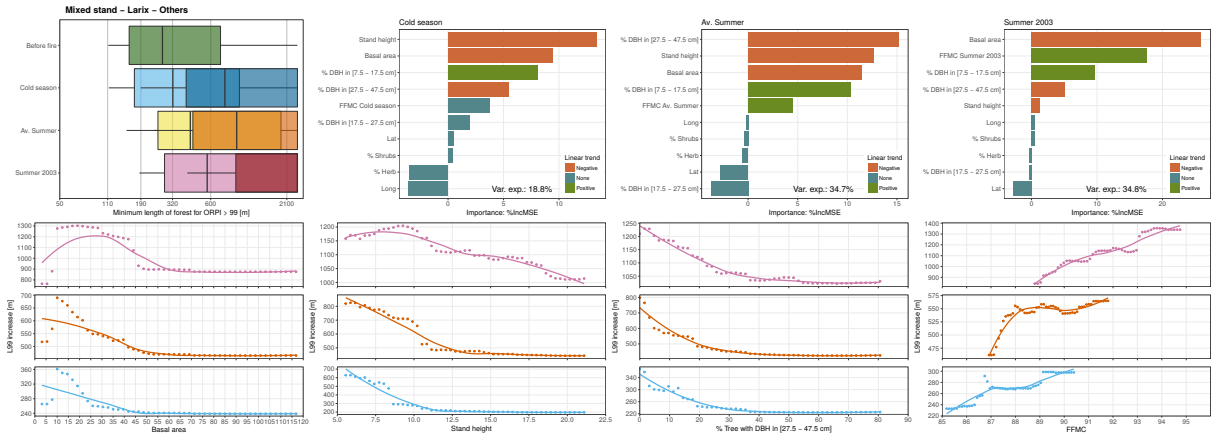

Figure C.15 – Result of regression forest for mixed stands dominated by *Larix decidua*.

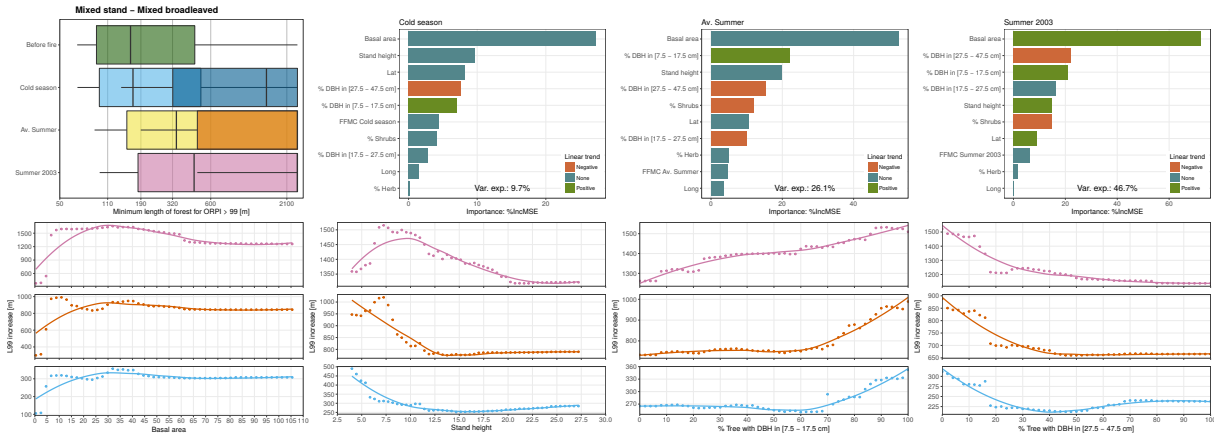

Figure C.16 – Result of regression forest for mixed stands of broadleaved species.

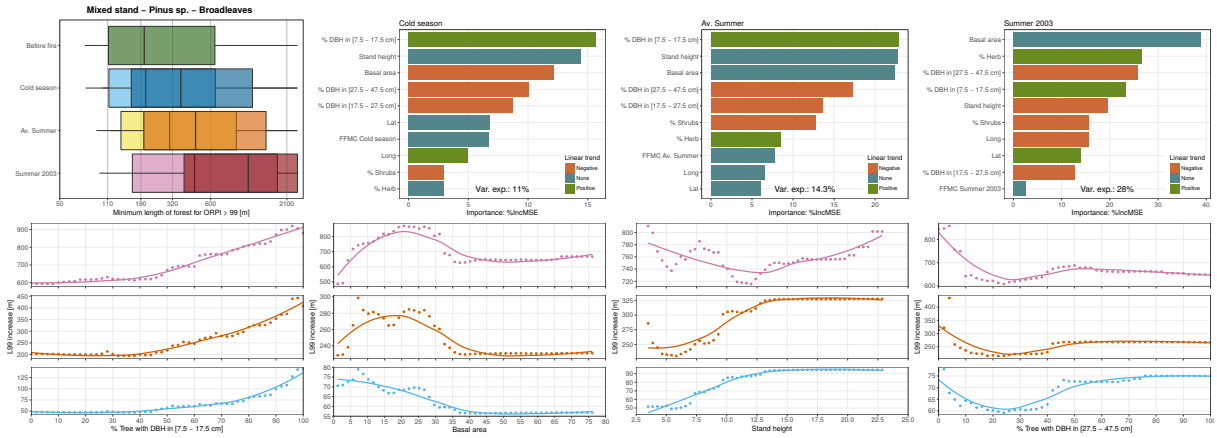

Figure C.17 – Result of regression forest for mixed stands dominated by *Pinus sp.*.

CHAPITRE 3

Synthèse de la partie IV

Dans cette partie, nous nous sommes intéressés aux effets des incendies sur la capacité de protection des forêts contre les chutes de blocs. Les différentes méthodes mises au point et les principaux résultats obtenus auparavant (parties II et III) ont été mobilisés pour proposer une approche méthodologique selon deux échelles d'analyse et de prise de décision : celle du peuplement forestier et celle de régions bioclimatiquement homogènes. Les principaux résultats et enseignements de cette partie sont détaillés ci-après.

Effet cascade à l'échelle du peuplement forestier.

Ce travail de thèse a permis d'identifier les types de peuplements les plus sujets à d'importantes pertes de leur capacité de protection contre les chutes de blocs. Il s'agit principalement des taillis (environ 42000 ha soit 14% de la superficie totale des forêts de protection des Alpes françaises) et, dans une moindre mesure, des futaies feuillues pures (60000 ha, 20% de la surface). Les incendies survenant pendant la saison froide ont généralement un faible effet sur la capacité de protection des forêts. Cependant, les feux d'été correspondant aux conditions moyennes observées ces dernières décennies et surtout les feux avec les conditions de l'été 2003 peuvent sérieusement altérer les capacités de protection. Dans le cas du scénario feu le plus extrême, l'effet protecteur est ainsi généralement réduit de 35 à 70% en moyenne pour les peuplements résineux et de 60 à 100% en moyenne pour les peuplements feuillus.
Par ailleurs, les résultats de la régression par forêt aléatoire permettent, pour chaque type de peuplement, d'identifier des gammes de valeurs optimales pour les caractéristiques forestières permettant de limiter l'effet des feux sur la capacité de protection initiale.

Deux zones particulièrement sujettes à des effets cascades importants.

L'analyse spatiale conduite dans ce travail de thèse a mis en avant deux zones particulièrement susceptibles de connaître des effets cascades importants en cas de feux. Ainsi, les basses altitudes des Alpes du Nord sont les plus sujettes à des effets cascades, essentiellement en cas de feux d'été affectant les forêts de protection. En effet, cette zone présente des forêts initialement très efficaces (majoritairement des taillis de bas de versant) qui voient leurs capacités de protection très fortement réduite en cas d'incendie d'été. La deuxième zone potentiellement la plus touchée par des effets cascade correspond aux faibles altitudes des Alpes du Sud. Dans cette zone, l'aléa incendie est très élevé (en fréquence et en intensité) mais la surface de forêt de protection est assez faible. Les quelques forêts de protection sont ainsi exposées à des feux plus dévastateurs qui entrainent une forte diminution de leur capacité de protection.

Les zones situées à haute altitude présentent des effets cascades potentiels similaires en cas d'incendie avec une très faible perte de la capacité de protection en cas de feu d'hiver, modérée en cas d'incendie d'été moyen et forte en cas de feu d'été extrême. Cependant, ces zones diffèrent par le nombre d'enjeux exposés aux chutes de blocs (plus nombreux dans le Nord) et par le niveau d'aléa incendie (plus élevé dans le Sud).

Cinquième partie

Synthèse générale et perspectives

CHAPITRE 1

Synthèse générale

Cette synthèse vise à résumer et mettre en perspective les principaux résultats obtenus au cours de ce travail de thèse. Les avancées concernant les aléas chute de blocs et incendie, étudiés indépendamment l'un de l'autre, sont d'abord présentées. Elles sont suivies des principaux enseignements concernant l'analyse multi-aléas. Les apports de ce travail de thèse sont rappelés dans le contexte de la problématique générale mais aussi dans une perspective plus large.

1.1 Évaluation de la capacité de protection contre les chutes de blocs des forêts des Alpes françaises

L'évaluation de la capacité de protection des forêts contre les chutes de blocs a été réalisée à partir de modélisations numériques effectuées avec le modèle Rockyfor3D. L'analyse de sensibilité du modèle, réalisée sur les variables d'entrées non forestières, montre l'importance relative de chaque variable et a permis d'éclairer le choix des paramètres par défaut utilisés pour toute la suite du travail. Ainsi, l'ensemble des résultats sur l'aléa chutes de blocs présentés dans cette thèse sont conservateurs dans le sens où les paramètres de sol choisis favorisent la propagation des blocs le long d'un versant. La chaîne de modélisation mise en place et les modifications apportées au modèle ont permis de simuler la propagation de dizaines de milliers blocs sur près de 4000 forêts des Alpes françaises de structures et compositions différentes tout en enregistrant la trajectoire (positions, vitesses) de chaque bloc virtuellement lancé.

Jusqu'à présent, les indicateurs de l'effet protecteur des forêts renseignaient principalement sur le nombre de blocs piégés en forêt (réduction de la fréquence), appelé "effet barrière" dans ce travail. Or, ce n'est pas le seul effet de la forêt puisqu'une partie de l'énergie cinétique du bloc est réduite (réduction de l'intensité) à chaque impact contre un arbre. Nous avons nommé ce processus "effet tampon". Afin de détailler le plus précisément possible la capacité de protection d'une forêt, trois indicateurs quantitatifs ont été définis dans cette thèse en comparant les données de trajectoire des blocs enregistrées lors de simulations avec forêt et sans forêt. Le premier indicateur, *BARI*, évalue l'effet barrière et retourne la proportion de blocs arrêtés en forêt. Le second, *MIRI*, quantifie l'effet tampon et retourne la réduction de l'énergie maximale des blocs. Enfin, le dernier indicateur, *ORPI*, est une combinaison des deux premiers et renseigne sur la réduction globale de l'aléa en tenant compte à la fois de l'effet barrière et de l'effet tampon. *BARI* et *MIRI* trouveront plutôt une application auprès des gestionnaires du risque tandis que *ORPI* a tout spécialement été conçu pour faire partie des indicateurs courants utilisés par les gestionnaires forestiers de montagne car il résume l'effet protecteur global d'une forêt en une

seule valeur. C'est d'ailleurs pour cette raison que seul *ORPI* a été utilisé par la suite pour synthétiser la perte de capacité de protection après feu.

Ces trois indicateurs ont permis d'identifier les paramètres forestiers qui influencent le plus la capacité de protection. Ainsi, le fait que les indicateurs soient calculés en fonction de la longueur boisée du versant fait de cette variable un paramètre clé dans l'évaluation de la capacité de protection des forêts. La surface terrière et le diamètre moyen des tiges (tous deux calculés en prenant en compte les arbres de diamètre $\geq$ 7.5 cm) sont ensuite apparus comme les plus importants. Si ces deux derniers paramètres ont souvent été cités dans les travaux menés sur l'effet protecteur des forêts, la longueur de forêt a, quant à elle, très peu été mise en avant, notamment lors de la vulgarisation de ces recherches. En effet, dans les guides de sylvicultures de montagne français, si les recommandations en termes de surface terrière sont fréquentes, les mentions à la longueur de forêt sont très rares et bien souvent limitées à la recommandation générale de "*maintenir ou atteindre une longueur boisée supérieure à 250 m*". Ce travail de thèse montre qu'il est tout à fait possible d'obtenir une excellente protection avec des longueurs de forêts inférieures et à l'inverse, une protection faible avec des longueurs supérieures. Ainsi, la capacité de protection dépend bien du triptyque longueur boisée, surface terrière et diamètre moyen. Donner une plage de valeurs cible pour l'une de ces variables sans prendre en compte les deux autres peut conduire à des non-sens. C'est à partir de ces trois paramètres qu'une méthode permettant d'évaluer rapidement chacun des indicateurs de protection a été proposée (Chapitre II.2).

La longueur de forêt nécessaire pour atteindre une réduction globale de l'aléa de 99% (c.-à-d. $ORPI \geq 99$), L_{99}, a par la suite été utilisée afin de comparer l'effet protecteur des principaux types de peuplements forestiers des Alpes françaises (Chapitre II.3). Différents enseignements ressortent de cette analyse. Tout d'abord, sur près de 4000 forêts réparties sur l'ensemble des Alpes françaises, 57% d'entre elles présentent une capacité de protection excellente à bonne avec 99% de l'aléa réduit après seulement 190 m de versant boisé. Le point commun à ces forêts est un important capital sur pied avec de fortes densités de tiges (> 800 tiges$\cdot$ha^{-1}) et des surfaces terrières élevées (> 30 m$^2\cdot$ha^{-1}). À l'opposé, 17% des forêts étudiées offrent une faible capacité de protection. Ce sont généralement des forêts subalpines dominées par le pin à crochets, le pin cembro ou le mélèze avec un nombre de tiges réduit (< 300 tiges$\cdot$ha^{-1}) et une surface terrière très faible (< 15 m$^2\cdot$ha^{-1}).

Cette analyse a aussi souligné un gradient décroissant de la capacité de protection quand la proportion d'essences feuillues diminue. Ainsi, les peuplements offrant la meilleure capacité de protection sont les taillis devant les futaies feuillues puis les futaies mixtes. Les futaies résineuses offrent généralement le niveau de protection le plus faible. De plus, à proportion de feuillus équivalente, les peuplements dominés par des essences tolérantes à l'ombre (sapin, épicéa, hêtre) présentent une meilleure capacité de protection que ceux dominés par des essences pionnières comme les pins, les mélèzes ou les chênes. Enfin, l'importance de la diversité forestière en termes de structure et de composition est apparue essentielle. En effet, les peuplements avec une distribution hétérogène des diamètres et composés de plusieurs essences différentes offrent généralement une meilleure protection que les peuplements réguliers et purs.

En conclusion, ce travail de thèse propose une méthode complète et définit trois indicateurs quantitatifs afin d'évaluer la capacité de protection d'une forêt contre les chutes de blocs. Un état des lieux complet de la capacité de protection des différents types de peuplements forestiers rencontrés dans les Alpes françaises a ensuite été réalisé à partir de ces indicateurs. Ce travail a ainsi permis d'identifier les peuplements les plus efficaces et d'apporter des éléments de réponse aux lacunes des guides de sylvicultures de montagne.

1.2 Évaluation de l'aléa incendie dans les forêts des Alpes françaises

L'évaluation de l'aléa incendie dans les forêts des Alpes françaises s'est effectuée en deux parties. Tout d'abord, les évolutions spatiales et temporelles des conditions météorologiques favorables aux feux ont été étudiées sur l'ensemble du territoire (Chapitre III.2). Le travail d'analyse spatiale effectué et le type des données météorologiques quotidiennes disponibles sur la période 1959-2015 ont permis une cartographie précise à une résolution fine (25 m), prenant en compte l'évolution de ces variables en fonction de l'altitude. Ainsi pour chaque pixel de 25 m, les principaux composants déterminants de l'aléa feu-météo (intensité, fréquence, longueur et saisonnalité des périodes favorables aux incendies) ont été déterminés et leurs tendances temporelles analysées.

L'analyse sur les soixante dernières années permet d'identifier trois points chauds où l'aléa feu-météo est modéré à fort et en nette augmentation. La zone la plus critique concerne les hautes altitudes et vallées internes des Alpes du Sud qui ont subi une augmentation significative de toutes les composantes de l'aléa (intensité, fréquence, longueur et saisonnalité) au cours des dernières décennies. Ainsi, si l'aléa était relativement modéré dans les années soixante, il atteint désormais régulièrement les plus hauts niveaux. La deuxième zone correspond aux basses altitudes des Alpes du Sud qui sont particulièrement sujettes aux feux intenses en raison d'un climat à tendance méditerranéenne combinant températures élevées, longue période sans précipitation et épisodes ventés fréquents. Dans cette zone, toutes les composantes de l'aléa atteignent régulièrement les plus hauts niveaux observés dans les Alpes françaises. En revanche, contrairement à la première zone, la tendance temporelle est moins marquée même si elle augmente également. Enfin, le dernier point chaud concerne les basses altitudes des Alpes du Nord. En condition normale, cette zone connaît un aléa faible à modéré. En revanche, lors d'épisodes caniculaires importants comme lors de l'été 2003, l'aléa atteint un niveau élevé propice à l'ignition et à la propagation de feux importants et intenses. La fréquence de ces épisodes extrêmes, tout comme les autres composantes de l'aléa, a connu une nette augmentation depuis les années soixante même si la tendance est plus modérée que dans le sud des Alpes. Malgré ces trois points chauds, il est important de noter que certaines parties des Alpes françaises restent exposées à un aléa faible et stable au cours des dernières décennies. Cela concerne principalement les hautes altitudes (> 800 m) des Alpes du Nord caractérisées par des températures fraîches et des précipitations bien réparties tout au long de l'année. Jusqu'à présent, ce climat frais et relativement humide atténuait l'effet de l'augmentation globale des températures et a permis de maintenir l'aléa feu-météo à un niveau modéré même lors de l'été anormalement chaud de 2003.

Les résultats de l'analyse spatio-temporelle ont été utilisés pour l'évaluation de la mortalité des arbres après des incendies de différentes intensités (Chapitre III.3). Elles ont notamment permis la définition de trois scénarios de feux fondés sur les conditions climatiques moyennes observées sur la période 1959-2015 de novembre à avril (feu d'hiver) et de juin à septembre (feu d'été) ainsi que celles observées lors de l'été exceptionnel de 2003 (feu d'été extrême). Ces trois scénarios de feux ont été appliqués sur les mêmes forêts que celles utilisées dans l'évaluation de l'aléa chutes de blocs en utilisant le modèle FlamMap. Les résultats des simulations ont ensuite été utilisés pour prédire la mortalité des arbres suite au passage d'un incendie. Cette mortalité dépend de l'intensité du feu, du temps de résidence du front de flammes et des caractéristiques de l'arbre (épaisseur d'écorce, hauteur totale et hauteur de la base du houppier). Elle a été calculée à l'aide de plusieurs équations de mortalité identifiées dans la littérature et en fonction de deux temps de résidence du front de flammes : 30 secondes (temps minimum nécessaire pour qu'un feu subsiste) et un temps maximum théorique (entre 1 et 5 minutes) qui dépend de la charge de combustible et de son taux d'humidité. Pour les principales essences des Alpes françaises, les résultats obtenus ont été comparés à des observations de terrain après des incendies réels ou à

des données empruntées dans la littérature. Ce travail à l'échelle de l'arbre a permis d'identifier les espèces les moins résistantes au feu (sapin, hêtre, pin à crochets, pin cembro) ainsi que les équations de mortalité les plus adaptées à chacun des trois scénarios de feu.

Les résultats principaux à l'échelle du peuplement forestier montrent que les incendies survenant pendant la saison froide (60% des feux dans les Alpes françaises) ont un impact très limité sur les forêts. En revanche, ceux intervenant en été (et *a fortiori* lors d'un été exceptionnellement sec et chaud comme en 2003) peuvent conduire à des taux de mortalité importants surtout dans les taillis et les futaies dominées par des essences feuillues.

En conclusion, ce travail de thèse établit un état des lieux complet de l'évolution de l'aléa feu-météo dans les Alpes françaises et met en avant un contraste important entre les Alpes du Nord, avec un aléa qui augmente dans le temps mais qui reste limité aux étés exceptionnels et cantonné aux basses altitudes, et les Alpes du Sud avec un aléa fort qui a montré une évolution importante dans les soixante dernières années. L'évaluation de la mortalité post-feu souligne quant à elle une vulnérabilité importante des types de peuplements dominés par les feuillus et en particulier des taillis. Ainsi, les peuplements offrant la meilleure protection contre les chutes de blocs semblent aussi être les plus vulnérables en cas d'incendie.

1.3 Analyse multi-aléas et effets cascades

L'analyse multi-aléas réalisée au cours de ce travail de thèse vise à évaluer l'influence du passage d'un feu sur l'efficacité de la protection contre les chutes de blocs des forêts de montagne (Chapitre IV.2). Ce travail a été conduit pour deux échelles d'analyse et de prise de décision : au niveau du peuplement forestier et au niveau de quatre régions bioclimatiquement homogènes.

La mortalité post-feu obtenue au chapitre III.3 pour les arbres de 4438 placettes forestières réparties dans les Alpes françaises a été introduite dans la chaîne de modélisation de la capacité de protection contre les chutes de blocs. Ainsi, pour chaque placette forestière, la même forêt initiale a été utilisée, à la différence près que pour chacun des trois scénarios feux, les arbres présentant une probabilité de mortalité post-incendie supérieure à 50% ont été supprimés. Les résultats présentés sont ainsi conservateurs, d'autant plus que les arbres morts peuvent temporairement contribuer à réduire l'aléa chute de blocs. L'indicateur *ORPI* défini précédemment, ainsi que la longueur de forêt nécessaire pour réduire l'aléa chutes de blocs de 99% (L_{99}) ont ensuite été calculés à partir des résultats de simulations afin de comparer la capacité de protection avant et après feu.

L'étude à l'échelle du peuplement forestier a permis d'identifier les types de peuplements les plus sujets à d'importantes pertes de leur capacité de protection contre les chutes de blocs. Il s'agit principalement des taillis (environ 42000 ha soit 14% de la superficie totale des forêts de protection des Alpes françaises) et, dans une moindre mesure, des futaies feuillues pures (60000 ha, 20% de la surface). Ce résultat s'explique en partie par la localisation de ces types de peuplements qui se trouvent aux altitudes les plus basses caractérisées par des conditions climatiques plus favorables aux feux. Pour les taillis, il faut ajouter à cela des arbres présentant de faibles diamètres (donc de faibles épaisseurs d'écorce) et des hauteurs relativement basses qui diminuent leur résistance au feu. Cette baisse d'efficacité de la protection est également présente, bien que dans une moindre mesure, dans les peuplements dominés par les conifères. Les incendies survenant pendant la saison froide ont généralement un faible effet sur la capacité de protection des forêts. Cependant, les feux d'été correspondant aux conditions moyennes observées ces dernières décennies et surtout les feux avec les conditions de l'été 2003 peuvent sérieusement altérer les capacités de protection. Dans le cas du scénario feu le plus extrême, l'effet protecteur est ainsi généralement réduit de 35 à 70% en moyenne pour les peuplements résineux et de 60 à

100% en moyenne pour les peuplements feuillus.

En complément de ces résultats, une analyse a été réalisée afin d'identifier les caractéristiques forestières optimales propres à chacun des peuplements forestiers des Alpes françaises dans l'optique de limiter la perte de la capacité de protection suite à un feu.

L'analyse spatiale réalisée dans ce travail de thèse a permis d'identifier les forêts avec une fonction de protection potentielle contre les chutes de blocs ainsi que la proportion d'enjeux (routes, voies ferrées et bâtiments) exposés à l'échelle des Alpes françaises. Les résultats concernant la perte de la capacité de protection après différents scénarios de feux à l'échelle du peuplement forestier ont ensuite été utilisés afin d'identifier les effets cascades potentiels au sein des quatre régions bioclimatiquement homogènes des Alpes françaises.

Il ressort de cette analyse que les basses altitudes des Alpes du Nord sont les plus sujettes à des effets cascades importants essentiellement en cas de feux d'été affectant les forêts de protection. En effet, cette zone présente la plus forte concentration d'enjeux exposés. Sans feu, les forêts sont particulièrement efficaces en réduisant l'aléa chutes de blocs de 90% au niveau de 75% des enjeux. Après un feu d'été, la proportion d'enjeux présentant le même niveau de protection diminue fortement : seulement 10% en cas de feu d'été moyen et 5% en cas d'un feu extrême. C'est la plus importante perte de capacité de protection observée parmi les quatre zones d'études.

La deuxième zone potentiellement la plus touchée par des effets cascade correspond aux faibles altitudes des Alpes du Sud. Dans cette zone, le nombre d'enjeux menacés par les chutes de blocs est relativement faible, mais l'aléa incendie est le plus élevé de la zone alpine. Les forêts de cette zone offrent une protection modérée contre les chutes de blocs, mais elles sont ainsi exposées à des feux plus fréquents et plus intenses. Leur effet protecteur en cas d'incendie (en particulier les feux d'été) subit ainsi une forte diminution.

Les deux zones à haute altitude présentent des effets cascades potentiels similaires en cas d'incendie avec une très faible perte de la capacité de protection en cas de feu d'hiver, modérée en cas d'incendie d'été moyen et forte en cas de feu d'été extrême. Cependant, ces zones diffèrent par le nombre d'enjeux exposés aux chutes de blocs (plus nombreux dans le Nord) et par le niveau d'aléa incendie (plus élevé dans le Sud).

En conclusion, ce travail de thèse propose une méthode permettant de quantifier la diminution de la capacité de protection contre les chutes de blocs d'une forêt suite à un incendie. Cette méthode a été utilisée pour identifier les effets cascades potentiels au sein des principaux types de peuplements forestiers des Alpes françaises et évaluer leurs répercussions à d'autres niveaux sur les enjeux humains.

CHAPITRE 2

Perspectives scientifiques et applications

2.1 Évaluation de l'aléa chutes de blocs et de la capacité de protection des forêts

Vers une cartographie de la fonction de protection.

Cette étude propose une méthode afin d'identifier les forêts de protection potentielles à large échelle. En l'absence de données spatiales concernant les caractéristiques forestières (surface terrière, diamètre moyen ou densité de tiges), la capacité de protection a été évaluée simplement en fonction de la longueur boisée du versant et du type de peuplement dominant. Lorsque les caractéristiques forestières sont disponibles, ce qui peut être le cas sur les zones couvertes par Lidar, il est possible d'aller beaucoup loin dans la cartographie de la fonction de protection (Monnet et al., 2017). Une spatialisation des indices proposés dans cette thèse serait ainsi envisageable à moyen terme, ce qui faciliterait la prise en compte de la forêt dans les scénarios et analyses de risque.

Quantification de la probabilité de départ des blocs.

Dans ce travail de thèse, l'évaluation de l'aléa chutes de blocs porte essentiellement sur la phase de propagation. La probabilité d'occurrence du phénomène n'est donc pas prise en compte. Outre sa capacité de protection, la forêt pourrait aussi servir de bio-indicateur de la fréquence des chutes de blocs à travers une analyse dendrogéomorphologique des cicatrices sur les arbres liées à des impacts de blocs. Des recherches récentes vont d'ailleurs dans ce sens en utilisant la cartographie des impacts sur les arbres pour déduire une fréquence du phénomène gravitaire (Favillier et al., 2015).

Évolution dans le temps de la capacité de protection.

Le point précédent revêt aussi une certaine importance lorsqu'on s'intéresse à l'évolution naturelle de la capacité de protection dans le temps. En effet, une forêt située dans une zone avec une activité importante de chutes de blocs peut être fragilisée par les impacts répétés sur les arbres. À cela s'ajoute l'évolution naturelle des peuplements qui peut passer par des stades limitant la capacité de protection. Jusqu'à présent, l'évolution de la capacité de protection au cours d'un cycle sylvogénétique a peu été étudiée (Cordonnier et al., 2008). Pour les futures recherches sur le sujet, mon travail de thèse apporte une méthode simple mais robuste pour quantifier la capacité de protection mais aussi pour intégrer l'effet de perturbations naturelles (tempêtes, sécheresses...) comme cela a été réalisé pour les incendies.

Vers une analyse économique de l'aléa chutes de blocs.

Les indicateurs quantitatifs sont très utiles pour évaluer la valeur économique d'un service écosystémique (Lasseur, 2017; Getzner et al., 2017). L'effet protecteur des forêts est particulièrement propice à ce type d'étude (Dupire, 2011) et la méthode et les indicateurs proposés dans ce travail pourraient permettre une évaluation rapide. En cas de spatialisation des indicateurs, l'analyse économique pourrait même être réalisée à échelle supérieure (par exemple nationale ou celle de l'arc alpin) avec un niveau de précision élevé.

Amélioration des modèles existants.

Pour mener à bien ce travail de thèse, plusieurs modifications ont été apportées au modèle Rockyfor3D : (1) la sauvegarde des trajectoires des blocs (vitesse, position), (2) la modification du fichier arbre pour prendre en compte les capacités mécaniques des arbres, (3) le remplacement de la hauteur de chute initiale par une vitesse d'entrée dans le peuplement et (4) la prise en compte d'une seule rugosité moyenne du sol contre trois valeurs dans le modèle initial. Si ces modifications ne sont pas forcément toutes utiles pour une utilisation classique, le passage de trois variables de rugosité de sol à une seule serait certainement une avancée car il s'agit d'un paramètre prépondérant (cf. analyse de sensibilité) très difficile à apprécier sur le terrain.
Par ailleurs, l'intégration des résultats des récentes études mécaniques portant sur les rebonds (Bourrier et al., 2009) et les impacts sur les arbres (Toe et al., 2017a) permettrait une description plus précise des processus mécaniques impliqués lors d'une chute de blocs.

Création d'outils opérationnels en ligne pour évaluer la capacité de protection.

Rockfor^{NET} (Berger et al., 2007) est actuellement le seul outil en ligne disponible pour évaluer rapidement la capacité de protection d'une forêt. Ce modèle repose sur des équations empiriques fondées sur un nombre restreint d'observations. Par ailleurs, seules des estimations sur le nombre de blocs piégés en forêt sont fournies. Ce travail de thèse porte sur un nombre important de forêts couvrant une large variabilité en termes de structure et de composition. De plus, il ajoute des informations sur la réduction de l'intensité de l'aléa. Avec l'amélioration des capacités de calcul, il serait aujourd'hui possible de mettre en ligne la chaîne de modélisation utilisée dans cette thèse. L'utilisateur pourrait ainsi simplement fournir un profil topographique, la dimension des blocs et les trois variables forestières clés (longueur de forêt, diamètre moyen et surface terrière) et obtiendrait en retour les valeurs de *BARI*, *MIRI* et *ORPI*.

Prises en compte de la forêt par les gestionnaires du risque.

La mise en place des outils présentés précédemment serait un argument de poids pour que les forêts soient mieux prises en compte par les gestionnaires du risque, notamment lorsqu'ils dimensionnent des ouvrages de protection (filet ou merlon). En effet, même s'ils reconnaissent l'effet de la forêt, les gestionnaires manquent aujourd'hui de données quantitatives fiables. La forêt est ainsi sous-évaluée lors d'un dimensionnement alors que sa présence pourrait permettre d'installer des structures plus petites et donc de réduire les coûts d'installation et de maintenance.

Mise à jour des guides de sylvicultures.

Enfin, ce travail pourrait alimenter une mise à jour des guides de sylvicultures de montagne. Par exemple, la longueur de la bande boisée sur le versant, pourtant essentielle pour une évaluation précise de la capacité de protection, est très largement négligée dans ces guides. Les valeurs "optimales" des grandeurs forestières sont ainsi données sans prendre en compte cette longueur. Cela peut conduire à des non-sens comme par exemple le fait de garder une forte densité d'arbres, qui va compliquer le renouvellement de la forêt, dans les zones où la longueur boisée est suffisamment longue pour que le même niveau de protection soit atteint avec une densité plus faible.

2.2 Évaluation de l'aléa feux de forêt dans les Alpes françaises

Étude sur les vecteurs d'ignition dans les Alpes.

Dans ce travail de thèse, les vecteurs d'ignition des incendies n'ont pas été étudiés. Il s'agit pour autant d'un élément important dans l'évaluation de l'aléa feux de forêt et d'un facteur limitant les incendies sur cette zone d'étude. En effet, lors d'épisodes caniculaires comme pendant l'été 2003, le nombre de feux recensés, bien qu'important comparé à une année classique, est finalement limité compte tenu des conditions météorologiques très sèches et de la teneur en eau de la végétation très basses observées. Il semble ainsi que les vecteurs d'ignition dans les Alpes soient différents de ceux, plus connus, de la zone méditerranéenne (Curt et al., 2016). Des investigations sur cette thématique sont ainsi nécessaires pour compléter les résultats de cette étude (Arndt et al., 2013).

Spatialisation des indices feu-météo pour les scénarios climatiques futurs.

Dans cette étude, la spatialisation des indices feu-météo s'est limitée à la période 1959-2015 pour laquelle des informations de qualité sur les variables météorologiques observées étaient disponibles. Pour confirmer les tendances spatio-temporelles identifiées, il serait intéressant d'effectuer une spatialisation prospective des indices feu-météo pour chaque scénario climatique. Cela pourrait notamment être réalisé à partir des données CMIP5/EUROCORDEX (http://cordex.org/) qui fournissent des informations de projections très précises des climats attendus en Europe.

Typologie des combustibles pour les Alpes.

À ce jour, il n'existe aucune typologie de la végétation combustible concernant le territoire alpin. Un réseau de placettes de description du combustible a été initié lors d'une thèse précédente (Fréjaville, 2015) et complété au cours de cette thèse notamment pour l'étage collinéen des Alpes du Nord. Il serait très intéressant de densifier ce réseau de placette dans l'optique d'obtenir une typologie des combustibles pour la zone alpine qui soit utilisable dans les principaux modèles de comportement du feu (Behave, Firesite, FlamMap, etc.).

Informations sur le comportement du feux dans les bases de données incendie.

Les bases de données feux de forêts actuellement disponibles en France (BDIFF, 2017; Prométhée, 2017) fournissent des informations intéressantes sur la localisation et la surface brûlée par un incendie. Afin d'alimenter les recherches sur les feux de forêts en France, il serait pertinent d'ajouter des informations basiques sur le comportement du feu dans ces bases de données. Par exemple, la hauteur de flamme ainsi que la vitesse de propagation et la largeur du front de flammes pourraient être renseignées sous forme de classes. Cela permettrait d'estimer l'intensité d'un feu afin de valider les résultats de simulations ou encore de la mettre en relation avec les dégâts observés sur la végétation.

Mise en place d'un suivi de la mortalité post-feu.

Les données de mortalité post-feu sont très rares pour ce qui concerne les peuplements alpins. La méthodologie mise en place par Maringer et al. (2016b) pour suivre l'évolution de la mortalité dans les peuplements de hêtre pourrait ainsi être étendue à d'autres types de peuplements ayant été exposés à un incendie. La mise en place d'un réseau transalpin de placettes de suivi de mortalité pourrait décupler les informations et apporter une source de données utiles à une meilleure compréhension et prédictibilité de la mortalité.

2.3 Renforcer l'analyse multi-aléas pour la prise en compte des effets cascades

Généralisation de la méthode à d'autres perturbations et aléas naturels.

La méthode générale développée au cours de ce travail de thèse est généralisable à d'autres perturbations. Il faut pour cela évaluer la mortalité après la perturbation pour appliquer par la suite la même méthode de comparaison de la capacité de protection avant/après la perturbation. Cela pourrait par exemple être réalisé pour les tempêtes, sécheresses ou encore les attaques d'insectes comme les scolytes, qui localement peuvent causer des mortalités au moins aussi importantes que celles observées après un incendie. De la même façon, les effets cascades suite au passage d'un incendie de forêt pourrait être étudiés pour d'autres aléas naturels sur lesquels la forêt agit. Cela a notamment été proposé pour les processus d'érosion (Johansen et al., 2001) et de crues torrentielles (Nunes et al., 2017).

Essais mécaniques sur des arbres brûlés.

Dans ce travail de thèse, les capacités mécaniques des arbres identifiés comme morts suite au passage d'un incendie ont été considérées comme nulles. En réalité, les arbres brûlés conservent certainement une capacité à réduire l'énergie des blocs, au moins temporairement. Il serait ainsi intéressant d'évaluer ces capacités, si possible, directement sur le terrain. Les méthodes développées pour suivre l'évolution de la dégradation des propriétés mécaniques du bois dans les ouvrages de protection (Barré, 2017) pourraient trouver ici une autre application. Cela permettrait une prise en compte plus nuancée de la mortalité des arbres.

Vers des compromis entre efficacité de la protection et vulnérabilité aux incendies.

Ce travail de thèse fournit des plages de valeurs optimales pour chacun des principaux types de peuplements forestiers afin de limiter la perte de capacité de protection. Il serait intéressant d'aller plus loin dans cette analyse afin d'identifier des modes de gestion et des structures de peuplement à privilégier pour maintenir une bonne capacité de protection tout en limitant la vulnérabilité aux incendies.

Mise en place d'outils d'aide à la décision.

L'analyse spatiale conduite dans la dernière partie de ce travail de thèse permet de localiser les forêts avec une forte capacité de protection et d'estimer la perte de cette fonction en cas d'incendie. Les différentes cartes créées pour cette analyse pourraient alimenter un outil d'aide à la décision pour les gestionnaires, les aménageurs ou les services de protection, permettant d'identifier des zones prioritaires où des moyens de luttes contre les incendies devraient être engagés en cas de feu afin de limiter la perte de capacité de protection et les dégâts sur les enjeux situés à l'aval.

Bibliographie

Ager, A. A., N. M. Vaillant, and M. A. Finney (2011). "Integrating fire behavior models and geospatial analysis for wildland fire risk assessment and fuel management planning". In: *Journal of Combustion* 2011.

Alexander, M. E. (1982). "Calculating and interpreting forest fire intensities". In: *Canadian Journal of Botany* 60.4, pp. 349–357.

Amatulli, G., A. Camia, and J. San-Miguel-Ayanz (2013). "Estimating future burned areas under changing climate in the EU-Mediterranean countries". In: *Science of The Total Environment* 450–451, pp. 209 –222.

Ancelin, P., C. Barthelon, F. Berger, M. Cardew, C. Chauvin, B. Courbaud, L. Descroix, L. K. A. Dorren, J. Fay, P. Gaudry, X. Gauquelin, J. Genin, D. Joud, P. Loho, E. Mermin, F. Plancheron, A. Prochasson, F. Rey, D. Rubeaud, and L. Wlerick (2006). *Guide des sylvicultures de montagne : Alpes du Nord françaises*. Cemagref, CRPF Rhône-Alpes, ONF.

Archibald, S., D. P. RoyY, B. W. Van Wilgen, and R. J. Scholes (2009). "What limits fire ? An examination of drivers of burnt area in Southern Africa". In: *Global Change Biology* 15.3, pp. 613–630.

Arndt, N, H Vacik, V Koch, A Arpaci, and H Gossow (2013). "Modeling human-caused forest fire ignition for assessing forest fire danger in Austria". In: *iForest - Biogeosciences and Forestry* 6.6, pp. 315–325.

Arpaci, A., C. S. Eastaugh, and H. Vacik (2013). "Selecting the best performing fire weather indices for Austrian ecoregions". In: *Theoretical and Applied Climatology* 114.3-4, pp. 393–406.

Barré, J.-B. (2017). "Evaluation du niveau de dégradation du bois dans les ouvrages de protection par spectroscopie proche infrarouge et analyse vibratoire". PhD thesis. Grenoble, France: Université Grenoble Alpes.

Barré, J.-B., F. Bourrier, D. Bertrand, M.-F. Thévenon, and F. Rey (2017a). "Decay extent assessment of small-diameter silver fir logs degraded in natural conditions in the French Northern Alps using NIRS and vibration resonance methods". In: *Ecological Engineering* 109, pp. 240–248.

Barré, J.-B., F. Bourrier, L. Brancheriau, D. Bertrand, and F. Rey (2017b). "Effects of fungal decay on elasticity and damping of small-diameter silver fir logs assessed by the transverse vibration resonant method". In: *Wood Science and Technology*, pp. 1–18.

Barré, J.-B., F. Bourrier, L. Cécillon, L. Brancheriau, D. Bertrand, M.-F. Thévenon, and F. Rey (2017c). "Predicting mechanical degradation indicators of silver fir wooden strips using near infrared spectroscopy". In: *European Journal of Wood and Wood Products*, pp. 1–13.

Bartko, J. J. (1966). "The intraclass correlation coefficient as a measure of reliability". In: *Psychological Reports* 19.1, pp. 3–11.

Bauer, G., T. Speck, J. Blömer, J. Bertling, and O. Speck (2010). "Insulation capability of the bark of trees with different fire adaptation". In: *Journal of Materials Science* 45.21, pp. 5950–5959.

BDIFF (2017). *BDIFF : Base de données sur les incendies de forêt en France*. URL: http://bdiff.ifn.fr/.

Bebi, P., F. Kienast, and W. Schönenberger (2001). "Assessing structures in mountain forests as a basis for investigating the forests' dynamics and protective function". In: *Forest Ecology and Management* 145.1-2, pp. 3–14.

Bebi, P., D. Kulakowski, and C. Rixen (2009). "Snow avalanche disturbances in forest ecosystems—State of research and implications for management". In: *Forest Ecology and Management* 257.9. Disturbances in Mountain Forests : Implications for Management, pp. 1883–1892.

Bedia, J., S. Herrera, D. Martín, N. Koutsias, and J. Gutiérrez (2013). "Robust projections of Fire Weather Index in the Mediterranean using statistical downscaling". In: *Climatic Change* 120.1-2, pp. 229–247.

Bedia, J., S. Herrera, A. Camia, J. Moreno, and J. Gutiérrez (2014). "Forest fire danger projections in the Mediterranean using ENSEMBLES regional climate change scenarios". In: *Climatic Change* 122.1-2, pp. 185–199.

Beniston, M. (2005). "Climatic change and its possible impacts in the Alpine region". In: *Journal of Alpine Research* 93.2, pp. 25–32.

Berger, F., C. Quetel, and L. K. Dorren (2002). "Forest : a natural protection mean against rockfalls, but with which efficiency". In: *International Congress Interpraevent*, pp. 815–826.

Berger, F. and L. K. Dorren (2007). "Principles of the tool Rockfor.net for quantifying the rockfall hazard below a protection forest". In: *Schweizerische Zeitschrift für Forstwesen* 158.6, pp. 157–165.

Berretti, R., L. Caffo, P. Camerano, F. De Ferrari, A. Domaine, A. Dotta, F. Gottero, J.-C. Haudeman, F. Letey C. Meloni, F. Motta, and P.-G. Terzuolo (2006). *Selvicoltura nelle foreste di protezione*. Compagnia delle Foreste.

Bertrand, D., F. Bourrier, I. Olmedo, M. Brun, F. Berger, and A. Limam (2013). "Experimental and numerical dynamic analysis of a live tree stem impacted by a Charpy pendulum". In: *International Journal of Solids and Structures* 50.10, pp. 1689–1698.

Bessie, W. C. and E. A. Johnson (1995). "The Relative Importance of Fuels and Weather on Fire Behavior in Subalpine Forests". In: *Ecology* 76.3, pp. 747–762.

Blarquez, O. and C. Carcaillet (2010). "Fire, Fuel Composition and Resilience Threshold in Subalpine Ecosystem". In: *PLOS ONE* 5.8, pp. 1–8.

Bortoletto, G and J. Moreschi (2003). "Physical–mechanical properties and chemical composition of Pinus taeda mature wood following a forest fire". In: *Bioresource Technology* 87.3, pp. 231–238.

Bourrier, F., L. Dorren, F. Nicot, F. Berger, and F. Darve (2009). "Toward objective rockfall trajectory simulation using a stochastic impact model". In: *Geomorphology* 110.3–4, pp. 68–79.

Bourrier, F., F. Berger, P. Tardif, L. Dorren, and O. Hungr (2012). "Rockfall rebound : comparison of detailed field experiments and alternative modelling approaches". In: *Earth Surface Processes and Landforms* 37.6, pp. 656–665.

Bourrier, F., L. Dorren, and O. Hungr (2013). "The use of ballistic trajectory and granular flow models in predicting rockfall propagation". In: *Earth Surface Processes and Landforms* 38.4, pp. 435–440.

Bova, A. S. and D. M. B. (2005). "Linking surface-fire behavior, stem heating, and tissue necrosis". In: *Canadian Journal of Forest Research* 35.4, pp. 814–822.

Bradstock, R. A. (2010). "A biogeographic model of fire regimes in Australia : current and future implications". In: *Global Ecology and Biogeography* 19.2, pp. 145–158.

Brang, P., W. Schönenberger, E. Ott, and B. Gardner (2001). "Forests as Protection from Natural Hazards". In: *The Forests Handbook*. Ed. by J. Evans. Vol. 2. Blackwell Science Ltd., Oxford, pp. 53–81.

Brauner, M., W. Weinmeister, P. Agner, S. Vospernik, and B. Hoesle (2005). "Forest management decision support for evaluating forest protection effects against rockfall". In: *Forest Ecology and Management*. Decision Support in Multi Purpose Forestry Decision Support in Multi Purpose Forestry Selected papers from the symposium on 'Development and Application of Decision Support Tools in Multiple Purpose Forest Management' 207.1–2, pp. 75–85.

Breiman, L. (2001). "Random Forests". In: *Machine Learning* 45.1, pp. 5–32.

BRGM, CETE, DGPR, DDT(06-38-74), IFSTTAR, Irstea, and ONF-RTM (2014). *Méthodologie de l'élaboration du volet "aléa rocheux" d'un PPRn*. Tech. rep. Groupe de travail MEZAP, Ministère de l'écologie, du développement durable et de l'énergie, p. 49.

Briner, S., R. Huber, P. Bebi, C Elkin, D. R. Schmatz, and A. Grêt-Regamey (2013). "Trade-Offs between Ecosystem Services in a Mountain Region". In: *Ecology and Society* 18.3.

Brown, J. K. and N. V. DeByle (1987). "Fire damage, mortality, and suckering in aspen". In: *Canadian Journal of Forest Research* 17.9, pp. 1100–1109.

Budimir, M. E. A., P. M. Atkinson, and H. G. Lewis (2014). "Earthquake-and-landslide events are associated with more fatalities than earthquakes alone". In: *Nat. Hazards* 72.2, pp. 895–914. ISSN: 1573-0840.

Burylo, M., C. Hudek, and F. Rey (2011). "Soil reinforcement by the roots of six dominant species on eroded mountainous marly slopes (Southern Alps, France)". In: *{CATENA}* 84.1–2, pp. 70 –78.

Byram, G. (1959). "Combustion of forest fuels". In: *Forest fire : control and use*. Ed. by K. Davis. McGraw-Hill : New York, pp. 61–89.

Carcaillet, C. (1998). "A spatially precise study of Holocene fire history, climate and human impact within the Maurienne valley, North French Alps". In: *Journal of Ecology* 86.3, pp. 384–396.

Castebrunet, H., N. Eckert, G. Giraud, Y. Durand, and S. Morin (2014). "Projected changes of snow conditions and avalanche activity in a warming climate : the French Alps over the 2020-2050 and 2070-2100 periods". In: *The Cryosphere* 8.5, pp. 1673–1697.

Catry, F., F. Rego, F. Moreira, P. Fernandes, and J. Pausas (2010). "Post-fire tree mortality in mixed forests of central Portugal". In: *Forest Ecology and Management* 260.7, pp. 1184 –1192.

Cerdà, A. (1998). "Changes in overland flow and infiltration after a rangeland fire in a Mediterranean scrubland". In: *Hydrological Processes* 12.7, pp. 1031–1042.

Christen, M. (2012). "Integral hazard management using a unified software environment". In: *12th Congress Interpraevent, Grenoble, France*, pp. 77–86.

Cohen, J. (1960). "A coefficient of agreement for nominal scales". In: *Educational and Psychological Measurement* 20.1, pp. 37–46.

Coles, S., J. Bawa, L. Trenner, and P. Dorazio (2001). *An introduction to statistical modeling of extreme values*. Vol. 208. Springer, London.

Conedera, M, L Lucini, E Valese, D Ascoli, and G. Pezzatti (2010). "Fire resistance and vegetative recruitment ability of different deciduous trees species after low-to moderate-intensity surface fires in southern Switzerland". In: *VI International Conference on Forest Fire Research, Coimbra, Portugal*.

Congalton, R. G. (1991). "A review of assessing the accuracy of classifications of remotely sensed data". In: *Remote Sensing of Environment* 37.1, pp. 35–46.

Cordonnier, T., B. Courbaud, F. Berger, and A. Franc (2008). "Permanence of resilience and protection efficiency in mountain Norway spruce forest stands : A simulation study". In: *Forest Ecology and Management* 256.3, pp. 347–354.

Corominas, J., R. Copons, J. Moya, J. M. Vilaplana, J. Altimir, and J. Amigó (2005). "Quantitative assessment of the residual risk in a rockfall protected area". In: *Landslides* 2.4, pp. 343–357.

Coudour, B. (2015). "Influence de la végétation et du relief dans les feux de forêt extrêmes : étude de l'accumulation, de la dégradation et des propriétés de combustion des composés organiques volatiles issus des feux de forêt". PhD thesis. Poitiers.

Coutard, J.-P. and B. Francou (1989). "Rock Temperature Measurements in Two Alpine Environments : Implications for Frost Shattering". In: *Arctic and Alpine Research* 21.4, pp. 399–416.

Curt, T., A. Schaffhauser, L. Borgniet, C. Dumas, R. Estève, A. Ganteaume, M. Jappiot, W. Martin, A. N'Diaye, and B. Poilvet (2011). "Litter flammability in oak woodlands and shrublands of southeastern France". In: *Forest Ecology and Management* 261.12, pp. 2214 –2222.

Curt, T., L. Borgniet, and C. Bouillon (2013). "Wildfire frequency varies with the size and shape of fuel types in southeastern France : Implications for environmental management". In: *Journal of Environmental Management* 117, pp. 150 –161.

Curt, T., T. Fréjaville, and S. Lahaye (2016). "Modelling the spatial patterns of ignition causes and fire regime features in southern France : implications for fire prevention policy". In: *International Journal of Wildland Fire* 25.7, pp. 785–796.

Cutler, D. R., T. C. Edwards, K. H. Beard, A. Cutler, K. T. Hess, J. Gibson, and J. J. Lawler (2007). "Random forest for classification in ecology". In: *Ecology* 88.11, pp. 2783–2792.

De Graff, J. V., B. Shelmerdine, A. Gallegos, and D. Annis (2015). "Uncertainty Associated with Evaluating Rockfall Hazard to Roads in Burned Areas". In: *Environmental & Engineering Geoscience* 21.1, pp. 21–33.

Dickinson, M. B. and E. A. Johnson (2004). "Temperature-dependent rate models of vascular cambium cell mortality". In: *Canadian Journal of Forest Research* 34.3, pp. 546–559.

Dickinson, M. and E. Johnson (2001). "Chapter 14 - Fire Effects on Trees". In: *Forest Fires*. Ed. by E. A. Johnson and K. Miyanishi. San Diego: Academic Press, pp. 477 –525.

Doche, O (1997). *Etude expérimentale de chutes de blocs en forêt*. Tech. rep. 97/0898. Cemagref, Grenoble.

Dorren, L. K. A., F. Berger, and U. S. Putters (2006a). "Real-size experiments and 3-D simulation of rockfall on forested and non-forested slopes". In: *Natural Hazards and Earth System Sciences* 6.1, pp. 145–153.

Dorren, L. K. A., F. Berger, M. Frehner, M. Huber, K. Kühne, R. Métral, A. Sandri, R. Schwitter, J.-J. Thormann, and B. Wasser (2015). "Das neue NaiS-Anforderungsprofil Steinschlag". In: *Schweizerische Zeitschrift fur Forstwesen* 166.1, pp. 16–23.

Dorren, L. K. A. (2003). "A review of rockfall mechanics and modelling approaches". In: *Progress in Physical Geography* 27.1, pp. 69–87.

Dorren, L. K. A., F. Berger, C. le Hir, E. Mermin, and P. Tardif (2005). "Mechanisms, effects and management implications of rockfall in forests". In: *Forest Ecology and Management* 215.1–3, pp. 183–195.

Dorren, L. K. A. and F. Berger (2006b). "Stem breakage of trees and energy dissipation during rockfall impacts". In: *Tree Physiology* 26.1, pp. 63–71.

Dorren, L. K. (2015). *Rockyfor3D (v5.2) revealed - Transparent description of the complete 3D rockfall model*. ecorisQ. URL: www.ecorisq.org.

Dumas, D. (2013). "Changes in temperature and temperature gradients in the French Northern Alps during the last century". In: *Theoretical and Applied Climatology* 111, pp. 223–233.

Dupire, S., F. Bourrier, J.-M. Monnet, S. Bigot, L. Borgniet, F. Berger, and T. Curt (2016b). "The protective effect of forests against rockfalls across the French Alps : Influence of forest diversity". In: *Forest Ecology and Management* 382, pp. 269–279.

Dupire, S., T. Curt, and T. Fréjaville (In Prep. (a)). "Predicting potential post-fire tree mortality in the French Alps". In:

Dupire, S. and T. Curt (In Prep. (b)). "Forest fires in mountain forests with a protection function against rockfalls : assessing cascading effects". In:

Dupire, S. (2011). *Projet Interreg Forêts de protection. Action 2.4.1 Etude économique. Démarche et principaux résultats.* Tech. rep. Laboratoire d'Economie Forestière. AgroParisTech-INRA. Nancy, France.

Dupire, S., F. Bourrier, J.-M. Monnet, S. Bigot, L. Borgniet, F. Berger, and T. Curt (2016a). "Novel quantitative indicators to characterize the protective effect of mountain forests against rockfall". In: *Ecological Indicators* 67, pp. 98–107.

Dupire, S., T. Curt, and S. Bigot (2017). "Spatio-temporal trends in fire weather in the French Alps". In: *Science of The Total Environment* 595.Supplement C, pp. 801 –817.

Durand, Y., M. Laternser, G. Giraud, P. Etchevers, B. Lesaffre, and L. Mérindol (2009). "Reanalysis of 44 yr of climate in the French Alps (1958-2002) : methodology, model validation, climatology, and trends for air temperature and precipitation". In: *Journal of Applied Meteorology and Climatology* 48, p. 429.

Dussauge-Peisser, C., A. Helmstetter, J.-R. Grasso, D. Hantz, P. Desvarreux, M. Jeannin, and A. Giraud (2002). "Probabilistic approach to rock fall hazard assessment : potential of historical data analysis". In: *Natural Hazards and Earth System Science* 2.1/2, pp. 15–26.

Ebel, B. A. and J. A. Moody (2017). "Synthesis of soil-hydraulic properties and infiltration timescales in wildfire-affected soils". In: *Hydrological Processes* 31.2, pp. 324–340.

Eckert, N., E. Parent, T. Faug, and M. Naaim (2009). "Bayesian optimal design of an avalanche dam using a multivariate numerical avalanche model". In: *Stochastic Environmental Research and Risk Assessment* 23.8, pp. 1123–1141.

Einhorn, B., N. Eckert, C. Chaix, L. Ravanel, P. Deline, M. Gardent, B. V, D. Richard, G. Giraud, and P. Schoeneich (2015). "Climate change and natural hazards in the Alps". In: *Journal of Alpine Research* 103.2.

Eskelson, B. N. I., H. Temesgen, V. Lemay, T. M. Barrett, N. L. Crookston, and A. T. Hudak (2009). "The roles of nearest neighbor methods in imputing missing data in forest inventory and monitoring databases". In: *Scandinavian Journal of Forest Research* 24.3, pp. 235–246.

Evans, S. and O. Hungr (1993). "The assessment of rockfall hazard at the base of talus slopes". In: *Canadian Geotechnical Journal* 30.4, pp. 620–636.

Falaise, G (2001). *Prévention des mouvements de versants et des instabilités de falaises : confrontation des méthodes d'étude d'éboulements rocheux dans l'arc Alpin.* Tech. rep.

Favillier, A., J. Lopez-Saez, C. Corona, D. Trappmann, D. Toe, M. Stoffel, G. Rovéra, and F. Berger (2015). "Potential of two submontane broadleaved species (Acer opalus, Quercus pubescens) to reveal spatiotemporal patterns of rockfall activity". In: *Geomorphology* 246, pp. 35 –47.

Fernandes, P. M., J. A. Vega, E. Jiménez, and E. Rigolot (2008). "Fire resistance of European pines". In: *Forest Ecology and Management* 256.3, pp. 246 –255.

Fink, A. H., T. Brücher, A. Krüger, G. C. Leckebusch, J. G. Pinto, and U. Ulbrich (2004). "The 2003 European summer heatwaves and drought –synoptic diagnosis and impacts". In: *Weather* 59.8, pp. 209–216.

Finney, M. A. (2006). "An Overview of FlamMap Fire Modeling Capabilities". In: *In : Andrews, Patricia L.; Butler, Bret W., comps. Fuels Management-How to Measure Success : Conference Proceedings. 28-30 March 2006; Portland, OR. Proceedings RMRS-P-41. Fort Collins,*

CO : U.S. Department of Agriculture, Forest Service, Rocky Mountain Research Station. 041, pp. 213–220.

Flannigan, M. D., B. M. Wotton, G. A. Marshall, W. J. de Groot, J. Johnston, N. Jurko, and A. S. Cantin (2016). "Fuel moisture sensitivity to temperature and precipitation : climate change implications". In: *Climatic Change* 134.1, pp. 59–71.

Fonseca, F., T. de Figueiredo, C. Nogueira, and A. Queirós (2017). "Effect of prescribed fire on soil properties and soil erosion in a Mediterranean mountain area". In: *Geoderma* 307.Supplement C, pp. 172 –180.

Frayssines, M. (2005). "Contribution à l'évaluation de l'aléa éboulement rocheux (rupture)". PhD thesis. Université Joseph-Fourier - Grenoble I.

Fréjaville, T. (2015). "Vulnérabilité des forêts de montagne des Alpes occidentales au changement de régime d'incendie". PhD thesis. Aix-Marseille, France: Aix-Marseille Université.

Fréjaville, T., T. Curt, and C. Carcaillet (2013). "Bark flammability as a fire-response trait for subalpine trees". In: *Frontiers in Plant Science* 4, p. 466.

Fréjaville, T. and T. Curt (2014). "Pyroclimatic classification of Mediterranean and mountain landscapes of south-eastern France". In: *Advances in Forest Fire Research.* Coimbra: Imprensa da Universidade de Coimbra, pp. 1249–1255.

— (2015). "Spatiotemporal patterns of changes in fire regime and climate : defining the pyroclimates of south-eastern France (Mediterranean Basin)". In: *Climatic Change* 129.1, pp. 239–251.

Fréjaville, T., T. Curt, and C. Carcaillet (2016). "Tree cover and seasonal precipitation drive understorey flammability in Alpine mountain forests". In: *Journal of Biogeography* 43.9, pp. 1869–1880.

Fuhr, M., F. Bourrier, and T. Cordonnier (2015). "Protection against rockfall along a maturity gradient in mountain forests". In: *Forest Ecology and Management* 354, pp. 224–231.

Ganteaume, A., A. Camia, M. Jappiot, J. San-Miguel-Ayanz, M. Long-Fournel, and C. Lampin (2013). "A Review of the Main Driving Factors of Forest Fire Ignition Over Europe". In: *Environmental Management* 51.3, pp. 651–662.

Getzner, M., G. Gutheil-Knopp-Kirchwald, E. Kreimer, H. Kirchmeir, and M. Huber (2017). "Gravitational natural hazards : Valuing the protective function of Alpine forests". In: *Forest Policy and Economics* 80, pp. 150 –159.

Gibson, C. M., M. R. Turetsky, K. Cottenie, E. S. Kane, G. Houle, and E. S. Kasischke (2016). "Variation in plant community composition and vegetation carbon pools a decade following a severe fire season in interior Alaska". In: *Journal of Vegetation Science* 27.6, pp. 1187–1197.

Gill, J. C. and B. D. Malamud (2016). "Hazard interactions and interaction networks (cascades) within multi-hazard methodologies". In: *Earth System Dynamics* 7.3, pp. 659–679.

Gill, J. C. and B. D. Malamud (2014). "Reviewing and visualizing the interactions of natural hazards". In: *Reviews of Geophysics* 52.4, pp. 680–722.

Gilleland, E. and R. W. Katz (2016). "extRemes 2.0 : An Extreme Value Analysis Package in R". In: *Journal of Statistical Software* 72.8, pp. 1–39.

Gini, C. (1921). "Measurement of inequality of incomes". In: *The Economic Journal* 31.121, pp. 124–126.

Giordano, A. (1994). *L'érosion et la lutte contre l'érosion en forêt méditerranéenne.* Marseill (France).

Gobiet, A., S. Kotlarski, M. Beniston, G. Heinrich, J. Rajczak, and M. Stoffel (2014). "21st century climate change in the European Alps — A review". In: *Science of The Total Environment* 493, pp. 1138 –1151.

Gobron, N., B. Pinty, F. Mélin, M. Taberner, M. M. Verstraete, A. Belward, T. Lavergne, and J.-L. Widlowski (2005). "The state of vegetation in Europe following the 2003 drought". In: *International Journal of Remote Sensing* 26.9, pp. 2013–2020.

Granström, A. (2001). "Fire Management for Biodiversity in the European Boreal Forest". In: *Scandinavian Journal of Forest Research* 16.sup003, pp. 62–69.

Groot, W. J. de, Wardati, and Y. Wang (2005). "Calibrating the fine fuel moisture code for grass ignition potential in Sumatra, Indonesia". In: *International Journal of wildland fire* 14.2, pp. 161–168.

Gsteiger, P (1993). "Steinschlagschutzwald. Ein Beitrag zur Abgrenzung, Beurteilung und Bewirtschaftung". In: *Schweizerische Zeitschrift für Forstwesen* 144, pp. 115–132.

Guirimand, M. (2013). *Les forêts à fonction de protection vis-à-vis des chutes de blocs sur le territoire du Parc naturel régional du Vercors*. Tech. rep., p. 110.

Gutsell, S. and E. Johnson (1996). "How fire scars are formed : coupling a disturbance process to its ecological effect". In: *Canadian Journal of Forest Research* 26.2, pp. 166–174.

Géorisques (2017). *Géorisques - Mieux connaître les risques sur le territoire*. Accessed : 2017-01-05. URL: http://www.georisques.gouv.fr/.

Götmark, F. and C. Kiffer (2014). "Regeneration of oaks (Quercus robur/Q. petraea) and three other tree species during long-term succession after catastrophic disturbance (windthrow)". In: *Plant Ecology* 215.9, pp. 1067–1080.

Hantson, S., S. Pueyo, and E. Chuvieco (2015). "Global fire size distribution is driven by human impact and climate". In: *Global Ecology and Biogeography* 24.1, pp. 77–86.

Hantz, D., J. M. Vengeon, and C. Dussauge-Peisser (2003). "An historical, geomechanical and probabilistic approach to rock-fall hazard assessment". In: *Natural Hazards and Earth System Sciences* 3.6, pp. 693–701.

Harris, R. M. B., T. A. Remenyi, G. J. Williamson, N. L. Bindoff, and D. M. J. S. Bowman (2016). "Climate–vegetation–fire interactions and feedbacks : trivial detail or major barrier to projecting the future of the Earth system ?" In: *Wiley Interdisciplinary Reviews : Climate Change* 7.6, pp. 910–931.

Hartford, R. A. and W. H. Frandsen (1992). "When it's hot, it's hot... or maybe it's not !(Surface flaming may not portend extensive soil heating)". In: *International Journal of Wildland Fire* 2.3, pp. 139–144.

Heim, A. (1932). *Bergsturz und menschenleben*. 20. Fretz & Wasmuth.

Helfenstein, J. and F. Kienast (2014). "Ecosystem service state and trends at the regional to national level : A rapid assessment". In: *Ecological Indicators* 36, pp. 11 –18.

Hewitt, K. (1997). "Risk and disasters in mountain lands". In: *Mountains of the World : A Global Priority*. Ed. by B. Messerli and J.-D. Ives. New York and Carnforth: Parthenon Publishing, pp. 371–408.

— (2014). *Regions of risk : a geographical introduction to disasters*. Routledge, p. 400.

Hollander, M., D. A. Wolfe, and E. Chicken (2013). *Nonparametric statistical methods*. John Wiley & Sons.

Inbar, M, M Tamir, and L Wittenberg (1998a). "Runoff and erosion processes after a forest fire in Mount Carmel, a Mediterranean area". In: *Geomorphology* 24.1, pp. 17 –33. ISSN: 0169-555X.

— (1998b). "Runoff and erosion processes after a forest fire in Mount Carmel, a Mediterranean area". In: *Geomorphology* 24.1, pp. 17 –33.

IPCC (2012). *Managing The Risks of Extreme Events and Disaster to Advance Climate Change Adaptation. A Special Report of Working Groups I and II of the Intergovernmental Panel on Climate Change*. Ed. by C. B. Field, V. Barros, T. F. Stocker, D. Qin, D. J. Dokken, K. L. Ebi, M. M. D., K. J. Mach, P. G.-K., A. K. Allen, T. M., and M. P. M. Cambridge (UK) and New York, (USA): Cambridge University Press, p. 582.

Jahn, J (1988). "Entwaldung und Steinschlag". In: *International Congress Interpraevent 1988 in Graz*, pp. 185–198.

Jancke, O., L. K. A. Dorren, F. Berger, M. Fuhr, and M. Köhl (2009). "Implications of coppice stand characteristics on the rockfall protection function". In: *Forest Ecology and Management* 259.1, pp. 124 –131.

Johansen, M. P., T. E. Hakonson, and D. D. Breshears (2001). "Post-fire runoff and erosion from rainfall simulation : contrasting forests with shrublands and grasslands". In: *Hydrological Processes* 15.15, pp. 2953–2965.

Joly, D., T. Brossard, H. Cardot, J. Cavailhes, M. Hilal, and P. Wavresky (2010). "Types of climates on continental France, a spatial construction". In: *Cybergeo : European Journal of Geography*.

Jomelli, V., V. P. Pech, C. Chochillon, and D. Brunstein (2004). "Geomorphic variations of debris flows and recent climatic change in the French Alps". In: *Climatic Change* 64.1, pp. 77–102.

Kappes, M. S., M. Keiler, K. von Elverfeldt, and T. Glade (2012). "Challenges of analyzing multi-hazard risk : a review". In: *Natural Hazards* 64.2, pp. 1925–1958.

Kaufman, L. and P. J. Rousseeuw (1990). "Partitioning Around Medoids (Program PAM)". In: *Finding Groups in Data : An Introduction to Cluster Analysis*. Hoboken, NJ, USA: John Wiley and Sons, Inc., pp. 68–125.

Keeley, J. E. (2009). "Fire intensity, fire severity and burn severity : a brief review and suggested usage". In: *International Journal of Wildland Fire* 18.1, pp. 116–126.

Kohler, T., M. Giger, H. Hurni, C. Ott, U. Wiesmann, S. Wymann von Dach, and D. Maselli (2010). "Mountains and climate change : a global concern". In: *Mountain Research and Development* 30.1, pp. 53–55.

Kolström, T. and S. Kellomäki (1993). "Tree survival in wildfires." In: *Silva Fennica* 27.4.

Kunstler, G., S. Lavergne, B. Courbaud, W. Thuiller, G. Vieilledent, N. E. Zimmermann, J. Kattge, and D. A. Coomes (2012). "Competitive interactions between forest trees are driven by species' trait hierarchy, not phylogenetic or functional similarity : implications for forest community assembly". In: *Ecology Letters* 15.8, pp. 831–840.

Lahaye, S., T. Curt, L. Paradis, and C. Hély (2014). "Classification of large wildfires in South-Eastern France to adapt suppression strategies". In: *Advances in Forest Fire Research*. Coimbra: Imprensa da Universidade de Coimbra, pp. 696–708.

Lambert, S., F. Bourrier, and D. Toe (2013). "Improving three-dimensional rockfall trajectory simulation codes for assessing the efficiency of protective embankments". In: *International Journal of Rock Mechanics and Mining Sciences* 60, pp. 26–36.

Lasseur, R. (2017). "Cartographie multi-échelles des services écosystémiques : caractérisation des associations spatiales et apports de la télédétection". PhD thesis. Grenoble, France: Université Grenoble Alpes.

Lawson, B. D., O. Armitage, and others (2008). *Weather guide for the Canadian forest fire danger rating system*. Nat. Resour. Can., Can. For. Serv.

Le Meur, E., M. Gerbaux, M. Schäfer, and C. Vincent (2007). "Disappearance of an Alpine glacier over the 21st Century simulated from modeling its future surface mass balance". In: *Earth and Planetary Science Letters* 261.3–4, pp. 367 –374.

Leine, R. I., A. Schweizer, M. Christen, J. Glover, P. Bartelt, and W. Gerber (2014). "Simulation of rockfall trajectories with consideration of rock shape". In: *Multibody System Dynamics* 32.2, pp. 241–271.

Lied, K (1977). "Rockfall problems in Norway". In: *ISMES* 90, pp. 51–53.

Linder, P., P. Jonsson, and M. Niklasson (1998). "Tree mortality after prescribed burning in an old-growth Scots pine forest in northern Sweden". In: *Silva Fennica* 32.4.

Loehman, R. A., E. Reinhardt, and K. L. Riley (2014). "Wildland fire emissions, carbon, and climate : Seeing the forest and the trees – A cross-scale assessment of wildfire and carbon dynamics in fire-prone, forested ecosystems". In: *Forest Ecology and Management* 317.Supplement C, pp. 9 –19.

Luterbacher, J., D. Dietrich, E. Xoplaki, M. Grosjean, and H. Wanner (2004). "European seasonal and annual temperature variability, trends, and extremes since 1500". In: *Science* 303.5663, pp. 1499–1503.

Mansuy, N., E. Thiffault, D. Paré, P. Bernier, L. Guindon, P. Villemaire, V. Poirier, and A. Beaudoin (2014). "Digital mapping of soil properties in Canadian managed forests at 250 m of resolution using the k-nearest neighbor method". In: *Geoderma* 235–236, pp. 59 –73.

Maringer, J., D. Ascoli, L. K. A. Dorren, P. Bebi, and M. Conedera (2016a). "Temporal trends in the protective capacity of burnt beech forests (Fagus sylvatica L.) against rockfall". In: *European Journal of Forest Research*, pp. 1–17.

Maringer, J., D. Ascoli, N. Küffer, S. Schmidtlein, and M. Conedera (2016b). "What drives European beech (Fagus sylvatica L.) mortality after forest fires of varying severity ?" In: *Forest Ecology and Management* 368.Supplement C, pp. 81 –93. ISSN: 0378-1127.

Maroschek, M., W. Rammer, and M. Lexer (2014). "Using a novel assessment framework to evaluate protective functions and timber production in Austrian mountain forests under climate change". In: *Regional Environmental Change*, pp. 1–13.

Matsuoka, N. and H. Sakai (1999). "Rockfall activity from an alpine cliff during thawing periods". In: *Geomorphology* 28.3–4, pp. 309–328.

McHugh, C. W., T. E. Kolb, and J. L. Wilson (2003). "Bark Beetle Attacks on Ponderosa Pine Following Fire in Northern Arizona". In: *Environmental Entomology* 32.3, pp. 510–522.

Meyn, A., P. S. White, C. Buhk, and A. Jentsch (2007). "Environmental drivers of large, infrequent wildfires : the emerging conceptual model". In: *Progress in Physical Geography* 31.3, pp. 287–312.

Michaletz, S. T. and E. A. Johnson (2007). "How forest fires kill trees : A review of the fundamental biophysical processes". In: *Scandinavian Journal of Forest Research* 22.6, pp. 500–515.

Mignan, A., S. Wiemer, and D. Giardini (2014). "The quantification of low-probability–high-consequences events : part I. A generic multi-risk approach". In: *Nat. Hazards* 73.3, pp. 1999–2022. ISSN: 1573-0840.

Mitsopoulos, I., G. Mallinis, A. Karali, C. Giannakopoulos, and M. Arianoutsou (2016). "Mapping fire behaviour under changing climate in a Mediterranean landscape in Greece". In: *Regional Environmental Change* 16.7, pp. 1929–1940.

Modugno, S., H. Balzter, B. Cole, and P. Borrelli (2016). "Mapping regional patterns of large forest fires in Wildland–Urban Interface areas in Europe". In: *Journal of Environmental Management* 172, pp. 112 –126.

Monnet, J.-M., F. Bourrier, S. Dupire, and F. Berger (2017). "Suitability of airborne laser scanning for the assessment of forest protection effect against rockfall". In: *Landslides* 14.1, pp. 299–310.

Montz, B. E., G. A. Tobin, and R. R. Hagelman (2017). *Natural hazards : explanation and integration*. Guilford Publications.

Moreira, F., O. Viedma, M. Arianoutsou, T. Curt, N. Koutsias, E. Rigolot, A. Barbati, P. Corona, P. Vaz, G. Xanthopoulos, F. Mouillot, and E. Bilgili (2011). "Landscape – wildfire interactions in southern Europe : Implications for landscape management". In: *Journal of Environmental Management* 92.10, pp. 2389 –2402. ISSN: 0301-4797.

Moretti, M., M. Conedera, P. Duelli, and P. J. Edwards (2002). "The effects of wildfire on ground-active spiders in deciduous forests on the Swiss southern slope of the Alps". In: *Journal of Applied Ecology* 39.2, pp. 321–336.

Morin, X., L. Fahse, M. Scherer-Lorenzen, and H. Bugmann (2011). "Tree species richness promotes productivity in temperate forests through strong complementarity between species". In: *Ecology Letters* 14.12, pp. 1211–1219.

Moriondo, M, P Good, R Durao, M Bindi, C Giannakopoulos, and J Corte-Real (2006). "Potential impact of climate change on fire risk in the Mediterranean area". In: *Climate Research* 31.1, pp. 85–95.

Moris, J. V., G. Vacchiano, S. Ravetto Enri, M. Lonati, R. Motta, and D. Ascoli (2017). "Resilience of European larch (Larix decidua Mill.) forests to wildfires in the western Alps". In: *New Forests* 48.5, pp. 663–683.

Moritz, M. A., M.-A. Parisien, E. Batllori, M. A. Krawchuk, J. Van Dorn, D. J. Ganz, and K. Hayhoe (2012). "Climate change and disruptions to global fire activity". In: *Ecosphere* 3.6, pp. 1–22.

Motta, R. and J.-C. Haudemand (2000). "Protective Forests and Silvicultural Stability". In: *Mountain Research and Development* 20.2, pp. 180–187.

Mucherino, A., P. J. Papajorgji, and P. M. Pardalos (2009). "k-Nearest Neighbor Classification". In: *Data Mining in Agriculture*. New York, NY: Springer New York, pp. 83–106.

Müller, M. M., H. Vacik, G. Diendorfer, A. Arpaci, H. Formayer, and H. Gossow (2013). "Analysis of lightning-induced forest fires in Austria". In: *Theoretical and Applied Climatology* 111.1, pp. 183–193.

Müller, M. M., H. Vacik, and E. Valese (2015). "Anomalies of the Austrian forest fire regime in comparison with other Alpine countries : A research note". In: *Forests* 6.4, pp. 903–913.

Naaim-Bouvet, F. and D. Richard (2015). *Les risques naturels en montagne*. Versailles Cedex: Éd. Quae. ISBN: 978-2-7592-2386-2.

Newman, J. P., H. R. Maier, G. A. Riddell, A. C. Zecchin, J. E. Daniell, A. M. Schaefer, H. van Delden, B. Khazai, M. J. O'Flaherty, and C. P. Newland (2017). "Review of literature on decision support systems for natural hazard risk reduction : Current status and future research directions". In: *Environmental Modelling and Software* 96, pp. 378 –409.

Nicot, F., B. Cambou, and G. Mazzoleni (2001). "From a constitutive modelling of metallic rings to the design of rockfall restraining nets". In: *International Journal for Numerical and Analytical Methods in Geomechanics* 25.1, pp. 49–70.

Notaro, S. and A. Paletto (2012). "The economic valuation of natural hazards in mountain forests : an approach based on the replacement cost method". In: *Journal of Forest Economics* 18.4, pp. 318–328.

Nunes, A. N. and L. Lourenço (2017). "Increased vulnerability to wildfires and post fire hydrogeomorphic processes in Portuguese mountain regions : what has changed ?" In: *Open Agriculture* 2.1, pp. 70–82.

Olmedo, I., F. Bourrier, D. Bertrand, F. Berger, and A. Limam (2015). "Felled Trees as a Rockfall Protection System : Experimental and Numerical Studies". In: *Engineering Geology for Society and Territory - Volume 2 : Landslide Processes*. Ed. by G. Lollino, D. Giordan, G. B. Crosta, J. Corominas, R. Azzam, J. Wasowski, and N. Sciarra. Cham: Springer International Publishing, pp. 1889–1893.

Ordóñez, J. L., J. Retana, and J. M. Espelta (2005). "Effects of tree size, crown damage, and tree location on post-fire survival and cone production of Pinus nigra trees". In: *Forest Ecology and Management* 206.1, pp. 109 –117.

Ozenda, P. and H. Wagner (1975). *Les séries de végétation de la chaine alpine et leurs équivalences dans les autres systèmes phytogéographiques*. Laboratoire de biologie végétale de l'Université de Grenoble.

Pachauri, R. K., M. R. Allen, V. R. Barros, J. Broome, W. Cramer, R. Christ, J. A. Church, L. Clarke, Q. Dahe, P. Dasgupta, and others (2014). *Climate change 2014 : synthesis report. Contribution of Working Groups I, II and III to the fifth assessment report of the Intergovernmental Panel on Climate Change*. IPCC.

Pardini, G., M. Gispert, M. Emran, and S. Doni (2017). "Rainfall/runoff/erosion relationships and soil properties survey in abandoned shallow soils of NE Spain". In: *Journal of Soils and Sediments* 17.2, pp. 499–514.

Peila, D., S. Pelizza, and F. Sassudelli (1998). "Evaluation of Behaviour of Rockfall Restraining Nets by Full Scale Tests". In: *Rock Mechanics and Rock Engineering* 31.1, pp. 1–24.

Perret, S., F. Dolf, and H. Kienholz (2004). "Rockfalls into forests : Analysis and simulation of rockfall trajectories — considerations with respect to mountainous forests in Switzerland". In: *Landslides* 1.2, pp. 123–130.

Peterson, D. L. and K. C. Ryan (1986). "Modeling postfire conifer mortality for long-range planning". In: *Environmental Management* 10.6, pp. 797–808.

Pielou, E. C. (1966). "The measurement of diversity in different types of biological collections". In: *Journal of Theoretical Biology* 13, pp. 131 –144.

Piton, G., S. Carladous, A. Recking, J. M. Tacnet, F. Liébault, D. Kuss, Y. Quefféléan, and O. Marco (2016). "Why do we build check dams in Alpine streams ? An historical perspective from the French experience". In: *Earth Surface Processes and Landforms*, pp. 91–108.

Poumadère, M., C. Mays, S. Le Mer, and R. Blong (2005). "The 2003 Heat Wave in France : Dangerous Climate Change Here and Now". In: *Risk Analysis* 25.6, pp. 1483–1494.

Power, M. J., J. Marlon, N. Ortiz, P. J. Bartlein, S. P. Harrison, F. E. Mayle, A. Ballouche, R. H. W. Bradshaw, C. Carcaillet, and al (2008). "Changes in fire regimes since the Last Glacial Maximum : an assessment based on a global synthesis and analysis of charcoal data". In: *Climate Dynamics* 30.7, pp. 887–907.

Price, M. F., G. Gratzer, L. A. Duguma, T. Kohler, D. Maselli, and R. Romeo (2011). *Mountain Forests in a Changing World - Realizing values, addressing challenges*. Rome: FAO/MPS and SDC.

Prométhée (2017). *PROMÉTHÉE 2 : La banque de données sur les incendies de forêts en région Méditerranéenne en France*. URL: http://www.promethee.com/.

Quintana-Segui, P., P. Le Moigne, Y. Durand, E. Martin, F. Habets, M. Baillon, C. Canellas, L. Franchisteguy, and S. Morel (2008). "Analysis of near-surface atmospheric variables : Validation of the SAFRAN analysis over France". In: *Journal of applied meteorology and climatology* 47.1, pp. 92–107.

Quintana-Seguí, P., M. Turco, S. Herrera, and G. Miguez-Macho (2016). "Validation of a new SAFRAN-based gridded precipitation product for Spain and comparisons to Spain02 and ERA-Interim". In: *Hydrology and Earth System Sciences Discussions* 2016, pp. 1–26.

Radtke, A., D. Toe, F. Berger, S. Zerbe, and F. Bourrier (2014). "Managing coppice forests for rockfall protection : lessons from modeling". In: *Annals of Forest Science* 71.4, pp. 485–494.

Rammer, W., M. Brauner, H. Ruprecht, and M. Lexer (2015). "Evaluating the effects of forest management on rockfall protection and timber production at slope scale". In: *Scandinavian Journal of Forest Research* 30.8, pp. 719–731.

Ravanel, L. and P. Deline (2011). "Climate influence on rockfalls in high-Alpine steep rockwalls : The north side of the Aiguilles de Chamonix (Mont-Blanc massif) since the end of the 'Little Ice Age'". In: *The Holocene* 21.2, pp. 357–365.

Reineking, B., P. Weibel, M. Conedera, and H. Bugmann (2010). "Environmental determinants of lightning-v. human-induced forest fire ignitions differ in a temperate mountain region of Switzerland". In: *International Journal of Wildland Fire* 19.5, pp. 541–557.

Reinhard, M., M. Rebetez, and R. Schlaepfer (2005). "Recent climate change : Rethinking drought in the context of Forest Fire Research in Ticino, South of Switzerland". In: *Theoretical and Applied Climatology* 82.1, pp. 17–25.

Rey, F. (2017). "Ecologie ingénieriale : une recherche finalisée au service de l'ingénierie et du génie écologiques". In: *Revue d'écologie - La Terre et la vie* 72.

Reynolds, A. P., G. Richards, B. Iglesia, and V. J. Rayward-Smith (2006). "Clustering Rules : A Comparison of Partitioning and Hierarchical Clustering Algorithms". In: *Journal of Mathematical Modelling and Algorithms* 5.4, pp. 475–504.

Rigolot, E (2002). "Fuel-break assessment with an expert appraisement approach". In: *Forest Fire Research and Wildland Fire Safety, Proceedings of the IV International Conference on Forest Fire Research/2002 Wildland Fire Safety Summit.* University of Coimbra. Coimbra (Portugal). Millpress (Rotterdam).

Rigolot, E. (2004). "Predicting postfire mortality of Pinus halepensis Mill. and Pinus pinea L." In: *Plant Ecology* 171.1, pp. 139–151.

Ritchie, A. M. (1963). "Evaluation of rockfall and its control". In: *Highway research record* 17.

Robert, N., C. Vidal, A. Colin, H. Jean-Christophe, N. Hamza, and C. Cluzeau (2010). "National Forest Inventories reports : France". In: *National Forest Inventories—Pathways for Common Reporting.* Ed. by E. Tomppo, T. Gschwantner, M. Lawrence, and R. E. McRoberts. Springer, pp. 207–221.

Rohner, B., C. Bigler, J. Wunder, P. Brang, and H. Bugmann (2012). "Fifty years of natural succession in Swiss forest reserves : changes in stand structure and mortality rates of oak and beech". In: *Journal of Vegetation Science* 23.5, pp. 892–905.

Rothermel, R. C. (1991). *Predicting behavior and size of crown fires in the Northern Rocky Mountains.* Tech. rep. USDA Forest Service. Intermountain Research Station, p. 46.

Rothermel, R. C. et al. (1972). *A mathematical model for predicting fire spread in wildland fuels.* Tech. rep. USDA Forest Service. Intermountain Research Station, p. 40.

Ruffault, J, V Moron, R. M. Trigo, and T Curt (2016). "Objective identification of multiple large fire climatologies : an application to a Mediterranean ecosystem". In: *Environmental Research Letters* 11.7.

Ruffault, J., V. Moron, R. M. Trigo, and T. Curt (2017a). "Daily synoptic conditions associated with large fire occurrence in Mediterranean France : evidence for a wind-driven fire regime". In: *International Journal of Climatology* 37.1, pp. 524–533.

Ruffault, J. and F. Mouillot (2017b). "Contribution of human and biophysical factors to the spatial distribution of forest fire ignitions and large wildfires in a French Mediterranean region". In: *Int. J. Wildland Fire* 26.6, pp. 498–508.

Schumacher, S. and H. Bugmann (2006). "The relative importance of climatic effects, wildfires and management for future forest landscape dynamics in the Swiss Alps". In: *Global Change Biology* 12.8, pp. 1435–1450.

Schunk, C., C. Wastl, M. Leuchner, and A. Menzel (2017). "Fine fuel moisture for site- and species-specific fire danger assessment in comparison to fire danger indices". In: *Agricultural and Forest Meteorology* 234–235, pp. 31 –47.

Scott, A. C. and I. J. Glasspool (2006). "The diversification of Paleozoic fire systems and fluctuations in atmospheric oxygen concentration". In: *Proceedings of the National Academy of Sciences* 103.29, pp. 10861–10865.

Selby, M. (1993). "Mass wasting of soils". In: *Hillslope materials and processes. Second Edition. Oxford University Press, Oxford*, pp. 249–355.

Shakesby, R. A., J. A. Moody, D. A. Martin, and P. R. Robichaud (2016). "Synthesising empirical results to improve predictions of post-wildfire runoff and erosion response". In: *International Journal of Wildland Fire* 25.3, pp. 257–261.

Sidoroff, K., T. Kuuluvainen, H. Tanskanen, and I. Vanha-Majamaa (2007). "Tree mortality after low-intensity prescribed fires in managed Pinus sylvestris stands in southern Finland". In: *Scandinavian Journal of Forest Research* 22.1, pp. 2–12.

Skowronski, N. S., S. Haag, J. Trimble, K. L. Clark, M. R. Gallagher, and R. G. Lathrop (2016). "Structure-level fuel load assessment in the wildland–urban interface : a fusion of airborne

laser scanning and spectral remote-sensing methodologies". In: *International Journal of Wildland Fire* 25.5, pp. 547–557.

Spalt, K. W. and W. E. Reifsnyder (1962). *Bark characteristics and fire resistance : a literature survey*. Tech. rep. Southern Forest Experiment Station, USDA Forest Service, p. 24.

Stirling, G. and B. Wilsey (2001). "Empirical Relationships between Species Richness, Evenness, and Proportional Diversity". In: *The American Naturalist* 158.3, pp. 286–299.

Stoffel, M., A. Wehrli, R. Kühne, L. K. A. Dorren, S. Perret, and H. Kienholz (2006). "Assessing the protective effect of mountain forests against rockfall using a 3D simulation model". In: *Forest Ecology and Management* 225.1–3, pp. 113–122.

Stoffel, M., C. Corona, J. A. Ballesteros-Cánovas, and J. M. Bodoque (2013). "Dating and quantification of erosion processes based on exposed roots". In: *Earth-Science Reviews* 123, pp. 18 –34.

Straub, D. and M. Schubert (2008). "Modeling and managing uncertainties in rock-fall hazards". In: *Georisk : Assessment and Management of Risk for Engineered Systems and Geohazards* 2.1, pp. 1–15.

Swezy, D. M. and J. K. Agee (1991). "Prescribed-fire effects on fine-root and tree mortality in old-growth ponderosa pine". In: *Canadian Journal of Forest Research* 21.5, pp. 626–634.

Tibshirani, R., G. Walther, and T. Hastie (2001). "Estimating the number of clusters in a data set via the gap statistic". In: *Journal of the Royal Statistical Society : Series B (Statistical Methodology)* 63.2, pp. 411–423.

Tinner, W., P. Hubschmid, M. Wehrli, B. Ammann, and M. Conedera (1999). "Long-term forest fire ecology and dynamics in southern Switzerland". In: *Journal of Ecology* 87.2, pp. 273–289.

Tinner, W., M. Conedera, E. Gobet, P. Hubschmid, M. Wehrli, and B. Ammann (2000). "A palaeoecological attempt to classify fire sensitivity of trees in the southern Alps". In: *The Holocene* 10.5, pp. 565–574.

Tinner, W., M. Conedera, B. Ammann, and A. F. Lotter (2005). "Fire ecology north and south of the Alps since the last ice age". In: *The Holocene* 15.8, pp. 1214–1226.

Toe, D. and F. Berger (2015). "Regional Mapping of Forest with a Protection Function Against Rockfall". In: *Engineering Geology for Society and Territory*. Ed. by G. Lollino, D. Giordan, G. B. Crosta, J. Corominas, R. Azzam, J. Wasowski, and N. Sciarra. Vol. 2. Cham: Springer International Publishing, pp. 1957–1959.

Toe, D. (2016). "Characterisation of the protection function of coppice stands against rockfall hazard". PhD thesis. Grenoble, France: Université Grenoble Alpes.

Toe, D., F. Bourrier, L. Dorren, and F. Berger (2017a). "A Novel DEM Approach to Simulate Block Propagation on Forested Slopes". In: *Rock Mechanics and Rock Engineering*, pp. 1–15.

Toe, D., F. Bourrier, I. Olmedo, J.-M. Monnet, and F. Berger (2017b). "Analysis of the effect of trees on block propagation using a DEM model : implications for rockfall modelling". In: *Landslides* 14.5, pp. 1603–1614.

— (2017c). "Analysis of the effect of trees on block propagation using a DEM model : implications for rockfall modelling". In: *Landslides* 14.5, pp. 1603–1614.

Toppe, R. (1987). "Terrain models-A tool for natural hazard mapping". In: *Avalanche formation, movement and effects, IAHS Publ* 162, pp. 629–638.

Trappmann, D. and M. Stoffel (2013). "Counting scars on tree stems to assess rockfall hazards : A low effort approach, but how reliable ?" In: *Geomorphology* 180–181, pp. 180 –186.

Trappmann, D., M. Stoffel, and C. Corona (2014). "Achieving a more realistic assessment of rockfall hazards by coupling three-dimensional process models and field-based tree-ring data". In: *Earth Surface Processes and Landforms* 39.14, pp. 1866–1875.

Turner, W. R., K. Brandon, T. M. Brooks, R. Costanza, G. A. B. d. Fonseca, and R. Portela (2007). "Global Conservation of Biodiversity and Ecosystem Services". In: *BioScience* 57.10, pp. 868–873.

Vacchiano, G., R. Berretti, E. B. Mondino, F. Meloni, and R. Motta (2016). "Assessing the Effect of Disturbances on the Functionality of Direct Protection Forests". In: *Mt. Res. Dev.* 36.1, pp. 41–55.

Valese, E, M Conedera, H Vacik, A Japelj, A Beck, G Cocca, H Cvenkel, N Di Narda, A Ghiringhelli, A Lemessi, et al. (2011). "Wildfires in the Alpine region : first results from the ALP FFIRS project". In: *Proc. Fifth International Wildfire Conference, South Africa.*

Valese, E., M. Conedera, A. C. Held, and D. Ascoli (2014). "Fire, humans and landscape in the European Alpine region during the Holocene". In: *Anthropocene* 6, pp. 63 –74.

Valor, T., J. R. González-Olabarria, M. Piqué, and P. Casals (2017). "The effects of burning season and severity on the mortality over time of Pinus nigra spp. salzmannii (Dunal) Franco and P. sylvestris L." In: *Forest Ecology and Management* 406.Supplement C, pp. 172 –183.

Van Wagner, C. E. (1977). "Conditions for the start and spread of crown fire". In: *Canadian Journal of Forest Research* 7.1, pp. 23–34.

Van Wagner, C. (1970). *On the value of temperature data in forest fire research.* Petawawa forest experiment station.

— (1987). *Development and structure of the Canadian Forest Fire Weather Index System.* Vol. 35. Canadian Forestry Service, Forestry Technical Report 35.

Varner, J. M., F. E. Putz, J. J. O'Brien, J. K. Hiers, R. J. Mitchell, and D. R. Gordon (2009). "Post-fire tree stress and growth following smoldering duff fires". In: *Forest Ecology and Management* 258.11, pp. 2467 –2474.

Venäläinen, A., N. Korhonen, O. Hyvärinen, N. Koutsias, F. Xystrakis, I. R. Urbieta, and J. M. Moreno (2014). "Temporal variations and change in forest fire danger in Europe for 1960–2012". In: *Natural Hazards and Earth System Sciences* 14.6, pp. 1477–1490.

Vidal, J.-P., E. Martin, L. Franchistéguy, M. Baillon, and J.-M. Soubeyroux (2010). "A 50-year high-resolution atmospheric reanalysis over France with the Safran system". In: *International Journal of Climatology* 30.11, pp. 1627–1644.

Vidrih, R., M. Ribičič, and P. Suhadolc (2001). "Seismogeological effects on rocks during the 12 April 1998 upper Soča Territory earthquake (NW Slovenia)". In: *Tectonophysics* 330.3–4, pp. 153–175.

Viegas, D. X., G. Bovio, A. Ferreira, A. Nosenzo, and B. Sol (2000). "Comparative study of various methods of fire danger evaluation in southern Europe". In: *International Journal of wildland fire* 9.4, pp. 235–246.

Vilà, M., J. Vayreda, L. Comas, J. J. Ibáñez, T. Mata, and B. Obón (2007). "Species richness and wood production : a positive association in Mediterranean forests". In: *Ecology Letters* 10.3, pp. 241–250.

Volkwein, A., K. Schellenberg, V. Labiouse, F. Agliardi, F. Berger, F. Bourrier, L. Dorren, W. Gerber, and M. Jaboyedoff (2011). "Rockfall characterisation and structural protection - a review". In: *Natural Hazards and Earth System Sciences* 11, p. 2617 –p. 2651.

Wallenius, T. H., A. Pitkänen, T. Kuuluvainen, J. Pennanen, and H. Karttunen (2005). "Fire history and forest age distribution of an unmanaged Picea abies dominated landscape". In: *Canadian Journal of Forest Research* 35.7, pp. 1540–1552.

Wasser, B and M Frehner (1996). *Minimale Pflegesmassnahmen für Wälder mit Schutzfunktion.* Bern: Wegleitung. Bundesamt für Umwelt, Wald und Landschaft (BUWAL).

Wastl, C., C. Schunk, M. Leuchner, G. B. Pezzatti, and A. Menzel (2012). "Recent climate change : long-term trends in meteorological forest fire danger in the Alps". In: *Agricultural and Forest Meteorology* 162–163, pp. 1 –13.

Wehrli, A., A. Zingg, H. Bugmann, and A. Huth (2005). "Using a forest patch model to predict the dynamics of stand structure in Swiss mountain forests". In: *Forest Ecology and Management* 205.1, pp. 149–167.

Wehrli, A., L. K. Dorren, F. Berger, A. Zingg, W. Schönenberger, and P. Brang (2006). "Modelling long-term effects of forest dynamics on the protective effect against rockfall". In: *Forest Snow and Landscape Research* 80.1, pp. 57–76.

Weiner, J. and O. T. Solbrig (1984). "The Meaning and Measurement of Size Hierarchies in Plant Populations". In: *Oecologia* 61.3, pp. 334–336.

Whalley, W. (1984). "Rockfalls". In: *Slope instability*, pp. 217–256.

Wick, L. and A. Möhl (2006). "The mid-Holocene extinction of silver fir (Abies alba) in the Southern Alps : a consequence of forest fires ? Palaeobotanical records and forest simulations". In: *Vegetation History and Archaeobotany* 15.4, p. 435.

Wilcoxon, F. (1945). "Individual comparisons by ranking methods". In: *Biometrics bulletin* 1.6, pp. 80–83.

Woltjer, M., W. Rammer, M. Brauner, R. Seidl, G. M. J. Mohren, and M. J. Lexer (2008). "Coupling a 3D patch model and a rockfall module to assess rockfall protection in mountain forests". In: *Journal of Environmental Management* 87.3, pp. 373–388.

Wotton, B. M. (2009). "Interpreting and using outputs from the Canadian Forest Fire Danger Rating System in research applications". In: *Environmental and Ecological Statistics* 16.2, pp. 107–131.

Zumbrunnen, T., P. Menéndez, H. Bugmann, M. Conedera, U. Gimmi, and M. Bürgi (2012). "Human impacts on fire occurrence : a case study of hundred years of forest fires in a dry alpine valley in Switzerland". In: *Regional Environmental Change* 12.4, pp. 935–949.

Évaluation des effets des incendies sur la capacité de protection des forêts contre les chutes de blocs dans les Alpes françaises

Résumé

Les forêts de montagne sont particulièrement efficaces pour atténuer les effets dévastateurs de certains aléas naturels comme les chutes de blocs. Cette capacité de protection peut cependant être altérée par d'autres aléas naturels tels que les incendies, susceptibles d'être plus fréquents et intenses en raison des changements climatiques. Ce travail de thèse a pour objectif d'évaluer les effets des incendies sur la capacité de protection des forêts contre les chutes de blocs dans les Alpes françaises. Il propose une méthode originale pour quantifier la capacité de protection d'une forêt contre les chutes de blocs avant et après un incendie et alimente les connaissances sur ces deux aléas naturels et les risques associés. L'analyse multi-aléas conduite en fin de thèse permet d'appréhender les effets cascades potentiels à l'échelle du peuplement forestier ainsi que pour quatre territoires bioclimatiquement homogènes des Alpes françaises.

Mots-clés : Forêts de montagne · Aléas naturels · Alpes françaises · Chutes de blocs · Feux de forêt · Analyse multi-aléas · Effets cascades · Forêts de protection · Changements climatiques · Services écosystémiques · Simulations numériques

Assessing wildfires effects on the protection capability of forests against rockfalls in the French Alps

Abstract

Mountain forests are a particularly efficient nature based-solution to mitigate the damages caused by natural hazards such as rockfalls. This protection capability can however be altered by other natural hazards such as fires, likely to be more frequent and intense in the context of climate change. This PhD thesis aims at assessing the effects of fires on the protection capability of forests against rockfalls in the French Alps. It proposes an original method to quantify the protection capabilities of a forest against rockfalls before and after a fire and improve the knowledge of these two natural hazards and their associated risks. The multi-hazard analysis conducted at the end of the thesis makes it possible to understand the potential cascading effects in the main forest types and four bioclimatically homogeneous territories of the French Alps.

Keywords : Mountain forests · Natural hazards · French Alps · Rockfalls · Forest fire · Multi-hazard analysis · Cascading effect · Protection forest · Climate changes · Ecosystem services · Numerical modelling